

ҚАЗАҚСТАН РЕСПУБЛИКАСЫ  
ҒЫЛЫМ ЖӘНЕ ЖОҒАРЫ БІЛІМ МИНИСТРЛІГІ  
SATBAYEV UNIVERSITY  
МЕТАЛЛУРГИЯ ЖӘНЕ КЕН БАЙЫТУ ИНСТИТУТЫ

ISSN 2616-6445 (Online)  
ISSN 2224-5243 (Print)  
DOI 10.31643/2018/166445

# Минералдық шикізаттарды кешенді пайдалану

—❖— **4(331)** —❖—

**Комплексное  
Использование  
Минерального  
Сырья**

**Complex  
Use of  
Mineral  
Resources**

**ҚАЗАН-ЖЕЛТОҚСАН 2024  
ОCTOBER-DECEMBER 2024  
ОКТАБРЬ-ДЕКАБРЬ 2024**

**ЖЫЛЫНА 4 РЕТ ШЫҒАДЫ  
QUARTERLY JOURNAL  
ВЫХОДИТ 4 РАЗА В ГОД**

**ЖУРНАЛ 1978 ЖЫЛДАН БАСТАП  
ШЫҒАДЫ JOURNAL HAS BEEN  
PUBLISHING SINCE 1978 ЖУРНАЛ  
ИЗДАЕТСЯ С 1978 ГОДА**

**АЛМАТЫ - 2024**

Б а с р е д а к т о р техника ғылымдарының докторы, профессор **Багдаулет КЕНЖАЛИЕВ**

Р е д а к ц и я а л қ а с ы :

Тех. ғыл. канд. **Ринат Абдулвалиев**, Металлургия және байыту институты, Алматы, Қазақстан;  
Ph.D, проф. **Akçil Ata**, Сулейман Демирел университеті, Испарта, Түркия;  
Ph.D, доцент **Rouholah Ashiri**, Исфахан технологиялық университеті, Исфахан, Иран;  
Проф., др. **Craig E. Banks**, Манчестер Метрополитен университеті, Ұлыбритания;  
Тех. және физ.-мат. ғыл. др. **Валерий Володин**, Металлургия және байыту институты, Алматы, Қазақстан;  
Ph.D, проф. **Didik Nurhadiyanto**, Джокьякарта мемлекеттік университеті, Индонезия;  
Тех. ғыл. др., проф. **Ұзақ Жапбасбаев**, Сәтбаев университеті, Алматы, Қазақстан;  
Др. **Khaldun Mohammad Al Azzam**, Әл-Ахлия Амман университеті, Амман 19328, Иордания;  
Др. **Kyoung Tae Park**, Корея сирек металдар институты (KIRAM), Корея өнеркәсіптік технологиялар институты (KITECH), Корея Республикасы;  
Др. **Jae Hong Shin**, Корея өнеркәсіптік технологиялар институты, Корея Республикасы;  
Др. **Malgorzata Rutkowska-Gorczyca**, Вроцлав технологиялық университеті, Вроцлав, Польша;  
Др., проф. **Abdul Hafidz Yusoff**, Университет Малайзии Келантан, 16100, Келантан, Малайзия;  
Тех. ғыл. др., **Гүлнәз Молдабаева**, Сәтбаев университеті, Алматы, Қазақстан;  
Проф., др. **Heri Retnawati**, Джокьякарта мемлекеттік университеті (Universitas Negeri Yogyakarta), Индонезия;  
Проф. **Mishra Brajendra**, Вустер Политехникалық институты, Вустер, АҚШ;  
Проф., т.ғ.д., **El-Sayed Negim**, Ұлттық зерттеу орталығы, Каир, Египет;  
Ph.D **Muhammad Noorazlan Abd Azis**, Сұлтан Идрис атындағы білім беру университеті, Перак, Малайзия;  
Тех.ғыл.кан., проф., академик **Ержан И. Кульдеев**, Сәтбаев университеті, Алматы, Қазақстан;  
Тех.ғыл.кан., проф. **Қанай Рысбеков**, Сәтбаев университеті, Алматы, Қазақстан;  
Ph.D, проф. **Dimitar Peshev**, Химиялық технология және металлургия университеті, София, Болгария;  
Тех. ғыл. др., **Сергей Квятковский**, Металлургия және байыту институты, Алматы, Қазақстан;  
Тех. ғыл. др., проф. **Arman Shah**, Сұлтан Идрис білім беру университеті, Малайзия;  
Жетекші ғылыми қызметкер, др. **Dilip Makhija**, JSW Cement Ltd, Мумбай, Үндістан.

Ж а у а п т ы х а т ш ы

**Гулжайна Касымова**

**Редакция мекен жайы:**

Металлургия және кен байыту институты

050010, Қазақстан Республикасы, Алматы қ., Шевченко к-сі, Уәлиханов к-нің қиылысы, 29/133,

Fax. +7 (727) 298-45-03, Tel. +7-(727) 298-45-02, +7 (727) 298-45-19

E mail: journal@kims-imio.kz, product-service@kims-imio.kz

<http://kims-imio.com/index.php/main>

---

«Минералдық шикізаттарды кешенді пайдалану» журналы ғылыми жұмыстардың негізгі нәтижелерін жариялау үшін Қазақстан Республикасы Білім және ғылым министрілігінің Білім және ғылым сапасын қамтамасыз ету комитеті ұсынған ғылыми басылымдар тізіміне енгізілген.

Меншік иесі: «Металлургия және кен байыту институты» АҚ

Журнал Қазақстан Республикасының Ақпарат және коммуникация министрлігінің Байланыс, ақпараттандыру және бұқаралық ақпарат құралдары саласындағы мемлекеттік бақылау комитетінде қайта тіркелген

2016 ж. 18 қазандағы № 16180-Ж Куәлігі

Editor-in-chief Dr. Sci. Tech., professor **Bagdaulet KENZHALIYEV**

Editorial board:

Cand. of Tech. Sci. **Rinat Abdulvaliyev**, Institute of Metallurgy and Ore Beneficiation, Kazakhstan;  
Ph.D., Prof. **Akçil Ata**, Süleyman Demirel Üniversitesi, Isparta, Turkey;  
Ph.D **Rouholah Ashiri**, associate prof. of Isfahan University of Technology, Isfahan, Iran;  
Prof., Dr. **Craig E. Banks**, Manchester Metropolitan University, United Kingdom;  
Dr. Tech., Phys-math. Sci., prof. **Valeryi Volodin**, Institute of Metallurgy and Ore Beneficiation, Almaty, Kazakhstan;  
Prof., Ph.D., **Didik Nurhadiyanto**, Yogyakarta State University, Yogyakarta, Indonesia;  
Dr.Sci.Tech., Prof. **Uzak K. Zhapbasbayev**, Satbayev University, Almaty, Kazakhstan;  
Dr. **Khaldun Mohammad Al Azzam**, Department of Pharmaceutical Sciences, Pharmacological and Diagnostic Research Center, Faculty of Pharmacy, Al-Ahliyya Amman University, Amman 19328, Jordan;  
Dr. **Kyoung Tae Park**, Korea Institute for Rare Metals (KIRAM), Korea Institute of Industrial Technology (KITECH), Republic of Korea;  
Dr. **Jae Hong Shin**, Korea Institute of Industrial Technology, Republic of Korea;  
Dr.Sc. **Malgorzata Rutkowska-Gorczyca**, Wroclaw University of Science and Technology, Wroclaw, Poland;  
Associate Prof., Dr **Abdul Hafidz Yusoff**, Universiti Malaysia Kelantan, 16100, Kelantan, Malaysia;  
Dr.Sci.Tech. **Gulnaz Moldabayeva**, Satbayev University, Almaty, Kazakhstan;  
Prof., Dr. **Heri Retnawati**, Yogyakarta State University (Universitas Negeri Yogyakarta), Indonesia;  
Prof. **Mishra Brajendra**, Worcester Polytechnic Institute, Worcester, United States;  
Prof., Dr. Sci. Tech. **El-Sayed Negim**, Professor of National Research Centre, Cairo, Egypt;  
Ph.D. **Muhammad Noorazlan Abd Azis**, associate prof. of Sultan Idris Education University, Perak, Malaysia;  
Prof., Dr. Sci. Tech., academician **Yerzhan I. Kuldeyev**, Satbayev University, Almaty, Kazakhstan;  
Prof., Dr. Sci. Tech. **Kanay Rysbekov**, Satbayev University, Almaty, Kazakhstan;  
Professor, Ph.D. **Dimitar Peshev**, University of Chemical Technology and Metallurgy, Sofia, Bulgaria;  
Dr.Sci.Tech. **Sergey A. Kvyatkovskiy**, Institute of Metallurgy and Ore Beneficiation, Kazakhstan;  
Prof., Dr. Sci. Tech. **Arman Shah**, Universiti Pendidikan Sultan Idris, Tanjong Malim, Malaysia;  
Lead Scientist, Dr. **Dilip Makhija**, JSW Cement Ltd, Mumbai, India.

Executive secretary

**Gulzhaina Kassymova**

**Address:**

Institute of Metallurgy and Ore Beneficiation  
29/133 Shevchenko Street, corner of Ch. Valikhanov Street, Almaty, 050010, Kazakhstan  
Fax. +7 (727) 298-45-03, Tel. +7-(727) 298-45-02, +7 (727) 298-45-19  
E mail: journal@kims-imio.kz, product-service@kims-imio.kz  
<http://kims-imio.com/index.php/main>

---

The Journal “Complex Use of Mineral Resources” is included in the List of publications recommended by the Committee for Control in the Sphere of Education and Science of the Ministry of Education and Science of the Republic of Kazakhstan for the publication of the main results of scientific activities.  
Owner: “Institute of Metallurgy and Ore Beneficiation” JSC

The Journal was re-registered by the Committee for State Control in the Sphere of Communication, Information and Mass Media of the Ministry of Information and Communication of the Republic of Kazakhstan.

Certificate № 16180-Ж since October 18, 2016

Главный редактор доктор технических наук, профессор **Багдаулет КЕНЖАЛИЕВ**

Редакционная коллегия:

Кан. хим. н. **Ринат Абдулвалиев**, Институт Metallургии и Обогащения, Алматы, Казахстан;  
Ph.D, проф. **Akçil Ata**, Университет Сулеймана Демиреля, Испарта, Турция;  
Ph.D, доцент, **Rouhollah Ashiri**, Исфahanский технологический университет, Исфahan, Иран;  
Др. тех. н., проф. **Craig E. Banks**, Манчестерский столичный университет, Соединенное Королевство;  
Др. тех. н. и физ.-мат. н. **Валерий Володин**, Институт Metallургии и Обогащения, Казахстан;  
Др. тех. н., доцент **Didik Nurhadiyanto**, Джокьякартский государственный университет, Индонезия;  
Др. тех. н., проф. Узак **Жапбасбаев**, КазНИТУ имени К. И. Сатпаева, Алматы, Казахстан;  
Др. **Khalidun Mohammad Al Azzam**, Аль-Ахлия Амманский университет, Амман 19328, Иордания;  
Др. **Kyoung Tae Park**, Корейский институт редких металлов (KIRAM), Корейский институт промышленных технологий (KITECH), Республика Корея;  
Др. **Jae Hong Shin**, Корейский институт промышленных технологий, Республика Корея;  
Др. **Malgorzata Rutkowska-Gorczyca**, Вроцлавский политехнический университет, Вроцлав, Польша;  
Др. проф. **Abdul Hafidz Yusoff**, Университет Малайзии, Келантан, 16100, Келантан, Малайзия;  
Др. тех. н., **Гульназ Молдабаева**, КазНИТУ имени К.И. Сатпаева, Алматы, Казахстан;  
Проф., др. **Heri Retnawati**, Факультет математики и естественных наук Джокьякартского государственного университета (Universitas Negeri Yogyakarta), Индонезия;  
Ph.D, проф. **Mishra Brajendra**, Вустерский политехнический институт, Вустер, США;  
Др. тех. н., проф. **El-Sayed Negim**, Национальный исследовательский центр, Каир, Египет;  
Ph.D, доцент, **Muhammad Noorzalan Abd Azis**, Образовательный университет Султана Идриса, Перак, Малайзия;  
К.т.н., проф., академик **Ержан И. Кульдеев**, КазНИТУ имени К. И. Сатпаева, Алматы, Казахстан;  
К.т.н., проф. **Канай Рысбеков**, КазНИТУ имени К. И. Сатпаева, Алматы, Казахстан;  
Ph.D, проф. **Dimitar Peshev**, Университет химической технологии и металлургии, София, Болгария;  
Др. тех. н. **Сергей Квятковский**, Институт Metallургии и Обогащения, Алматы, Казахстан;  
Кан. хим. н., проф. **Arman Shah**, Педагогический университет Султана Идриса, Танджунг Малим, Малайзия;  
Ведущий научный сотрудник, др. **Dilip Makhija**, JSW Cement Ltd, Мумбаи, Индия.

Ответственный секретарь

**Гулжайна Касымова**

Адрес редакции:

Институт Metallургии и Обогащения  
050010, Республика Казахстан, г. Алматы, ул. Шевченко, уг. ул. Валиханова, 29/133,  
Fax. +7 (727) 298-45-03, Tel. +7 (727) 298-45-02, +7 (727) 298-45-19  
E mail: journal@kims-imio.kz, product-service@kims-imio.kz  
<http://kims-imio.com/index.php/main>

---

Журнал «Комплексное использование минерального сырья» включен в Перечень изданий, рекомендуемых Комитетом по контролю в сфере образования и науки Министерства образования и науки Республики Казахстан для публикации основных результатов научной деятельности.  
Собственник: АО «Институт металлургии и обогащения»

Журнал перерегистрирован в Комитете государственного контроля в области связи, информатизации и средств массовой информации  
Министерства информации и коммуникации Республики Казахстан  
Свидетельство № 16180-Ж от 18 октября 2016 г.





## Study of the material composition of refractory gold-bearing ore from the Aktobe deposit

Barmenshinova M.B., \*Motovilov I.Y., Telkov Sh.A., Omar R.S.

Satbayev University, Almaty, Kazakhstan

\*Corresponding author email: E-mail: i.motovilov@satbayev.university

Received: October 2, 2023  
Peer-reviewed: November 13, 2023  
Accepted: December 12, 2023

### ABSTRACT

The study of the material composition of gold-bearing ores includes the determination of quantitative chemical and mineral composition, forms of noble metals, granulometric composition, and physical and mechanical properties to choose the direction for the development of an effective technology of their complex enrichment. This work is devoted to the study of the material composition of refractory gold-bearing ore of Aktobe deposit. It was determined that the content of gold is 1.55-1.6 g/t, the mass fraction of silver is 42-43 g/t, and the content of sulphur is low and is 1-1.1% respectively. Of non-ferrous metals, zinc 0.17%, and lead 0.15% are present in insignificant amounts, and the content of harmful impurities antimony and arsenic are insignificant and amounted to 0.01 and 0.05%. The ore sample has a relatively uncomplicated mineral composition: rock-forming minerals represented by quartz, potassium feldspar, calcite, and mica predominate significantly. Ore minerals are represented by pyrite up to 10 %, limonite up to 0.5 %, galena 0.15-0.2 %, sphalerite 0.17-0.2 % and gold. Physical and mechanical properties of the ore were determined. According to the category of crushability, the ore belongs to the category of medium hardness. According to Bond's method, the "index of network  $W_i$ " of ball milling was determined for the initial ore, which was 19.3 kW·h/t· $\mu\text{m}^{0.5}$ . Based on the obtained data on the study of material composition, further research will be directed to the study of gravity and flotation enrichment.

**Keywords:** gold, silver, chemical analysis, mineralogical analysis, granulometric analysis, physical and mechanical properties.

### Information about the authors:

**Barmenshinova Madina Bohembaevna**

Candidate of Technical Sciences, Associate Professor, Head of the Department of "Metallurgy and Mineral Processing", Satbayev University, Satpayev 22, Almaty, Kazakhstan. E-mail: m.barmenshinova@satbayev.university

**Motovilov Igor Yurievich**

Doctor PhD, Associate Professor at the Department of Metallurgy and Mineral Processing, Satbayev University, Satpayev 22, Almaty, Kazakhstan. E-mail: i.motovilov@satbayev.university

**Telkov Shamil Abdulaevich**

Candidate of Technical Sciences, Associate Professor, Professor of the Metallurgy and Mineral Processing Department, Satbayev University, Satpayev 22, Almaty, Kazakhstan. E-mail: s.telkov@satbayev.university

**Omar Rakymzhan Sultanbekuly**

Master of Technical Sciences, Engineer of the Metallurgy and Mineral Processing Department, Satbayev University, Satpayev 22, Almaty, Kazakhstan. E-mail: r.omar@satbayev.university

## Introduction

The Aktobe deposit is located in the Moyinkum region of Zhambyl province and is part of the Mynaral ore field. The Mynaral ore field differs from other ore fields of the Chu-Ili ore belt by its peculiar history of geological development, volcanism, magmatism and mineralisation. The discovery of a significant number of occurrences and points of ore mineralisation within its boundaries, as well as a huge number of hypogenic halos, allows us to reasonably distinguish the Mynaral ore cluster as a gold-bearing territory.

Within this field, relatively recently (1984-88) performed prospecting works revealed 20 ore occurrences and about 30 occurrences and points of mineralisation of gold, 1 of silver, 9 of molybdenum, 6 of lead, 3 of beryllium, 3 of manganese and 2 of copper.

The prevalence of gold mineralisation over other metals is overwhelming. This characterises the manifested specialisation of the ore field for gold.

Concerning the study, within the limits of the ore field the conducted works revealed about 50 ore occurrences and manifestations of gold, 5 of

which were most fully studied by mining and drilling works, which gave the justification to separate them into one deposit, called Mynaralskoye, with reserves of 30.0 tonnes of gold with an average grade of 12.0 g/t and vein thickness from 1.0 m to 3 m. Currently, this deposit has been mined to a depth of 240.0 metres from the surface by underground mining. The remaining 45 gold occurrences remained poorly explored and underexplored due to the collapse of the USSR and, as a consequence, the cessation of state budgetary allocations. In 2017, TOO "Mynaral Gold" and TOO "Mynaral Resources", having obtained the subsoil use right for the Mynaral ore field, explored the Aktobe deposit of 4.7 tonnes of gold according to the JORC system.

Based on the above, the question arose about the study of the material composition of the sample of gold-bearing ore of the Aktobe to choose a further direction for the development of rational technology of its processing.

### Experimental part

This research was carried out in the non-profit joint-stock company " K.I. Satpayev KazNITU" at the Department of "Metallurgy and Mineral Processing" under the grant project №AP19680182 "Development of an effective technology of complex enrichment and processing of refractory gold-bearing raw materials of the Aktobe deposit".

The object of the study was the gold-bearing ore of the Aktobe deposit of the Republic of Kazakhstan.

Used methods of studying the material composition of the ore sample:

- chemical composition [[1], [2], [3]] - determined by spectral, chemical, and assay analysis;

- mineral composition [[3], [4], [5]] - determined by macroscopic study of samples under a binocular loupe MBS-1 and microscopic study of anschliffts on a polarising microscope Leica DM2500 M. For more detailed confirmation of the mineral composition of the ore, X-ray diffractometric analysis was made.

- physical properties [[6], [7]]:

- Granulometric composition [[8], [9]] - determined by sieve analysis;

- Ore density - measured by pycnometer;

- Bulk density of ore - measured by weighing in a vessel of known volume;

Ore strength according to Protodiakonov [[10], [11]] - is determined by the instrument of determination of the strength of POC;

Bond grindability index - determined by Bond's method [[12], [13], [14], [15], [16], [17], [18], [19]].

Sampling for the above analyses was carried out using standard techniques recommended in the study of minerals for enrichment, the meaning of which is the relationship between the size and weight of the sample taken, which with sufficient reliability preserved all the properties of the original process sample and the ore of the deposit.

### Discussing the results

*Chemical composition:*

The results of the chemical composition of the ore are summarised in Table 1.

**Table 1** – Chemical composition of initial ore

Element	Mass fraction
Gold, g/t	1.57
Silver, g/t	42.50
Quartz, %	64.50
Aluminium oxide, %	18.11
Calcium oxide, %	0.76
Iron, %	2.14
Sulphur (total), %	1.06
Copper, %	0.01
Lead, %	0.15
Zinc, %	0.17
Arsenic, %	0.05
Antimony, %	0.01

The results of atomic-emission semi-quantitative spectral analysis are shown in Table 2.

According to the results of the assay, chemical and atomic-emission semi-quantitative spectral analyses, the average gold grade in the ore sample received for testing was 1.57 g/t. The silver grade was 42.50 g/t.

The iron and sulphur content of the ore was 2.14% and 1.06% respectively.

Copper content was minimal, lead 0.15 %, zinc 0.17 %.

The content of harmful impurities in the form of arsenic and antimony is minimal.

*Mineral composition*

The material composition was studied by X-ray diffractometric analysis on an automated diffractometer DRON-3 with <sup>55</sup>NiCa-radiation, β-filter.

**Table 2** – Results of atomic-emission analysis of initial ore

Element	Concentration, %	Element	Concentration, %
Au	<0.0002	Ni	0.003
Ag	0.004	Mo	0.002
Al	>>1.0	V	0.005
Si	>>1.0	Ga	0.0015
Fe	>>1.0	Ge	<0.0002
K	>1.0	Sr	0.03
Mg	0.5	Bi	<0.0002
Na	0.2	Nb	<0.001
Mn	0.15	Cd	0.001
Ti	0.3	Te	<0.002
Ca	≤1.0	Tl	<0.0005
Cu	0.003	Hg	<0.003
Zn	0.1	Y	0.003
Sn	0.001	Yb	0.002
Cr	0.002	Be	0.00015
W	<0,002	Ba	0.1
Pb	0.15	Ce	0.01
As	0.05	La	0.002
Sb	0.005	Co	0.003
Sc	0.002	Zr	0.01
Li	0.003	In	<0.0005
P	0.15	Ta	<0.01
Pd	<0.0002	Re	<0.0003
Pt	<0.001	Os	<0.001

Results of semi-quantitative X-ray phase analysis (Table 3), diffractogram of the sample (Fig.1).

**Table 3** – Results of semi-quantitative X-ray phase analysis

Mineral	Formula	Concentration, %
Quartz	SiO <sub>2</sub>	79.1
Potassium feldspar	KAlSi <sub>3</sub> O <sub>8</sub>	7.2
Pyrite	FeS <sub>2</sub>	6.0
Calcite	Ca(CO <sub>3</sub> )	4.6
Mica	KAl <sub>2</sub> (AlSi <sub>3</sub> O <sub>10</sub> )(OH) <sub>2</sub>	3.1

The ore sample has a relatively uncomplicated mineral composition: rock-forming minerals represented by quartz, potassium feldspar, calcite and mica predominate significantly. Ore minerals are represented by pyrite up to 10 %, limonite up to 0.5 %, galena 0.15-0.2 %, sphalerite 0.17-0.2 %, gold and silver, which were determined by X-ray diffractometric analysis and confirmed by microscope examination of anschliffs.

Pyrite is observed in two generations, pyrite I - in the form of intergrowths and phenocrysts of individual idiomorphic grains up to 1.0 mm in size, mostly cubic in shape (squares in the anschliff section).

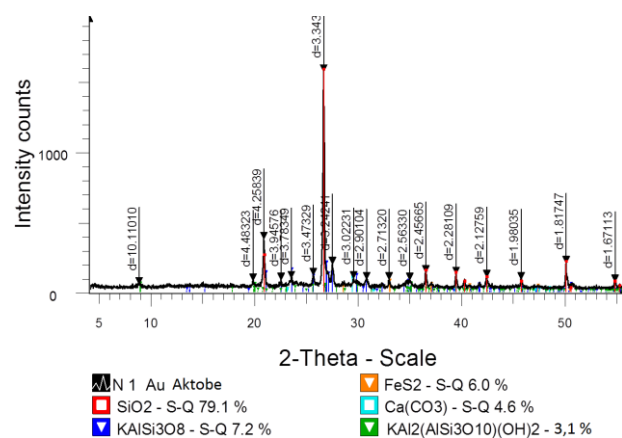


**Figure 2** - Diffractogram of a sample of initial ore from the Aktobe deposit

Pyrite II forms fine-grained inclusions in the clastic material of the breccia, up to 0.014 mm in size, the shape of grains is mainly pentagon dodecahedra. Most of the pyrite is observed in association with sphalerite and galena, which intensively replace and corrode it (Figure 3).

Sphalerite forms continuous aggregates and veins, anhedral grains with emulsion phenocrysts of pyrite, from 0.05 to 1.2 mm in size, and often replaces pyrite with the formation of loop structures. Sphalerite is medium-grained, with light-yellow internal reflexes (cleophane) (Figure 3).

Galena is less abundant, as a later mineral by the degree of formation, it performs interstices in non-metallic minerals, and forms veins and mesh-like inclusions. It intensively replaces pyrite and sphalerite. It rarely forms large accumulations (Figure 3).

Limonite forms thread-like, net-like inclusions around the grains of nonmetallic minerals, and iron

hydroxides form crusts with concentric-zonal structures along the cracks (Figure 4 b).

One inclusion of nugget gold, elongated in shape, 0.035x0.01 mm in size, straw-yellow in colour with high reflection was found in the cavity of limonite leaching (Figure 4 a).

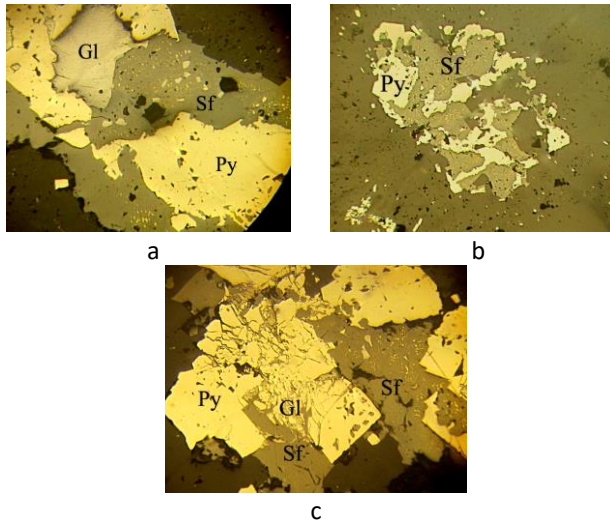


**Figure 3** - a) sphalerite (Sf) intergrowth corroding pyrite (Py) and galena (Gl), b) replacement of pyrite (Py) by sphalerite (Sf) with formation of loop structure, c) sphalerite (Sf) and pyrite (Py) intergrowth, pyrite is corroded by galena (Gl) along cracks

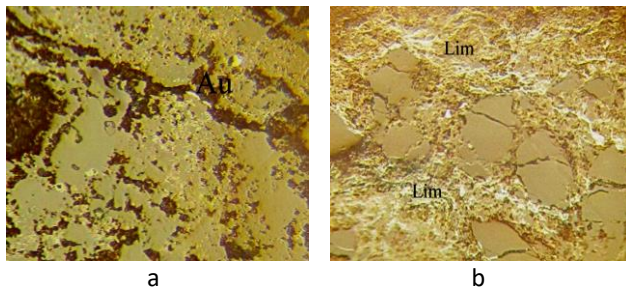


**Figure 4** - a) inclusion of nugget gold (Au) in the leach fracture; b) filamentous limonite (Lim) efflorescence enveloping grains of non-metallic minerals

#### Physical properties

The results of sieve analysis of a sample of gold-bearing ore crushed to 3.3 mm with gold and silver distribution by size class are presented in Table 4.

The sieve analysis results presented in Table 4 showed that the weighted average grade of gold in the analysed ore was 1.56 g/t and silver 42.91 g/t.

The distribution of gold content by size class is uneven. The gold content in the largest class of - 3.3+1.6 mm size class was 1.05 g/t and with decreasing coarseness of classes increases up to 3.37 g/t.

The distribution of silver content by size class is uneven. The silver content in the largest class of - 3.3+1.6 mm was 37.29 g/t and with decreasing coarseness of classes increased to 78.75 g/t.

Table 5 shows the results of the determination of the physical-mechanical properties of the ore sample of the Aktobe deposit.

**Table 4** – Results of sieve analysis of initial ore

Grain size class, mm	Output, %	Content, g/t		Recovery, %	
		Au	Ag	Au	Ag
-3.3+1.6	20.13	1.05	37.29	13.50	17.49
-1.6+1	31.83	1.07	35.17	21.77	26.09
-1+0.63	12.45	1.12	35.71	8.93	10.36
-0.63+0.32	13.45	2.07	40.17	17.86	12.59
-0.32+0.16	7.88	2.06	51.33	10.41	9.43
-0.16+0.074	4.92	2.33	60.17	7.36	6.90
-0.074+0.0	9.34	3.37	78.75	20.17	17.14
Total	100.0	1.56	42.91	100.0	100.0

**Table 5** – Physical and mechanical properties of ore sample

Indices	Unit of measurement	Values
pt - specific weight (density)	g/cm <sup>3</sup>	2.69
pb - bulk density	g/cm <sup>3</sup>	1.50
η - porosity	%	44
f - Protodiakonov's coefficient of strength	-	12.12
Bond crushability index	kWh/h/t·mcm <sup>0.5</sup>	19.3

Ore hardness according to Protodyakonov was 12.12 - the ore is categorised as medium hardness in terms of crushability. The bond crushability index was 19.3 kWh·h/t·μm<sup>0.5</sup>, the ores of Aktobe deposit are classified as medium crushable.

Comparison of the results of the study of the material composition of gold-bearing ore of the deposit "Aktobe" with the results of earlier studies [[3], [20]], carried out on similar gold-bearing ores, it is established that further research on the development of technology enrichment of ore of the deposit "Aktobe" is advisable to continue with the study of gravity and flotation enrichment.

## Conclusions

Based on the results of research on the material composition of ore of the deposit "Aktobe" the following main conclusions can be made:

- according to the results of assay analysis, the average gold content in the studied ore was 1.57 g/t and silver 42.50 g/t;

- the main host mineral is quartz, potassium feldspar, calcite and mica are also present;

- ore minerals are represented by pyrite up to 10 %, limonite up to 0.5 %, galena 0.15-0.2 %, sphalerite 0.17-0.2 %;

- harmful impurities in the form of arsenic and antimony are practically absent, as well as minimal copper content;

- a microscope examination of the samples revealed that the ore is represented by nested disseminated aggregates of galena-sphalerite-pyrite composition. The main ore mineral - pyrite is observed in the form of anhedral and phenocrysts, individual idiomorphic grains, ranging in size from 0.02 to 1.5 mm in association with sphalerite and galena, developing mainly along fractures. Nugget gold is found in a void in brecciated, intensely leached rock represented by limonite and iron

hydroxides. The grain is elongated, 0.035x0.01 mm in size, straw-yellow in colour with high reflection;

- the main components in the ore of the deposit "Aktobe", representing industrial value, are gold and silver.

Based on the obtained data on the study of material composition, further research will be directed to the study of gravity and flotation enrichment with the development of the optimal technological scheme for the enrichment of gold-bearing ore of the deposit Aktobe with the writing of technological regulations.

**Conflict of interest.** On behalf of all authors, the correspondent author declares that there is no conflict of interest.

**Acknowledgements.** This research is funded by the Committee of Science of the Ministry of Science and Higher Education of the Republic of Kazakhstan (grant #AP19680182).

**Cite this article as:** Barmenshinova MB, Motovilov IYu, Telkov ShA, Omar RS. Study of the material composition of refractory gold-bearing ore from the Aktobe deposit. Kompleksnoe Ispolzovanie Mineralnogo Syra = Complex Use of Mineral Resources. 2024; 331(4):5-11. <https://doi.org/10.31643/2024/6445.34>

## Ақтөбе кен орнының құрамында алтыны бар қиын өңделетін кендерінің заттай құрамын зерттеу

Барменшинова М.Б., Мотовилов И.Ю., Телков Ш.А., Омар Р.С.

Сәтбаев Университеті, Алматы, Қазақстан

### ТҮЙІНДЕМЕ

Құрамында алтыны бар кендердің заттай құрамын зерттеу, оларды кешенді байытудың тиімді технологиясын әзірлеу бағытын таңдау мақсатында сандық химиялық және минералдық құрамдарды, асыл металдардың қандай түрде болатындығын, гранулометриялық құрамын, физика-механикалық қасиеттерін анықтауды қамтиды. Бұл жұмыс Ақтөбе кен орнының құрамында алтыны бар кендерінің заттай құрамын зерттеуге арналған. Алтынның мөлшері 1,55 – 1,6 г/т, күмістің массалық үлесі 42-43 г/т, күкірт мөлшері төмен және сәйкесінше 1-1, 1% құрайды. Түсті металдардың құрамында аз мөлшерде мырыш 0,17%, қорғасын 0,15%, сурьма мен мышьяқтың зиянды қоспаларының мөлшері шамалы 0,01 және 0,05% болады. Кен салыстырмалы түрде қарапайым минералдық құрамға ие: онда кварц, калийлі дала шпаты, кальцит, слюда сияқты тау жыныстарын құрайтын минералдар басым. Кен минералдарының құрамында пирит 10% дейін, лимонит 0,5% дейін галенит 0,15-0,2 %, сфалерит 0,17-0,2% және алтын бар. Кеннің физикалық-механикалық қасиеттері анықталды. Ұсату категориясы бойынша кен орташа қаттылық санатына жатады. Бонд әдісі бойынша бастапқы кен үшін шарлы ұнтақтаудың "Wi таза жұмыс индексі" анықталды. Ол 19,3 кВт·сағ/т·мкм<sup>0,5</sup> құрады. Заттай құрамды зерттеу бойынша алынған мәліметтер негізінде одан әрі зерттеулер гравитациялық және флотациялық байыту зерттеулеріне бағытталады.

**Түйін сөздер:** алтын, күміс, химиялық талдау, минералогиялық талдау, гранулометриялық талдау, физика-механикалық қасиеттері.

### Авторлар туралы ақпарат:

Техника ғылымдарының кандидаты, қауымдастырылған профессор, "Металлургия және пайдалы қазбаларды байыту" кафедрасының меңгерушісі, Сәтбаев Университеті, Сәтбаев көш. 22, Алматы, Қазақстан. E-mail: [m.barmenshinova@satbayev.university](mailto:m.barmenshinova@satbayev.university)

Мақала келді: 2 қазан 2023  
Сараптамадан өтті: 13 қараша 2023  
Қабылданды: 12 желтоқсан 2023

Барменшинова Мадина Богембаевна



<b>Мотовилов Игорь Юрьевич</b>	<i>PhD докторы, "Металлургия және пайдалы қазбаларды байыту" кафедрасының қауымдастырылған профессоры, Сәтбаев Университеті, Сәтбаев көш. 22, Алматы, Қазақстан. E-mail: i.motovilov@satbayev.university</i>
<b>Телков Шамиль Абдулаевич</b>	<i>Техника ғылымдарының кандидаты, доцент, "Металлургия және пайдалы қазбаларды байыту" кафедрасының профессоры, Сәтбаев Университеті, Сәтбаев көш. 22, Алматы, Қазақстан. E-mail: s.telkov@satbayev.university</i>
<b>Омар Рақымжан Сұлтанбекұлы</b>	<i>Техника ғылымдарының магистрі, "Металлургия және пайдалы қазбаларды байыту" кафедрасының инженері, Сәтбаев Университеті, Сәтбаев көш. 22, Алматы, Қазақстан. E-mail: r.omar@satbayev.university</i>

## Изучение вещественного состава упорной золотосодержащей руды месторождения Актөбе

Барменшинова М.Б., Мотовилов И.Ю., Телков Ш.А., Омар Р.С.

*Satbayev University, Алматы, Казахстан*

### АННОТАЦИЯ

Изучение вещественного состава золотосодержащих руд включает определение количественного химического и минерального составов, форм нахождения благородных металлов, гранулометрического состава, физико-механических свойств с целью выбора направления для разработки эффективной технологии их комплексного обогащения. Данная работа посвящена изучению вещественного состава упорной золотосодержащей руды месторождения Актөбе. Определено, что содержание золота – 1,55-1,6 г/т, массовая доля серебра составляет 42-43 г/т, содержание серы низкое и составляет 1-1,1% соответственно. Из цветных металлов в незначительных количествах присутствует цинк 0,17%, свинец 0,15%, содержание вредных примесей сурьмы и мышьяка незначительные и составили 0,01 и 0,05 %. Проба руды имеет сравнительно несложный минеральный состав: существенно преобладают породообразующие минералы, представленные кварцем, калиевым полевым шпатом, кальцитом, слюдой. Рудные минералы представлены пиритом до 10 %, лимонитом до 0,5 % галенитом 0,15-0,2 %, сфалеритом 0,17-0,2 % и золотом. Определены физико-механические свойства руды. По категории дробимости, руда относится к категории средней твердости. По методу Бонда определен «индекс чистой работы  $W_i$ » шарового измельчения для исходной руды, который составил 19,3 кВт·ч/т·мкм<sup>0,5</sup>. На основании полученных данных по изучению вещественного состава, дальнейшие исследования будут направлены на изучение гравитационной и флотационной обогатимости.

**Ключевые слова:** золото, серебро, химический анализ, минералогический анализ, гранулометрический анализ, физико-механические свойства.

### Информация об авторах:

<b>Барменшинова Мадина Богембаевна</b>	<i>Кандидат технических наук, ассоциированный профессор, заведующий кафедрой «Металлургии и обогащения полезных ископаемых», Satbayev University, улица Сатпаева 22, Алматы, Казахстан. E-mail: m.barmenshinova@satbayev.university</i>
<b>Мотовилов Игорь Юрьевич</b>	<i>Доктор PhD, ассоциированный профессор кафедры «Металлургии и обогащения полезных ископаемых», Satbayev University, улица Сатпаева 22, Алматы, Казахстан. E-mail: i.motovilov@satbayev.university</i>
<b>Телков Шамиль Абдулаевич</b>	<i>Кандидат технических наук, доцент, профессор кафедры «Металлургии и обогащения полезных ископаемых», Satbayev University, улица Сатпаева 22, Алматы, Казахстан. E-mail: s.telkov@satbayev.university</i>
<b>Омар Рақымжан Сұлтанбекұлы</b>	<i>Магистр технических наук, инженер кафедры «Металлургии и обогащения полезных ископаемых», Satbayev University, улица Сатпаева 22, Алматы, Казахстан. E-mail: r.omar@satbayev.university</i>

## References

- [1] Zelenov VI, Metodika issledovaniya zoloto- i serebrosoderzhashchikh rud [Methodology of research of gold-and silver-bearing ores]. Moscow: Nedra. 1989. (in Russ.).
- [2] Bekpulatov ZhM, Khudayberdiyev FT. Izucheniye veshchestvennogo sostava i razrabotka tekhnologii pererabotki zolotosoderzhashchey proby rudy odnogo iz mestorozhdeniy respubliki Uzbekistan [Study of material composition and development of technology of processing of gold-bearing ore sample of one of the deposits of the Republic of Uzbekistan]. Mezhdunarodnyy nauchnyy zhurnal Innovatsionnaya nauka = International scientific journal Innovative Science. 2017; 4(3):20-23. (in Russ.).
- [3] Kenzhaliyev BK, Koizhanova AK, Atanova OV, Magomedov DR, Nurdin H. Research and development of gold ore processing technology. Kompleksnoe Ispolzovanie Mineralnogo Syra = Complex Use of Mineral Resources. 2024; 329(2):63-72. <https://doi.org/10.31643/2024/6445.17>

- [4] Umarova IK, Mengilbayev DA, Makhmarezhbov DB. Izucheniye mineralogicheskogo sostava upornykh zolotosoderzhashchikh rud mestorozhdeniya Auminzov [Study of mineralogical composition of refractory gold-bearing ores of Auminzov deposit]. Scientific Progress. 2021; 2(5):199-205. (in Russ.).
- [5] Fedotov PK, Senchenko AE, Fedotov KV, Burdonov AE, Vlasova VE. Technology for processing low-sulfide gold-quartz ore. Izvestiya Tomskogo politekhnicheskogo universiteta. Geoaktivny inzhenerii = Bulletin of the Tomsk Polytechnic University. Geo Assets Engineering. 2022; 333(6):178-189. <https://doi.org/10.18799/24131830/2022/6/3540>
- [6] Leonov SB, Belkova ON. Issledovaniye poleznykh iskopayemykh na obogatimost [Studies of mineral resources for mineral processing]. Moscow: Internet Engineering. 2001.
- [7] Marchevskaya VV, Mukhina TN. Izucheniye fiziko-mekhanicheskikh svoystv gornyykh porod mestorozhdeniy malosulfidnykh rud Kolskogo poluostrova [Study of Physical and Mechanical Properties of Rocks of Low-Sulphide Ore Deposits of the Kola Peninsula]. Vestnik Kolskogo nauchnogo tsentra RAN = Bulletin of the Kola Scientific Centre of the Russian Academy of Sciences. 2011; 3:35-39. (in Russ.).
- [8] Shautenov MR, Telkov ShA, Begalinov AB, Motovilov IYu, Akkazina NT. Granulometricheskii sostav i kharakter raspredeleniya redko-zemelnykh elementov rudy kory vyvetrivaniya [Granulometric composition and character of distribution of rare-earth elements of weathering crust ores]. Gornyy zhurnal Kazakhstana = Mining Journal of Kazakhstan 2013; 1-2:88-93. (in Russ.).
- [9] Semushkina LV, Narbekova SM. On the possibility of flotation processing of technogenic gold-containing waste from enrichment plants. Challenges of Science. 2021; IV:40-47. <https://doi.org/10.31643/2021.06>
- [10] Avdeyev AN, Sosnovskaya EL, Bolotnev AYU, Batzhargal D. Osobennosti izucheniya fiziko-mekhanicheskikh svoystv mnogoletnemerzlykh massivov gornyykh porod pri otsenke geomekhanicheskikh usloviy rudnykh mestorozhdeniy [Peculiarities of studying physical and mechanical properties of perennially frozen rock massifs at estimation of geomechanical conditions of ore deposits]. Nauki o Zemle i nedropolzovaniye = Earth Sciences and Subsoil Use. 2019; 42(2):240-253. (in Russ.). <https://doi.org/10.21285/2541-9455-2019-42-2-240-253>
- [11] Avdeyev AN, Sosonovskaya EL, Bolotnev AYU. Otsenka koeffitsiyenta kreposti gornyykh porod kosvennymi metodami [Estimation of rock strength coefficient by indirect methods]. Izvestiya vysshikh uchebnykh zavedeniy. Gornyy zhurnal = Proceedings of Higher Educational Institutions. Mining Journal. 2021; 3:28-35. (in Russ.). <https://doi.org/10.21440/0536-1028-2021-3-28-35>
- [12] Bond FC. The third theory of comminution. Transactions on AIME Mining Engineering. 1952; 193:484-494.
- [13] Taranov VA, Aleksandrova TN. Otsenka prochnostnykh svoystv rudy kak faktor povysheniya effektivnosti protsessa izmelcheniya [Estimation of ore strength properties as a factor of increasing the efficiency of the grinding process]. Gornyy informatsionno-analiticheskiy byulleten = Mining information-analytical bulletin. 2015; 4:119-123. (in Russ.).
- [14] Motovilov IYu, Telkov ShA, Barmenshinova MB, Nurmanova AN. Examination of the preliminary gravity dressing influence on the Shalkiya deposit complex ore. Non-ferrous metals. 2019; 2:3-8. <https://doi.org/10.17580/nfm.2019.02.01>
- [15] Lvov VV, Chitalov LS. Sovremennyye tendentsii podkhodov k raschetu rudopodgotovitelnykh protsessov apparatov dlya pererabotki rud tsvetnykh metallov [Modern tendencies of approaches to calculation of ore preparation processes of apparatuses for processing of non-ferrous metal ores]. Tsvetnyye metally = Non-ferrous metals. 2020; 10:20-26. (in Russ.). <https://doi.org/10.17580/tsm.2020.10.03>
- [16] Telkov ShA, Motovilov IYu, Barmenshinova MB. Issledovaniye vliyaniya predvaritelnoy kontsentratsii na izmelchayemost polimetallicheskikh rud [Investigation of influence of preliminary concentration on pulverisability of polymetallic ores]. Vestnik KazNITU = Bulletin of KazNRTU. 2020; 4:623-628. (in Russ.).
- [17] Telkov SA, Motovilov IY, Abisheva ZS, Barmenshinova MB. Study of the gravity enrichment of Shalkiya deposit lead-zinc ores. XXX International Mineral Processing Congress Proceedings IMPC 18-22 October 2020 Cape Town South Africa. 2020, 821-833.
- [18] Telkov ShA, Motovilov IYu, Barmenshinova MB, Abisheva ZS. Izucheniye gravitatsionno-flotatsionnogo obogashcheniya svintsovo-tsinkovoy rudy mestorozhdeniya Shalkiya [Gravity-flotation concentration of lead-zinc ore at the Shalkiya deposit]. Obogashcheniye rud = Ore dressing. 2021; 6:3-9. (in Russ.). <https://doi.org/10.17580/or.2021.06.02>
- [19] Chitalov LS, Lvov VV. Sravnitel'naya otsenka metodov opredeleniya rabocheho indeksa sharovogo izmelcheniya Bonda [Comparative evaluation of methods for determining the working index of Bond ball milling]. Gornyy informatsionno-analiticheskiy byulleten = Mining information-analytical bulletin. 2021; 1:130-145. (in Russ.). <https://doi.org/10.25018/0236-1493-2021-1-0-130-145>
- [20] Koyzhanova AK, Kenzhaliev BK, Magomedov DR, Abdyldaev NN. Development of a combined processing technology for low-sulfide gold-bearing ores. Obogashchenie Rud. 2021; 2:3-8. <https://doi.org/10.17580/or.2021.02.01>



DOI: 10.31643/2024/6445.35

Engineering and Technology

## Modified bitumen-polymer mastic to protect metal coatings from corrosion

<sup>1\*</sup> Sabergaliyev M.M., <sup>2</sup> Yeligbayeva G.Z., <sup>3</sup> Khassanov D.A., <sup>1</sup> Muradova S.R., <sup>2</sup> Orazalin Z.K.,  
<sup>1</sup> Ainakulova D.T., <sup>1</sup> Sharipov R.Kh., <sup>1,2</sup> Negim El-Sayed

<sup>1</sup> School of Materials Science and Green Technologies, Kazakh-British Technical University, Almaty, Kazakhstan

<sup>2</sup> School of Petroleum Engineering, Satbayev University, Almaty, Kazakhstan

<sup>3</sup> Faculty of Energy and Oil and Gas Industry, Kazakh-British Technical University, Almaty, Kazakhstan

\* Corresponding author email: m\_sabergaliyev@kbtu.kz

Received: November 28, 2023

Peer-reviewed: December 8, 2023

Accepted: December 14, 2023

### ABSTRACT

The protection of metallic structures against corrosion remains a pivotal challenge across numerous industries. In recent years, the amalgamation of modified bitumen with epoxy resin has emerged as a promising avenue in the pursuit of enhanced corrosion protection. This novel composite material showcases exceptional potential in thwarting the deleterious effects of corrosion, offering an innovative solution to safeguard vital infrastructure, industrial components, and diverse metallic substrates. The synergistic properties stemming from the combination of modified bitumen and epoxy resin present an intriguing prospect for superior durability, chemical resistance, and structural integrity, thereby fostering advancements in the realm of anti-corrosion coatings. This scientific article endeavours to explore the efficacy, mechanisms, and potential applications of this composite material as an effective barrier against corrosion, shedding light on its transformative impact within corrosion mitigation strategies. In this study, bitumen was modified using epoxy resin ELM-NG900Z and hardener in a ratio of 1.0: 5: 1.5 respectively. The modified bitumen was further tested by mechanical tests and solvent tests. The samples of modified bitumen successfully passed the tests and showed results better than the reference (epoxy resin without bitumen).

**Keywords:** Bitumen-epoxy resin, Bitumen, epoxy, corrosion.

**Sabergaliyev Murat Meirgalievich**

#### Information about authors:

2nd year master's student in the specialty "Materials Science and Technology of New Materials." Kazakh-British Technical University, School of Materials Science and Green Technologies, st. Tole bi, 59, 050000, Almaty, Kazakhstan. Email: m\_sabergaliyev@kbtu.kz

**Yeligbayeva Gulzhakhan Zhakparovna**

School of Petroleum Engineering, Satbayev University, 22 Satpayev Street, 050013, Almaty, Kazakhstan. Email: g.yeligbayeva@satbayev.university

**Khassanov Dauren Airatovich**

2nd year master's student, Faculty of Energy and Oil and Gas Industry, Kazakh-British Technical University, Almaty, Kazakhstan. Email: daurenkhassanoff@gmail.com

**Muradova Sabina Rustamkyzy**

Master's Degree in Materials Science and Technology of New Materials, School of Materials Science and Green Technologies, Kazakh-British Technical University, st. Tole bi 59, 050000, Almaty, Kazakhstan. Email: sab.muradova.01@mail.ru

**Orazalin Zhandos Kairatuly**

School of Petroleum Engineering, Satbayev University, 22 Satpayev Street, 050013, Almaty, Kazakhstan. Email: zhandos1403@bk.ru

**Ainakulova Dana Tulegenkyzy**

Ph.D. student at Materials Science and Technology of New Materials, School of Materials Science and Green Technologies, Kazakh-British Technical University, st. Tole bi 59, 050000, Almaty, Kazakhstan. Email: da\_ainakulova@kbtu.kz

**Sharipov Rustam Khasanovich**

Kazakh-British Technical University, School of Materials Science and Green Technologies, Kazakhstan. E-mail: r.sharipov@kbtu.kz

**Negim Attia El-Sayed**

Ph.D., Professor at School of Materials Science and Green Technologies, Kazakh-British Technical University, st. Tole bi 59, 050000, Almaty, Kazakhstan. Professor at Geology and Oil-gas Business Institute named after K. Turyssov, Department of Petroleum Engineering, Satbayev University, Almaty, Kazakhstan. Email: a.negim@kbtu.kz

### Introduction

Bitumen-epoxy resin refers to a composite material formed by combining bitumen, a viscous and hydrophobic organic substance derived from

petroleum, with epoxy resin, a thermosetting polymer created by the reaction between epoxide compounds and hardening agents [[1], [2], [3], [4], [5], [6]]. This amalgamation results in a hybrid material exhibiting enhanced properties, including



improved adhesion, corrosion resistance, durability, and flexibility, making it suitable for various applications in anti-corrosion coatings, construction, waterproofing, and infrastructure protection as shown in Table 1 [7].

There are several advantages associated with bitumen-epoxy resin combinations for anti-corrosion coatings:

**Enhanced Adhesion:** The combination of bitumen with epoxy resins creates coatings with excellent adhesion properties, ensuring strong bonding to various substrates, including metals and concrete surfaces.

**Superior Corrosion Resistance:** This composite material offers robust protection against corrosion caused by moisture, chemicals, salts, and environmental factors, extending the lifespan of coated surfaces [[8], [9], [10]].

**Improved Durability:** Bitumen-epoxy resin coatings exhibit enhanced durability, resisting abrasion, impact, and wear, which is particularly beneficial in high-traffic or harsh industrial environments.

**Chemical and Weather Resistance:** The coatings show remarkable resistance to a wide range of chemicals, acids, solvents, and extreme weather conditions, maintaining their protective qualities in diverse settings [11].

**Flexibility and Toughness:** The combination provides flexibility and toughness to the coatings, allowing them to withstand substrate movement and deformation without cracking or compromising the protective layer.

**Excellent Waterproofing Properties:** Bitumen-epoxy resin coatings create an impermeable barrier, effectively preventing water ingress and protecting against moisture-related corrosion [12].

**Enhanced Structural Integrity:** Coated surfaces benefit from improved structural integrity, as these coatings provide a strong barrier against corrosion-induced deterioration, maintaining the integrity of underlying structures.

**Versatility in Applications:** These coatings can be applied to various substrates, making them suitable for different industries, including roofing, pavement, waterproofing, marine, and industrial flooring.

**Cost-Effectiveness:** The long-lasting protection offered by bitumen-epoxy resin coatings can reduce maintenance costs and extend the service life of structures and components, resulting in cost savings over time.

**Environmental Benefits:** Certain formulations can be tailored to be low in volatile organic compounds (VOCs), reducing environmental impact during application while providing effective corrosion protection [[13], [14], [15], [16]].

The combination of bitumen with epoxy resins in anti-corrosion coatings presents a robust solution that combines multiple advantageous properties, making it a valuable choice for protecting a wide array of surfaces prone to corrosion [[17], [18], [19]].

This paper aims to modify bitumen using epoxy resin and hardener in a ratio of 3.5: 1.0. the mechanical and chemical properties were investigated.

**Table 1** - Possible applications of bitumen-epoxy resin

Nature of hydrocarbon binder	Additives	Utilization	Ref.
Bituminous emulsion		Anticorrosion paint binders for gravel	6
Bitumen		Waterproof paints; sprayed paints	7.8
Bitumen, tar	(CH <sub>3</sub> ) <sub>2</sub> SO <sub>4</sub> (30-60%)	Reinforced anticorrosion paints	9
Bitumen	Liquid polybutadiene	Anticorrosion paint	10
Bitumen	Styrene/butadiene/ styrene copolymer	Pavement coating	11
Bitumen- asphalt		Moisture-proof coatings	12-15

## Main provisions

Bitumens are natural or synthetic, there are various applications in industry. It is a little bit cheap product, that the physicochemical properties can be modified. Among applications of bitumens are road and building materials, pavements, roofs, and coatings.

The interesting results were obtained by authors [[20], [21]] who investigated the parameters of the compatibility or incompatibility of epoxy resins with a given bitumen. Thus, they modified epoxy resins by using new aliphatic and cycloaliphatic epoxy resins mixed with bitumen and compared their performance when admixed with a hardening agent. The results showed that the aromaticity and aliphaticity of the epoxy resins were not the only determined the homogeneity of the resulting mixtures.

The authors [13] found that the compatibility of a resin with a bitumen arose from the flexibility of epoxy resins. The technique that provides the polarity of molecules in terms of hydrophilic/lipophilic balance. This provides a compatible model molecule that has been synthesized on a large scale and has the following structure of epoxy resins (Figure 1):

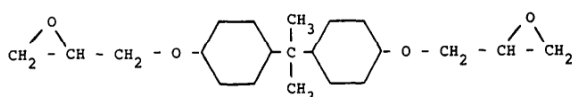


**Figure 1** – Structure of epoxy resin

Other authors [14, 15] investigated the mixing ratios of epoxy with bitumen to find compatible ratios. They demonstrated that epoxy resins with 50% in the mixture increase the mechanical characteristics of the same mixtures without epoxy resins and are considerable for highway applications.

However, such applications developed for various commercial activities as given in Table 1. Table 1 lists a wide range of applications of bitumen-epoxy resin blends. The improvement in the physical and mechanical properties of resin and bitumen using substituted phenols, such as t-butyl and nonyl phenols, to the mixtures [[16], [17], [18], [19], [20], [21], [22]].

## Material and methods

To create a modified bitumen-epoxy coating, waterproofing bitumen No. 24 from Technicol, Almaty, Kazakhstan. Epoxy resin ELM-NG900Z and Hardener 1816: ELM-NG 34H from Elcos Marketing LLP, Almaty, Kazakhstan.

The processes of coating are given in Figure 2. Firstly, Metal plates were cleaned pre-washed using water, and dried before coating. The preparation of samples is an important factor to avoid any problem during coating such as dirt or dust on the plates.

Secondly, the preparation mixture of bitumen and epoxy resin in the presence of hardener. Epoxy resin is a two-component substance. It necessarily includes a hardener, which starts the process of polymerization (hardening) of the composition.

6.5 grams of bitumen, 50 grams of epoxy resin, and 15 grams of hardener were mixed very well at room temperature.

Further, because of mixing the above materials, a modified bitumen-epoxy coating was obtained and applied to metal samples.

The bitumen-epoxy content was poured onto the plate itself and evenly applied. The application was carried out using a stainless-steel applicator to obtain a more uniform coating Figure 3.

The mechanical properties of the coating films including impact resistance, bending strength, adhesion, and scratch resistance were investigated. The names of tests Figure 4 shows the types of equipment for tests mechanical properties.

Impact resistance test (Figure 4-a) – A coated metal sample was placed between the upper part of the die and a graduated vertical tube. The load was lifted to a maximum height of 100 cm and dropped. Next, the sample was extracted from the tester and evaluated for damage to the coating and substrate.

The bending strength test (Figure 4-b) - was carried out by bending the test sample at an angle of 180° around cylindrical or conical rods. There is a bending lever with rollers on the frame, which is adjustable in height, and a sliding vice for clamping samples, which ensures perfect and uniform bending of the test samples. The presence of damage to the test sample (cracks, delamination) was determined visually.

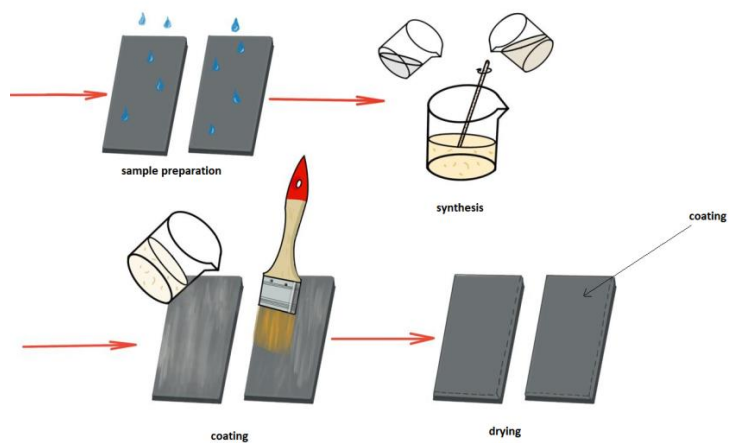


Figure 2 - the process of coating samples

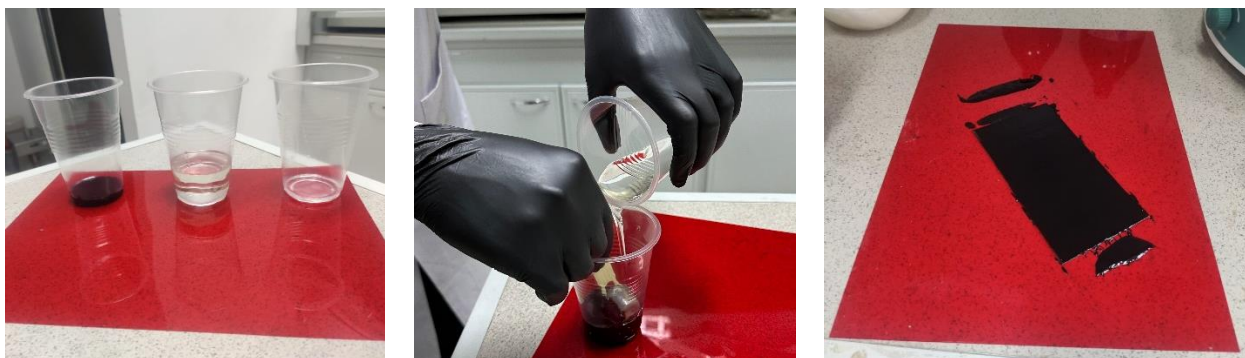


Figure 3 – The coating process

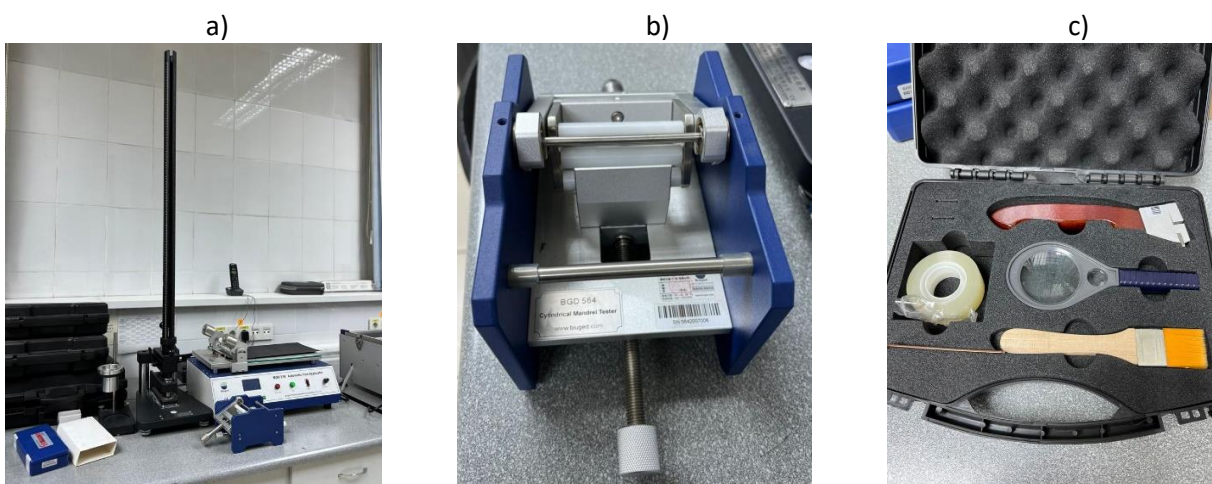


Figure 4 – a) BGD 305 Tubular Impact Tester, b) BGD 564 Cylindrical Mandrel Tester, c) BGD 504/6 Economic Cross Hatch Tester

The resistance of the coating to scratches on the surface (Figure 4-c) was determined by carrying out two transverse notches on the coating with a multi-blade cutting tool, after which the adhesive resistance of the tape coating to separation from the substrates was evaluated. The adhesive strength of the adhesive tape is equal to 9.5 N for a width of 25 mm and is transparent, which ensures proper adhesion to the coating.

Also, anticorrosive properties in solutions of 10, 20, and 30% NaCl, NaOH, and H<sub>2</sub>SO<sub>4</sub> were studied on the obtained samples with bitumen-epoxy coating.

As a comparison, uncoated metal plates were also immersed in the solutions. The samples were kept in each of the solutions for 7 days (Figure 5). After 7 days, the coatings were examined for corrosion

### Results and discussion

From the data given in Figure 6, the coating based on bitumen-epoxy resin has passed all the tests for the mechanical properties of the coating.

The results of the mechanical properties are presented in Table 2.

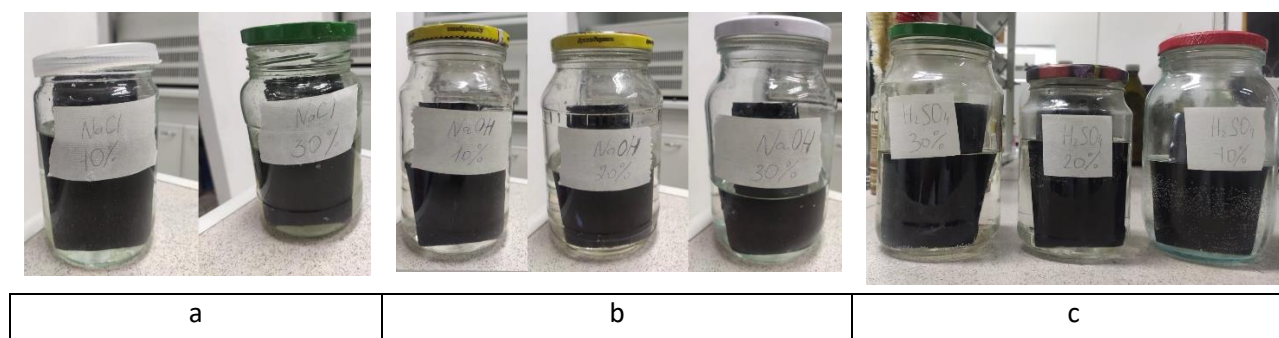


Figure 5 – a) NaCl solution, b) NaOH solution, c) H<sub>2</sub>SO<sub>4</sub> solution

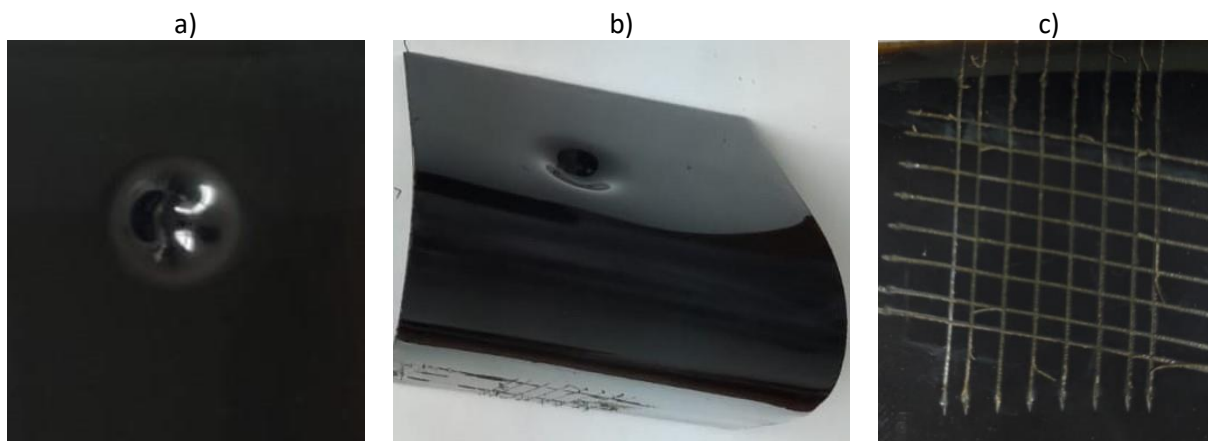


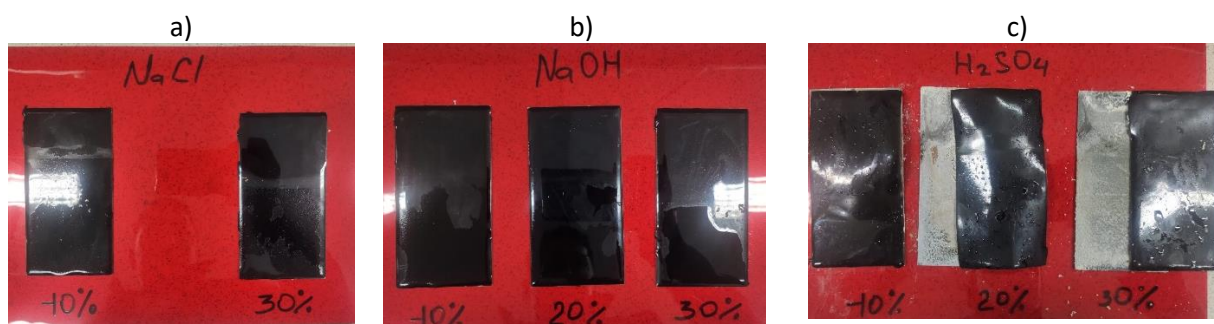
Figure 6 – a) impact resistance test results, b) bending strength test results, c) results of the coating's scratch resistance on the surface

Table 2 - The results of the mechanical properties

Sample	Polymer	Research	Results
Metal plate	Bitumen-epoxy resin	Impact resistance test	Passed
Metal plate	Bitumen-epoxy resin	Bending strength test	Passed
Metal plate	Bitumen-epoxy resin	The resistance of the coating to scratches on the surface	Passed

passed = excellent, failed = bad





**Figure 7** – Metal plates with bitumen-epoxy coating, after 7 days in solutions with a concentration of 10%, 20%, 30%, at room temperature a) NaCl, b) NaOH, c) H<sub>2</sub>SO<sub>4</sub>,

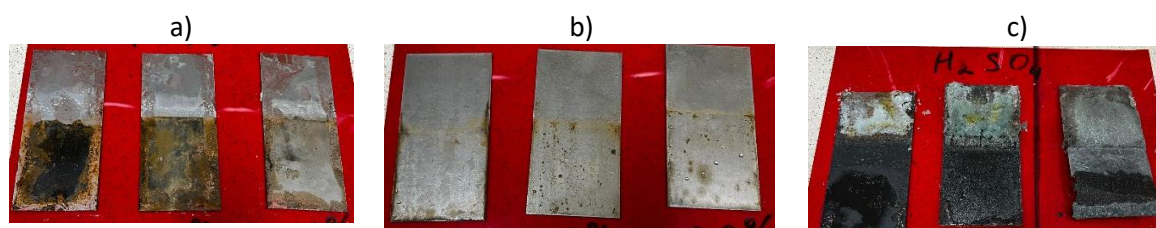


**Figure 8** – Metal plates without coating, after 7 days in solutions with a concentration of 10%, 20%, and 30%, at room temperature a) NaCl, b) NaOH, c) H<sub>2</sub>SO<sub>4</sub>

**Table 3** - The results of the anticorrosive properties

Sample	Polymer	Solution	with coating			without coating		
			10%	20%	30%	10%	20%	30%
Metal plate	Bitumen-epoxy resin	NaCl	E	E	E	P	P	P
Metal plate	Bitumen-epoxy resin	NaOH	E	E	E	P	G	G
Metal plate	Bitumen-epoxy resin	H <sub>2</sub> SO <sub>4</sub>	E	G	G	P	P	P

When submerged for 7 days, E = excellent, G = good, and P = bad.

As can be seen from Figure 7, metal plates with bitumen-epoxy coating withstood all concentrations of solutions of NaCl, NaOH, H<sub>2</sub>SO<sub>4</sub>. However, in the H<sub>2</sub>SO<sub>4</sub> solution, the coating itself peeled off in solutions with 20% and 30% concentration. Whereas all metal plates without coating are completely corroded Figure 8.

The results of the study of bitumen-epoxy coatings for anticorrosive properties in solutions of 10, 20, 30% NaCl, NaOH, H<sub>2</sub>SO<sub>4</sub> are presented in Table 3.

### Conclusion

The combination of modified bitumen with epoxy resins offers a universal solution that improves the properties of both materials. It provides increased durability, flexibility, adhesion and resistance to various environmental influences

and structural loads, which makes it a valuable choice for various applications in construction and infrastructure. Based on the results obtained and the properties of coatings based on bitumen-epoxy resins, it can be concluded that the coating based on bitumen-epoxy resin has a wide range of applications. The best ratio of epoxy resin to hardener was 3.5% to 1.0% to enhance the mechanical and chemical properties of bitumen.

**Acknowledgements.** This work was supported by the Ministry of Science and Education of the Republic of Kazakhstan, a competition for grant funding for scientific and technical projects 2023–2025. Project No. AP19676595 “Development of high electrically conductive paint for corrosion prevention in concrete structures”.

**Conflicts of interest.** The authors declare no conflicts of interest, financial or otherwise.

**Cite this article as:** Sabergaliyev MM, Yeligbayeva GZ, Khassanov DA, Muradova SR, Orazalin ZK, Ainakulova DT, Sharipov RK, Negim El-Sayed. Modified bitumen-polymer mastic to protect metal coatings from corrosion. Kompleksnoe Ispolzovanie Mineralnogo Syra = Complex Use of Mineral Resources. 2024; 331(4):12-20. <https://doi.org/10.31643/2024/6445.35>

## Металл жабындарды коррозиядан қорғауға арналған модификацияланған битум-полимерлі мастика

<sup>1\*</sup>Саберғалиев М.М., <sup>2</sup>Елигбаева Г.Ж., <sup>3</sup>Хасанов Д.А., <sup>1</sup>Мурадова С.Р., <sup>2</sup>Оразалин Ж.К.,  
<sup>1</sup>Айнакулова Д.Т., <sup>1</sup>Шарипов Р.Х., <sup>1,2</sup>Негим Эльсайд

<sup>1</sup> Материалтану және жасыл технологиялар мектебі, Қазақ-Британ техникалық университеті, Алматы, Қазақстан

<sup>2</sup> Мұнай өнеркәсіп мектебі, Сәтбаев университеті, Алматы, Қазақстан

<sup>3</sup> Энергетика және мұнай-газ индустриясы мектебі, Қазақ-Британ техникалық университеті, Алматы, Қазақстан

ТҮЙІНДЕМЕ	
Мақала келді: 28 қараша 2023 Сараптамадан өтті: 8 желтоқсан 2023 Қабылданды: 14 желтоқсан 2023	Металл конструкцияларын коррозиядан қорғау көптеген салаларда маңызды міндеттердің бірі болып қала береді. Соңғы жылдары модификацияланған битумды эпоксидті шайырмен біріктіру коррозиядан қорғауды арттырудың перспективалы бағыты болды. Бұл жаңа композициялық материал маңызды инфрақұрылымды, өнеркәсіптік құрамдас бөліктерді және әртүрлі металл субстраттарды қорғау үшін инновациялық шешім ұсына отырып, коррозияның зиянды әсерлерімен күресудің ерекше әлеуетін көрсетеді. Модификацияланған битум мен эпоксидті шайырды қосу арқылы пайда болған синергиялық: ұзаққа жарамдылық, химиялық төзімділік және құрылымдық тұтастық сияқты қасиеттер жақсарады, осылайша коррозияға қарсы жабындар саласында жетістіктерге қол жеткізіледі. Бұл зерттеу жұмысында осы композициялық материалдың коррозияға қарсы тосқауыл ретінде тиімділігі, механизмдері мен әлеуетті қолданылуы қарастырылып, оның коррозияға қарсы стратегиялардағы трансформациялық әсерлеріне жол ашады. Бұл зерттеуде битум эпоксидті шайыр ELM-NG900Z және 1,0: 5: 1,5 қатынасында қатайтқышты қолдану арқылы өзгертілді. Механикалық сынақтар мен еріткіштерді пайдалану арқылы модификацияланған битумға қосымша сынақтар жүргізілді. Модификацияланған битум үлгілері сынақтардан сәтті өтті және эталонға (битумсыз эпоксидті шайыр) қарағанда жақсы нәтиже көрсетті. <b>Түйін сөздер:</b> Битумды эпоксидті шайыр, битум, эпоксидті шайыр, коррозия.
<b>Саберғалиев Мурат Меурғалиевич</b>	<b>Авторлар туралы ақпарат:</b> «Материалтану және жаңа материалдар технологиясы» мамандығының 2 курс магистранты. Қазақ-Британ техникалық университеті, Материалтану және жасыл технологиялар мектебі, көш. Төле би, 59, 050000, Алматы, Қазақстан. Email: <a href="mailto:m_sabergaliyev@kbtu.kz">m_sabergaliyev@kbtu.kz</a>
<b>Елигбаева Гүлжахан Жақпаровна</b>	Мұнай инженериясы кафедрасы, Сәтбаев университеті, Сәтбаев көшесі, 22, Алматы 050013, Қазақстан. Email <a href="mailto:g.yeligbayeva@satbayev.university">g.yeligbayeva@satbayev.university</a>
<b>Хасанов Даурен Айратович</b>	Энергетика және мұнай-газ индустриясы мектебі, Қазақ-Британ техникалық университеті, Алматы, Қазақстан. Email: <a href="mailto:daurenkhassanoff@gmail.com">daurenkhassanoff@gmail.com</a>
<b>Мурадова Сабина Рустамқызы</b>	Магистр, Материалтану және жаңа материалдар технологиясы, Материалтану және жасыл технологиялар мектебі, Қазақ-Британ Техникалық Университеті, Төле би көш., 59, 050000, Алматы, Қазақстан. Email: <a href="mailto:sab.muradova.01@mail.ru">sab.muradova.01@mail.ru</a>
<b>Оразалин Жандос Қайратұлы</b>	Мұнай инженериясы кафедрасы, Сәтбаев университеті, Сәтбаев көшесі, 22, Алматы 050013, Қазақстан. Email: <a href="mailto:zhandos1403@bk.ru">zhandos1403@bk.ru</a>
<b>Айнакулова Дана Тулегенқызы</b>	Ph.D. докторант Материалтану және жаңа материалдар технологиясы, Материалтану және жасыл технологиялар мектебі, Қазақ-Британ Техникалық Университеті, Төле би көш., 59, 050000, Алматы, Қазақстан. Email: <a href="mailto:da_ainakulova@kbtu.kz">da_ainakulova@kbtu.kz</a>
<b>Шарипов Рустам Хасанович</b>	Қазақ-Британ техникалық университеті, Материалтану және жасыл технологиялар мектебі, Қазақстан. E-mail: <a href="mailto:r.sharipov@kbtu.kz">r.sharipov@kbtu.kz</a>
<b>Негим Аттиа Эльсайд</b>	Ph.D., Материалтану және жасыл технологиялар мектебінің профессоры, Қазақ-Британ Техникалық Университеті, Төле би көш., 59, 050000, Алматы, Қазақстан. Профессор Қ. Тұрысов атындағы Геология және мұнай-газ ісі институты, Мұнай Инженериясы Кафедрасы, Сәтбаев Университеті, Сәтбаев көш. 22а, 050013, Алматы, Қазақстан. Email: <a href="mailto:a.negim@kbtu.kz">a.negim@kbtu.kz</a>

## Модифицированная битумно-полимерная мастика для защиты металлических покрытий от коррозии

<sup>1\*</sup>Саберғалиев М.М., <sup>2</sup>Елигбаева Г.Ж., <sup>3</sup>Хасанов Д.А., <sup>1</sup>Мурадова С.Р., <sup>2</sup>Оразалин Ж.К.,  
<sup>1</sup>Айнакулова Д.Т., <sup>1</sup>Шарипов Р.Х., <sup>1,2</sup>Негим Эльсайд

<sup>1</sup> Школа материаловедения и зеленых технологий, Казахстанско-Британский Технический Университет, г. Алматы, Казахстан

<sup>2</sup> Кафедра Нефтяной Инженерии, Сатбаев Университет, ул. Сатбаева 22а, 050013, г. Алматы, Казахстан

<sup>3</sup> Факультет Энергии и Нефтегазовой Индустрии, Казахстанско-Британский Технический Университет, г. Алматы, Казахстан

Поступила: 28 ноября 2023 Рецензирование: 8 декабря 2023 Принята в печать: 14 декабря 2023	<p><b>Аннотация</b>          Защита металлических конструкций от коррозии остается одной из важнейших задач во многих отраслях промышленности. В последние годы соединение модифицированного битума с эпоксидной смолой стало перспективным направлением в деле усиления защиты от коррозии. Этот новый композиционный материал демонстрирует исключительный потенциал в борьбе с пагубным воздействием коррозии, предлагая инновационное решение для защиты жизненно важных объектов инфраструктуры, промышленных компонентов и различных металлических подложек. Синергетические свойства, обусловленные сочетанием модифицированного битума и эпоксидной смолы, открывают захватывающие перспективы для повышения долговечности, химической стойкости и структурной целостности, способствуя тем самым прогрессу в области антикоррозионных покрытий. Данная научная статья посвящена изучению эффективности, механизмов и потенциальных возможностей применения этого композитного материала в качестве эффективного барьера против коррозии, проливая свет на его преобразующее воздействие в рамках стратегий борьбы с коррозией. В данном исследовании битум был модифицирован с использованием эпоксидной смолы ELM-NG900Z и отвердителя в соотношении 1,0:5:1,5 соответственно. Модифицированный битум был подвергнут дальнейшим испытаниям с помощью механических испытаний и испытаний с растворителем. Образцы модифицированного битума успешно прошли испытания и показали результаты лучше эталона (эпоксидная смола без битума).</p> <p><b>Ключевые слова:</b> Битумно-эпоксидная смола, битум, эпоксидная смола, коррозия.</p>
<b>Сабергалиев Мурат Меургалиевич</b>	<p><b>Информация об авторах:</b>          Магистрант 2-го курса по специальности "Материаловедение и технология новых материалов". Казахско-Британский технический университет, Школа материаловедения и зеленых технологий, ул. Толе би, 59, 050000, Алматы, Казахстан. Email: m_sabergaliyev@kbtu.kz</p>
<b>Елигбаева Гульжахан Жақпаровна</b>	<p>Кафедра Нефтяной Инженерии, Самбаев Университет, ул. Самбаева 22а, 050013, г. Алматы, Казахстан. Email g.yeligbayeva@satbayev.university</p>
<b>Хасанов Даурен Айратович</b>	<p>Факультет Энергии и Нефтегазовой Индустрии, Казахстанско-Британский Технический Университет, г. Алматы, Казахстан. Email: daurenkhasanoff@gmail.com</p>
<b>Муратова Сабина Рустамқызы</b>	<p>Магистр по специальности Материаловедения и Технологии Новых Материалов, Школа материаловедения и зеленых технологий, Казахстанско-Британский технический университет, ул. Толе би, 59, 050000, Алматы, Казахстан. Email: sab.muratova.01@mail.ru</p>
<b>Оразалин Жандос Кайратулы</b>	<p>Кафедра Нефтяной Инженерии, Самбаев Университет, ул. Самбаева 22а, 050013, г. Алматы, Казахстан. Email: zhandos1403@bk.ru</p>
<b>Айнакулова Дана Тулегенқызы</b>	<p>Ph.D. докторант Материаловедения и Технологии Новых Материалов, Школы материаловедения и зеленых технологий, Казахстанско-Британский технический университет, ул. Толе би, 59, 050000, Алматы, Казахстан. Email: da_ainakulova@kbtu.kz</p>
<b>Шарипов Рустам Хасанович</b>	<p>Казахско-Британский технический университет, Школа материаловедения и зеленых технологий, Казахстан. E-mail: r.sharipov@kbtu.kz</p>
<b>Негим Аттиа Эльсайд</b>	<p>Ph.D., Профессор Школы материаловедения и зеленых технологий, Казахстанско-Британский технический университет, ул. Толе би, 59, 050000, Алматы, Казахстан. Профессор Института геологии и нефтегазового дела им. К. Турысова, Кафедра Нефтяной Инженерии, Самбаев Университет, ул. Самбаева 22а, 050013, г. Алматы, Казахстан. Email: a.negim@kbtu.kz</p>

## References

- [1] Syrmanova K, Negim E, Kaldybekova J, Tuleuov A. M. Epoxylitane compositions modification with using thermoplastic polyurethane. Orient J Chem. 2016; 32(1):1-7.
- [2] Apostolidis P, Liu X, Erkens SMJG, & Scarpas A. Evaluation of epoxy modification in bitumen. Construction and Building Materials. 2019; 208:361-368.
- [3] Apostolidis P, Liu X, Kasbergen C, van de Ven MFC, Pipintakos G, & Scarpas A. Chemo-rheological study of hardening of epoxy modified bituminous binders with the finite element method. Transportation Research Record. 2018; 2672(28):190-199.
- [4] Cong P, Tian Y, Liu N, & Xu P. Investigation of epoxy-resin-modified asphalt binder. Journal of Applied Polymer Science. 2016; 133(21).
- [5] Zhou W, Xia Y, Tsai FC, Jiang T, Zhao H, & Wen J. Effects of compound curing agent on the thermo-mechanical properties and structure of epoxy asphalt. International Journal of Pavement Engineering. 2017; 18(10):928-936.
- [6] Lu Q, & Bors J. Alternate uses of epoxy asphalt on bridge decks and roadways. Construction and Building Materials. 2015; 78:18-25.
- [7] Sun Y, Zhang Y, Xu K, Xu W, Yu D, Zhu L, ... & Cheng R. Thermal, mechanical properties, and low-temperature performance of fibrous nanoclay-reinforced epoxy asphalt composites and their concretes. Journal of Applied Polymer Science. 2015; 132(12).
- [8] Yin H, Jin H, Wang C, Sun Y, Yuan Z, Xie H, ... & Cheng R. Thermal, damping, and mechanical properties of thermosetting epoxy-modified asphalts. Journal of Thermal Analysis and Calorimetry. 2014; 115:1073-1080.
- [9] Xiao Y, Van De Ven MFC, Molenaar AAA, Su Z, & Zandvoort F. Characteristics of two-component epoxy modified bitumen. Materials and structures. 2011; 44:611-622.
- [10] Dauletov Y, Abdiyev K, Toktarbay Z, et al. Radical Polymerization and Kinetics of N, N-diallyl-N, N-dimethylammonium Chloride and Vinyl Ether of Monoethanolamine. Fibers Polym. 2018; 19:2023-2029. <https://doi.org/10.1007/s12221-018-6947-3>

- [11] Fischer HR, & Cernescu A. Relation of chemical composition to asphalt microstructure—Details and properties of microstructures in bitumen as seen by thermal and friction force microscopy and by scanning near-field optical microscopy. *Fuel*. 2015; 153:628-633.
- [12] Li H, & Li SQ. Research on asphalt oil corrosion mechanism. *Highw. Eng*. 2016; 41:229-231.
- [13] Makhmetova A, Negim E-S, Ainakulova D, Yeligbayeva G, & Khatib J. An Overview of Epoxy Resins as coating to protect metals from corrosion. *Kompleksnoe Ispolzovanie Mineralnogo Syra = Complex Use of Mineral Resources*. 2023; 328(1):20-32.
- [14] Li Q, Li K, Zhao K, Sun G, & Luo S. Fuel oil corrosion resistance of asphalt mixtures. *Construction and Building Materials*. 2019; 220:10-20.
- [15] Gao X, Pang L, Xu S, Lv Y, & Zou Y. The Effect of Silicone Resin on the Fuel Oil Corrosion Resistance of Asphalt Mixture. *Sustainability*. 2022; 14(21):14053.
- [16] Jin FL, Li X, & Park SJ. Synthesis and application of epoxy resins: A review. *Journal of industrial and engineering chemistry*. 2015; 29:1-11.
- [17] Xiang Q, & Xiao F. Applications of epoxy materials in pavement engineering. *Construction and Building Materials*. 2020; 235:117529.
- [18] Cong P, Luo W, Xu P, & Zhang Y. Chemical, and physical properties of hot mixing epoxy asphalt binders. *Construction and Building Materials*. 2019; 198:1-9.
- [19] Ainakulova D, Muradova S, Khaldun MAA, Bekbayeva L, Megat-Yusoff P, Mukatayeva Z, Ganjian E, & Negim E-S. Analytical Review of Conductive Coatings, Cathodic Protection, and Concrete. *Kompleksnoe Ispolzovanie Mineralnogo Syra = Complex Use of Mineral Resources*. 2023; 329(2):92-102.
- [20] Ignatenko VY, Kostyuk AV, Kostina JV, Bakhtin DS, Makarova VV, Antonov SV, & Ilyin SO. Heavy crude oil asphaltenes as a nanofiller for epoxy resin. *Polymer Engineering & Science*. 2020; 60(7):1530-1545.
- [21] Syrmanova K, Negim E, Kaldybekova J, Suleimenova M, Baizhanova S. Study of modification process of the epoxy/itane composites. *Industrial Technology and Engineering*. 2015; 3:75-83.
- [22] Muradova S, Negim E-S, Makhmetova A, Ainakulova D, & Mohamad N. An Overview of the Current State and the Advantages of using acrylic resins as anticorrosive coatings. *Kompleksnoe Ispolzovanie Mineralnogo Syra = Complex Use of Mineral Resources*. 2023; 327(4):90-98.





DOI: 10.31643/2024/6445.36

Engineering and Technology



## Polyurethane as a versatile polymer for coating and anti-corrosion applications: A review

<sup>1\*</sup>Yeligbayeva G., <sup>2</sup>Khaldun M. A., <sup>3</sup>Abdassalam A. Alfergani, <sup>4</sup>Tleugaliyeva Zh., <sup>4</sup>Karabayeva A.,  
<sup>1,5</sup>Bekbayeva L., <sup>6</sup>Zhetpisbay D.S., <sup>7</sup>Shadin N.A., <sup>1</sup>Atabekova Z.

<sup>1</sup>School of Petroleum Engineering, Satbayev University, Almaty, Kazakhstan

<sup>2</sup>Department of Chemistry, School of Science, The University of Jordan, 11942, Amman, Jordan

<sup>3</sup>Chemistry Department, Faculty of Education, Sirte University, Sirte, Libya

<sup>4</sup>School of Materials Science and Green Technologies, Kazakh-British Technical University, Almaty, Kazakhstan.

<sup>5</sup>National Nanotechnology Open Laboratory, Al-Faraby Kazakh National University, Almaty, Republic of Kazakhstan

<sup>6</sup>Department of Biochemistry, School of General Medicine-1, S.D. Asfendiyarov KazNMU, Almaty, Kazakhstan

<sup>7</sup>Department of Chemistry, Institute of Natural Sciences and Geography, Abai Kazakh National Pedagogical University, Almaty, Kazakhstan

\*Corresponding author e-mail: g.yeligbayeva@satbayev.university

Received: November 23, 2023

Peer-reviewed: December 8, 2023

Accepted: December 15, 2023

### ABSTRACT

The development of polyurethane materials and process optimization are currently the subjects of extensive study. Polyurethane is characterized by high physicochemical and operational properties. Polyurethanes have high wear resistance, and oil and gasoline resistance. They have excellent thermophysical and elastic properties. This allows the use of polyurethanes in many industries where materials with high-performance properties are required. Polyurethanes are widely used in many industrial applications, protective coating manufacturing, and anti-corrosion agent applications. A significant number of studies have been conducted to improve the physical, mechanical, and operational properties of polyurethane polymers, in particular the anti-corrosion properties of modified polyurethane coatings. The properties of polyurethane polymers for various applications can be improved by changing monomers and their ratios and the process of preparations. Preparation of polyurethane polymers based on polyols and isocyanate monomers using a polyaddition process in the presence of a catalyst as well as solvents including toluene, xylene, and acetone. There are different factors affecting the physical and mechanical properties of polyurethane polymers were investigated by different techniques. The factors were types of isocyanates, polyols, OCN/OH ratios, solvents, catalysts, and temperatures. Generally, the polyols are responsible for the flexibility of the polyurethane polymers and isocyanates are responsible for the rigidity of the polyurethane polymer and crosslinking between the backbone of the polymer. Because of the flexibility of its chemistry, they may modify the coating's characteristics based on the intended use. The effects of different polyols and polyisocyanates' chemistry are assessed. The hydrophobicity, thermal stability, and mechanical and anti-corrosion properties of polyurethane polymers were investigated. As a result, the properties of polyurethane polymers such as hydrophobicity, thermal stability, and mechanical and anti-corrosion properties were all enhanced when all the above factors. An outline of the most modern, financially successful methods for creating protective polyurethane coatings and using them as anti-corrosion agents is given in this review article.

**Keywords:** Polyurethane, coating, anti-corrosion, polyols, polyisocyanates.

<b>Yeligbayeva Gulzhakhan Zhakparovna</b>	School of Petroleum Engineering, Satbayev University, 22 Satpayev Street, 050013, Almaty, Kazakhstan. Email: g.yeligbayeva@satbayev.university
<b>Khaldun M. Al Azzam</b>	Department of Chemistry, School of Science, The University of Jordan, 11942, Amman, Jordan. Email: azzamkha@yahoo.com
<b>Abdassalam A. Alfergani</b>	Chemistry Department, Faculty of Education, Sirte University, Sirte, Libya. Email: abdassalamtameem@yahoo.com
<b>Tleugaliyeva Zhanetta Ashatovna</b>	School of Materials Science and Green Technologies, Kazakh-British Technical University, 59 Tole bi Street, 050000, Almaty, Kazakhstan. Email: z_tleugaliyeva@kbtu.kz
<b>Karabayeva Aykumis Yermekkyzy</b>	School of Materials Science and Green Technologies, Kazakh-British Technical University, 59 Tole bi Street, 050000, Almaty, Kazakhstan. Email: a_karabayeva@kbtu.kz
<b>Lyazzat Bekbayeva</b>	National Nanotechnology Open Laboratory, Al-Faraby Kazakh National University, al-Farabi av., 050040, Almaty, Republic of Kazakhstan. Email: lyazzat_bk2019@mail.ru
<b>Zhetpisbay D.S.</b>	Department of Biochemistry, School of General Medicine-1, S.D. Asfendiyarov KazNMU, 480012, Tole bi, 88, Almaty, Kazakhstan. Email: zhetpisbay.d@kaznmu.kz
<b>Shadin N.A.</b>	Department of Chemistry, Institute of Natural Sciences and Geography, Abai Kazakh National Pedagogical University, 30 Kazybek Bi str., Almaty, Kazakhstan. Email: nugen_87@mail.ru
<b>Z.B. Atabekova</b>	School of Petroleum Engineering, Satbayev University. Engineer. Email: zau888@mail.ru

## Introduction

Several years ago, the coating industry used various polymers to manufacture a wide range of coating goods such as acrylic, epoxy, alkyds, polyurea, and polyurethane. Polyurethane was created via polyaddition polymerization of several formulations containing isocyanates and polyols [[1], [2], [3]]. Additives were also applied by the method and product type. They were made without solvent using different isocyanate monomers such as aliphatic and aromatic, and different polyols such as polycarbonate, polyester, and polyether since their toxicity polluted the atmosphere and harmed the ozone layer.

The primary purpose of this review is to screen and adapt prepolymers based on aliphatic and aromatic polyurethane polymers for industrial coatings, particularly anti-corrosion coating. These prepolymers will be environmentally sustainable and have the greatest physical properties. The project will focus on the development of anti-corrosion coatings based on polyurethane prepolymers, both aliphatic and aromatic. An

alternate isocyanate and hydroxyl ratio should be studied to produce the desired product. When combined with additives such as fillers, thickeners, plasticizers, and crosslinking agents, the product produces the appropriate anti-corrosion coatings for pipeline applications. The current study aimed to develop the technology and find the materials and polymers that play important roles to reduce or prevent the corrosion rate of metals.

## Polyurethane

Polyurethanes (Pus) are one-of-a-kind polymeric materials with a wide range of physical and chemical characteristics that have been employed in a variety of applications, including foams, coatings, adhesives, and thermoplastic elastomers [[3], [4], [5], [6], [7], [8]]. Material selection, polymer design, production conditions, and application procedures can all be used to create PUs. Polyurethane chemistry is based on isocyanate reactivity toward hydroxyl and amine groups. The isocyanate group's reactivity is

attributed to the positive charge of the carbon atom in the N=C=O group's cumulated double-bond system, as seen in Figure 1.

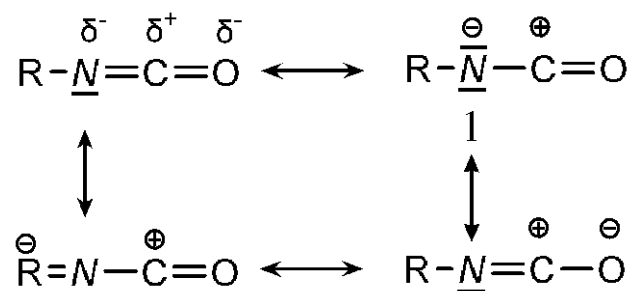
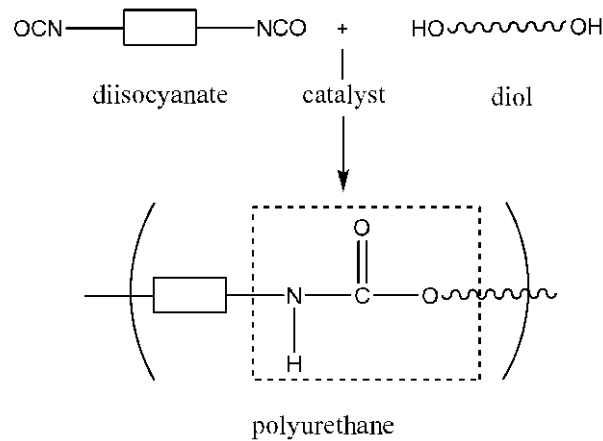


Figure 1 - Resonance structure of the isocyanate group

Isocyanates react with all molecules containing "active" hydrogen atoms, including water, hydroxyl, and amine groups, at temperatures ranging from 60 to 90 °C depending on catalyst type and concentration [9]. The exothermic, reversible process produces urethane. Polyurethane polymers or polyurethane-polyurea polymers containing both urethane and urea groups are used to make PUs, which are created by polyaddition reactions of polyols, polyisocyanates, and polyamines, as illustrated in Figure 2. Polyisocyanate is a molecule that has two or more isocyanate functional groups, while polyol contains two or more hydroxyl groups [10]. Because urea groups are known to interact via bifurcated hydrogen bonds, they are good functionality for usage in hard segments of thermoplastic elastomers. Compared to urethanes and amides, they have a stronger hydrogen bond. Poor melt processibility and insufficient solubility in organic solvents are two disadvantages of these elastomers, though. The temperatures at which urea segments melt or soften are significantly greater than their thermal breakdown temperatures due to the extremely strong bifurcate hydrogen bonding between urea groups.

As illustrated in Figure 3, more "active" hydrogen atoms are present in the urethane and urea groups that are produced, and these groups can react with isocyanate to produce allophanates and biurets.



**Figure 2** - Polyaddition reaction between diisocyanate and diol

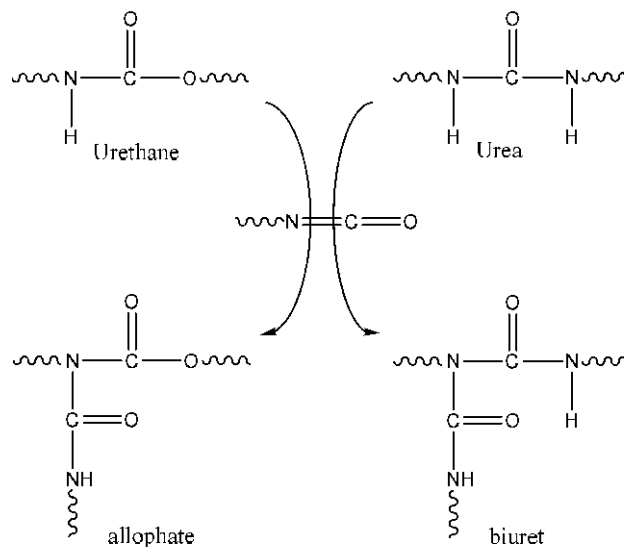


**Figure 3** - Urethane and urea groups reacted with isocyanates

Polyols and additives like catalysts, cross-linkers, and polyisocyanates—which produce the polymer's hard segments—make up the raw ingredients for polyurethanes. The polymer's soft segments are inexorably formed by the transistor.

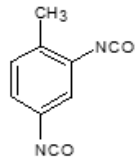
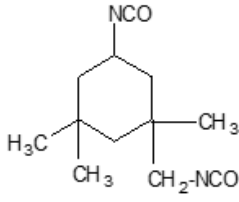


### Polyisocyanates

The primary products needed to create polyurethane polymers are isocyanates containing two or more functional groups [11]. PUs' cost and quality are determined by the kind of diisocyanates used, such as aliphatic and aromatic dimethyl cyanide. The bulk of diisocyanates produced worldwide are aromatic isocyanates, despite their low UV resistance. However, because of their strong UV resistance, aliphatic and cycloaliphatic isocyanates are also crucial for the production of

polyurethane materials for outdoor applications. Aliphatic isocyanates are strongly advised. This is because the reactivity of an isocyanate group with an aromatic connection is much higher than that of an aliphatic one. The lower cost of aromatic isocyanates compared to aliphatic isocyanates is another consideration. Isocyanates are distinguished by the percentage of NCO content and their functionality, which reflects the number of NCO groups present in a molecule. Table 1 lists the most regularly utilized isocyanates in the manufacturing of polyurethanes.

The authors studied the properties of segmented PU produced from various diisocyanates [12]. Using 4,4'-diphenylmethane diisocyanate (MDI), 2,4-toluene diisocyanate (TDI) and its isomers, hydrogenated 4,4'-diphenylmethane diisocyanate (HMDI), and 1,6-hexane diisocyanate

**Table 1** - The most prevalent diisocyanates used in the manufacturing of polyurethane

No.	Chemical name	Abbreviation	Structure
1	toluene -2,4 -diisocyanate	TDI	
2	Hexamethylene diisocyanate	HMDI	OCN — C <sub>6</sub> H <sub>12</sub> — NCO
3	Isophorone diisocyanate	IPDI	
4	4,4'-Methylene bis phenylene diisocyanates	MDI	OCN — Ph — CH <sub>2</sub> — Ph — NCO
5	Cyclohexane-1,4-diisocyanate	CHDI	
6	p-Phenylene -1,4 -diisocyanate	PPDI	

(HDI), they discovered that the diisocyanate structure had a significant influence on the mechanical characteristics of the PUR.

They explained that the hard segment's symmetry and chemical makeup were to blame for the impact. Based on variations in the interatomic bond type, Caraculacu et al. [13] established a new general categorization of many probable isocyanate addition methods. Beginning with the most recent developments in physicochemical techniques, new information was discovered about the structure of isocyanates and the various hydroxyl compound relationships that resulted from additional procedures. It was discovered that the symmetrical diols' intramolecular hydrogen bonding significantly influenced the two OH group reactivities.

### Polyols

Alcohols having several hydroxy groups are known as polyols, and they are the main reactants with isocyanates. These substances are characterized by their hydroxyl number (OH number, in mg KOH/g), which is inversely related to molecular weight. Based on their chemical makeup,

polyols can be categorized as acrylic, polyester, polyether, or polycarbonate polyols. Polypropylene glycol (PPG), polyethylene oxide, or polyethylene glycol (PEG), and polytetrahydrofuran, or PTMEG, are the three categories into which polyether polyols fall. Polyols come in mixed aliphatic-aromatic and aromatic forms, as well as in both aromatic and aliphatic forms [14]. When compared to isocyanates, polyols typically have relatively low toxicity. The common polyol types are seen in Figure 4, with each type identified by its backbone structure. Nowadays, polyethers form the basis for over 75% of the polyols used to make polyurethane [15].

The final product's characteristics, polyurethane polymers, are greatly influenced by two essential properties of polyols: functionality and equivalent weight. The average number of functional groups that react to isocyanate in each polyol molecule is known as polyol functionality. The following definition of polyol equivalent weight is applicable:

Equivalent weight = Molecular weight of polyols/functionality of polyols = 56100/hydroxyl number

The hydroxyl number (mg KOH/g) is the number of milligrams of potassium hydroxide present in one

gram of polyols [16]. Acrylic polyols are typically employed in high-performance applications that need UV stability. Acrylic polyols are used in polyurethane coatings for automobile finishes because they are chemical resistant and long-lasting. The chemical composition of the monomers employed in acrylic polyol-based PU coatings has a significant impact. Figure 5 is an example of an acrylic polyol reaction preparation.

Polyols provide flexibility to the network chains' backbone, which is why they are referred to as soft segments or domains in PUs. Polyether polyols are the byproducts of a reaction between alkali initiators and monomers such as ethylene oxide and

propylene oxide. Polyols utilized in polyurethane production are hydroxyl-terminated long-chain macroglycols with varying molecular weights [17]. The structure of polyol is an important aspect in determining polyurethane characteristics.

Polyols can be made from epoxy resins that have secondary hydroxyl groups [18]. Special silicone resins are ideal for heat-resistant PU coatings. Vinyl polymers, alone or in conjunction with other polyols, can be utilized efficiently as polyols. Vegetable or plant oils, such as castor oil, linseed oil, tall oil, and others, can also be utilized as polyols. Because coal tar includes many groups containing active hydrogen, it may also be utilized to make polyols.

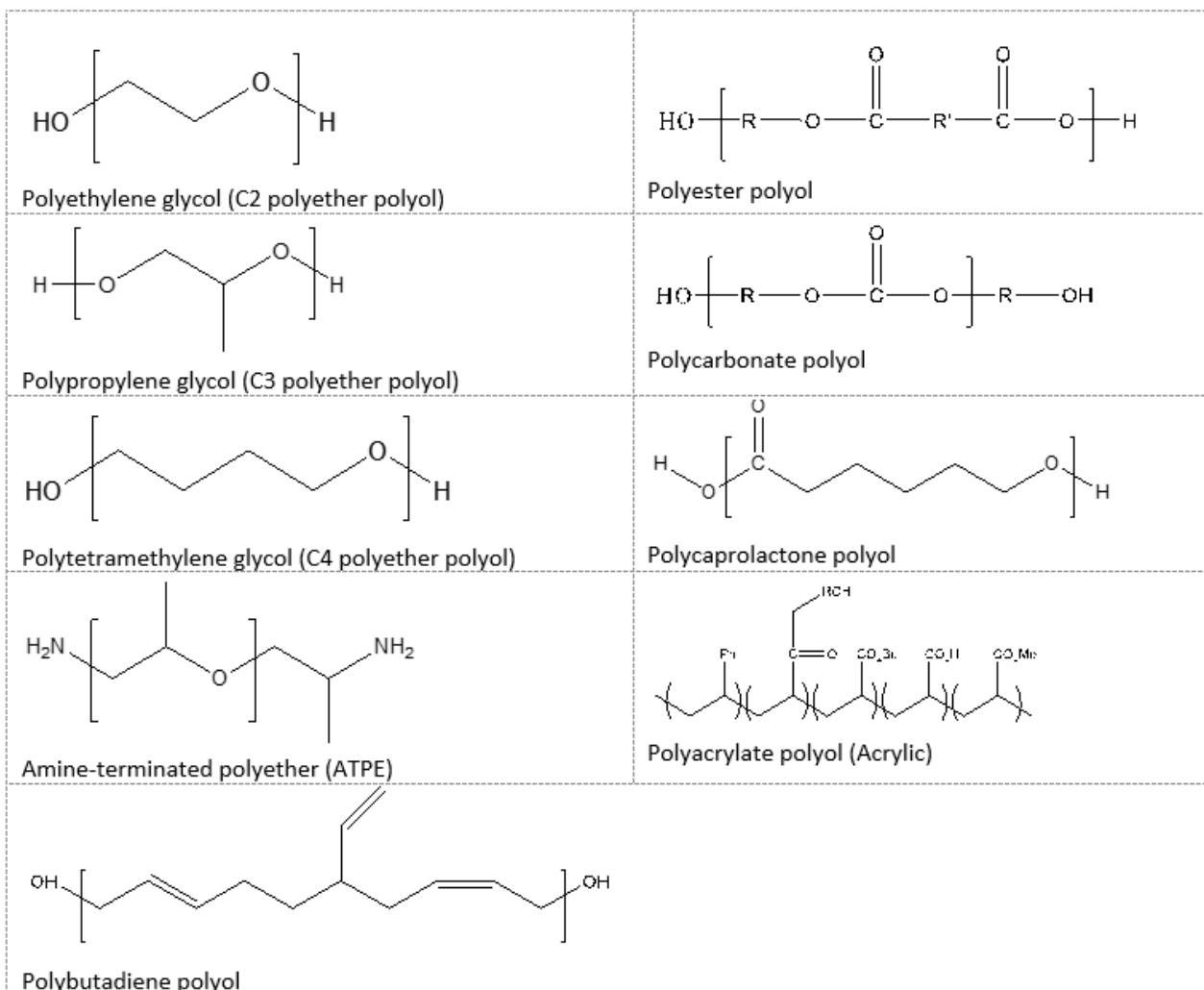


Figure 4 - Common polyol types

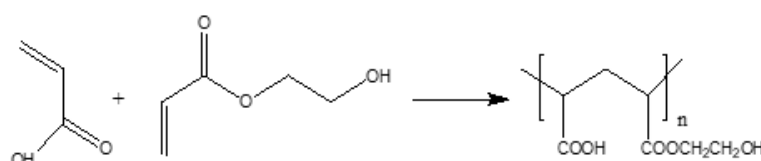


Figure 5 - Preparation of acrylic polyol

Polyester polyols can be made using a variety of methods, including polycondensation of hydroxyl acids or diacids and diol or ring-opening polymerization of lactone. Polyester produced from a combination of two or more diacids reacting with various glycols is a popular commercial product [[19], [20]].

The invention describes polyester polyols with an average equivalent weight between 200 and 4,000. These polyols are made by reacting alpha and omega dicarboxylic acids with butane 1,4-diol, hexane 1,6-diol, propane 1,3-diol, or pentane 1,5-diol. The resulting polyols with three to six hydroxyl groups are then used to create PUR pourable elastomers with enhanced resistance to hydrolysis [21].

The molecular weight and structure of soft segments also affect polyurethane shape. Typically, soft segments with average molecular weights of 1000–5000 are used in the manufacturing of thermoplastic polyurethanes. Phase separation is greater in polyether urethanes than in polyester urethanes due to the reduced compatibility of the polyether soft segments with the polar hard segments.

Both polyester urethane and polyether exhibit changes in characteristics as soft segments' molecular weight is increased. The impact of increasing the molecular weight of the soft segment on the microphase separation and viscoelastic characteristics of polyester polyurethanes was investigated by Velankar and Cooper [22]. DSC, SAXS, and rheology were used to describe a range of polyester urethanes with variable block lengths (soft segment MW = 830, 1250, 2000, and 3000) and constant composition (soft segment  $\approx$  50 wt%). PUs made with SS MW 830 and 1250 were single-phase materials, according to DSC and SAXS data.

These two PUs exhibited rheological behavior that was similar to homopolymer melts and reasonably consistent with Rouse's theoretical predictions. The amount of microphase separation increased gradually with SS MW, according to DSC, SAXS, and rheological study (Time Temperature Superposition) for PUs with SS MW 2000 and 3000. Furthermore, a substantial relationship between soft segment length was observed for both the relaxation time and the Newtonian viscosity.

Korley et al. [23] investigated the effects of crystallinity in the soft segment phase, which is made up of polyether soft blocks with varying inclinations toward crystallization. The authors of this work looked at the morphology and mechanical behavior of a range of polyurethanes with different

hard segment contents that contained PEO (1000 and 4600 g/mol) and PEO-PPO-PEO (1900 g/mol) soft segments. In comparison to polyurethanes including PEO-PPO-PEO soft segments, it was shown that toughness was enhanced and the storage modulus of polyurethane below the  $T_m$  of the soft block was raised by soft segment crystallinity in PEO (1000 g/mol). The results of the study demonstrated that organized soft segment areas, which dissipate energy and contribute to the overall deformation process, not only provide extensibility but also reinforce the polyurethane matrix during the process.

Strictly speaking, the urethane process is catalyzed if the catalysts raise the rate of reaction without getting consumed themselves. The most often utilized catalysts are tertiary amines, such as tetramethyl butane diamine (TMBDA) and 1,4-diazo bicyclo (2,2,2)-octane (DABCO), and organo compounds, such as dibutyl tin dilaurate (DBTDL).

A segmented structure with flexible, polyol chains, and rigid segments, as well as segmental length, crystallizability, intra- and inter-segment interactions like hydrogen bonding, overall compositions, and molecular weight, are the characteristics of polyurethane resins [24]. Polyurethane has unique mechanical, thermal, and elastomeric qualities because of its hydrogen-bonding architecture. Because of its flexible chain and lower glass transition temperature than room temperature, the polyester section is referred to as the "soft segment." Instead of a covalent bond being chemically cross-linked, polyurethanes include a large number of hydro gross linkages, which allow them to rearrange upon mechanical deformation [25]. After the tension is released, the hydrogen bond reorganizes and regains its deformation strength. Urethane coatings have a limited capacity for self-healing due to intermolecular hydrogen bonding. This characteristic makes it possible to create polyurethanes that are resistant to solvent swelling and abrasion. Foams, coatings, adhesives, and thermoplastic elastomers are just a few of the applications for polyurethane, a special polymeric substance with a broad variety of physical and chemical characteristics (1–10). Polyurethane holds a prominent place in various applications, particularly in the coating sector, due to its high-quality coating layer that exhibits resistance to solvents, weather stability, and mechanical qualities. The polyurethane coatings industry comprises two main systems. One is referred to as a one-component (1K) system, where the substrate is



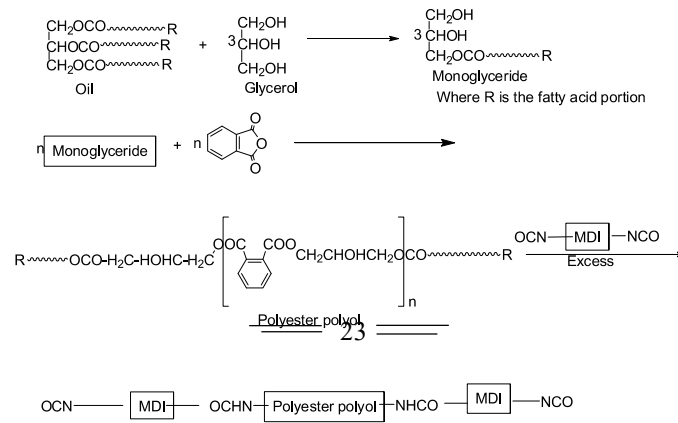


Figure 6 - Reaction sequence of the preparation of polyurethanes

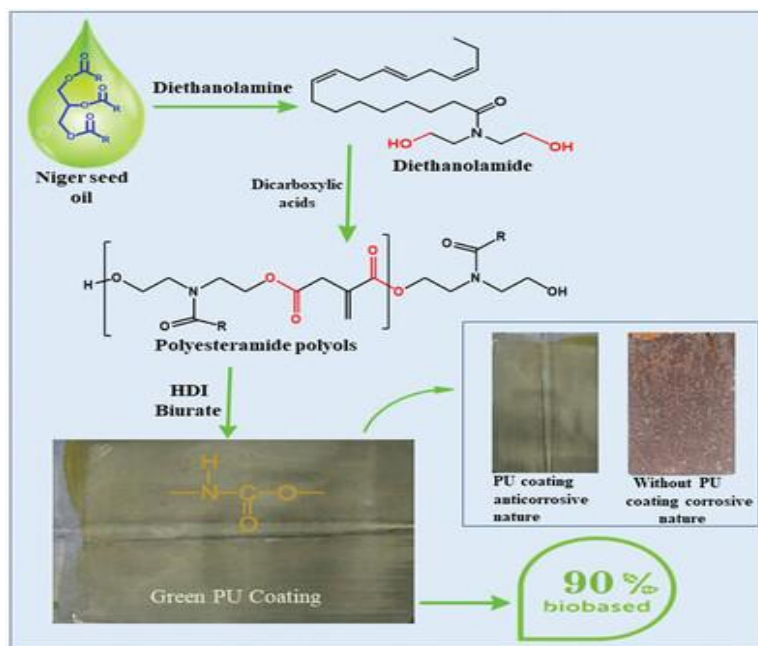


Figure 7 - Green PU coating from Niger-seed oil

physically cured after being covered with high molecular weight polyurethane. The other system consists of two components, hydroxyl functional polymers, and polyisocyanate hardeners with an ng NCO group.

To create monoglycerides, polyester polyol was made using esterified soybean oil and a glycerol:1:3 molar ratio [26]. Polyester polyols were created using a ratio-based reaction between the produced monoglycerides and phthalic anhydride. To create polyester–polyurethane coatings, PU prepolymer (Figure 6) was created by polyaddition reaction of diphenylmethane diisocyanate with polyester polyols at NCO/OH ratios of 1.2, 1.4, and 1.6 using toluene as a solvent. A high NCO/OH ratio is generally considered typical since it results in

tougher, more solvent-resistant coatings. The produced coatings exhibited attributes such as chemical resistance, impact resistance, pencil hardness, and flexibility. As the number of hard segments in the sample increases, so do the produced coatings' favorable attributes.

Velayutham et al. [[27], [28]] used polyester polyols with varied oleic acid concentrations to create PU coatings. To create PU coatings, the polyols reacted with aromatic isocyanate (toluene 2,4-diisocyanate, or TDI). The physical characteristics of PU coatings on mild steel panels were examined about different NCO/OH ratios and polyols' oleic acid concentrations. Physical-chemical characteristics such as solvent resistance, adhesive qualities, drying time, pencil hardness,

corrosion/chemical resistance determination, and solvent resistance were described together with the characterization of PU coatings using IR spectroscopy analysis. The best overall coating qualities are shown by the coatings made from polyol with a 28% content. The mechanical and anticorrosive capabilities of all the coatings increased progressively as the NCO/OH ratio rose.

Niger seed oil (NSO) was used by Ranjeet et al. [29] to create a PU covering (Figure 7). Niger seed oil is amidated with diethanolamine to create polyesteramide polyols, which are then esterified with several biobased dicarboxylic acids (phthalic, itaconic, and dimer) to add the necessary hydroxyl group functionality. Hexamethylene diisocyanate biuret (HDI-B) and synthetic polyesteramide polyols are used to make the polyurethane coatings. The gel content method is used to show the cross-link density of PU coatings, and the saltwater immersion technique is used to conduct the corrosion investigation. By using differential scanning calorimetry and thermogravimetric analysis, the glass transition temperature ( $T_g$ ) and thermal stability of the PU coatings are also investigated.

Common polymeric coatings like polyurethane offer surfaces in the food processing, marine, and biomedical sectors flexibility, durability, and resistance to abrasion (Figure 8). Because of its adjustable chemistry, polyurethane has enormous potential for materials of the future. Many studies have been conducted on the modification of polyurethane to provide it additional properties like antibacterial, non-fouling, anticorrosive activity, or high heat resistance. Traditional solvent-borne polyurethane

(PU) based on 4,4'-Methylenebis (phenyl isocyanate) (MDI), which is often used in food processing facilities, boat hulls, and floor coverings, was produced by Rudlong and Goddard 2023 [30]. The polyurethane included 1%, 2%, and 3% perfluoropolyether (PFPE).

Wetability and hydrophobicity were assessed using a dynamic water contact angle. The addition of perfluoropolyether blocks (PU-co-1PFPE  $131.5^\circ \pm 8.0$ , PU-co-2PFPE  $130.9^\circ \pm 5.8$ , and PU-co-3PFPE  $128.8^\circ \pm 5.2$ ) significantly advanced the water contact angle in comparison to the control polyurethane ( $93.6^\circ \pm 3.6$ ). The surface orientation of fluorine provided support for the lower critical surface tensions of PU-co-3PFPE-modified polyurethane ( $12.54 \text{ mN m}^{-1}$  as opposed to  $17.19 \text{ mN m}^{-1}$  for unmodified polyurethane).

Because of its superior mechanical and thermal qualities as well as outstanding chemical resistance, epoxy resins find extensive usage in the adhesive, automotive, paint, and aerospace sectors. Nevertheless, the overall impact resistance of these materials is weakened following external impact due to the propagation of cracks in epoxy polymers. As a result, many impact modifiers have been created to lessen epoxy polymers' brittleness. Polyurethanes (PU) can increase the toughness of polymers by acting as impact modifiers. While the fact that polyurethanes (PUs) phase-separate in the polymer matrix during curing is widely known, it has proven difficult to reattach PUs to the matrix to improve the mechanical characteristics of polymers.

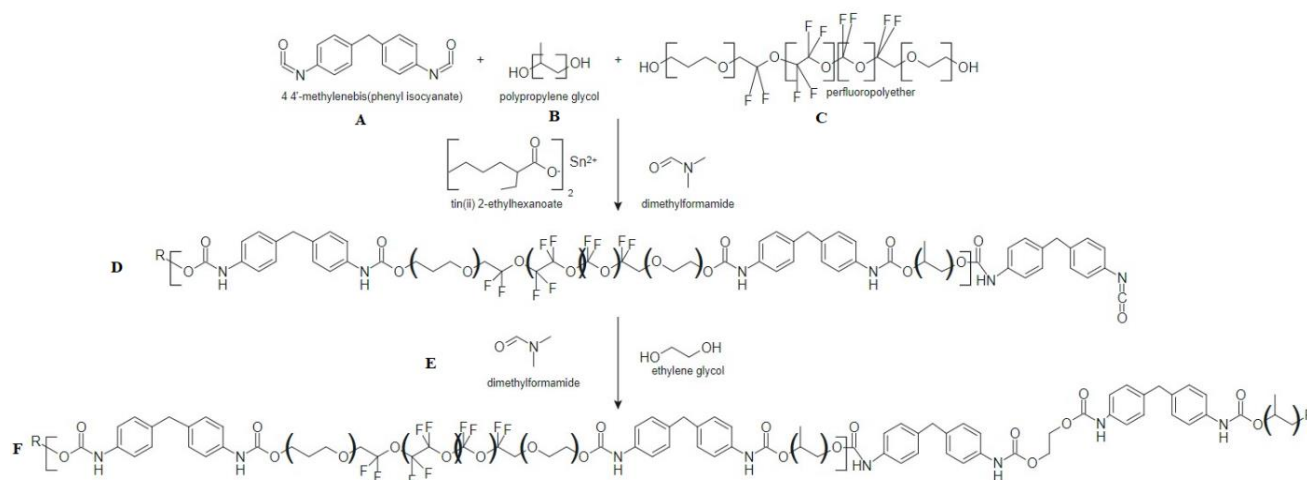


**Figure 8** - A two-step prepolymer reaction of MDI (A), PPG (B), and PFPE (C) forms the prepolymer (D). Chain extender (E) added to form final PU-co-PFPE polymer (F).



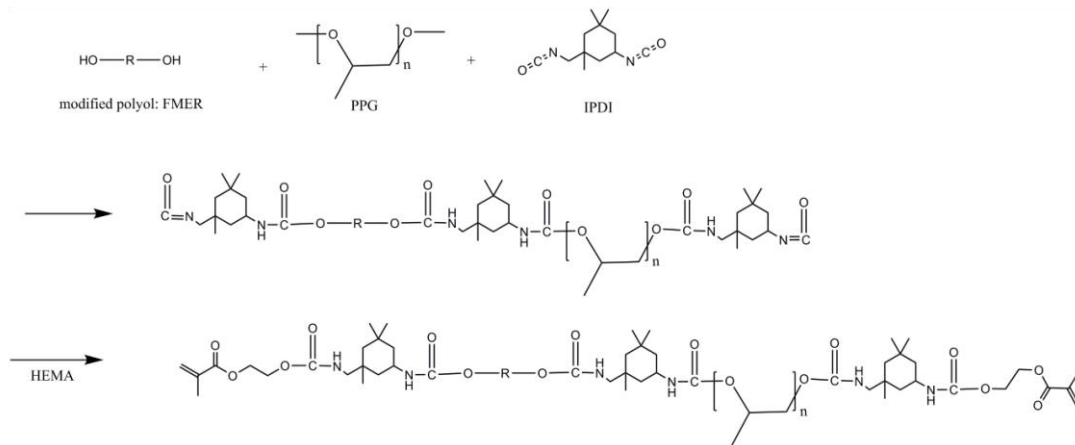


**Figure 9** - PU reaction strategy including the reaction of isophorone diisocyanate (FMEP-PU) with hydrogenated epoxy polyol modified by fatty acids

Unlike previous research that concentrated on changing capping agents to establish a network topology between the polymer matrix and PU, Kim et al., 2019 [31] included epoxy functional groups into polyol backbones. By using gel permeation chromatography, we were able to verify the molecular weight of the produced PU. Additionally, the produced material was mixed with the epoxies, and the resultant materials' mechanical and thermal characteristics were assessed. We also measured impact resistance, flexural strength, and tensile strength. The impact strength and mechanical strength of the epoxy compositions were improved and sustained up to 10 phr of PU by the addition of PU (Figure 9).

In 2019, Zaimahwati et al. [32] polyurethane (PU) nanocomposite that has been prepared using castor oil and coated with montmorillonite nanoparticles. After synthesizing polyols from castor oil and organic montmorillonite nanoparticles, polyurethanes (PU) were prepared, evaluated, and used as coating materials for polyurethane nanocomposites. Organic montmorillonite nanoparticles were added to polyols to create a polyurethane nanocomposite, which was then combined with toluene diisocyanate. Using thermogravimetric analysis (TGA) equipment, the thermal properties of polyurethane nanocomposites were used to evaluate their efficacy as heat-resistant coatings. Subsequently, the adhesive strength and morphological characteristics of the material coating were assessed. The results showed that the addition of montmorillonite improved both the adhesive strength of the material coating applied to the material's surface and the heat resistance of the material's film surface layer.

The impact of diisocyanate symmetry and hydrogen bonding on microphase morphology was examined by Yilgor et al. [33]. Their investigation into segmented polyether ureas and non-chain extended polyether urethanes produced some intriguing findings on the microphase separation of these polymers. The researchers observed that polyurethanes prepared with symmetrical diisocyanates, namely 1,4-phenylene diisocyanate (PPDI), 1,6-hexamethylene diisocyanate (HDI), and 1,4-cyclohexyl diisocyanate (CHDI), exhibited a microphase morphology in which the soft segment matrix was permeated by hard segments that resembled ribbons. Conversely, polyurethanes based on diisocyanates that are not symmetrical, such as 1,3-phenylene diisocyanate (MPDI), 2,6- and 2,4-toluene diisocyanate (TDI), bis (4-isocyanate cyclohexyl)methane (HMDI), and MDI, did not exhibit microphase morphology at ambient temperature. All polyether areas, in contrast to their urethane counterparts, showed microphase morphology at room temperature, irrespective of the diisocyanate's structure or symmetry. Their research demonstrates the critical influence that hard segment symmetry has on polyurethane microphase formation. PU coatings are available in several varieties. Solvent-based coatings, or conventional PU coatings, have dominated the industrial coating industry in recent decades. More restrictive laws about volatile organic compound (VOC) emissions, however, nevertheless pose a threat to this position. Because of this, producers of paint and suppliers of raw materials are creating substitute technologies that work just as well but are more environmentally friendly.

Coatings containing volatile organic compounds (VOCs) are becoming more and more appealing since they offer excellent protection and address environmental issues. Eco-friendly polyurethane coatings include a subclass known as polyurethane-urea hybrid coatings [34]. The reason for the interest in this kind of coating is that it has been claimed to have better mechanical qualities than traditional polyurethanes, which improves the organic film's overall performance [35]. An important part of this scenario involves high-solid systems. Hybrid coatings made entirely of solid polyurethane and urea have been created in this work. Different NCO/OH molar ratios and methylene diphenyl diisocyanate (MDI) were used in the preparation of the coatings. By employing differential scanning calorimetry (DSC) and electrochemical impedance spectroscopy (EIS), the impacts of the structural properties on the physical aging behavior and the electrochemical responsiveness of the hybrid coatings were assessed. The optimum combination of attributes, including low sensitivity to physical aging and excellent corrosion resistance, was demonstrated by the coating with the greatest NCO/OH ratio, according to the findings [36]. The kind of diisocyanate and the NCO/OH molar ratio affect the performance of polyurethane and polyurethane-urea hybrid coatings [[37], [38]]. Mishra and colleagues (2019) noted that increased NCO/OH ratios also resulted in enhanced heat stability for PU-based coatings. According to Negim et al. [39], elongation at break and viscosity declined as the NCO/OH ratio rose, while the tensile strength,

hardness, and rip strength of water dispersion polyurethanes escalated. In addition to the urethane/urea hard components, this behavior is linked to the increased production of molecular groups such as allophanate or biurate connections [40].

Two-step solution polymerization was used to create a variety of moisture-cured polyurethane/polysiloxane (PUs) copolymers (Figure 10). Alkoxysilane was utilized as an end-capping agent, and amine-terminated polysiloxane (PDMS) and polyester diol were combined as mixed soft segments to react with a 4,4'-diphenylmethane diisocyanate (MDI). The impact of changing building block structures, such as the NCO/OH ratio and polyester diol structure, on the characteristics and morphology of polyurethanes (PUs) were investigated. Investigations were conducted into the tensile, dielectric, thermal stability, surface, and water-repellent qualities. The findings demonstrated that differences in molecular architecture had a significant impact on the appearance and characteristics of PUs [41].

Without the use of a catalyst or solvent, Prabhakar et al., 2005 [42] synthesized NCO-terminated polyurethane of polypropylene glycol (PPG)-1000 and isophoron diisocyanate (IPDI) with an NCO/OH ratio of 1.2:1. The produced prepolymer was structurally investigated using 1D and 2D NMR spectroscopy. To provide a clear description of the assessment of the urethane groups and to

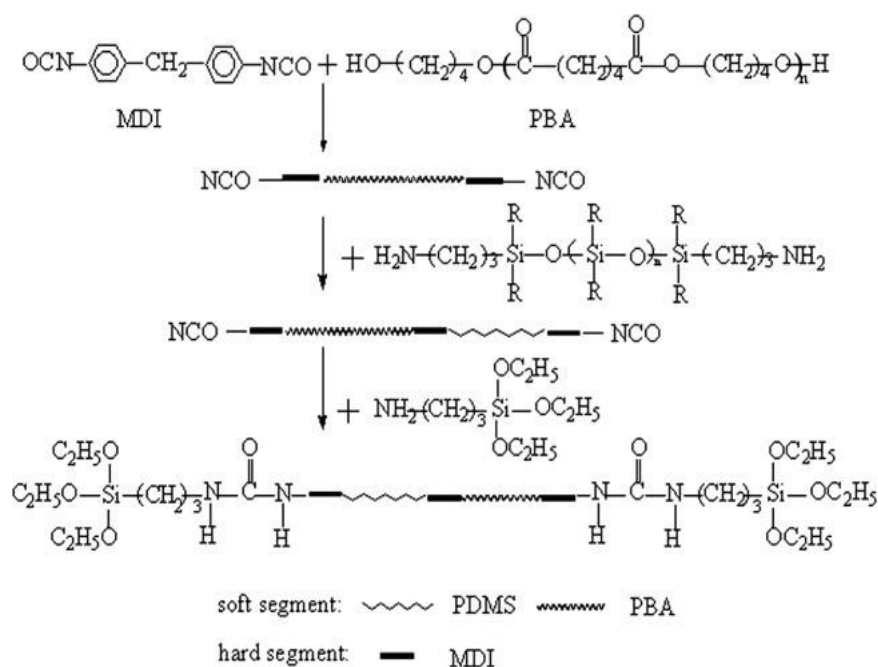


Figure 10 - Synthesis of the polyurethane/polysiloxane copolymer

track the reactivity of isocyanate groups with the hydroxyl function of PPG,  $^1\text{H}$  NMR spectra, and dibutyl amine back-titration were employed.  $^{13}\text{C}$  NMR spectroscopy was used to crosscheck the % conversion data for the methanol end-capped prepolymer in the urethane zone. The secondary NCO group is more reactive than the primary group, according to the findings.

In 2003, [43] Semsarzadeh and Navarchian synthesized Poly(urethane-isocyanurate)s created by reacting poly(propylene glycol) and toluene diisocyanate at varied stoichiometric ratios (1-3) with varying amounts of ferric acetylacetonate (FeAA) and dibutyltin dilaurate (DBTDL). Using Fourier transform IR spectroscopy, the impact of the catalyst type and concentration, as well as the NCO/OH ratio, on the degree of urethane and isocyanurate synthesis were investigated. With a rise in the stoichiometric ratio or DBTDL concentration, it was seen that the proportion of the trimer group and the trimer/urethane content rose. Thermogravimetric (TG) analysis was used to examine the thermal breakdown of the polyurethanes in an inert environment.

The TG curves showed three phases of disintegration, with 355 to 385 °C serving as the major degradation temperature. The effects of the NCO/OH ratio, catalyst type and concentration, and heating rate on the thermal stability of the polyurethanes were determined. We estimated the activation energies of thermal decomposition by use of the Kissinger, Flynn-Wall, and Ozawa methods. The swelling behavior of solid polyurethanes in toluene showed that as DBTDL concentration and/or NCO/OH ratio increased, the crosslink density increased and the swelling ratio and average molecular weight between crosslinks decreased. It was demonstrated that the sol fraction of solid polyurethanes decreased with an increase in the stoichiometric ratio or the amount of DBTDL.

Rummi et al. (2013) [44] studied that by reacting a molar excess of diphenylmethane diisocyanate (MDI) with polypropylene glycol (PPG) for two hours at 60°C, polyurethane prepolymers were produced. It investigated how different NCO/OH molar ratios and polyol molecular weights affected the polyurethane plaster cast's tack-free time, setting time, diametral compression strength, percent elongation, and tensile strength. When the NCO/OH molar ratio increases, the cast's tack-free period and setting time reduce but its diametral compression strength increases. Using a universal testing

apparatus, tensile strength was determined to increase as the NCO/OH ratio increased, even though the percentage of elongation had the opposite tendency. As the polyol molecular weight rises, the cast's tack-free and setting times increase while its diametral compression strength decreases. The tensile and diametral compression strengths of blended polyols, such as PPG 1000 and PPG 400 mixed in a 50/50 ratio, are equivalent to those of their unblended equivalents. Compared to fiberglass cast, polyester cast has a higher % elongation and diametral compression strength.

Polyaniline/graphene was used as an anticorrosion filler by Kewen et al., 2016 [45] to create a conductive coating based on aqueous polyurethane. Potentiodynamic polarization curves, electrochemical impedance spectroscopy (EIS), and salt spray were used to evaluate the coating. The maximum conductivity for polyurethane coating was achieved with a polyaniline/graphene ratio of 0.75 wt% and a graphene concentration of 4 wt%. Youtong Wu et al., 2019 [46] used SG-ZP mixtures as an additive to create an aqua polyurethane-based surface. Tafel curves and EIS analysis were used to test the obtained coating. The 0.5 wt% sulfonated graphene/zinc phosphate ratio produced satisfactory results, with a corrosion current density of 0.4252  $\mu\text{A}/\text{cm}^2$  and a charged transfer resistance ( $R_{ct}$ ) of 10.937  $10^3 \text{ cm}^2$ . Cui et al., 2020 [47] investigated if smart anticorrosion coatings outperformed traditional ones. The paper introduced the linked ideas of self-healing and nano-container development. The present issues, their optimization, and potential future consequences have all been explored.

Pei-Ying Tsai et al., 2018 [48] used a complex PU/Gr coating with a ratio of 0,2,4, and 8wt.% for Gr. The anti-corrosion and mechanical capabilities of the mixture were evaluated using EIS, salt spray, and cross-cut tests. At normal conditions, anti-friction properties were evaluated using a tribometer and the ball-on-disc technique. Complexes containing 4 and 8% gr. The friction coefficient data showed that increasing the graphite (Gr) content to 8% reduced the anti-friction qualities of the PU/Gr composite coatings by 61% compared to the standard coating.

Thi Xuan Hang et al., 2015 [49] showed that treatment with 2-aminoethyl-3-aminopropyltrimethoxysilane (APS) resulted in the precipitation of nanosized ZnO. ZnO-APS nanomaterial characterization was performed by UV-Vis, SEM, TEM, and XRD spectroscopy. Under

QUV testing conditions, the degradation of polyurethane coatings containing nano ZnO at a weight percentage of 0.1 and nano ZnO-APS at two weight percentages, 0.1 and 0.5 wt%, was assessed. The findings demonstrate that the nano ZnO-APS particle sizes range from 10 to 15 nm and have a spherical shape. The polyurethane coating's UV resistance was enhanced by nano ZnO, and its effectiveness was further enhanced by surface modification using APS. Notably, the UV resistance of the polyurethane coating was markedly enhanced by the addition of nano ZnO-APS at 0.1 wt%.

Huibin Zhu et al., 2020, [50] used a one-step spray-coating approach to develop superhydrophobic films with flexibility, mechanical robustness, and thermal stability. The coatings, which had a micro-nano structure and a  $T_g$  greater than 221°C, kept contact angles over 150 degrees. They were extremely flexible, with a friction value of 1.70. Electrochemical corrosion studies indicated their extraordinary resistance ( $I_{corr}$  reaching  $8.90 \times 10^{-5}$  A  $cm^{-2}$  under particular conditions), making them promising for harsh environment applications.

Yao Tong et al. 2017, [51] investigated the use of graphite and graphene particles to improve the specific conductance and anti-corrosion characteristics of polyurethane (PU) coatings. In terms of electrical conductance, a hybrid composite including carbon nanotubes outperformed single filler systems, with a significant advantage reported at 5 wt% loading (0.77 S/m, whereas the single filler system remained non-conductive). The conductive mechanism has been discovered. Lower filler loadings in the coatings increased anti-corrosion properties. Resistance readings from Electrochemical Impedance Spectroscopy (EIS) and the four-point probe technique were compared and discussed.

Mahmudzadeh et al. 2019, [52] investigated a cost-effective and ecologically friendly approach for decreasing graphene oxide in an hour using *Urtica dioica* leaves extract at 90°C. The elimination of oxygen functional groups was verified by Raman spectroscopy. Even after accelerated weathering, the decreased graphene oxide increased the corrosion resistance of polyurethane coatings and displayed remarkable protection efficacy, topping 99% in low-frequency impedance studies.

Xiaoyun Yea et al., (2019), [53] demonstrated the fabrication of zinc oxide (ZnO) array/polyurethane (PU) nanocomposite coatings on stainless steel substrates. ZnO arrays were grown

from seeds and then mixed with PU. The coatings' structure, wettability, mechanical characteristics, and corrosion resistance were all evaluated. The ZnO arrays have a hexagonal wurtzite structure and are somewhat more hydrophilic. Mechanical qualities improved as ZnO concentration increased, and the coatings demonstrated good corrosion resistance. Infrared radiation performance improved slightly as well. This innovative organic/inorganic nanocomposite coating is a viable strategy for creating functional coatings with improved corrosion resistance and mechanical properties in a variety of polymer systems.

Hui Wang et al., (2021) [54] investigated a novel anticorrosive coating capable of self-healing in the event of damage. Using Diels-Alder (DA) bonding, a PU prepolymer is combined with a modified CeO<sub>2</sub> furan to form this covering. These DA bonds are efficient in preserving mild steel against corrosion following coating degradation. The photothermal characteristics of dopamine allow this coating to self-heal in settings similar to infrared irradiation for 20 seconds. The mechanical and anticorrosive properties of the coating remained nearly unaltered after such self-healing. The proposed coating (PU DA-d@CeNPs5) exhibited good mechanical properties ( $38.89 \pm 0.52$  MPa), adhesion qualities (12 MPa), and an impedance modulus at 0.01 Hz equivalent to  $1.29 \times 10^9$ -ohm  $cm^2$ . Even after 100 days of continuous immersion, the impedance modulus at 0.01 Hz can still surpass 107 ohms/ $cm^2$ .

Polyurethane foam waste (PUR) was used and treated with dicarboxylic acids (DA) by Godinho et al., (2021) [55]. Using spectrum analysis, the ratio of PUT and DA was regulated, and the findings indicated that the recycled polyol (RP) has an appropriate hydroxyl number and acidity to form a new polyurethane (PU). This novel substance was utilized to make polyurethane coatings for wood (PUC). When compared to a typical polyol coating, the coating generated from RP has a higher hardness, but less gloss and more hydrophobicity.

Hui Yuan et al. [56] investigated the influence of water-based polyurethane, silicon dioxide, and fillers on the characteristics of modified silicate coatings. Coatings containing 10% polyurethane and 4% silica demonstrated superior mechanical qualities as well as resistance to heat and acids. The changed coatings outperformed the unmodified coatings in terms of strength, heat resistance, and acid resistance by 25.1%, 34.1%, and 32.4%, respectively. A thick microstructure with an



interpenetrating network was revealed by microstructural investigation. The coatings were also found to be less permeable, which increased their properties. Heat resistance at high temperatures (250°C) was fulfilled by the modified coatings.

Fengyuan Zhanga et al., (2020) [57] effectively created water-based polyurethane composites (WPC) containing functionalized graphene oxide (PAFG) generated from polyethyramines. The inclusion of nanoparticles at the optimum concentration improved the characteristics of WPU composites significantly. In comparison to pure WPU, the contact angle with water and water absorption in the WPU composite improved significantly to 98.5°C and 3.01 wt.%, respectively, from 70.5°C and 8.31 wt.%. Furthermore, there were significant improvements in thermal stability and mechanical qualities, particularly with the addition of 0.05 wt.% PAFG. With a 10% mass loss, the decomposition temperature of the WPU composite climbed to 322°C, which was 29.3°C higher than that of pure WPU. When compared to pure WPU, the tensile strength of WPU containing 0.05 wt.% PAFG improved by 130.92%. In terms of electrochemical data, after 31 days of immersion, the  $|Z|$  value at 0.01 Hz for WPU dropped, whereas WPU/PAFG0.05 remained steady. This demonstrates that 0.05 wt.% PAFG significantly improves the barrier characteristics of the WPU coating.

Jiahua et al., (2012) [58] used the sol-gel process to construct fluorescent silica shells of varying thicknesses on spherical carbonyl iron (CIP) particles. For metal particle surface compatibility with TEOS, hydrolysis, and condensation of tetraethyl orthosilicate (TEOS) were combined with the usage of gelatin B and 3 aminopropyltriethoxysilane (APTES). This results in a protective silica shell with variable thickness. The silica shell increases the particles' anti-corrosion and heat resistance. SIP and CIP-silica self-healing polyurethane coatings demonstrated increased anti-corrosion and heat resistance.

Tuan et al., (2022) [59] researched a novel anticorrosive coating that may self-repair when damaged. This coating is made of polyurethane acrylate (PUA) with lithium salt added as a polymer electrolyte. UV radiation was used to approve PUA and lithium salt mixtures, resulting in thin coatings with high heat resistance and ionic conductivity. The best conductivity was exhibited by PUA with a 25% mass fraction of lithium salt. The coating's

mechanical and structural properties, as well as its capacity to self-heal under near-infrared illumination, were also investigated.

Cheng et al., (2020) [60] created and tested ecologically friendly non-isocyanate polyurethane (NIPU) anti-corrosion coatings. The synthesis and formulation of these coatings employing several materials, including amine terminated NIPU, TEOS, and BPA epoxy, are the main emphasis of this work. The study evaluates the anti-corrosion performance of NIPU coatings with varying TEOS concentrations and finds that the best anti-corrosion behavior was shown by coatings containing 5% TEOS. Spectroscopic and microscopy methods have demonstrated that variations in anti-corrosion performance are related to the organic/inorganic micro-phase separation.

This research advances our understanding of how TEOS affects the anti-corrosion properties of NIPU coatings. Pavan et al., 2021, [61] investigate the synthesis of bio-renewable materials such as vegetable oils, outlining chemical changes and prospective uses. The analysis also tackles the obstacles and promising technology in the eco-friendly transition of the coatings sector.

Aqdas et al. (2015) [62] emphasize the benefits of ecologically friendly waterborne polyurethane (WPU) coatings, such as reduced VOC emissions and desired characteristics. It goes over current advances in WPU coatings, such as UV-cured and hyper-branched polyurethanes. It also investigates strategies to improve mechanical strength and flame retardancy using additives such as nanoparticles and fire retardants. By incorporating two commercially available inhibitors, Ravindra et al., 2015, [63] increased the anti-corrosive capabilities of polyurethane coatings. The encapsulating technique and its impacts on coating performance are explored, and improved corrosion inhibition efficiency is demonstrated.

Jing Li et al. (2016), [63] discovered that adding the following chemicals to a waterborne polyurethane matrix in the following order improves the anticorrosive characteristics of polyurethane: graphene oxide, moderately reduced graphene oxide, and functionalized graphene. Impedance Electrochemical Spectroscopy and salt spray testing confirmed that the additives are anti-corrosive. The chemical and dispersion states of graphene within polyurethane, according to the findings, impact the material's capacity to resist corrosion. The inclusion of 0.2 wt% of reduced graphene oxide improves the

anticorrosive capabilities of graphene-reinforced polyurethane composite coatings. The findings of the Electrochemical Impedance Spectroscopy demonstrated that, after 235 hours of immersion in a 3.5 wt% NaCl solution, there was no under-painting corrosion and that the impedance modulus at 0.1 Hz was constant at 109 U. This was true over the whole 235-hour period, with very little variation noted.

When 0.2 wt% reduced graphene oxide is added, the anticorrosive properties of graphene-reinforced polyurethane composite coatings are enhanced. After 235 hours of immersion in a 3.5 weight percent NaCl solution, the findings of the Electrochemical Impedance Spectroscopy revealed that under-painting corrosion did not occur and that the impedance modulus at 0.1 Hz was constant at 109 U. This was true throughout the whole 235-hour period, with very little variation detected.

According to Ashraf et al. (2015) [64], a Transmission electron microscopy image indicated that zinc oxide nanoparticles generated by direct precipitation have a pseudospherical shape and diameter of roughly 20.0 nm. Zinc oxide nanoparticles are uniformly disseminated in polyurethane by ultrasonication at loading levels ranging from 0.1 to 2.0 wt.% to improve polymer characteristics. The coatings were shown to be efficient at inhibiting both Gram-positive and Gram-negative bacteria growth. When ZnO NPs are used, the number of organisms growing on the coating's surface decreases. Moreover, better mechanical and corrosion resistance at lower concentrations was obtained by increasing the weight % of ZnO NPs. Scanning electron microscopy data served as the foundation for the conclusions.

Pooneh et al. (2018) [65] showed that the covalent functionalization of graphene oxide nanosheets by 3-glycidyloxypropyl) trimethoxysilane additions contributes to the improvement of mechanical performance and corrosion resistance. The study of nanomaterials was conducted using Fourier transform infrared spectroscopy (FT-IR), thermogravimetric analysis (TGA), field emission scanning electron microscopy (FE-SEM), and X-ray diffraction (XRD). The physical-mechanical characteristics of the coating with nanosheets were assessed by the use of tensile tests and dynamic mechanical thermal analysis (DMTA). In addition, the impact of GO and fGO nanosheets on the surface fracture morphology of polyurethane coating during tensile testing was investigated using

SEM analysis. The results of the study showed that the addition of fGO nanosheets enhanced the mechanical, anti-corrosion, and physical properties of the PU coatings by fortifying the interfacial bonds between the coating and the GO nanosheets. To understand the mechanism of the trimethoxysilane-polyurethane interaction, GO surface quantum mechanics techniques were used.

According to research by Abhijit et al., 2020 [66], polyurethane is a very versatile material that can be created to order when additives and nanoparticles are added. This enables a wide range of properties, including soft-touch coatings and rigid construction materials. The material's mechanical, chemical, and biological characteristics may be adjusted to meet specific needs, which has piqued the interest of several businesses as well as the scientific community. The chemistry of the constituent parts of polyurethane is examined in this study, along with recent advancements and applications in the medical, automotive, coatings, adhesives, sealants, paints, textiles, marine, wood composites, and apparel sectors.

Xiaohua et al., 2013 [67] demonstrated that LipolTM, a bio-based polyol, was made using a variety of vegetable oils. The oligomer dispersion and chemical structures of these polyols were investigated. The polyols were used to create polyurethane coatings with a bio-based content of about 60%. The coatings exhibited satisfactory mechanical and thermo-mechanical properties. The flax PU, which comes from oil that has a high linolenic acid content, had the highest performance because of its low solvent swelling, high glass transition temperature, strong cross-linked networks, resistance to abrasion and water, and hardness.

The goal of this investigation was to determine how various hardeners influenced the protective properties of polyurethane coatings, as investigated by Ewa et al. 2014 [68]. It was necessary to comprehend any modifications to the mechanical qualities, crosslink density, and chemical structure. After being applied to mild steel panels, the wet adhesion, abrasion resistance, and anti-corrosive properties of unpigmented polyurethane coatings with different hardener concentrations were evaluated. The electrical and abrasion resistance of coatings with a greater hardener ratio was demonstrated by the findings. The coating with the stoichiometric hardener ratio exhibited the least degree of adherence. According to the FTIR data, the

coatings' urethane group count dropped when the hardener ratio dropped. The study concluded that electrochemical impedance spectroscopy and DC resistance are helpful methods for determining how well the coatings will hold up over time.

The combination of poly (ethylene glycol) with epoxidized vegetable oil has been researched by Mandar et al., 2015 [69] to create novel polyester polyols. A sustainable method of extracting oil from cottonseed and karanja was used. The molecular weight of the poly (ethylene glycol) was altered. The polyols' spectrum properties and end groups were looked at. These polyols were utilized to replace dipen tene with xylene in ecologically friendly polyurethane coatings. Along with their physical and thermal characteristics, the resultant polyurethanes were evaluated for adhesion, gloss, hardness, impact resistance, and flexibility. These coatings showed promise for industrial use.

Tsao-Cheng Huang and colleagues (2017) [70] investigated the feasibility of ZrP/PU nanocomposite films to ensure consumption security. The electrochemical experiments confirmed the improved consumption resistance of ZrP/PU coatings on steel surfaces as compared with pure PU coatings. The connecting of ZrP nanoplatelets into the PU lattice further strengthened dampness obstructing characteristics. Ying Liang et al. (2020) [71] investigated the use of polydimethylsiloxane and acetylated starch in the manufacturing of bio-based polyurethane coating. The research was done and it was found that an acetylated starch-based polyurethane coating with a 0.5–3% polydimethylsiloxane content has anti-corrosion properties.

The enhancement of the anti-erosion characteristics of aluminum (Al) coatings by the creation of superhydrophobic surfaces was examined by Xiuyong Chen et al. (2014) [72]. The cycle involves using a suspension fire splashing technology to save polyurethane (PU)/nano-Al<sub>2</sub>O<sub>3</sub> composites by first curve showering Al coatings onto steel substrates. The result is the successful production of superhydrophobic PU/nano-Al<sub>2</sub>O<sub>3</sub>-Al coatings with a large spectrum of consumption that are safe. The super hydrophilicity/superhydrophobicity of the coatings may be adjusted by varying the concentration of PU in the initial suspension. A specific layer with 2.0 weight percent PU exhibits excellent hydrophobicity, with water droplets sliding at around 6.5°C and making contact at about 151°C.

For maritime foundations, the PU/nano-Al<sub>2</sub>O<sub>3</sub>-Al coatings with their solid enemy of consumption capabilities and superhydrophobic qualities can be employed as protective layers.

Four polyurethane saps—polyurethane (PU), epoxy-changed polyurethane (EPU), fluorinated polyurethane (FPU), and epoxy-altered fluorinated polyurethane (EFPU)—were used to create natural cement for the production of coatings with low infrared emissivity, according to a review by Yajun Wang et al. (2011) [73]. It is anticipated that the investigation will examine how these various tar networks affect the guarantee of low infrared emissivity coatings' usage. A neutral salt shower test has been employed to assess the goal, and coatings have been examined using Fourier-change infrared spectroscopy (FTIR) and scanning electron microscopy (SEM). Remarkably, the natural glue covering consolidating EFPU demonstrated exceptional erosion resistance. The simultaneous existence of epoxy aggregates and nuclear fluorine in the EFPU fastener was attributed to this improved presentation.

Fluorine-containing epoxy (FO) compounds that were combined using 2,2,3,3-tetrafluoro-1-propanol (TFP) and epichlorohydrin (ECH) in a single step were investigated by Xia Wang et al. (2015) [74]. A controlled sub-atomic weight fluorinated polyglycol was produced by cationic polymerization. Fluorinated polyurethane (FPO) and FO designs were detailed using techniques such as gel pervasion chromatography (GPC), FTIR, and NMR. Then, using a room temperature relieving procedure, FPO and methyl diphenylenediisocyanate (MDI) were combined to make a two-part fluorinated polyurethane coating. The concentration also evaluated the film surface using SEM (filtering electron microscope) imaging, as well as protection against the salt spray and water resistance.

The combination and representation of silicone-based covering materials that combine siloxane and polyurethane/polyurea copolymer were studied by Anna M. Mikhailova et al. (2012), [75]. Primary study, subatomic representation, warm properties, mechanical qualities, attachment, morphology, and consumption execution are all covered in the analysis, which reveals that aspects other than those covered in the hard part have an influence on the defensive and anticorrosion characteristics. To evaluate these covering materials' defensive and anticorrosion qualities, electrochemical impedance spectroscopy (EIS) was used. Indeed, the assessment

demonstrates that the hard part content does not apply only to these qualities. FT-IR spectroscopy was used to study the formation of the pre-blended copolymer and the ensuing silicone-polyurethane/polyurea copolymer (SPPU) with varying hard fragment (HS) percentages.

In their study on the enhancement of polyurethane-urea coatings, Yixing Zeng et al. (2023), [76] emphasized the importance of the isocyanate file in fitting the properties of polyurethane-urea coatings, providing a methodical approach to safeguarding metal and metal offices while encouraging the practical application of harmful to destructive materials. The coatings were assembled using conductive mica particles as fillers and aromatic isocyanate, amino-ended polyether, polyol derived from castor oil, and polyaspartic pitch as reactants. The review investigated how the isocyanate file affected the polyurethane-urea coatings' synthetic structure, static conductivity, and consumption hindrance. Higher cross-connectivity inside the covering was achieved by expanding the isocyanate file, albeit at the expense of decreased smallness and electrostatic conductivity. The organization of carbon dioxide increases in the overlying layer was blamed for this alteration. Salt shower tests and electrochemical impedance spectroscopy revealed that when the isocyanate record increased, the covering's ability to counter-consume on entire surfaces increased, but its appearance in areas with abandons decreased. Coatings with an isocyanate list of 1.0–1.1 demonstrated excellent electrostatic conductivity and erosion resistance, making them suitable for protecting metal and metallic workplaces.

To improve the enemy of consumption properties due to hydrophobicity and obstruction impacts, Mengting Moa et al. (2016) [77] developed functionalized graphene-supported polyurethane coatings with explicit surface surfaces. This resulted in less water contact and further developed the dispersion opposition of harmful substances. To improve their adversary of consumption qualities, the review focuses on the creation of PU nanocomposite coatings supported by functionalized graphene (FG). Its anti-erosive characteristics were further enhanced by the PU composite covering's surface and all-around dispersed FG. This improvement can be attributed to

the hydrophobic concept of the coatings, which reduces water cooperation and increases the pathway's convolution for the dispersion of harmful media. The majority of these components strengthen the ultimate FG/PU composite covering's defense against erosion. Transmission electron microscopy, examining electron microscopy, nuclear power microscopy, X-beam photoelectron spectrometry, Raman spectroscopy, Fourier change infrared spectroscopy, and other techniques were used to illustrate the main and morphological characteristics of the PU composite coatings. The coatings exhibited a unique round cone shape with distinct characteristics (widths of 8  $\mu\text{m}$  distributed eight, six, and four  $\mu\text{m}$  apart, respectively).

### Conclusions and Future Perspectives

There has been a steady and robust increase in the need for materials based on polyurethane throughout time. Particle filters (PUs) are widely used as coatings to prevent corrosion on metals. A chance to include new green PU formulations was presented by the growing recognition on a worldwide scale of the significance of environmental and human health. As a result, there has been a lot of interest in the design and development of highly effective polyurethanes (PUs) that are less harmful to the environment than their conventional equivalents made from polyols and polyisocyanates derived from petroleum. The current research on the application of such green polyurethanes—waterborne and bio-based polyurethanes in particular—as protective coatings is gathered in this review.

**Acknowledgments.** The work was financially supported by the Ministry of Science and Education of the Republic of Kazakhstan, program-targeted financing out of competitive procedures for 2023–2025. Project No. (BR21881822), entitled “Development of Technological Solutions for Optimizing Geological and Technical Operations When Drilling Wells and Oil Production at the Late Stage of Field Exploitation”.

**Conflicts of interest.** The authors declare no conflict of interest.



**Cite this article as:** Yeligbayeva G, Khaldun MA, Abdassalam A Alfergani, Tleugaliyeva Zh, Karabayeva A, Bekbayeva L, Zhetpisbay DS, Shadin N.A., Atabekova Z. Polyurethane as a versatile polymer for coating and anti-corrosion applications: A review. *Kompleksnoe Ispolzovanie Mineralnogo Syra = Complex Use of Mineral Resources.* 2024; 331(4):21-41. <https://doi.org/10.31643/2024/6445.36>

## Полиуретан қаптауға және коррозиядан қорғауға арналған универсалды полимер ретінде: Шолу

<sup>1\*</sup>Елигбаева Г.Ж., <sup>2</sup>Халдун М.А., <sup>3</sup>Абдассалам А. Альфергани, <sup>4</sup>Тлеугалиева Ж.А., <sup>4</sup>Карабаева А. Е., <sup>1,5</sup>Бекбаева Л.К., <sup>6</sup>Жетписбай Д.Ш., <sup>7</sup>Шадин Н.А., <sup>1</sup>Атабекова З.Б.

<sup>1</sup>Сәтбаев университеті, Мұнай өнеркәсібі мектебі, Алматы, Қазақстан

<sup>2</sup>Фармакологиялық және диагностикалық зерттеу орталығы (PDRС), Амман университеті Әл Ахлия, Амман, 19328, Иордания

<sup>3</sup>Химия бөлімі, білім беру факультеті, Сирт университеті, Сирт, Ливия

<sup>4</sup>Материалтану және жасыл технологиялар мектебі, Қазақ-Британ техникалық университеті, Алматы, Қазақстан

<sup>5</sup>Химия және химиялық технология факультеті, әл-Фараби атындағы ҚазҰУ, Алматы, Қазақстан

<sup>6</sup>С.Ж. Асфендияров атындағы ҚазҰМУ, Жалпы медицина мектебі, Алматы, Қазақстан

<sup>7</sup>Абай атындағы Қазақ ұлттық педагогикалық университеті, Жаратылыстану және география институты, Алматы, Қазақстан

Мақала келді: 23 қараша 2023  
Сараптамадан өтті: 8 желтоқсан 2023  
Қабылданды: 15 желтоқсан 2023

### ТҮЙІНДЕМЕ

Полиуретанды материалдарды әзірлеу және технологиялық процестерді оңтайландыру қазіргі уақытта ауқымды зерттеулердің тақырыбы болып табылады. Полиуретан жоғары физика-химиялық және пайдалану қасиеттерімен сипатталады. Полиуретандар тозуға, майға және бензинге төзімді. Олар керемет жылу физикалық және созылғыш қасиеттерге ие. Бұл полиуретандарды жоғары эксплуатациялық қасиеттері бар материалдарды қажет ететін көптеген салаларда қолдануға мүмкіндік береді. Полиуретандар сонымен қатар көптеген салаларда коррозияға қарсы агент ретінде қорғағыш жабындарын өндіруде кеңінен қолданылады. Полиуретанды полимерлердің физика-механикалық және эксплуатациялық қасиеттерін, атап айтқанда модификацияланған полиуретанды жабындардың коррозияға қарсы қасиеттерін жақсартуға арналған көптеген зерттеулер жүргізілді. Полиуретанды полимерлердің әртүрлі қолдануларға арналған қасиеттерін мономерлер мен олардың арақатынасын, сондай-ақ өндіріс процесінің өзін өзгерту арқылы жақсартуға болады. Полиолдар мен изоцианат мономерлеріне негізделген полиуретанды полимерлерді алу катализатордың қатысуымен полимерлеу процесіне де, толуол, ксилол және ацетон сияқты еріткіштерді қолдануға да негізделген. Әртүрлі әдістермен зерттелген полиуретанды полимерлердің физика-механикалық қасиеттеріне әсер ететін бірнеше факторлар бар. Мұндай факторларға изоцианаттардың, полиолдардың түрлері, ОСN/ОН қатынасы, еріткіштер, катализаторлар және температура жатады. Әдетте, полиолдар полиуретанды полимерлердің иілгіштігіне жауап береді, ал изоцианаттар полиуретанды полимердің қаттылығына және полимердің негізгі бөлігінің бірігуіне (тігілуіне) жауап береді. Реагенттердің химиялық құрамын өзгерту арқылы пайдалану мақсатына байланысты жабынның сипаттамалары өзгертіледі. Қорытынды әсер әртүрлі полиолдар мен полиизоцианаттардың химиялық құрамымен анықталады. Полиуретанды полимерлердің гидрофобтылығы, ыстыққа төзімділігі, механикалық және коррозияға қарсы қасиеттері зерттелді. Нәтижесінде гидрофобтылық, ыстыққа төзімділік, механикалық және коррозияға қарсы қасиеттер сияқты полиуретанды полимерлердің қасиеттері жоғарыда аталған факторлардың әсерінен жақсарды. Бұл шолу мақаласы қорғаныш полиуретанды жабындарды жасаудың және оларды коррозияға қарсы агент ретінде пайдаланудың ең заманауи, қаржылық табысты әдістеріне қысқаша сипаттама береді.

**Түйін сөздер:** Полиуретан, жабын, коррозияға қарсы, полиолдар, полиизоцианаттар.

### Авторлар туралы ақпарат:

<b>Елигбаева Гульжан Жақпаровна</b>	Химия ғылымдарының докторы, профессор, Мұнай инженериясы кафедрасы, Сәтбаев университеті, Сәтбаев көшесі, 22, Алматы 050013, Қазақстан. Email: <a href="mailto:g.yeligbayeva@satbayev.university">g.yeligbayeva@satbayev.university</a>
<b>Халдун М. Аль Аззам</b>	Химия кафедрасы, Жаратылыстану ғылымдары мектебі, Иордания университеті, 11942, Амман, Иордания. Email: <a href="mailto:azzamkha@yahoo.com">azzamkha@yahoo.com</a>
<b>Абдассалам А. Альфергани</b>	Химия бөлімі, білім беру факультеті, Сирт университеті, Сирт, Ливия. Email: <a href="mailto:abdassalamtameem@yahoo.com">abdassalamtameem@yahoo.com</a>
<b>Тлеугалиева Жанетта Асхатовна</b>	Материалтану және жасыл технологиялар мектебі, Қазақстан-Британ Техникалық Университеті Төле би көшесі, 59, 050000, Алматы, Қазақстан. Email: <a href="mailto:z_tleugaliyeva@kbtu.kz">z_tleugaliyeva@kbtu.kz</a>
<b>Карабаева Айкүміс Ермакқызы</b>	Материалтану және жасыл технологиялар мектебі, Қазақстан-Британ Техникалық Университеті Төле би көшесі, 59, 050000, Алматы, Қазақстан. Email: <a href="mailto:a_karabayeva@kbtu.kz">a_karabayeva@kbtu.kz</a>
<b>Бекбаева Ляззат</b>	Ұлттық ашық нанотехнология зертханасы, ҚазҰУ. Әл-Фараби, әл-Фараби даңғылы, 050040, Алматы, Қазақстан Республикасы. Email: <a href="mailto:lyazzat_bk2019@mail.ru">lyazzat_bk2019@mail.ru</a>
<b>Жетписбай Д.Ш.</b>	С.Ж. Асфендияров атындағы ҚазҰМУ, Жалпы Медицина Мектебі 1, Биохимия кафедрасы, 480012, Төле би көшесі, 88, Алматы, Қазақстан. Email: <a href="mailto:zhetpisbay.d@kazntmu.kz">zhetpisbay.d@kazntmu.kz</a>
<b>Шадин Н.А.</b>	Абай атындағы Қазақ Ұлттық Педагогикалық Университеті, Жаратылыстану және география институты, Химия кафедрасы, Қазыбек би көшесі, 30, Алматы, Қазақстан. Email: <a href="mailto:nugen_87@mail.ru">nugen_87@mail.ru</a>
<b>Атабекова З.Б.</b>	Сәтбаев университеті, Мұнай инженериясы кафедрасы, Инженер. Email: <a href="mailto:zau888@mail.ru">zau888@mail.ru</a>

# Полиуретан как универсальный полимер для нанесения покрытий и защиты от коррозии: Обзор

<sup>1\*</sup>Елигбаева Г.Ж., <sup>2</sup>Халдун М.А., <sup>3</sup>Абдассалам А. Альфергани, <sup>4</sup>Тлеугалиева Ж.А., <sup>4</sup>Карабаева А. Е.,  
<sup>1,5</sup>Бекбаева Л.К., <sup>6</sup>Жетписбай Д.Ш., <sup>7</sup>Шадин Н.А., <sup>1</sup>Атабекова З.Б.

<sup>1</sup>Сатбаев Университет, Кафедра Нефтяной Инженерии, Алматы, Казахстан

<sup>2</sup>Центр фармакологических и диагностических исследований (PDRC), Амманский университет Аль-Ахлия, Амман, 19328, Иордания

<sup>3</sup>Кафедра химии, педагогический факультет, Университет Сирта, Сирт, Ливия

<sup>4</sup> Факультет материаловедения и зеленых технологий, Казахстанско-Британский технический университет, Алматы, Казахстан

<sup>5</sup> Факультет химии и химической технологии КазНУ им. Аль-Фараби, Алматы, Казахстан

<sup>6</sup> КазНМУ им. Асфендиярова, лечебный факультет, Алматы, Казахстан

<sup>7</sup>Казахский национальный педагогический университет имени Абая, Институт естественных наук и географии, Алматы, Казахстан

<p>Поступила: 23 ноября 2023 Рецензирование: 8 декабря 2023 Принята в печать: 15 декабря 2023</p>	<p><b>Аннотация</b> Разработка полиуретановых материалов и оптимизация технологических процессов в настоящее время являются предметом обширных исследований. Полиуретан характеризуется высокими физико-химическими и эксплуатационными свойствами. Полиуретаны обладают высокой износостойкостью, масло- и бензостойкостью. Они имеют прекрасными теплофизические и эластичные свойства. Это позволяет применять полиуретаны во многих отраслях промышленности, где требуются материалы с высокими эксплуатационными свойствами. Полиуретаны также широко используются во многих отраслях промышленности при производстве защитных покрытий в качестве антикоррозионных средств. Было проведено значительное количество исследований, посвященных улучшению физико-механических и эксплуатационных свойств полиуретановых полимеров, в частности антикоррозионных свойств модифицированных полиуретановых покрытий. Свойства полиуретановых полимеров для различных применений могут быть улучшены путем изменения используемых мономеров и их соотношений, а также самого процесса получения. Получение полиуретановых полимеров на основе полиолов и изоцианатных мономеров основано как на процессе полиприсоединения в присутствии катализатора, так и применении растворителей, таких как толуол, ксилол и ацетон. Существуют различные факторы, влияющие на физико-механические свойства полиуретановых полимеров, которые были исследованы различными методами. Такими факторами были типы изоцианатов, полиолов, соотношения ОСN/ОН, растворители, катализаторы и температуры. Как правило, полиолы отвечают за гибкость полиуретановых полимеров, а изоцианаты отвечают за жесткость полиуретанового полимера и сшивку между основной частью полимера. Благодаря гибкому изменению химического состава реагентов они могут изменять характеристики покрытия в зависимости от предполагаемого использования. Конечный эффект определяется химическим составом различных полиолов и полиизоцианатов. Были исследованы гидрофобность, термостойкость, механические и антикоррозионные свойства полиуретановых полимеров. Как результат, свойства полиуретановых полимеров, такие как гидрофобность, термостойкость, механические и антикоррозионные свойства, улучшились под воздействием вышеперечисленных факторов. В этой обзорной статье дается краткое описание наиболее современных, финансово успешных методов создания защитных полиуретановых покрытий и использования их в качестве антикоррозионных средств.</p>
	<p><b>Ключевые слова:</b> Полиуретан, покрытие, антикоррозионное, полиолы, полиизоцианаты.</p>
<p><b>Елигбаева Гульжахан Жакпаровна</b></p>	<p><b>Информация об авторах:</b> Доктор химических наук, профессор, Кафедра Нефтяной Инженерии, Сатбаев Университет, ул. Сатбаева, 22, 050013, Алматы, Казахстан. Email: g.yeligbayeva@satbayev.university</p>
<p><b>Халдун М. Аль Аззам</b></p>	<p>Кафедра химии, Школа естественных наук, Иорданский университет, 11942, Амман, Иордания. Email: azzamkha@yahoo.com</p>
<p><b>Абдассалам А. Альфергани</b></p>	<p>Химический факультет, педагогический факультет, Сиртский университет, Сирт, Ливия. Email: abdassalamtameem@yahoo.com</p>
<p><b>Тлеугалиева Жанетта Асхатовна</b></p>	<p>Школа материаловедения и зеленых технологий, Казахстанско-Британский технический университет, ул. Толе би, 59, 050000, Алматы, Казахстан. Email: z_tleugalieva@kbtu.kz</p>
<p><b>Карабаева Айкумис Ермеккызы</b></p>	<p>Школа материаловедения и зеленых технологий, Казахстанско-Британский технический университет, ул. Толе би, 59, 050000, Алматы, Казахстан. Email: a_karabayeva@kbtu.kz</p>
<p><b>Бекбаева Ляззат</b></p>	<p>Национальная открытая лаборатория нанотехнологий, КазНУ им. Аль-Фараби, пр. Аль-Фараби, 050040, Алматы, Казахстан. Email: lyazzat_bk2019@mail.ru</p>
<p><b>Жетписбай Д.Ш.</b></p>	<p>Кафедра биохимии, Школа Общей Медицины, КазНМУ имени С.Д. Асфендиярова, 480012, ул. Толе би, 88, Алматы, Казахстан. Email: zhetpisbay.d@kaznmu.kz</p>
<p><b>Шадин Н.А.</b></p>	<p>Кафедра Химия, Институт естествознания и географии, Казахский Национальный Педагогический Университет имени Абая, ул.Казыбек би, 30, Алматы, Казахстан. nigen_87@mail.ru</p>
<p><b>Атабекова З.Б.</b></p>	<p>Школа Нефтяной Инженерии, Сатбаев Университет. Инженер. Email: zau888@mail.ru</p>

## References

- [1] Petrovic ZS, DooPyo H, Javn I, Erina N, Zhang F, Ilavsky J. Phase structure in segmented polyurethanes having fatty acid-based soft segment. *Polymer*. 2013; 54:372-380.
- [2] Diego Piazza, Debora S Silveira, Natalia P Lorandi. Polyester-based powder coatings with montmorillonit nanoparticle applied carbon steel. *Progress in organic Coatings*. 2012; 73:42-46.
- [3] Petrovic ZS, Cevallos MJ, Javni I, Schaefer DW, Justice R. *Journal of Polymer Science, Part B: Polymer Physics*. 2005; 43(22):3178-3190.
- [4] Velayutham TS, Abd Majid WH, Ahmad AB, Kang GY, Gan SN. *Progress in Organic Coatings*. 2009; 66:367-371.
- [5] Suhreta Husic, Ivan Javni, Zoran S. Petrovic. *Composites Science and Technology*. 2005; 65:19-25.
- [6] Wicks ZW, Jones PN, Pappas SP. *Organic Coatings: Science and Technology*. 2nd edition, John Wiley & Sons. Inc.: New York. 1999, 630.
- [7] Ingold CK. *Structure and Mechanism in Organic Chemistry*. 2nd edition, Cornell University Press: Ithaca, New York. 1969, 1129-113.
- [8] Das A, Mahanwar P. A brief discussion on advances in polyurethane applications. *Adv. Ind. Eng. Polym. Res*. 2020; 3:93-101.
- [9] Akindoyo JO, Beg MDH, Ghazali S, Islam MR, Jeyaratnam N, Yuvaraj AR. Polyurethane types, synthesis and applications. A review. *RSC Adv*. 2016; 6:114453-114482.
- [10] Yuan Y, Lee TR. Contact Angle and Wetting Properties. In *Surface Science Techniques*; Springer: Berlin-Heidelberg, Germany. 2013, 3-34.
- [11] Oertel G, Abele L. *Polyurethane Handbook: Chemistry, Raw Materials, Processing, Application, Properties*. Hanser Publishers. Distributed in USA By Scientific and Technical Books, Macmillan. 1985, 688.
- [12] Da-Kong Lee, Hong-Bing Tsai. Properties of segmented PUR derived from different diisocyanatos. *Journal of Applied Polymer Science*. 2000; 75(1):167-174.
- [13] Caraculacu AA, Coseri S. Isocyanates in polyaddition processes. Structure and reaction mechanisms. *Progress in Polymer Science*. 2001; 26:799-851.
- [14] Ionescu M. *Chemistry and Technology of Polyols for Polyurethanes*. Rapra Publishing. 2005, 392.
- [15] Ferrer MCC, Babb D, Ryan AJ. Characterization of polyurethane networks based on vegetable derived polyol . *Polymer*. 2008; 49(15):3279-3287.
- [16] Szycher M. *Szycher 's handbook of polyurethanes*. CRC Press: Florida. 1999, 1112.
- [17] Zhang C, Dai X, Wang Y, Sun G, Li P, Qu L, Sui Y, Dou Y. Preparation and corrosion resistance of ETEO modified graphene oxide/epoxy resin coating. *Coatings*. 2019; 9:46.
- [18] Hepburn C. *Polyurethane elastomers*. Elsevier Applied Science. 1992, 441.
- [19] Patent 6423816. US. Polyester polyols and their use as a binder component in two-component polyurethane coating composition. Wamprecht C, Sonntag M. 2002.
- [20] Patent 6184332. US. Polyester polyols and their use as the polyol component in two-component polyurethane paints. Santos D, Manuel A. 2001.
- [21] Patent 6809172. US. Polyester polyols and the use of polyester for producing polyurethane cast elastomers that have an improved resistance to hydrolysis. Barnes JM, Schneider M, Hoffmann A. 2004.
- [22] Velankar S, Cooper SL. Microphase Separation and Rheological Properties of Polyurethane Melts. 1. Effect of Block Length. *Macromolecules*. 1998; 31:9181-9192.
- [23] Korley LTJ, Pate BD, Thomas EL, Hammond PT. Effect of the Degree of Soft and Hard Segment Ordering on the Morphology and Mechanical Behavior of Semicrystalline Segmented Polyurethanes. *Polymer*. 2006; 47:3073-3082.
- [24] Matthew A. Hood, Bingbing Wang, James M Sands, John J La Scala, Frederick L Beyer, Christopher Y Li. Morphology control of segmented polyurethanes by crystallization of hard and soft segments. *Polymer*. 2020; 51(10):2191-2198.
- [25] Yan Wu, Kuling Wei, Yinglin Zhang, Chengcheng Miao. Fabrication of self-replenishing hydrophobic surfaces and self-cleaning coating based on self-crosslinkable PDMS-g-WPU emulsion. *Progress in Organic Coatings*. 2023; 175:107375.
- [26] Ismail Eid A, Motawie AM, Sadek EM. Synthesis and characterization of polyurethane coatings based on soybean oil-polyester polyols. *Egyptian Journal of Petroleum*. 2011; 20(2):1-8.
- [27] Velayutham TS, Abd Majid WH, Ahmad AB, Gan Yik Kang, Gan SN. Synthesis and characterization of polyurethane coatings derived from polyols synthesized with glycerol, phthalic anhydride and oleic acid. *Progress in Organic Coatings*. 2009; 66(4):367-371.
- [28] Velayutham TS, Abd Majid WH, Ahmad AB, Yik KG, Seng NG. The physical and mechanical properties of polyurethanes from oleic acid polyols. *Journal of Applied Polymer Science*. 2009; 112(6):3554-3559.
- [29] Ranjeet BD, Pavan MP, Yogeshsing NR, Ravindra DK. Synthesis and characterization of gree polyurethane coatings derived from Niger-seed-oil-based polyester amide polyols. *European Journal of Lipid Science and Technology*. 2002; 124(2):2100171.
- [30] Rudlong AM, Goddard JM. Synthesis and Characterization of Hydrophobic and Low Surface Tension Polyurethane. *Coatings*. 2023; 13(7):1133.
- [31] Kim TH, Kim M, Lee W, Kim H-G, Lim C-S, Seo B. Synthesis and Characterization of a Polyurethane Phase Separated to Nano Size in an Epoxy Polymer. *Coatings*. 2019; 9(5):319.
- [32] Zaimahwati, Yuniati, Jalal R, Rihayat T, Zhafiri S. Synthesis and characterization thermal of polyurethane. MMT from Castrol oil polyols for coating. *Conf. Ser.: Mater. Sci. Eng*. 2019; 536:012037.
- [33] Yilgor I, Yilgor E *Polym. Structure-morphology-property behavior of segmented thermoplastic polyurethanes and polyureas prepared without chain extenders*. *Polymer Reviews*. 2007; 47:487-510.
- [34] Yeh F, Hsiao BS, Sauer BB, Michel S, Siesler HW. Preparation, characterization and properties of novel bisphenol-A type novolac epoxy-polyurethane polymer with high thermal stability. *Macromolecules*. 2003; 36:1940.

- [35] Garrett JT, Runt J, Lin JS. Compression-molded polyurethane block copolymers. Evaluation of microphase compositions. *Macromolecules*. 2000; 33:6353.
- [36] Kausar A, Zulfiqar S, Sarwar MI. High performance segmented polyurethanes derived from a new aromatic diisocyanate and polyol. *Polym. Degrad. Stab.* 2013;98(1):368-686.
- [37] Mara CL, Renato AA, Isolda C. Effect of the NCO/OH Molar Ratio on the Physical Aging and on the Electrochemical Behavior of Polyurethane-Urea Hybrid Coating. *Int. J. Electrochem. Sci.* 2013; 8:4679-4689.
- [38] Mishra AK, Narayan R, Raju KVS, Aminabhavi TM. Hyperbranched polyurethane (HBPU)-urea and HBPU-imide coatings: effect of chain extender and NCO/OH ratio on their properties. *Prog Org Coat.* 2012; 74:134-141.
- [39] Negim E-SM, Bekbayeva L, Mun GA, Abilov ZA, Saleh MI. Effects of NCO/OH ratios on physico-mechanical properties of polyurethane dispersion. *World Appl. Sci. J.* 2011; 14:402.
- [40] García-Pacios V, Costa V, Colera M, Martín-Martínez JM. Waterborne polyurethane dispersions obtained with polycarbonate of hexanediol intended for use as coatings. *Prog. Org. Coat.* 2011; 71:136-146.
- [41] Hongmei J, Zhen Z, Wenhui S, Xinling W. Inc. Moisture-cured polyurethane/polysiloxane copolymers: Effects of the structure of polyester diol and NCO/OH ratio. *J Appl Polym Sci.* 2008; 108(6):3644-3651.
- [42] Prabhakar A, Chattopadhyay DK, Jagadeesh, Raju KVS. Structural investigations of polypropylene glycol; (PPG) and isochrone diisocyanate (IPDI)-based polyurethane prepolymer by 1D and 2D NMR spectroscopy. *Journal of Polymer Science. Part A: Polymer Chemistry.* 2005; 43(6):1196-1209.
- [43] Semsarzadeh MA, Navarchian AH. Effects of NCO/OH ratio and catalyst concentration on structure, thermal stability, and crosslink density of poly(urethane-isocyanurate). *Journal of Applied Polymer Sci.* 2003; 90(4):963-972.
- [44] Runumi G, Utpal KN, Sarwar MA, Dayal SM. Study of Effect of NCO/OH Molar Ratio and Molecular Weight of Polyol on the Physico-Mechanical Properties of Polyurethane Plaster Cast. *World Applied Sciences Journal.* 2013; 21(2):276-283.
- [45] Kewen Cai, Shixiang Zuo, Shipin Luo, Chao Yao, Wenjie Liu, Jianfeng Ma, Huihui Mao and Zhongyu Li. Preparation of polyaniline/graphene composites with excellent anti-corrosion properties and their application in waterborne polyurethane anticorrosive coatings. *RSC Advances.* 2016, 98.
- [46] Youtong Wu, Shaoguo Wen, Kaiming Chen, Jihu Wang, Guangyu Wang, Kai Sun. Preparation of sulfonated graphene/zinc phosphate mixtures as anti-corrosion additives in the aqua polyurethane tar. *Progress in Organic Coatings.* 2019; 132:409-416.
- [47] Gan Cui, Zhenxiao Bia, Shuaihua Wang, Jianguo Liu, Xiao Xing, Zili Li, Bingying Wang. A comprehensive review on smart anti-corrosive coatings. *Progress in Organic Coatings.* 2020; 148:105821.
- [48] Pei-Ying Tsai, Tzu-En Chen and Yueh-Lien Lee. Development and Characterization of Anticorrosion and Antifriction Properties for High Performance Polyurethane/Graphene Composite Coatings. *Coatings.* 2018; 7:250.
- [49] To Thi Xuan Hang, Ngo Thanh Dung, Trinh Anh Truc, Nguyen Thuy Duong, Bui Van Truoc, Pham Gia Vu, Thai Hoang, Dinh Thi Mai Thanh, Marie-Georges Olivier. Effect of silane modified nano ZnO on UV degradation of polyurethane coatings. *Progress in Organic Coatings.* 2015; 79:68-74.
- [50] Huibin Zhu, Weihong Hu, Sipei Zhao, Xin Zhang, Li Pei, Guizhe Zhao, and Zhi Wang. Flexible and thermally stable superhydrophobic surface with excellent anti-corrosion behavior. *Journal of Materials Science.* 2020; 55:2215-2225.
- [51] Yao Tong, Siva Bohm, Mo Song. The capability of graphene on improving the electrical conductivity and anti-corrosion properties of Polyurethane coatings. *Applied Surface Science.* 2017; 424:72-81.
- [52] Mahmudzadeh M, Yari H, Ramezanzadeh B, Mahdavian M. Urtica dioica extract as a facile green reductant of graphene oxide for UV resistant and corrosion protective polyurethane coating fabrication. *Journal of Industrial and Engineering Chemistry.* 2019; 78:125-136.
- [53] Xiaoyun Yea, Zhaopeng Wang, Lian Maa, Qianting Wang, Anni Chua. Zinc oxide array/polyurethane nanocomposite coating: fabrication, characterization and corrosion resistance. *Surface and Coatings Technology.* 2019; 358:497-504.
- [54] Hui Wang, Junhuai Xu, Xiaosheng Du, Zongliang Du, Xu Cheng, HaiBo Wang. A self-healing a polyurethane-based composite coating with high strength and anti-corrosion properties for metal protection. *Composites. Part B: Engineering.* 2021; 225:109273.
- [55] Godinho B, Gama N, Barros-Timmons A, Ferreira A. Recycling of different types of polyurethane foam wastes via acidolysis to produce polyurethane coatings. *Sustainable Materials and technology.* 2021; 29.
- [56] Hui Yuan, Yushuai Wang, Zhiyong Liu and Shiyu Li. A study on the properties and working mechanism of a waterborne polyurethane-modified silicatebased coating. *RSC (Royal Society of Chemistry) Adv.* 2019; 9:26817-26824.
- [57] Fengyuan Zhanga, Weiqu Liua, Liyan Lianga, Maiping Yanga, Shuo Wang, Hongyi Shia, Yankun Xiea, Ke Pia. Application of polyether amine intercalated graphene oxide as filler for enhancing hydrophobicity, thermal stability, mechanical and anti-corrosion properties of waterborne polyurethane. *Diamond and Related Materials.* 2020; 109:108077.
- [58] Jiahua Zhu, Suying Wei, Ian Y Lee, Sung Park, John Willis, Neel Haldolaarachchige, David P. Young Zhiping Luo and Zhanhu Guo. Silica stabilized iron particles toward anti-corrosion magnetic polyurethane nanocomposites. *RSC Advances.* 2012; 2:1136-1143.
- [59] Tuan Syarifah Rossyidah Tuan Naiwi, Min Min Aung, Marwah Rayung, Azizan Ahmad, Kai Ling Chai, Mark Lee Wun Fui, Emma Ziezie Mohd Tarmizi, Nor Azah Abdul Aziz. Dielectric and ionic transport properties of bio-based polyurethane acrylate solid polymer electrolyte for application in electrochemical devices. *Polymer Testing.* 2022; 106:107459.
- [60] Cheng Zhang, Kuan-Chen Huang, Haoran Wang, Qixin Zhou. Anti-corrosion non-isocyanate polyurethane polysiloxane organic/inorganic hybrid coatings. *Progress in Organic Coatings.* 2020; 148:105855.
- [61] Pavan M Paraskar, Mayur S Prabhudesai, Vinod M Hatkar, Ravindra D Kulkarni. Vegetable oil-based polyurethane coatings. *Progress in Organic Coatings.* 2021; 156:106267.
- [62] Aqdas Noreen, Khalid Mahmood Zia, Mohammad Zuber, Shazia Tabasum, and Muhammad Jawwad Saif. Recent trends in environmentally friendly water-borne polyurethane coatings: A review. *Korean Journal of Chemical Engineering.* 2015; 33:388-400.
- [63] Jing Li, Jincan Cui, Jiayun Yang, Yaya Li, Hanxum Qui, Junhe Yang. Reinforcement of graphene and its derivatives on the anticorrosive properties of waterborne polyurethane coatings. *Composites Science and Technology.* 2016; 129:30-37.

- [64] Ashraf M El Saeed, M Abd El-Fattah, Ahmed M Azzam. Synthesis of ZnO nanoparticles and studying its influence on the antimicrobial, anticorrosion and mechanical behavior of polyurethane composite for surface coating. *Dyes and Pigments*. 2015; 121:282-289.
- [65] Pooneh Haghdadeh, Mehdi Ghaffari, Bahram Ramezanzadehb, Ghasem Bahlakeh, Mohammad Reza Sae. The role of functionalized graphene oxide on the mechanical and anti-corrosion properties of polyurethane coating. *Journal of the Taiwan Institute of Chemical Engineers*. 2018; 86:199-212.
- [66] Abhijit Das, Prakash Mahanwar. A brief discussion on advances in polyurethane applications. *Advanced Industrial and Engineering Polymer Research*. 2020; 3:93-101.
- [67] Xiaohua Konga, Guoguang Liua, Hong Qi, Jonathan M Curtis. Preparation and characterization of high-solid polyurethane coating systems based on vegetable oil derived polyols. *Progress in Organic Coatings*. 2013; 76:1151-1160.
- [68] Ewa A Papaj, Douglas J Mills, Sina S Jamali. Effect of hardener variation on protective properties of polyurethane coating. *Progress in Organic Coatings*. 2014; 77:2086-2090.
- [69] Mandar S Gaikwada, Vikas V Gitea, Pramod P Mahulikar, Dilip G Hundiwalea, Omprakash S Yemul. Eco-friendly polyurethane coatings from cottonseed and karanja oil. *Progress in Organic Coatings*. 2015; 86:164-172.
- [70] Tsao-Cheng Huang, Guan-Hui Laia, Chen-En Li, Mei-Hui Tsai, Peng-Yun Wan, Yi-Hsiu Chung, Meng-Hung Lin. Advanced anti-corrosion coatings prepared from  $\alpha$ -zirconium phosphate/polyurethane nanocomposites. *RSC Advances*. 2017; 7:9908-9913.
- [71] Ying Liang, Dong Zhang, Mengyu Zhou, Yuzheng Xia, Xiaonong Chen, Susan Oliver, Shuxian Shi, Lei Lei. Bio-based omniphobic polyurethane coating providing anti-smudge and anti-corrosion protection. *Progress in Organic Coatings*. 2020; 148:105844.
- [72] Xiuyong Chen, Jianhui Yuan, Jing Huang, Kun Ren, Yi Liu, Shaoyang Lu, Hua Li. Large-scale fabrication of superhydrophobic polyurethane/nano-Al<sub>2</sub>O<sub>3</sub> coatings by suspension flame spraying for anti-corrosion applications. *Applied Surface Science*. 2014; 311:864-869.
- [73] Yajun Wang, Guoyue Xu, Huijuan Yu, Chen Hu, Xiaoxing Yan, Tengchao Guo, Jiufen Li. Comparison of anti-corrosion properties of polyurethane based composite coatings with low infrared emissivity. *Applied Surface Science*. 2011; 257:4743-4748.
- [74] Xia Wang, Jiaojiao Hu, Ying Li, Jinrui Zhang, Yuanyuan Ding. The surface properties and corrosion resistance of fluorinated polyurethane coatings. *Journal of Fluorine Chemistry*. 2015; 176:14-19.
- [75] Anna M Mikhailova, Moussa Tamboura, Meng Qiu Jia. Heat-Resistant and Anti-Corrosion Urethane-Silicone-based Coatings. *Silicon*. 2012; 4:197-208.
- [76] Yixing Zeng, Hongqiang Li, Jian Li, Jinxin Yang, Zhonghua Chen. Preparation and characterization of solvent-free anti-corrosion polyurethane-urea coatings. *Surfaces and Interfaces*. 2023, 36.
- [77] Mengting Moa, Wenjie Zhao, Zifei Chena, Eryong Liu, Qunji Xue. Corrosion inhibition of functional graphene reinforced polyurethane nanocomposite coatings with regular textures. *RSC Advances*. 2016; 6:7780-7790.



## Geochemistry of Rare Earth Elements in Pahang River Sediment, Malaysia

<sup>1</sup>Chang S.C., <sup>1\*</sup>Yusoff A.H., <sup>2</sup>Mohamed C.A.R., <sup>3,4</sup>Liu S.F., <sup>1</sup>Shoparwe N.F., <sup>1</sup>Husain N.A., <sup>5</sup>Azlan M.N.

<sup>1</sup>Gold Rare Earth and Material Technopreneurship Centre, Faculty of Bioengineering and Technology, Universiti Malaysia Kelantan, Jeli Campus, 17600 Jeli, Kelantan, Malaysia

<sup>2</sup>School of Environmental Science and Natural Resources, Universiti Kebangsaan Malaysia 43600 Bangi, Selangor, Malaysia

<sup>3</sup>Key Laboratory of Marine Geology and Metallogeny, Ministry of Natural Resources, Qingdao 266061, China

<sup>4</sup>Laboratory for Marine Geology, Qingdao National Laboratory for Marine Science and Technology, Qingdao266061, China

<sup>5</sup>Physics Department, Faculty of Science and Mathematics, University Pendidikan Sultan Idris, 35900 Tanjung Malim, Perak, Malaysia

\* Corresponding author email: hafidz.y@umk.edu.my

<p>Received: October 30, 2023 Peer-reviewed: December 2, 2023 Accepted: December 27, 2023</p>	<p><b>ABSTRACT</b> Rare earth elements (REE) are a set of 17 chemically similar metallic elements including 15 lanthanides, scandium and yttrium. The current status of REE as a global strategic commodity has encouraged the identification of REE ore deposits. This research is carried out to identify the mining feasibility of fluvial sediment REE and to understand the sediment's physical and chemical characteristics and effects on the geochemical behaviour of REE in the longest river of Peninsular Malaysia namely Pahang River. Surface sediment samples were collected along Pahang River (n=44) in approximately 10 km distance intervals. The sediment samples were analyzed using XRF to determine the major oxide content. Meanwhile, REE content in the sediment samples was extracted using the Total Digestion method and analysed using ICP-MS. The results show the average value of <math>\Sigma</math>REE at surface sediments of the Pahang River is 42.58 ppm and can be considered too low to be economically mined. Each area shows higher fractionation of light REE than heavy REE with negative europium anomalies, suggesting sediments in this area were derived from felsic rocks. The concentration of REE in Pahang River surface sediments was controlled by the porosity and organic matter as showed by the correlation of <math>\Sigma</math>REE with porosity (<math>R^2=0.65</math>) and organic matter content (<math>R^2=0.71</math>). In conclusion, this research's findings are generally useful for further REE mineral exploration and fluvial sediment environmental monitoring.</p>
	<p><b>Keywords:</b> XRD analysis; Rare Earth Elements; Pahang River, Organic Matter</p>
<p><b>Chang S.C</b></p>	<p><b>Information of the authors:</b> PhD Student at Gold, Rare Earth and Material Technopreneurship Centre, Faculty of Bioengineering and Technology, Universiti Malaysia Kelantan 17600 Jeli, Kelantan, Malaysia. Email: chang.shenchang@yahoo.com</p>
<p><b>Yusoff A.H</b></p>	<p>Associate Professor at Gold, Rare Earth and Material Technopreneurship Centre (GREAT), Faculty of Bioengineering and Technology, Universiti Malaysia Kelantan, 17600, Kelantan, Malaysia. Email: hafidz.y@umk.edu.my</p>
<p><b>Mohamed C.A.R</b></p>	<p>Professor at Marine Science Program at the Department of Earth Science and Environment, Faculty of Science and Technology, Universiti Kebangsaan Malaysia, 43600 Bangi, Selangor, Malaysia. Email: carmohd@ukm.edu.my</p>
<p><b>Liu S.F</b></p>	<p>Researcher at First Institute of Oceanography, Ministry of Natural Resources, Qingdao China, Email: liushengfa@fio.org.cn</p>
<p><b>Shoparwe N.F</b></p>	<p>Dr, Director at Gold, Rare Earth and Material Technopreneurship Centre (GREAT), Faculty of Bioengineering and Technology, Universiti Malaysia Kelantan, 17600 Jeli, Kelantan, Malaysia. Email: fazliani.s@umk.edu.my</p>
<p><b>Husain N.A</b></p>	<p>PhD Student at Gold, Rare Earth and Material Technopreneurship Centre, Faculty of Bioengineering and Technology, Universiti Malaysia Kelantan, Jeli Campus 17600 Jeli, Kelantan, Malaysia. Email: nazirahawang98@gmail.com</p>
<p><b>Azlan M.N</b></p>	<p>Dr, Senior Lecturer at Faculty of Science and Mathematics, University Pendidikan Sultan Idris, 35900 Tanjung Malim, Perak, Malaysia. Email: azlanmn@fsm.upsi.edu.my</p>

### Introduction

Located on the east coast of Peninsular Malaysia, the Pahang River (459 km) is the longest and river in Peninsular Malaysia with a main bedrock of granite and limestone; and sedimentary rock e.g. shale, sandstone, respectively [1], it contributes

annual fluvial sediment fluxes of 20.4 Mt discharge into the southern South China Sea [2]. Fluvial sediments as the particles or grains eroded from rocks and soils and then deposited on the river bed, carry traces of the parent earth materials [[3], [4], [5]], including rare earth elements (REEs) which are

a group of chemically similar, naturally occurring elements but present in trace amounts [6].

The current high-tech trend in the development and miniaturization of electronic products, clean energy generators, military systems, communication systems, and satellites which rely on the magnetic, luminescent, and electrochemical properties of REEs has immensely induced the increasing demand for REEs and economically making them a strategic commodity [[7], [8]]. Studying the elemental distribution via geochemistry in Pahang Rivers can help us not only to understand the systems and history of Earth, and inspect environmental conditions but more importantly to explore mineral deposits which are high anomalies of certain commercial elements or minerals over appreciable areas which are profitable to be mined [[9], [10], [11], [12], [13]].

Recent research has reported the potential of granite as an REE source [14], therefore, we expect Pahang River with a major granitic background might have the potential to develop fluvial REE mining. In this research, REEs were traced along the river sediments, as one of the geochemical mapping methods in regional and detailed scales is to trace the pathway of elemental movement and locate the source of elements or minerals. There are limited detailed studies available on the geochemistry and mineralogy of the tropical rivers from the East Coast of Peninsular Malaysia as previous studies were focused on the near- and estuary area [[6], [15]], therefore, geochemical studies focusing on REE from upper to lower courses of tropical river sediment is thus needed to decipher the broad view of the sediment provenance. This study was performed to characterize the chemical composition of Pahang River sediments in terms of major oxides and elements, minerals, and rare earth elements (REE) and evaluate the geochemical behaviour of REE in tropical Pahang Rivers.

### Experimental part

#### Sample Collection

The surface sediments were collected at 0 to 20cm from the river bed along the Pahang River by using an Ekman grab sampler, sealed in labelled transparent polyethylene (PE) bag and stored at 4°C for further processing. The coordinates of the sampling locations were acquired by global positioning system (GPS) Garmin GPSMAP 62s and mapped by geographic information system ArcGIS 10.2, as shown in Figure 1 and Table 1.

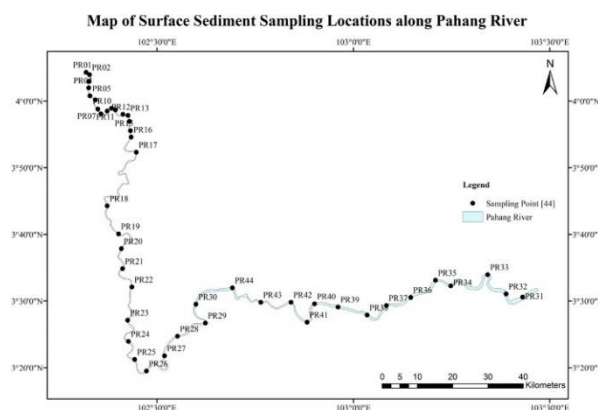


**Figure 1** - Map of surface sediment sampling location along the longest river in Peninsular Malaysia namely the Pahang River

**Table 1** - Coordinates of surface sediment sampling locations along the Pahang River

Sampling Locations	Latitude	Longitude
PR 01	04° 04' 19.20" N	102° 19' 08.40" E
PR 02	04° 03' 57.59" N	102° 19' 40.80" E
PR 03	04° 02' 56.40" N	102° 19' 33.59" E
PR 04	04° 01' 58.80" N	102° 19' 33.59" E
PR 05	04° 00' 46.79" N	102° 19' 44.39" E
PR 06	04° 00' 10.80" N	102° 20' 34.80" E
PR 07	03° 58' 47.99" N	102° 20' 56.40" E
PR 08	03° 58' 04.79" N	102° 21' 25.19" E
PR 09	03° 58' 30.00" N	102° 22' 22.80" E
PR 10	03° 58' 55.20" N	102° 23' 02.40" E
PR 11	03° 58' 40.80" N	102° 23' 38.40" E
PR 12	03° 58' 01.20" N	102° 24' 46.79" E
PR 13	03° 57' 50.39" N	102° 25' 33.60" E
PR 14	03° 56' 56.39" N	102° 25' 48.00" E
PR 15	03° 55' 33.60" N	102° 25' 55.20" E
PR 16	03° 54' 36.00" N	102° 26' 02.39" E
PR 17	03° 52' 19.19" N	102° 26' 49.20" E
PR 18	03° 44' 16.80" N	102° 22' 22.80" E
PR 19	03° 40' 04.80" N	102° 24' 07.20" E
PR 20	03° 37' 51.59" N	102° 24' 32.40" E
PR 21	03° 34' 51.60" N	102° 24' 43.20" E
PR 22	03° 32' 06.00" N	102° 26' 09.60" E
PR 23	03° 27' 07.19" N	102° 25' 29.99" E
PR 24	03° 23' 56.40" N	102° 25' 37.20" E
PR 25	03° 21' 14.40" N	102° 26' 34.79" E
PR 26	03° 19' 30.00" N	102° 28' 22.79" E
PR 27	03° 21' 46.80" N	102° 31' 08.40" E
PR 28	03° 24' 43.19" N	102° 33' 07.20" E
PR 29	03° 26' 41.99" N	102° 37' 22.80" E
PR 30	03° 29' 31.20" N	102° 35' 56.40" E
PR 31	03° 30' 35.99" N	103° 25' 51.59" E
PR 32	03° 31' 04.79" N	103° 23' 20.39" E
PR 33	03° 33' 57.59" N	103° 20' 31.19" E
PR 34	03° 32' 16.79" N	103° 14' 52.80" E
PR 35	03° 33' 07.20" N	103° 12' 32.40" E
PR 36	03° 30' 32.39" N	103° 08' 45.60" E
PR 37	03° 29' 20.39" N	103° 05' 02.40" E
PR 38	03° 27' 53.99" N	103° 02' 05.99" E
PR 39	03° 29' 05.99" N	102° 57' 39.59" E
PR 40	03° 29' 34.79" N	102° 54' 03.59" E
PR 41	03° 26' 49.20" N	102° 52' 55.20" E
PR 42	03° 29' 49.19" N	102° 50' 27.59" E
PR 43	03° 29' 49.19" N	102° 45' 50.39" E
PR 44	03° 31' 58.79" N	102° 41' 31.19" E

*Analysis of Major Oxides and REE in the sediment samples*

The sediment sample collected was weighted before and after being heated at 105°C with air ventilation of 50% in the oven until a constant weight was no longer reduced after repetitive heating. The sediment particles with mesh size below 250-µm were selected to be homogenized and pulverized to less than 45µm in a laboratory ball mill machine before sample digestion.

The samples were then analysed for major oxides analysis using Energy Dispersion XRF (EDXRF) which is outfitted with a rhodium (Rh) x-ray tube that operates at a voltage of 40 kV, and a current of 30µA for integration times ranging from 60-600 sec.

For REE analysis, about 0.2 g of the pulverized sediment sample was introduced into a 50-ml polytetrafluoroethylene (PTFE) beaker. 68% nitric acid (HNO3), 48% hydrofluoric acid (HF) and 50% hydrogen peroxide (H2O2) with a volumetric ratio of 4:3:2 with a total of 27 ml were poured carefully into the PTFE beaker and swirled to homogenize [[16], [17]]. All REE excluding Pm, were analyzed by Perkin-Elmer Elan DRC-e ICPMS at the laboratory of Universiti Kebangsaan Malaysia.

**Results and Discussion**

*Physical Characteristic and Organic Matter in Pahang River Sediments*

Pahang River sediments, as shown in Figure 2, were mainly dominated by relatively clear grains (PR01-PR05, PR08-PR11, PR13-15, PR21, PR28, PR30-PR32, PR35, PR37-39) and other greyish powdery coating grains instead of light brown of Kelantan River surface sediments due to different mineralogical composition and weathering conditions. Dry-bulk density of surface sediments along Pahang River, as shown in Figure 3 had a  $\bar{x} \pm s$  of  $1.44 \pm 0.45 \text{g/cm}^3$ , was least dense at PR42 ( $0.73 \text{g/cm}^3$ ) and was densest at PR10 ( $2.07 \text{g/cm}^3$ ). Organic matter content (OM) of Pahang surface sediments also had a fluctuated pattern with  $\bar{x} \pm s$  of  $3.23 \pm 3.19\%$ , highest OM at PR40 (10.05%), and lowest OM at PR28 (0.20%) as shown in Figure 3. Pahang River surface sediments OM shows a strong positive correlation with porosity ( $R^2=0.87$ ) suggesting their OM were highly influenced by the porosity as shown in Table 2.

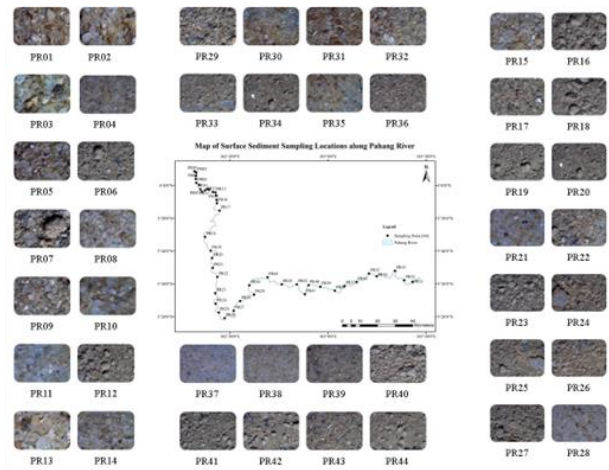


**Figure 2 - Pahang River surface sediments under stereoscopic at 5x magnification**

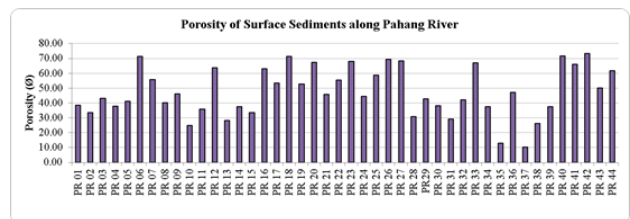


**Figure 3 - Porosity of surface sediments along Pahang River**

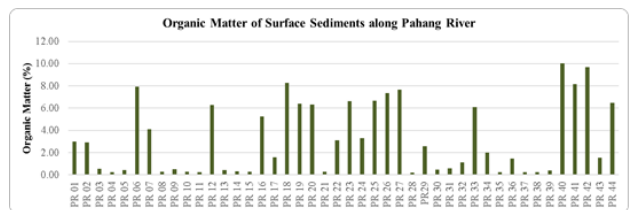


**Figure 4 - Organic matter content of surface sediments along the Pahang River**

**Table 2 - Correlation between physical characteristics of Pahang River surface sediments**

Correlation Coefficient, rPR	Organic Matter (%)	Dry-bulk density (g/cm <sup>3</sup> )	Porosity (φ)
Organic Matter (%)	1		
Dry-bulk density (g/cm <sup>3</sup> )	-0.875	1	
Porosity (φ)	0.875	-1	1

*Major Oxide in Pahang River Sediment*

The result of major oxides in sediments from the Pahang River is shown in Table 3. Maturity of Pahang river surface sediments was ranked as the following: PR08> PR24> PR30> PR10> PR21>PR02> PR28> PR13> PR11> PR32> PR15> PR03> PR14> PR29> PR04> PR09> PR01> PR34> PR31> PR05> PR12> PR36> PR35> PR17> PR25> PR37> PR07> PR38> PR16> PR41> PR18> PR33> PR39> PR20> PR19>

PR40> PR42> PR22> PR44> PR27> PR06> PR23> PR43> PR26. By applying the geochemical classification proposed by Herron (1988) [18], among 44 sampling locations along Pahang River, there are 22 subarkose, 7 wacke, 6 arkose, 3 litharenite, 3 quartz arenite and 3 shale as shown in Figure 5.

**Table 3 - Major Oxides of Pahang River surface sediments**

Location	Major Oxide Percentage (%wt)								
	Al <sub>2</sub> O <sub>3</sub>	CaO	Fe <sub>2</sub> O <sub>3</sub>	K <sub>2</sub> O	MgO	MnO	Na <sub>2</sub> O	SiO <sub>2</sub>	TiO <sub>2</sub>
PR 01	3.79	0.332	1.68	3.98	0.388	0.202	0.381	88.4	0.136
PR 02	3.4	0.113	0.594	2.83	0.242	0.179	0.265	91.4	0.127
PR 03	3.54	0.16	0.665	3.4	0.269	0.162		91.6	0.165
PR 04	3.94	0.101	0.684	3.98	0.259	0.168	0.102	90.7	
PR 05	4.37	0.102	0.769	4.69	0.265	0.109		89.5	0.1
PR 06	18.1	0.419	4.73	6.49	0.888	0.186		68	0.739
PR 07	9.73	0.25	2.11	5.74	0.377	0.121		81.2	0.302
PR 08	2.95	0.171	0.69	2.38	0.2	0.101		93.5	
PR 09	3.99	0.28	0.721	4.05	0.27	0.18		90.4	0.105
PR 10	3.21	0.186	0.811	2.82	0.28	0.264		92.2	0.146
PR 11	2.83		0.538	2.97	0.19	0.216		93.2	
PR 12	12.8	0.431	4.09	4.31	0.704	0.236		76.5	0.476
PR 13	3.14	0.125	0.812	2.89	0.236	0.105	0.214	92.3	0.102
PR 14	3.42	0.116	1.13	3.75	0.359	0.139		90.8	0.237
PR 15	3.19	0.162	0.594	3.35	0.176	0.212		92.3	
PR 16	14.1	0.469	3.88	5.69	0.846	0.183	0.314	73.6	0.518
PR 17	6.47	0.131	1.41	5.58	0.447	0.117	0.336	85.1	0.225
PR 18	18.2	0.373	4.98	5.83	0.921	0.191	0.12	68.2	0.751
PR 19	15.7	0.295	3.83	6.34	0.705	0.128		72	0.649
PR 20	15.3	0.436	3.89	6.33	0.765	0.17	0.137	72.1	0.612
PR 21	3.3	0.175	1.17	2.83	0.271	0.125		92.1	
PR 22	10.9	0.5	3	7.06	0.759	0.155		76.6	0.469
PR 23	17.2	0.519	5.97	6.54	0.725	0.159		67.4	0.708
PR 24	9.58	0.199	6.66	2.32	1.99	0.123		78.3	0.678
PR 25	14.4	0.277	3.56	5.18	0.643	0.148		74.9	0.538
PR 26	10.7	0.919	9.6	10.2	0.554	0.388	2.32	63.3	1.24
PR 27	16.7	0.527	4.64	6.47	0.807	0.238	0.48	68.8	0.725
PR 28	3.15	0.125	0.683	2.89	0.23	0.22		92.6	0.08
PR 29	4.53	0.471	1.54	3.63	0.348	0.153	0.376	87.8	0.265
PR 30	3.1	0.14	0.64	2.78	0.2	0.14		92.9	0.11
PR 31	5.79	0.117	1.18	4.31		0.195		88.2	0.141
PR 32	4.19	0.15	0.79	3.14	0.26	0.16		91.2	0.11
PR 33	13.2	0.474	4.12	6.25	0.85	0.206	0.65	72.9	0.583
PR 34	8.45	0.126	1.54	4.05	0.399	0.104		84.8	0.334
PR 35	1.91	0.387	1.77	5.83	0.187	0.187		89.1	0.09
PR 36	7.91	0.162	1.74	5.37	0.413	0.12		83.9	0.243
PR 37	2.02	0.413	1.71	6.19	0.25	0.88		88.4	0.102
PR 38	2.11	0.427	1.61	6.31		0.214		88.4	0.125
PR 39	2.27	0.41	2.05	7.46		0.271		86.5	0.105
PR 40	19.9	0.325	5.22	5.92	0.794	0.208		66.5	0.803
PR 41	18.9	0.241	4.75	5.78	0.783	0.119	0.117	68.2	0.751
PR 42	20	0.354	5.4	6	0.815	0.249		66	0.838
PR 43	5.4	0.532	3.41	10.5		0.224		78.5	0.565
PR 44	15.8	0.253	4.01	6.69	0.692	0.143		71.4	0.63

**Distribution of REEs in Pahang River Sediments**

Pahang River surface sediments had an average total REE of 42.581 ppm, LREE of 34.531 ppm HREE of 8.050 ppm as shown in Figure 6, and also in Table 4. PR06 with LREE 95.789 ppm and HREE 22.888 ppm contributing to a total REE 118.677 ppm was the highest among other Pahang River surface sediments, also having cerium being the main contributor as shown in Figure 7. The enrichment factor of each REE is also far below the economic value as illustrated in Figure 8. The spatial distribution of total REE was mapped in Figure 9.

**Map of Geochemical Classification of Surface Sediments along Pahang River**

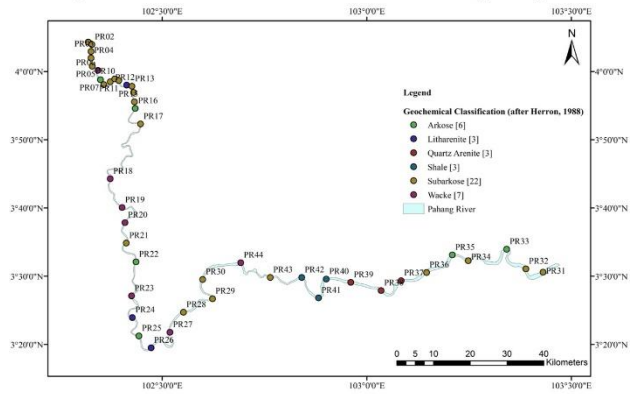


**Figure 5 - Map of geochemical classification of Pahang River surface sediments**

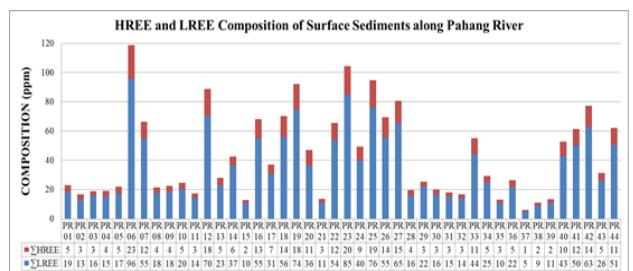


**Figure 6 - Total heavy rare earth elements (HREE) and light rare earth elements (LREE) composition (without decimal places) in Pahang River sediments.**

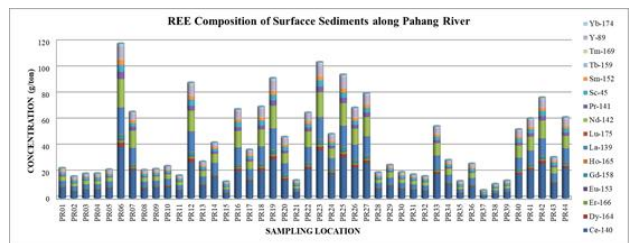


**Figure 7 - REE elemental composition in Pahang River surface sediments.**

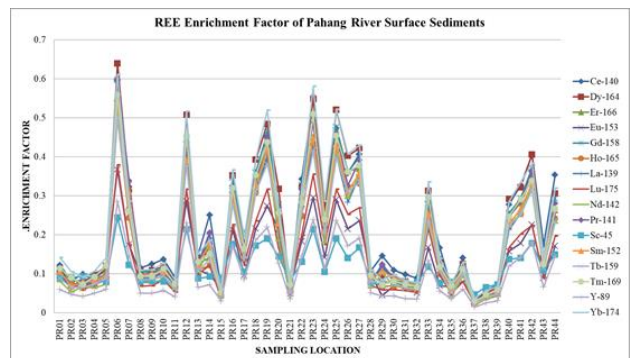


**Figure 8 - REE enrichment factor in Pahang River sediments**



**Table 4 - Total REEs of surface sediments along Pahang River**

Location	ΣLREE	ΣHREE	Total REE
PR01	18.527	4.537	23.064
PR02	13.179	3.483	16.662
PR03	15.603	3.218	18.822
PR04	15.186	3.774	18.959
PR05	17.262	4.664	21.926
PR06	95.789	22.888	118.677
PR07	54.641	11.623	66.264
PR08	17.507	4.019	21.526
PR09	18.267	4.078	22.345
PR10	20.073	4.540	24.613
PR11	14.224	3.138	17.362
PR12	70.406	18.264	88.670
PR13	22.864	5.155	28.019
PR14	36.535	6.113	42.648
PR15	10.441	2.283	12.724
PR16	54.835	13.399	68.235
PR17	30.536	6.607	37.143
PR18	55.736	14.441	70.177
PR19	74.311	17.805	92.117
PR20	36.394	10.611	47.005
PR21	10.932	2.748	13.680
PR22	53.841	11.751	65.591
PR23	84.791	19.595	104.386
PR24	39.846	9.363	49.210
PR25	75.970	18.828	94.799
PR26	55.253	14.164	69.417
PR27	65.230	15.349	80.579
PR28	15.749	3.930	19.680
PR29	21.958	3.461	25.419
PR30	16.463	3.450	19.914
PR31	15.127	2.968	18.095
PR32	14.000	2.794	16.794
PR33	44.104	11.074	55.179
PR34	24.546	4.700	29.246
PR35	10.375	2.684	13.059
PR36	21.726	4.715	26.441
PR37	4.922	1.153	6.075
PR38	8.928	1.938	10.866
PR39	11.005	2.394	13.399
PR40	42.858	9.908	52.767
PR41	49.740	11.509	61.249
PR42	62.832	14.393	77.226
PR43	26.182	5.285	31.467
PR44	50.676	11.393	62.069

**Map of Total Rare Earth Elements Distribution in Surface Sediments along Pahang River**

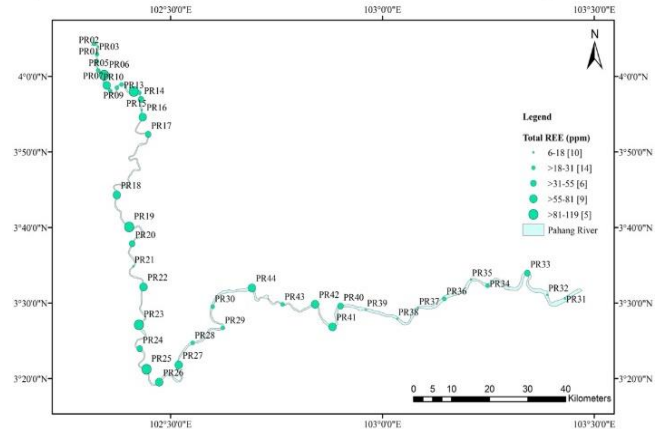


**Figure 9 - Maps of total REE in Pahang River sediments.**

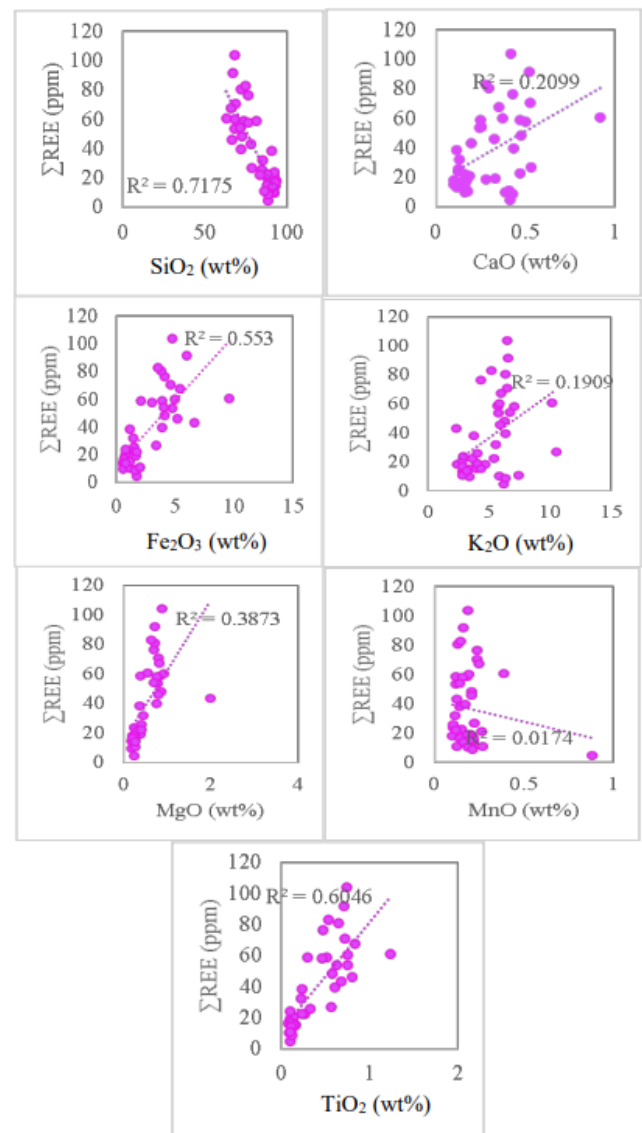


**Figure 10 - Relationship of Pahang River sediment total REE and major oxides**



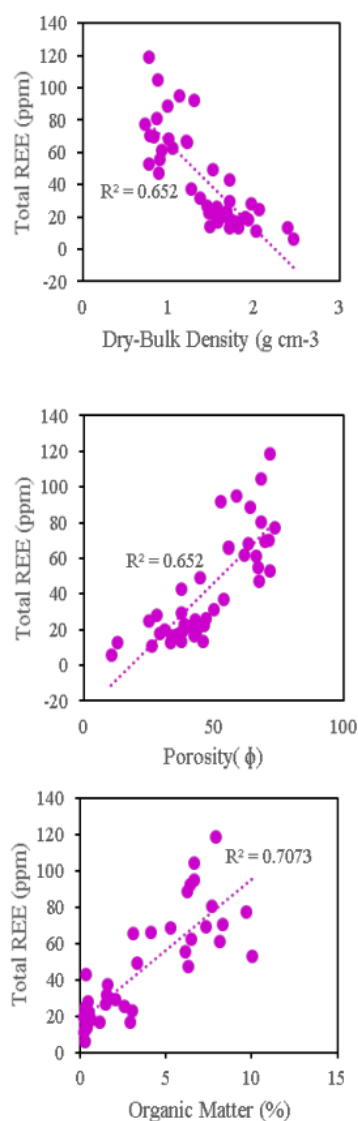


**Figure 11** - Correlation of Pahang River sediment total REE and physical characteristics.

#### *Geochemical behaviour of REE in Pahang River sediment*

The correlation of total REE in Pahang River sediments was made with oxides as shown in Figure 10. The strongest and weakest regression of surface sediment  $\Sigma$ REE was with  $\text{Al}_2\text{O}_3$  ( $R^2=0.749$ ) and  $\text{Na}_2\text{O}$  ( $r=0.0039$ ) respectively. Aluminium minerals in Pahang River surface sediments were thus inferred to have a profound effect on the occurrence of REE. Total REE in Pahang River surface sediment had a

moderate positive correlation with  $\text{Al}_2\text{O}_3$  ( $r=0.867$ ),  $\text{Fe}_2\text{O}_3$  ( $r=0.744$ ), and  $\text{TiO}_2$  ( $r=0.778$ ), showing REE concentrated in aluminium, iron, and titanium minerals; a moderate negative correlation with  $\text{SiO}_2$  ( $r=-0.848$ ) showing dilution effect of silicates in REE concentrations. REE in titanite has been proposed to interpret the growth of titanite [19]. Other than chemical influence, total REE also shows some correlations with physical characteristics: dry-bulk density and porosity ( $R^2=0.652$ ) and organic matter ( $R^2=0.7073$ ) as shown in Figure 11. As bulk density and porosity of sediments are mainly controlled by grain size, shape, packing, and distribution [20], it indicates grain size effect may be a factor controlling REE distribution in Pahang River sediments.

## Conclusions

Surface sediments collected along Pahang River had a total REE of 42.581 ppm, LREE of 34.53 ppm and HREE of 8.050 ppm. The rivers' sediments showed too low REE content and thus are not economically feasible to mine. The chondrite normalized REE showed a higher fraction of LREE to HREE in this area. Our results show the geochemical behaviour of REE in fluvial sediments was controlled by porosity and organic matter content. In addition, aluminium minerals in the Pahang River have a profound effect on REE occurrence.

**Conflicts of interest.** On behalf of all authors, the corresponding author states that there is no conflict of interest.

**Acknowledgments.** This project was supported financially through Universiti Malaysia Kelantan (UMK) research grant R/SGJP/A0100/01694A/002/2019/00581. Thanks also to technical support from the National University of Malaysia (UKM) and the First Institute of Oceanography (FIO), Ministry of Natural Resources, China for their willingness to share samples with us for this project. This project was also confounded by a UKM-FIO grant (ST-2016-005).

**Cite this article as:** Chang SC, Yusoff AH, Mohamed CAR, Liu SF, Shoparwe NF, Husain NA, Azlan MN. Geochemistry of Rare Earth Elements in Pahang River Sediment, Malaysia. Kompleksnoe Ispolzovanie Mineralnogo Syra = Complex Use of Mineral Resources. 2024; 331(4):42-50. <https://doi.org/10.31643/2024/6445.37>

## Малайзиядағы Паханг өзенінің шөгіндісіндегі сирек жер Элементтерінің геохимиясы

<sup>1</sup>Chang S.C., <sup>1\*</sup>Yusoff A.H., <sup>2</sup>Mohamed C.A.R., <sup>3,4</sup>Liu S.F., <sup>1</sup>Shoparwe N.F., <sup>1</sup>Husain N.A., <sup>5</sup>Azlan M.N

<sup>1</sup>Келантан Малайзия Университеті, Джели кампусы, 17600 Джели, Келантан, Малайзия

<sup>2</sup>Кебангсаан Малайзия Университеті, 43600 Банги, Селангор, Малайзия

<sup>3</sup>Табиғи ресурстар министрлігі, Циндао 266061, Қытай

<sup>4</sup>Циндао ұлттық теңіз ғылымы мен технологиясы зертханасы, Циндао266061, Қытай

<sup>5</sup>Пендикан Сұлтан Идрис университеті, 35900 Танджонг Малим, Перак, Малайзия

<p>Мақала келді: 30 қазан 2023 Сараптамадан өтті: 2 желтоқсан 2023 Қабылданды: 27 желтоқсан 2023</p>	<p><b>ТҮЙІНДЕМЕ</b></p> <p>Сирек жер элементтері (СЖЭ) – 15 лантаноидтарды, скандий және иттрийді қоса алғанда, 17 химиялық ұқсас металдық элементтердің жиынтығы. СЖЭ-ның жаһандық стратегиялық тауар ретіндегі ағымдағы мәртебесі СЖЭ кен орындарын анықтауды ынталандырады. Бұл зерттеу Малайзия түбегінің ең ұзын өзенінде, атап айтқанда Паханг өзенінде шөгінді СЖЭ өндірудің орындылығын анықтау және шөгінділердің физикалық және химиялық сипаттамаларының Малайзия түбегінің ең ұзын өзеніндегі СЖЭ геохимиялық әрекетіне әсерін түсіну үшін жүргізіледі. Жер үсті шөгінділерінің үлгілері Паханг өзенінің бойынан (n=44) шамамен 10 км қашықтықта жиналды. Шөгінді үлгілері негізгі оксид құрамын анықтау үшін РФТ көмегімен талданды. Сонымен қатар, шөгінді үлгілеріндегі ΣREE мәндері Total Digestion әдісімен алынған және ICP-MS көмегімен талданған. Нәтижелер Паханг өзенінің беткі шөгінділеріндегі ΣREE орташа мәндері миллионда 42,58 бөлігі ғана болатынын көрсетеді және оны экономикалық тұрғыдан өндіру үшін тым төмен. Әрбір аймақ теріс еуропий аномалиялары бар ауыр СЖЭ-ге қарағанда жеңіл СЖЭ фракциясының жоғарырақ екендігін көрсетеді, бұл осы аймақтағы шөгінділер қышқыл жыныстардан алынады. Паханг өзенінің беткі шөгінділеріндегі СЖЭ концентрациясы кеуектілікпен және органикалық заттармен анықталды, бұл ΣREE кеуектілігімен (R2=0,65) және органикалық заттардың мөлшерімен (R2=0,71) корреляция арқылы көрсетілген. Қорыта келгенде бұл зерттеудің нәтижелері СЖЭ минералдарын одан әрі барлау және өзен шөгінділеріне экологиялық мониторинг жасау үшін пайдалы.</p> <p><b>Түйін сөздер:</b> рентген құрылымдық талдау; сирек жер элементтері; Паханг өзені, органикалық заттар</p>
<p><b>Chang S.C</b></p>	<p><b>Авторлар туралы ақпарат:</b> PhD докторанты Алтын, сирек жер және материалдық технологиялар орталығында, биоинженерия және технология факультеті, Келантан Малайзия Университеті, 17600 Jeli, Келантан, Малайзия. Email: chang.shenchang@yahoo.com</p>
<p><b>Yusoff A.H</b></p>	<p>Алтын, сирек жер және материалдық технологиялар орталығының (GREAT) доценті, биоинженерия факультеті және технология кафедрасы, Келантан Малайзия Университеті, 17600, Келантан, Малайзия. Email: hafidz.y@umk.edu.my</p>
<p><b>Mohamed C.A.R</b></p>	<p>Жер туралы ғылым және қоршаған орта департаментінің Теңіз ғылымы бағдарламасының профессоры, Ғылым және технология факультеті, Кебангсаан Малайзия Университеті, 43600 Банги, Селангор, Малайзия. Email: carmohd@ukm.edu.my</p>
<p><b>Liu S.F</b></p>	<p>Бірінші Мұхиттану институтының ғылыми қызметкері, Табиғи ресурстар министрлігі, Циндао Қытай. Email: liushengfa@fio.org.cn</p>
<p><b>Shoparwe N.F</b></p>	<p>Доктор, алтын, сирек жер және материалдық технологиялар орталығы (GREAT) директоры, биоинженерия және технология факультеті, Келантан Малайзия Университеті, 17600 Jeli, Келантан, Малайзия. Email: fazliani.s@umk.edu.my</p>
<p><b>Husain N.A</b></p>	<p>PhD докторанты, Алтын, сирек жер және материалдық технологиялар орталығының биоинженерия және технология факультеті, Келантан университеті, Джели кампусы 17600 Джели, Келантан, Малайзия. Email: nazirahawang98@gmail.com</p>
<p><b>Azlan M.N</b></p>	<p>Доктор, ғылым-математика факультетінің аға оқытушысы, Пендикан Сұлтан Идрис университеті, 35900 Tanjong Malim, Перак, Малайзия. Email: azlanmn@fsm.ups.edu.my</p>

## Геохимия редкоземельных элементов в отложениях реки Паханг, Малайзия

<sup>1</sup>Chang S.C., <sup>1\*</sup>Yusoff A.H., <sup>2</sup>Mohamed C.A.R., <sup>3,4</sup>Liu S.F., <sup>1</sup>Shoparwe N.F., <sup>1</sup>Husain N.A., <sup>5</sup>Azlan M.N.

<sup>1</sup> Университет Малайзии Келантан, кампус Джели, 17600 Джели, Келантан, Малайзия

<sup>2</sup> Университет Малайзии Кебангсаан, 43600 Банги, Селангор, Малайзия

<sup>3</sup> Министерства природных ресурсов, Циндао 266061, Китай

<sup>4</sup> Национальная лаборатория морских наук и технологий Циндао, Циндао 266061, Китай

<sup>5</sup> Университет Пендикан Султан Идрис, 35900 Танджонг Малим, Перак, Малайзия

<p>Поступила: 30 октября 2023          Рецензирование: 2 декабря 2023          Принята в печать: 27 декабря 2023</p>	<p><b>АННОТАЦИЯ</b></p> <p>Редкоземельные элементы (РЗЭ) представляют собой набор из 17 химически схожих металлических элементов, в том числе 15 лантаноидов, скандия и иттрия. Текущий статус РЗЭ как глобального стратегического товара способствовал выявлению месторождений РЗЭ. Это исследование проводится для определения возможности добычи речных отложений РЗЭ и понимания влияния физических и химических характеристик отложений на геохимическое поведение РЗЭ в самой длинной реке полуострова Малайзия, а именно в реке Паханг. Пробы поверхностных отложений были собраны вдоль реки Паханг (n=44) на расстоянии примерно 10 км. Образцы отложений были проанализированы с помощью РФА для определения содержания основного оксида. Тем временем содержание РЗЭ в пробах отложений было экстрагировано методом полного расщепления и проанализировано с помощью ICP-MS. Результаты показывают, что средние значения <math>\Sigma\text{REE}</math> в поверхностных отложениях реки Паханг составляют 42,58 частей на миллион, и их можно считать слишком низкими для экономичной добычи. На каждом участке наблюдается более высокое фракционирование легких РЗЭ, чем тяжелых РЗЭ, с отрицательными аномалиями европия, что позволяет предположить, что отложения на этом участке произошли из кислых пород. Концентрация РЗЭ в поверхностных отложениях реки Паханг контролировалась пористостью и органическим веществом, о чем свидетельствует корреляция <math>\Sigma\text{PZЭ}</math> с пористостью (<math>R^2=0,65</math>) и содержанием органического вещества (<math>R^2=0,71</math>). В заключение можно сказать, что результаты этого исследования в целом полезны для дальнейшей разведки полезных ископаемых РЗЭ и экологического мониторинга речных отложений.</p>
	<p><b>Ключевые слова:</b> рентгеноструктурный анализ; Редкоземельные элементы; Река Паханг, органическое вещество</p>
<b>Chang S.C</b>	<p><b>Информация об авторах:</b>          Докторант, Южная Каролина, Центра технологического предпринимательства в области золота, редких земель и материалов, факультет биоинженерии и технологий, Университет Малайзии Келантан, 17600 Джели, Келантан, Малайзия.          Email: chang.shenchang@yahoo.com</p>
<b>Yusoff A.H</b>	<p>Доцент Центра технопредпринимательства по золоту, редкоземельным и материальным материалам (GREAT), факультет биоинженерии и технологий, Университет Малайзии Келантан, 17600, Келантан, Малайзия. Email: hafidz.y@umk.edu.my</p>
<b>Mohamed C.A.R</b>	<p>Профессор программы морских наук факультета наук о Земле и окружающей среды факультета науки и технологий Университета Малайзии Кебангсаан, 43600 Банги, Селангор, Малайзия. Email: cartohd@ukt.edu.my</p>
<b>Liu S.F</b>	<p>Научный сотрудник Первого института океанографии Министерства природных ресурсов, Циндао, Китай. Email: liushengfa@fio.org.cn</p>
<b>Shoparwe N.F</b>	<p>Доктор, директор Центра технопредпринимательства по золоту, редкоземельным и материальным материалам (GREAT), факультет биоинженерии и технологий, Университет Малайзии Келантан, 17600 Джели, Келантан, Малайзия. Email: fazliani.s@umk.edu.my</p>
<b>Husain N.A</b>	<p>Докторант Центра технологического предпринимательства по золоту, редкоземельным металлам и материалам, факультет биоинженерии и технологий, Университет Малайзии Келантан, кампус Джели, 17600 Джели, Келантан, Малайзия. Email: nazirahawang98@gmail.com</p>
<b>Azlan M.N</b>	<p>Доктор, старший преподаватель факультета естественных наук и математики Университета Пендидикан Султан Идрис, 35900 Танджонг Малим, Перак, Малайзия. Email: azlanmn@fsm.ups.edu.my</p>

## References

- [1] Department of Survey and Mapping Malaysia (JUPEM). Keluasan Malaysia (Malaysia Area). Retrieved on November 18, 2023. (in Malay.). [http://www.data.gov.my/data/ms\\_MY/dataset/keluasan-malaysia](http://www.data.gov.my/data/ms_MY/dataset/keluasan-malaysia)
- [2] Sathiamurthy E. River discharge characteristics of major east coast rivers of Peninsular Malaysia into South China Sea. 1<sup>st</sup> International Workshop on the Fluvial Supply to the South China Sea, Shanghai, China. 2008;
- [3] McLennan S, Murray R. Geochemistry. Springer: Dordrecht, Netherlands, Germany. Geochemistry of sediments. 1998, 282-292.
- [4] Boggs S. Principles of sedimentology and stratigraphy. 4<sup>th</sup> ed. Pearson Prentice Hall: Upper Saddle River, New Jersey, USA. 2006.
- [5] Nichols G. Sedimentology and Stratigraphy, 2<sup>nd</sup> ed. Wiley-Blackwell Malden: Massachusetts, USA. 2009.
- [6] Wu K, Liu S, Kandasamy S, Jin A, Lou Z, Li J, Shi X. Grain-size effect on rare earth elements in Pahang River and Kelantan River, Peninsular Malaysia: Implications for sediment provenance in the southern South China Sea. Continental Shelf Research. 2019; 189:103977. <https://doi.org/10.1016/j.csr.2019.103977>
- [7] Balaram V. Rare earth elements: A review of applications, occurrence, exploration, analysis, recycling, and environmental impact. Geoscience Frontiers. 2019; 10(4):1285-1303. <https://doi.org/10.1016/j.gsf.2018.12.005>
- [8] Kragh H. Chemical Sciences in the 20th Century: Bridging Boundaries. in Reinhardt C(Ed.). John Wiley & Sons: Weinheim, Germany. From geochemistry to cosmochemistry: The origin of a scientific discipline. 2008; 1915-1955:160-192.
- [9] Scott S. Treatise on Geochemistry in Holland H, Turekian K. (Eds). Elsevier: Italy. Volume Editor's Introduction. 2014; XXIII-XXV.

- [10] Yusof NN, Abd Azis MN, Yusoff NM. Exploring the Impact of Plasmonic Nanoparticles on Photoluminescence of Er<sup>3+</sup> - Doped Sodium Zinc Tellurite Glass for Solid-State Laser Applications. *Kompleksnoe Ispolzovanie Mineralnogo Syra*. 2023; 330(3):85-91. <https://doi.org/10.31643/2024/6445.32>
- [11] Volodin V, Tuleushev Y, Kenzhaliyev B, Trebukhov S. Thermal degradation of hard alloys of the niobiumcadmium system at low pressure. *Kompleksnoe Ispolzovanie Mineralnogo Syra*. 2020; 312(1):41-47. <https://doi.org/10.31643/2020/6445.05>
- [12] Shaari HR, Azlan MN, Azlina Y, et al. Investigation of Structural and Optical Properties of Graphene Oxide-Coated Neodymium Nanoparticles Doped Zinc-Tellurite Glass for Glass Fiber. *J Inorg Organomet Polym*. 2021; 31:4349-4359. <https://doi.org/10.1007/s10904-021-02061-7>
- [13] Azlan MN, Hajer SS, Halimah MK, et al. Comprehensive comparison on optical properties of samarium oxide (micro/nano) particles doped tellurite glass for optoelectronics applications. *J Mater Sci: Mater Electron*. 2021; 32:14174-14185. <https://doi.org/10.1007/s10854-021-05961-z>
- [14] Shafiee NS, Bahar AM, Ali Khan MM. Potential of Rare Earth Elements (REEs) in Gua Musang Granites, Gua Musang, Kelantan. *IOP Conference Series: Earth and Environmental Science*. 2020; 549:012027. <https://doi.org/10.1088/1755-1315/549/1/012027>
- [15] Shaari H, Nasir QM, Pan HJ, Mohamed C, Yusoff AH, Khalik WW, Anthony EJ. Sedimentation and sediment geochemistry in a tropical mangrove channel meander, Sungai Kerteh, Peninsular Malaysia. *Progress in Earth and Planetary Science*. 2020; 7(46). <https://doi.org/10.1186/s40645-020-00362-y>
- [16] Yusoff AH, Mohamed CAR. Natural Radionuclide of <sup>230</sup>Th in Malaysian Harbor Sediments. *International Journal of Advanced Science and Technology*. 2019; 28(18):65-71.
- [17] Wu K, Liu S, Shi X, Lou Z, Kandasamy S, Wu B, Mohamed CAR. Distribution of rare earth elements in surface sediments of the western Sunda Shelf: Constraints from sedimentology and mineralogy. *Continental Shelf Research*. 2020; 206:104198. <https://doi.org/10.1016/j.csr.2020.104198>
- [18] Herron MM. Geochemical Classification of Terrigenous Sands and Shales from Core or Log Data. *Journal of Sedimentary Petrology*. 1988; 58(5):820-829. <https://doi.org/10.1306/212F8E77-2B24-11D7-8648000102C1865D>
- [19] Scibiorski E, Kirkland CL, Kemp AS, Tohver E, Evans NJ. Trace elements in titanite: A potential tool to constrain polygenetic growth processes and timing. *Chemical Geology*. 2019; 509(8):1-19. <https://doi.org/10.1016/j.chemgeo.2019.01.006>
- [20] Flemming BW, Delafontaine MT. *Encyclopedia of Estuaries*. *Encyclopedia of Earth Science Series in Kennish MJ (Ed.)*. Springer:Dordrecht. Mass Physical Sediment Properties. 2016.



DOI: 10.31643/2024/6445.38

Earth sciences

## Analyzing geodetic leveling and subsidence of benchmarks: data and conclusions for Zhezkazgan and GEV-Lermontovo villages

<sup>1\*</sup> Zhunussova G.E., <sup>1</sup> Igemberlina M.B., <sup>2</sup> Abekov U.E.

<sup>1</sup> *Abylkas Saginov Karaganda Technical University, Karaganda, Kazakhstan*

<sup>2</sup> *Karaganda casting and engineering plant, Karaganda, Kazakhstan*

\*Corresponding author email: [lena\\_gulya@mail.ru](mailto:lena_gulya@mail.ru)

<p>Received: November 1, 2023 Peer-reviewed: November 20, 2023 Accepted: January 4, 2024</p>	<p><b>ABSTRACT</b></p> <p>This article analyzes geodetic leveling data at sites in the villages of Zhezkazgan and GEV-Lermontovo for the period from 2014 to 2020 using correlation matrices, statistical tests, and box plots. Using the rock displacement data on benchmarks along selected profile lines, detailed analyses were conducted in two groups (Group "A" with the data from 2018 to 2020 and Group "B" with the in-depth study of subsidence levels since 2014). In group "A", correlation matrices were analyzed and statistically significant relationships were determined between the levels of subsidence of the benchmarks. Group "B" was aimed at studying changes in the level of subsidence along the three profile lines for different periods. Using box plots, the distribution and variability of subsidence levels were visualized, anomalies were identified and potential problem areas were identified. The results indicate significant subsidence on profile line 115 caused by mining activities in the area of the Lermontovo hydraulic fracturing site. These studies are valuable information for geodesists and geologists and can be used to manage urban development, infrastructure stability, and environmental protection in the region. The results obtained are of interest for further studies and can serve as the basis for the development of appropriate strategies and remedial measures.</p>
	<p><b>Keywords:</b> instrumental observations, geodetic monitoring, geodesy, leveling, profile lines</p>
<p><b>Zhunussova G.E.</b></p>	<p><b>Information of the authors:</b> <i>Candidate of Technical Sciences, Abylkas Saginov Karaganda Technical University, 100027, Nursultan Nazarbayev Ave., No. 56, Karaganda, Kazakhstan. Email: <a href="mailto:lena_gulya@mail.ru">lena_gulya@mail.ru</a></i></p>
<p><b>Igemberlina M.B.</b></p>	<p><i>Master of Engineering, Abylkas Saginov Karaganda Technical University, 100027, Nursultan Nazarbayev Ave., No. 56, Karaganda, Kazakhstan. Email: <a href="mailto:igemberlina@mail.ru">igemberlina@mail.ru</a></i></p>
<p><b>Abekov U.E.</b></p>	<p><i>PhD, Karaganda casting and engineering plant, 100000, Orlov Street, No. 103/2, Karaganda, Kazakhstan. Email: <a href="mailto:ulan_abekov@mail.ru">ulan_abekov@mail.ru</a></i></p>

### Introduction

Monitoring, defined as the systematic observation of dynamic environmental conditions for control, analysis, and the prediction of changes, plays a pivotal role in assessing alterations in the natural world, often stemming from both natural phenomena, such as lithospheric plate movements and changes in weather conditions, and human activities, including soil reclamation and river channel modifications [1]. The progression of this field can be traced back to the 1990s when the widespread availability of Global Navigation Satellite Systems (GNSS) and the proliferation of GPS satellites enabled geodesists to meticulously track the Earth's crust movements with millimeter-level precision. This technological advancement shed light on the influence of seasonal shifts on tectonic movements and catalyzed investigations into surface load dynamics [2]. Nevertheless, satellite gravimetry exhibited certain limitations in the realm

of geodesy. These restrictions stemmed from its temporal constraints, as despite the possibility of continuous online monitoring, the frequency of observations remained restricted to a few times a year. The expansion of observations through this method was further hindered by the intricate use of offshore platforms that combined geodetic positioning through GNSS and acoustic distance measurements [3]. As a response to these challenges, high-precision digital levels were developed for geodetic monitoring. Although their theoretical significance is well-established, their practical utility necessitates additional research and a thorough error analysis. Contemporary literature predominantly centers on the implementation of information technology in the analysis of data obtained from digital leveling methods, GNSS, and 3D sensors [4]. However, there remains a notable paucity in the discourse about the process of scrutinizing the acquired data through robust statistical metrics.



To address this identified gap in the literature, this study focuses on the analysis of instrumental observations in the Zhezkazgan and GEV-Lermontovsky districts since 1997. The data procured was categorized, evaluated for correlations, and trends, and juxtaposed against established benchmarks. The analytical framework is built upon the utilization of the R programming language. The study aspires to uncover insights into the connections between subsidence levels, discernible trends, and deviations from standard subsidence patterns across distinct lines. The credibility of the findings is underpinned by rigorous statistical modeling and the computation of p-values.

### Experimental

A program for monitoring the subsidence of the earth's surface is being actively implemented at the Zhezkazgan field. The main measurement method used in this program is geodetic leveling used to analyze changes in surface level by accounting for differences in elevation.

### Discussing the results

The measurement process is carried out along the network of 148 profile lines with a total length of 48 kilometers. The process of instrumental measurements includes the leveling of ground benchmarks located on profile lines No. 78, 79, 80, and 81. Benchmarks are placed above the areas where field development work has been carried out and are oriented by the main streets of the central and southern parts of the village. Instrumental observations cover profile lines No. 33 Bis 166, 77, 78, 76, 79, 80, 81, and 169, the total length of which is 4.39 kilometers. The integrated monitoring and measurement approach provides the necessary data to thoroughly assess the impact of resource extraction on the land surface and utilities [5].

The geodetic points established on the earth's surface and used for observations were usually placed near profile lines to ensure collecting the necessary data on the boundaries of the displacement area and key parameters of the process of deformation of the earth's surface. For observations, working and auxiliary geodetic benchmarks were used, including short-term driving ones. Such benchmarks were made of bar or drill steel and had a length of 1.5-2.0 meters and a diameter of 15 to 20 millimeters. When laying

geodetic benchmarks in areas of the earth's surface where there was a risk of mechanical damage, the centers of the benchmarks were placed in special burials or holes [[6], [7]].

Observations of benchmarks at the geodetic station were carried out using a digital level. Such steps as Leica DNA03, lined invar slats, cast iron shoes and included the following:

1. Implementing planned and altitude reference reference points to the starting points and periodic monitoring of their immobility during observations.
2. Carrying out initial observations to determine the position of benchmarks at the observation station in the horizontal and vertical planes.
3. Measuring distances between benchmarks along profile lines.
4. Leveling all the benchmarks at the observation station.
5. Repeated observing the position of benchmarks at the observation station to determine the magnitude of their displacement.
6. Periodic surveys of cracks, failures and areas of collapse of the earth's surface [8].

Measurements in each period were performed in 2 series of observations. The information received was processed and the leveling of classes I and II was equalized by the requirements of the instructions [9]. Corrections are calculated with an accuracy of 1 mm. Their values are written with their signs above their corresponding excesses [10]. Collected over many years, multi-faceted data from different lines provides the completeness and reliability of the information needed to assess the impact of underground mining on the earth's surface and engineering infrastructure.

To identify the main relationships between the various geodetic profile lines, the lines were divided into two subgroups based on the available information. The first subgroup ("A") included profile lines with data from 2018 to 2020, while the second group ("B") focused on a more in-depth study of subsidence levels since the 2014s.

With the analysis of data available in group "A" for the period from 2018 to 2020, the priority task was to evaluate the correlation matrices. Correlation is a key concept in this statistical analysis that examines the relationship between variables in the context of their degree and direction [11]. The Pearson correlation coefficient, typically ranging from -1 to 1, indicates the strength and nature of the relationship between variables. A positive value means a positive correlation, indicating that as one variable increases, the other also tends to increase. Conversely, a negative value means a negative

correlation, where increasing one variable corresponds to decreasing another. A correlation of 0 implies that there is no linear relationship between the variables [12]. This type of analysis was aimed at quantifying the strength and direction of connections between pairs of profile lines and was justified by the temporal proximity of the selected period, which made it possible to reduce the effect of external factors on the data, making the analysis more targeted and reliable [13].

In addition to identifying relationships, the key objective of this analysis was also to determine which pairs of profile lineages exhibited statistically significant associations. For this purpose, the generally accepted “p” value was used, which represents the probability of observing a strong correlation calculated under the condition that there was no actual relationship between the variables. When the p-value is below a predetermined significance level, which in scientific studies is set at 0.05, the correlation is considered statistically significant, rejecting the null hypothesis and proving that there is a 95% chance that the trend found is not due to chance [[14], [15]]. To apply this statistical test, the following hypotheses were used:

- *Null hypothesis* ( $H_0$   $p \leq 0.05$ ): There is no relationship between the levels of subsidence of benchmarks from different lines.

- *Alternative hypothesis* ( $H_1$   $p > 0.05$ ): The relationship between the levels of subsidence of benchmarks from different lines is present and is not an accident based on statistical calculations.

Studying internal correlations in group “A” is of paramount importance, as it allows for identifying connections between the data that could be affected by common factors or events in a given period, which is valuable for making informed decisions and future forecasting [16].

Group “B” includes the data for three time intervals: 2014–2015, 2015–2018 and 2020–2024. The intervals were selected with the expectation that longer time periods could reveal broader and cyclical trends in the data [17]. These findings will be significant for long-term planning and identification of non-obvious patterns that might be missed in shorter intervals, such as in group “A”.

In addition to separate analysis by groups, a general statistical assessment of all the profile lines was also carried out. For each data line study, both minimum and maximum values were determined according to all available information. This synthesis study, which is necessary to assess the spread of data and identify extreme values, can help establish

control criteria and determine the limits of expected values in the future [18].

To demonstrate visually the distribution and variability of subsidence levels in each row, a box plot diagram method will be used. Box plots provide a condensed view of the distribution of data, showing the quartile mean and possible anomalies [19].

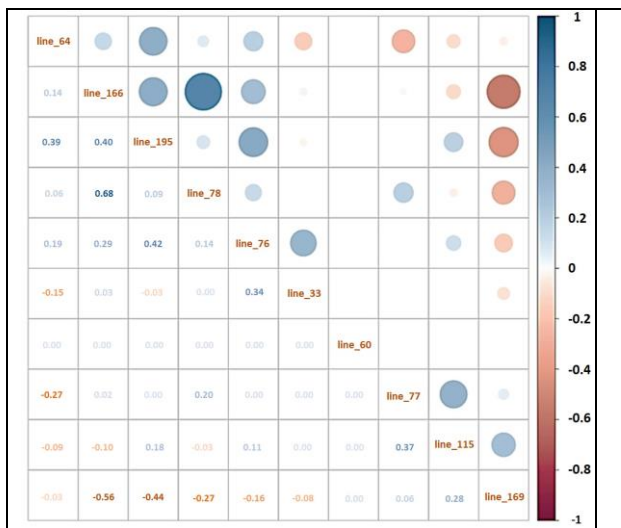
The overall line-by-line analysis process is presented in Table 1. All the analysis processes were carried out in the R programming language.

**Table 1 – Research methodology**

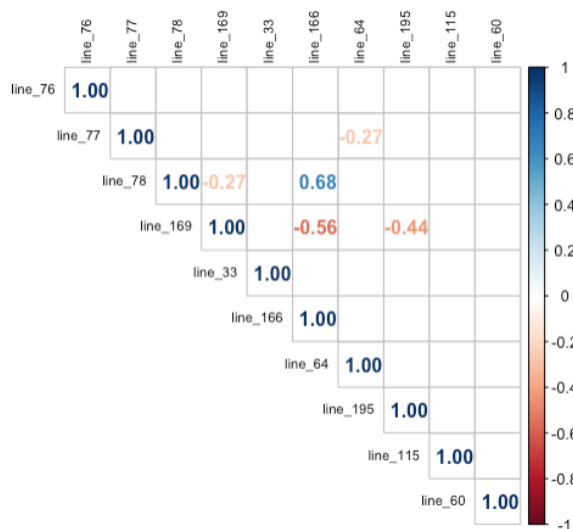
Characteristics of profile lines	Group A	Group B
Profile lines (Nos)	76. 77. 78. 169. 33. 166. 64. 195. 115. 60	79. 80. 81
Period	2018-2020	2014-2020
Analytical method	Correlation matrices and statistic test for significance	Identifying long-term regularities: cross analysis
General analysis for all the profile lines, building box plots		

**Group A.** In this study, we used the “corrplot” package in R to visualize the correlation matrix of the processed data [20]. The correlation matrix was calculated using rock displacement data on benchmarks along selected profile lines, organized using the order and eigenvalue method. The resulting correlation matrix shown in Figure 1a, provides a graphical representation of the relationships between variables: each cell in the matrix corresponds to the correlation coefficient between two variables, and the colors represent their intensities. And circular shapes are used to visually represent the strength and direction of these associations. This visualization technique allows quick and intuitive evaluating the relationships between variables, helping to identify potential patterns or relationships that may be of interest for further investigation. To the left of the cells is the color scale based on the Pearson correlation coefficient.

To highlight statistically significant relationships between variables, an additional correlation matrix plot was created (Figure 1b). This plot displays only statistically significant correlations based on the p value level  $\leq 0.05$ , and non-significant associations are represented by empty cells. Correlation coefficients are presented as numeric values in the upper triangle of the matrix, with black text and rotated 90 degrees to improve readability.



a)



b)

**Figure 1** – Correlation matrices based on the analyzing profile lines in the group A: general values (a) and statistically significant correlations (b)

In total, of the 45 possible combinations, 28 showed any linear relationship between benchmark subsidence levels between 2018 and 2020, of which only five pairs showed statistically significant correlations sufficient to accept the alternative hypothesis. The presence of nonsignificant correlations highlights the selectivity of these five major pairs of variables in the context of our study.

Firstly, there was observed a moderate negative correlation ( $r=-0.27$ ) between profile lines No. 74 and No. 64, which indicates the inverse relationship. This correlation suggests that as the values in line No. 74 increase, the values in line #64 tend to decrease.

The same inverse relationship is reflected in the correlation between profile lines No. 79 and No. 169, where a similar negative correlation was revealed ( $r = -0.27$ ). On the other hand, a strong positive

correlation ( $r=0.68$ ) was evident in the case of profile lines No.78 and No.166, confirming a strong linear relationship. In this scenario, as the values in line No. 78 increase, the values in line #166 show a corresponding increase. At the same time, the connection between line No. 169 and line No. 166 was characterized by a significant negative correlation ( $r= -0.56$ ), which indicates a pronounced inverse relationship. In this case, the increase in values on line No. 169 is associated with a decrease in values on line No. 166.

**Group B.** The data represent changes in the level of subsidence of benchmarks along profile lines No. 79, 80, and 81 for three separate periods. To begin with, each line will be considered separately, then a comparative analysis will be carried out.

Overall, on line No. 79 (Figure 2), the data shows a noticeable downward trend in altitude at most control points over the three periods. The rate of decline varies, with some indicators showing greater changes than others. Data for the period 2014–2015. show an initial decrease in height. At the same time, benchmark No. 13 demonstrates the most significant subsidence at the level of -8.5 mm. Likewise, most benchmarks continue their negative trend during 2014–2018. At the same time, benchmark No. 13 demonstrates a noticeable decrease of -10.5 mm. During the period 2014–2020, the pattern continues, however, it is noteworthy that during this period there was a sudden subsidence of -13.1 mm at benchmark No. 32. In general, the most significant changes occur in the period 2014–2018, and in 2014–2020 this trend continues.

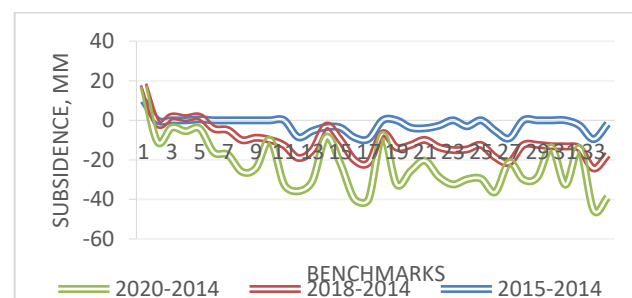


**Figure 2** – Plot of benchmark subsidence on profile line No. 79

On line No. 80 (Figure 3) the data shows short-term fluctuations in benchmark levels. These fluctuations suggest local variations in decline or rise that are not part of a broader long-term trend.

Throughout the period from 2014 to 2020, the data shows a stable pattern or a slight increase and a very gradual stabilization. In the initial period (2014–2015),

most indicators showed positive values, indicating a general trend of slight growth or stabilization. However, in the future, there was a noticeable variation on benchmark No. 10, where from 2014 to 2018 there was a significant decrease (-4.9 mm) in comparison with indicators No. 20 and No. 23, which showed positive levels of stabilization in the period from 2014 to 2020. Indicating the rise in the surrounding area. It is noteworthy to emphasize that signs about benchmarks Nos. 10, 22, and 24 exhibits more marked variations, suggesting the necessity for additional investigation into possible local issues. Conversely, such benchmarks as those Nos. 20 and 9 show consistent, albeit gradual, uplift, which may reflect regional geologic factors. In addition, Benchmarks Nos. 1, 2, and 7 show consistent patterns of uplift or slight subsidence over many years, which can provide valuable information to surveyors.

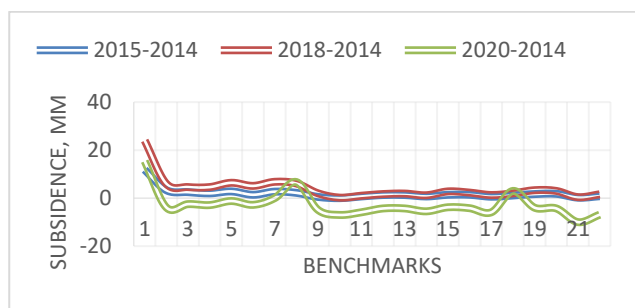


Figure 3 – Plots of benchmark subsidence on profile line No. 80

Examination of the line No. 81 data set (Figure 4) shows a consistent pattern of subsidence over three periods. At the same time, a significant decrease in height is recorded at control points. This subsidence pattern can have far-reaching consequences for the structural stability of buildings and infrastructure in the area. Benchmark No. 6 stands out as the most pronounced subsidence, decreasing by -6.8, -31.8, and -38.6 units over the corresponding time intervals. The other benchmarks also show a consistent decline in height, although not as steep as Benchmark No. 6.

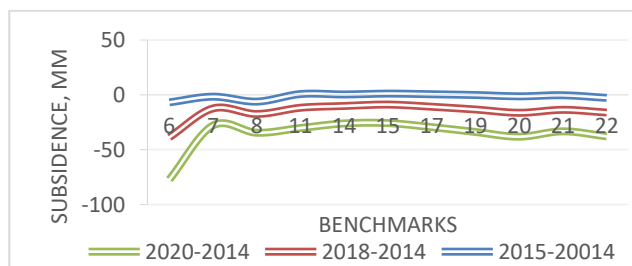


Figure 4 - Plots of benchmark subsidence on the profile line No. 81

In conclusion, the data set shows varied patterns of elevation change along lines 79, 80, and 81. While lines 79 and 81 consistently exhibit subsidence, line 80 exhibits variations in elevation with temporary stabilizations, likely due to local geologic conditions. These results highlight the need for in-depth geodetic and geological studies to identify the root causes of these changes and their potential implications for urban development, infrastructure stability, and environmental management in the affected regions.

**General analysis.** A box plot, also known as a box-and-whisker plot, is a graphical representation used to display the distribution and summary statistics of a numerical variable such as benchmark settlements. It consists of a rectangular “box” enclosing the interquartile range (IQR), which represents the middle 50% of the data. Within the box, a vertical line or “whisker” represents the median, which is the average value when sorting the data. The bottom and top edges of the box represent the first quartile (Q1) and third quartile (Q3), respectively that divide the data into four equal parts. The whiskers extend from the edges of the rectangle to the minimum and maximum values within a certain range, usually calculated as 1.5 times the IQR. Any data points outside this range are usually shown as individual points and are considered outliers. The boxplot provides a visual summary of the data's central tendency (median) scatter (IQR) and the presence of outliers. This is a valuable tool for comparing the distribution of a “linear” variable across different categories or periods, revealing potential patterns, skewness, and extreme values [21].

Among the identified results (Figure 5a, b), the boxplot for line No. 151 between 2018 and 2020 showed the greatest variability, as evidenced by a relatively wide interquartile range (IQR) with total variation starting from a maximum subsidence level of -50 mm. However, in comparison with other benchmark levels, no anomalies were identified in the case considered, while line No. 166 had the least variability during the same period. However, on a certain benchmark, an unusually low indicator was observed that did not fit into the maximum rate of change according to the average value along the profile line. The largest number of such emissions, indicating significant fluctuations in benchmarks within this category, was traced for line No. 80. All detected anomalies had a positive value. The changes indicated that certain benchmarks should be studied in more detail since they fall outside the typical range. The boxplot for profile line No. 33



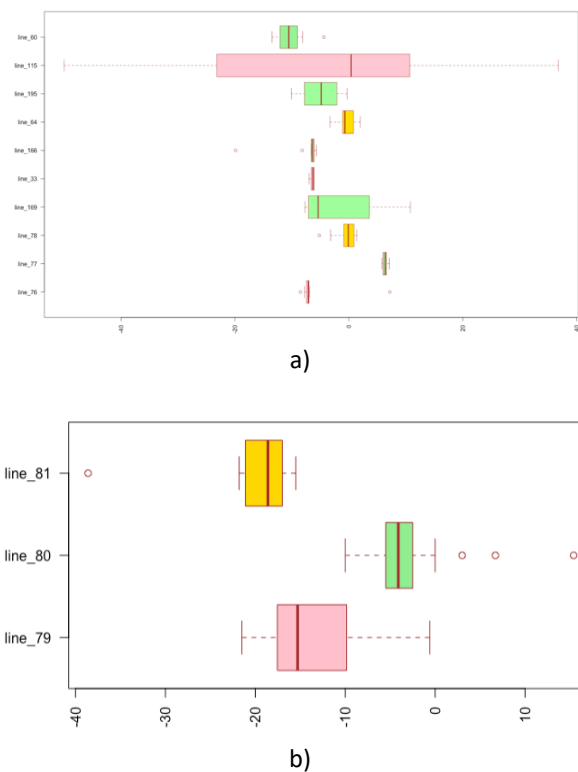


**Figure 5** – Box plot diagram for group A (a) and box plot diagram for group B (b)

showed the lowest variability with a relatively narrow IQR, suggesting that the rate of benchmark settlement remained more consistent and clustered around the median along the entire line.

In general, the geometric leveling paths laid at this site correspond to accuracy classes I and II. In the analysis carried out, from the results of instrumental observations carried out along the profile lines of the village Zhezkazgan and GEV-Lermontovo for the period from 2014 to 2020 there was revealed the greatest subsidence of the benchmarks along profile line No. 115, which ranges up to 50 mm. This is due to the fact that most of the territory of the village. The Lermontovo hydraulic fracturing site has been worked out, and the adjacent areas, in accordance with the deposit-by-deposit mining plans, are undergoing both primary and repeated development of reserves for different deposits, and there are also zones of multiple overlaps of mined-out areas.

**Conclusion.** As a result of the study based on the analysis of geometric leveling data in the village Zhezkazgan and GEV-Lermontovo for the period from 2014 to 2020, important conclusions were obtained significant for further geodetic, geological, and engineering research.

Firstly, a noticeable subsidence of the benchmarks was discovered in the areas under

consideration, especially on some profile lines. This indicates the possible effect of underground geology and mining on the structure of the land in these areas. Such changes have significant implications for the safety of residents and infrastructure, so systematic monitoring and analysis is required to effectively control and manage risks.

Secondly, correlation matrices made it possible to identify both statistically significant and insignificant relationships between subsidence levels on different profile lines. These results highlight the complexity of the relationships between different variables and the need for a deep understanding of the factors influencing land surface changes.

Thirdly, box plots made it possible to visualize the variability of data over different time periods and along different profile lines. The identified anomalies indicate the need for further in-depth research to accurately determine the causes of such deviations and develop measures to prevent possible negative consequences.

Based on these findings, additional geological and geodetic studies are recommended, considering regional geological features and mining history. This approach will help to accurately identify the factors influencing benchmark settlement and plan effective measures to address potential risks to the structural stability and safety of site occupants. Only such efforts will ensure sustainable development and guarantee the long-term safety of infrastructure.

## Final results

1. The in-depth analysis of instrumental observations along profile lines in the Zhezkazgan and GEV-Lermontov areas since 1997 made it possible to identify significant fluctuations in the levels of benchmarks subsidence on various profile lines within the period under review.

2. A significant part of the village area in the Lermontovo hydraulic fracturing site is subject to overworking, and there are also zones of multiple overlaps of mined-out areas, which causes significant fluctuations and anomalies in the levels of benchmark subsidence, exceeding the maximum rate of change.

3. Box plots constructed for Group A and Group B showed varying levels of variability and shifts in benchmarks depending on the profile lines,



indicating the need for additional research and monitoring in these areas.

4. The analysis of benchmark subsidence using digital levels and correlation matrices made it possible to identify statistically significant patterns and trends, which confirms the need for constant monitoring and control of the state of the earth's surface in these areas.

5. The development of observation programs at stations and the analysis of error sources are the key points to ensuring the accuracy and reliability of the

data when carrying out geodetic measurements and leveling on the specified profile lines.

These findings highlight the need for a systematic and comprehensive approach to monitoring and analyzing benchmark subsidence, especially under conditions of increased tectonic activity and geological changes in the studied areas.

**Conflicts of interest.** On behalf of all the authors, the corresponding author declares that there is no conflict of interest.

**Cite this article as:** Zhunussova GE, Igemberlina MB, Abekov UE. Analyzing geodetic leveling and subsidence of benchmarks: data and conclusions for Zhezkazgan and GEV-Lermontovo villages. *Kompleksnoe Ispolzovanie Mineralnogo Syra = Complex Use of Mineral Resources*. 2024; 331(4):51-59. <https://doi.org/10.31643/2024/6445.38>

## Геодезиялық нивелирлеу және реперлердің шөгүін талдау: Жезқазған және ГБК-Лермонтово кенттері бойынша мәліметтер мен қорытындылар

<sup>1</sup> Жунусова Г.Е., <sup>1</sup> Игемберлина М.Б., <sup>2</sup> Абеков У.Е.

<sup>1</sup> Әбілқас Сағынов атындағы Қарағанды техникалық университеті, Қарағанды, Қазақстан

<sup>2</sup> Қарағанды құю-машина жасау зауыты, Қарағанды, Қазақстан

<p>Мақала келді: 1 қараша 2023 Сараптамадан өтті: 20 қараша 2023 Қабылданды: 4 қаңтар 2024</p>	<p><b>ТҮЙІНДЕМЕ</b> Мақалада 2014-2020 жылдарға арналған Жезқазған және ГБК-Лермонтово кенттерінің учаскелерінің геометриялық орналасуы туралы мәліметтер корреляциялық матрицалар, статистикалық сынақтар және қорап диаграммасы арқылы талданған. Таңдалған профильді сызықтар бойынша реперлерде тау жыныстарының жылжуы туралы деректерді пайдалана отырып, егжей-тегжейлі талдаулар екі топта жүргізілді («А» тобы 2018 жылдан 2020 жылға дейінгі деректер және 2014 жылдан бастап шөгү деңгейі терең зерттелген «Б» тобы). «А» тобында корреляциялық матрицалар талданды және эталондық шөгү деңгейлері арасында статистикалық маңызды байланыстар анықталды. «Б» тобы әртүрлі кезеңдердегі үш профильдік сызық бойынша реперлердің шөгү деңгейіндегі өзгерістерді зерттеуге бағытталған. Қорап диаграммаларын пайдалана отырып, шөгү деңгейлерінің таралуы мен өзгермелілігі визуалды түрде көрсетілді, ауытқулар және ықтимал проблемалық аймақтар анықталды. Нәтижеде Лермонтово гидравликалық жару аймағында тау-кен жұмыстарын жүргізу нәтижесінде № 115 профиль сызығы бойынша айтарлықтай шөгү байқалады. Зерттеу деректері маркшейдерлер мен геологтарға құнды ақпарат береді және сонымен қатар аймақтағы қаланы дамыту, инфрақұрылымның тұрақтылығы мен қоршаған ортаны қорғауды басқару үшін пайдаланылуы мүмкін. Алынған нәтижелер кейінгі зерттеулер үшін қызығушылық тудырады және теріс салдарларды жою бойынша тиісті стратегиялар мен шараларды әзірлеу үшін негіз бола алады.</p> <p><b>Түйін сөздер:</b> аспаптық бақылаулар, геодезиялық мониторинг, геодезия, нивелирлеу, профильді сызықтар</p>
<p><b>Жунусова Г.Е.</b></p>	<p><b>Авторлар туралы ақпарат:</b> Техника ғылымдарының кандидаты, Әбілқас Сағынов атындағы Қарағанды техникалық университеті, 100027, Н.Назарбаев даңғылы, 56, Қарағанды, Қазақстан. E-mail: <a href="mailto:lena_gulya@mail.ru">lena_gulya@mail.ru</a></p>
<p><b>Игемберлина М.Б.</b></p>	<p>Техника ғылымдарының магистрі, Әбілқас Сағынов атындағы Қарағанды техникалық университеті, 100027, Н.Назарбаев даңғылы, 56, Қарағанды, Қазақстан. E-mail: <a href="mailto:igemberlina@mail.ru">igemberlina@mail.ru</a></p>
<p><b>Абеков У.Е.</b></p>	<p>PhD докторы, Қарағанды құю-машина жасау зауыты, 100000, Орлов көшесі, 103/2, Қарағанды, Қазақстан. E-mail: <a href="mailto:ulan_abekov@mail.ru">ulan_abekov@mail.ru</a></p>

## Анализ геодезического нивелирования и оседания реперов: данные и выводы для Жезказганского и ГРП-Лермонтово поселков

<sup>1</sup> Жунусова Г.Е., <sup>1</sup> Игемберлина М.Б., <sup>2</sup> Абеков У.Е.

<sup>1</sup> Карагандинский технический университет имени Абылкаса Сагинова, Караганда, Казахстан

<sup>2</sup> Карагандинский литейно-машиностроительный завод, Караганда, Казахстан

Поступила: 1 ноября 2023

Рецензирование: 20 ноября 2023

Принята в печать: 4 января 2024

### АННОТАЦИЯ

В данной статье проведен анализ данных геометрического нивелирования на объектах в пос. Жезказган и ГРП-Лермонтово за период с 2014 по 2020 гг. с использованием корреляционных матриц, статистических тестов и коробчатых диаграмм. Используя данные о смещении пород на реперах по выбранным профильным линиям, были проведены детальные анализы в двух группах (группа "А" с данными с 2018 по 2020 годы и группа "Б" с углубленным изучением уровня оседаний с 2014 года). В группе "А" был проведен анализ корреляционных матриц и определение статистически значимых связей между уровнями оседаний реперов. Группа "Б" была направлена на изучение изменений уровня оседаний реперов вдоль трех профильных линий за различные периоды. С использованием коробчатых диаграмм было визуализировано распределение и изменчивость уровня оседаний, выявлены аномалии и установлены потенциальные проблемные участки. Результаты указывают на значительные оседания, на профильной линии №115, вызванные горными работами в районе ГРП-Лермонтово. Данные изучения являются ценной информацией для специалистов-геодезистов и геологов, а также могут быть использованы для управления городским развитием, стабильностью инфраструктуры и охраной окружающей среды в данном регионе. Полученные результаты представляют интерес для проведения дальнейших исследований и могут послужить основой для разработки соответствующих стратегий и мер по устранению негативных последствий.

**Ключевые слова:** инструментальные наблюдения, геодезический мониторинг, геодезия, нивелирование, профильные линии

### Информация об авторах:

**Жунусова Г.Е.**

Кандидат технических наук, Карагандинский технический университет имени Абылкаса Сагинова, 100027, пр. Н.Назарбаева 56, Караганда, Казахстан. E-mail: lena\_gulya@mail.ru

**Игемберлина М.Б.**

Магистр технических наук, Карагандинский технический университет имени Абылкаса Сагинова, 100027, пр. Н.Назарбаева 56, Караганда, Казахстан. E-mail: igemberlina@mail.ru

**Абеков У.Е.**

Доктор PhD, Карагандинский литейно-машиностроительный завод, 100000, ул. Орлова 103/2, Караганда, Казахстан. E-mail: ulan\_abekov@mail.ru

## References

- [1] Sun X, Bao J, Li J, Zhang Y, Liu S, Zhou B. A digital twin-driven approach for the assembly-commissioning of high precision products. *Robotics and Computer-Integrated Manufacturing*. 2020; 61:101839. <https://doi.org/10.1016/j.rcim.2019.101839>
- [2] Heki K, Jin S. Geodetic study on earth surface loading with GNSS and GRACE. *Satellite Navigation*. 2023; 4(1):24. <https://doi.org/10.1186/s43020-023-00113-6>
- [3] Ishikawa T, Yokota Y, Watanabe SI, Nakamura Y. History of On-Board Equipment Improvement for GNSS-A Observation With Focus on Observation Frequency. *Frontiers in Earth Science*. 2020; 8:150. <https://doi.org/10.3389/feart.2020.00150>
- [4] Bures J, Bartonek D, Svabensky O, Vojkuvka M. Integrated information system of building structures monitoring. *International Multidisciplinary Scientific GeoConference SGEM*. 2017; 17:943-950. <https://doi.org/10.5593/sgem2017/21/S07.119>
- [5] Igemberlina MB, Seituly K. Otsenka geomekhanicheskogo sostoyaniya podrobotannoy territorii poselka Zhezkazgan [Assessment of the geomechanical condition of the undermined territory of the village of Zhezkazgan]. *Trudy Universiteta = University Proceedings*. 2020; 2(79):66-69. (in Russ.).
- [6] Tsentry i repery Gosudarstvennoy geodezicheskoy i nivelirnoy setey Respubliki Kazakhstan GKINP -19-024-09 [Centers and benchmarks of the State geodetic and leveling networks of the Republic of Kazakhstan GCINR-19-024-09]. Astana: 2009, 46. (in Russ.).
- [7] Instruksiya ob okhrane geodezicheskikh punktov [Instructions on the protection of geodetic points]. Moscow. 1984, 29. (in Russ.).
- [8] Instruksiya po nablyudeniym za sdvizheniyem gornyx porod i zemnoy poverkhnosti pri podzemnoy razrabotke rudnykh mestorozhdeniy [Instructions for observing the movement of rocks and the earth's surface during underground mining of ore deposits]. Moscow. 2007, 112. (in Russ.).
- [9] Instruksiya po nivelirovaniyu I, II, III i IV klassov [Leveling instructions I, II, III and IV classes]. Moscow. 2004, 231. (in Russ.).
- [10] Nizametdinov NF, Baryshnikov VD, Nizametdinov RF, Igemberlina MB, Staňková H, Batyrshaeva ZhM. Analysis of Ground Surface Displacements under the Influence of Repeated Mining Activities in the Zhezkazgan Area. *Journal of Mining Science*. 2021; 57(2):184-189. <https://doi.org/10.1134/S1062739121020022>

- [11] Brien CJ, James AT, Venables WN. An analysis of correlation matrices: Variables cross-classified by two factors. *Biometrika*. 1988; 75(3):469-476. <https://doi.org/10.2307/2336596>
- [12] Asuero AG, Sayago A, González AG. The correlation coefficient: An overview. *Critical reviews in analytical chemistry*. 2006; 36(1):41-59. <https://doi.org/10.1080/10408340500526766>
- [13] Hauke J, Kossowski T. Comparison of values of Pearson's and Spearman's correlation coefficients on the same sets of data. *Quaestiones geographicae*. 2011; 30(2):87-93. <https://doi.org/10.2478/v10117-011-0021-1>
- [14] Dahiru T. P-value, a true test of statistical significance? A cautionary note. *Annals of Ibadan postgraduate medicine*. 2008; 6(1):21-26. <https://doi.org/10.4314/aipm.v6i1.64038>
- [15] Altman D, Machin D, Bryant T, & Gardner M. eds. *Statistics with confidence: confidence intervals and statistical guidelines*. John Wiley & Sons. 2013.
- [16] Senthilnathan S. Usefulness of correlation analysis. Available at SSRN 3416918. 2019.
- [17] Chambers JC, Mullick SK, Smith DD. *How to choose the right forecasting technique*. Cambridge, MA, USA: Harvard University, Graduate School of Business Administration. 1971.
- [18] Schwertman NC, Owens MA, Adnan R. A simple more general boxplot method for identifying outliers. *Computational statistics & data analysis*. 2004; 47(1):165-174. <https://doi.org/10.1016/j.csda.2003.10.012>
- [19] McGill R, Tukey JW, Larsen WA. Variations of box plots. *The american statistician*. 1978; 32(1):12-16. <https://doi.org/10.1080/00031305.1978.10479236>
- [20] Package Corrplot. 2022; 26. <https://cran.r-project.org/web/packages/corrplot/corrplot.pdf>
- [21] Krzywinski M, Altman N. Visualizing samples with box plots: use box plots to illustrate the spread and differences of samples. *Nature Methods*. 2014; 11(2):119-121. <https://doi.org/10.1038/nmeth.2813>



DOI: 10.31643/2024/6445.39

Earth sciences

## Depletion of converter slags to waste in the Vanyukov furnace during pyrometallurgical copper production at JSC Almalyk MMC

<sup>1</sup>Yakubov M.M., <sup>1</sup>Yoqubov M.M., <sup>2</sup>Kholikulov D.B., <sup>2</sup>Maksudhodjaeva M.S.

<sup>1</sup>National research technological University MISIS in Almalyk<sup>\*</sup> Almalyk branch, Uzbekistan

<sup>2</sup>Almalyk branch of Tashkent state technical University, Republic of Uzbekistan

\* Corresponding author email: yakubovmahmud51@gmail.com

<p>Received: November 6, 2023 Peer-reviewed: December 4, 2023 Accepted: January 4, 2024</p>	<p><b>ABSTRACT</b></p> <p>The article shows the possibility of involving man-made formations in the pyrometallurgical production of copper in the form of slag and clinker-zinc production for the purpose of comprehensive extraction of non-ferrous and precious metals from them at Almalyk MMC JSC. Clinker, a technogenic waste from zinc production, contains a significant amount of reducing elements in the form of metallic iron and carbon, as well as gold in the amount of 2.3 g/t and silver 250 g/t. In research, clinker works as a reducer of magnetite contained in the converter slag during its depletion and in the process of depletion (reduction) of the converter slag, noble metals are extracted into matte, and then into blister copper up to 95-98%. Converter slags from copper production of Almalyk MMC JSC contain 2.0-3.5% copper, and they, as a circulating product, are depleted in a reverberatory furnace with copper extraction of 75%. To increase the yield of copper from converter slag in Vanyukov furnaces, it is necessary to first deplete the converter slag in reduction processes and then transfer it for processing. It was found that using clinker, a technogenic waste from zinc production with a particle size of +5 - -10 mm, the recovery of converter slag in a converter from magnetite to wustite using the developed technology in 10-15 minutes exceeded more than 50.0% (the amount of magnetite decreased from 21.9 % to 9.8%). As a result of processing recovered converter slags in the Vanyukov furnace, it was possible to reduce the copper content in converter slags of copper production from 2.2-3.5% to 0.58-0.72% in waste slag. To increase the yield of copper from converter slag in the reverberatory and Vanyukov furnaces, it is necessary to first deplete the converter slag in reduction processes and then transfer it for processing.</p> <p><b>Keywords:</b> copper, slag, converter slag, depletion, magnetite, extraction, clinker, concentrate.</p>
<p><b>Mahmud M. Yakubov</b></p>	<p><b>Information about authors:</b> Doctor of science, professor, "National research technological University MISIS in Almalyk" Almalyk branch, Uzbekistan. E-mail: yakubovmahmud51@gmail.com</p>
<p><b>Oybek M. Yoqubov</b></p>	<p>PhD, "National research technological University MISIS in Almalyk" Almalyk branch, Uzbekistan. E-mail: oybek.yoqubov6600@gmail.com</p>
<p><b>Doniyor B. Kholikulov</b></p>	<p>PhD, Almalyk branch of Tashkent state technical University, Republic of Uzbekistan. E-mail: doniyor_xb@mail.ru</p>
<p><b>Mukhtabar S. Maksudhodjaeva</b></p>	<p>PhD, Almalyk branch of Tashkent state technical University, Republic of Uzbekistan. E-mail: lawsecret@mail.ru</p>

### Introduction

As is known, when choosing a method for processing copper sulfide concentrate, autogenous furnaces began to be chosen. The advantage of autogenous smelting processes is that it obtains sufficient heat for melting and physical and chemical processes, slag and matte formation in the furnace, due to the oxidation of metal sulfides, it is possible to work without the consumption of external fuel, all the necessary heat for metallurgical smelting is provided exclusively through exothermic reactions in such processes as: "Outokumpu", "JMCO", "Ausmelt", "Isasmelt", CFP, smelting in Vanyukov furnaces, and others. Analyzing various

pyrometallurgical methods for processing sulfide copper-nickel concentrates at enterprises in many foreign countries, today the most promising technology for their processing is smelting in a two-zone Vanyukov furnace to produce copper-rich matte. At the same time, these furnaces still have additional advantages such as high productivity and the production of process gases rich in SO<sub>2</sub> content for the production of sulfuric acid [[1], [2]].

At Almalyk MMC JSC in 2016. The Vanyukov autogenous furnace was built and put into production; a second larger furnace and a flash smelting furnace are being designed.

It should be noted that in the world's ore deposits, reserves of high-quality copper and iron

ores are significantly reduced, as well as the emerging danger to the environment during their processing, associated with the removal of a huge amount of metallurgical technogenic waste, in the form of slag and tailings of the processing plant. An analysis of the forecast for raw materials in the mining and metallurgical industry shows that the raw material reserves of quarries and stockpiled ores do not meet the needs of the processing plant as early as 2020; a dilemma arises: either reduce production or attract resources with reduced consumer characteristics. In this regard, the possibility opens up for their effective use as secondary sources of iron, copper and noble metals. In the slags of the copper industry, the elemental proportion of iron was about 35.4%, and from the literature it is known that an iron content of at least 25% is economically feasible [[3], [4], [5], [6], [7]].

The dumps of the Almalyk MMC JSC plant have accumulated more than 1 billion 500 million tons of technogenic waste from the processing plant, 8.5 million tons of dump slag, and they contain more than 1.4 million tons of copper. In zinc production, clinker is a technogenic waste from Waeltzing zinc cakes; today more than 450 thousand tons of it have accumulated in dumps; it contains gold in the amount of 2.7-3.5 g/t and silver 160-250 g/t [[8], [9], [10]].

However, converter slags containing copper obtained by converting copper matte in the Vanyukov furnace itself are not processed; the technology does not allow it due to the oxidizing atmosphere in the reaction zone of the furnace; they are shipped to the enrichment plant, to the head of the enrichment process, and together with the ore undergo re-enrichment (crushing, grinding, flotation) to obtain copper sulfide concentrate. Of the total volume of converter slag produced during copper production at Almalyk MMC JSC, 30% is processed in reverberatory furnaces, and 70% is transferred to the plant's processing plant.

In order to reduce (dissolved, mechanical) losses of metals, in the production of copper by pyrometallurgical means in autogenous and classical furnaces, they adhere to the main task - the need for the copper content in the slag to be minimal, however, in the slag the high concentration of iron oxides, especially in the form of magnetite, on the contrary, sharply increases his. This occurs due to the fact that, being in excess, magnetite is able to separate from the dissolved state into the solid state and form an additional heterogeneous phase. In turn, the solid phase of magnetite during melting in

a reverberatory furnace forms a magnetite deposit in the bottom part (bottom) of the furnace, and when melting in the Vanyukova furnace, it bubbles (circulates) in the volume of the furnace in the form of a suspension-dirt, disrupting the production technology [[11], [12], [13], [14]].

Scientific research is being conducted around the world to reduce the excess magnetite content in iron silicate slags of copper production, its reduction to wustite in processes during pyrometallurgical copper production, using carbon (coke), natural gas or man-made waste containing reducing elements.

It has been substantiated that the recovered converter slag to a residual magnetite content of 18-28% to 8-10% can be loaded in liquid and solid form into melting furnaces without a negative impact on the smelting process and without fear of magnetite release into the solid phase [[15], [16]].

The concentration of magnetite-oxide of ferric iron in slag can be quite high and range from 5% to 24%. An increased content of magnetite during the smelting process can lead to disruption of the smelting technology, which in turn leads to an increase in copper losses with waste slag. In the pyrometallurgical production of copper, one of the important points when melting sulfide copper concentrates in smelting furnaces is the reduced content of magnetite in the waste slag. For example, in a reverberatory furnace, magnetite in an amount of 2-9% can be supplied with the concentrate [[17], [18], [19], [20]].

Magnetite content of 2-9% may be present in concentrates as shown in Fig. 1 - Fig. 4 thin sections of ore from the Kalmakir mine of the Almalyk MMC made at the State Enterprise IMR.

The reduction of iron oxide from the ferric state is possible when it is reduced to ferrous oxide. The converter slag magnetite reducer can be not only coke, natural gas, metallic iron, but also technogenic raw materials that contain these elements. Such technogenic raw materials, which contain carbon and iron, can be clinker, as well as noble metals Au and Ag.

#### **Selection and justification of research objects.**

The main objects of research were industrial converter slags of Almalyk MMC JSC, the chemical composition of which is given in Table 1. Both stale, accumulated and freshly formed converter slags were subjected to chemical analysis.

To conduct laboratory studies and clarify the main reactions occurring during the reduction process during conversion, the clinker composition was used, which is given in table. 2.



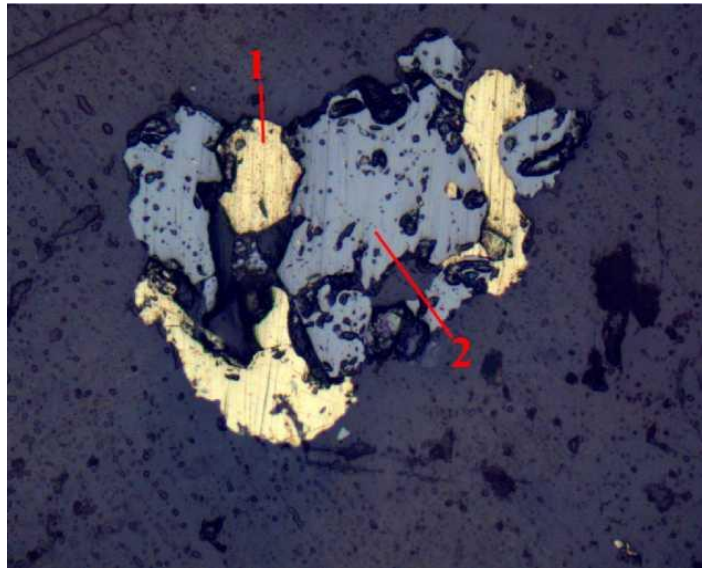


**Fig. 1** - Fragments of samples containing 1-chalcopyrite, 2-magnetite (magnification x200)

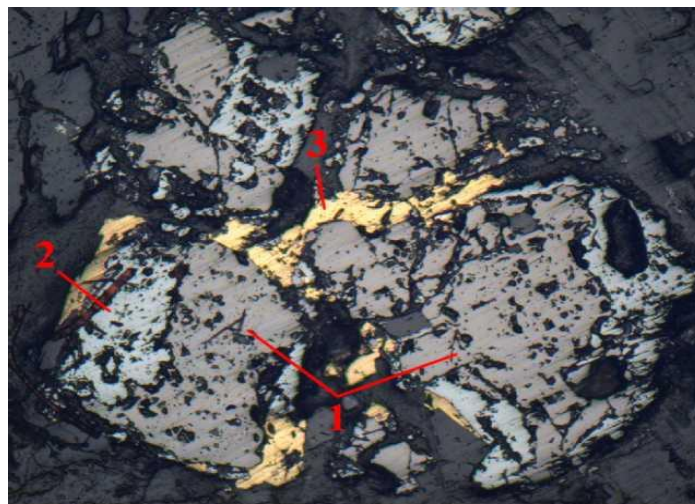


**Fig. 2** - Fragments of samples containing 1-hematite, 2-magnetite, 3-chalcopyrite (magnification x200)

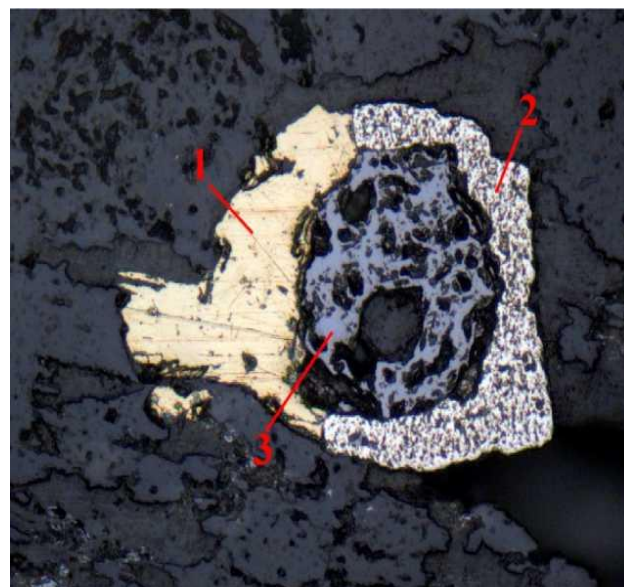


**Fig.3** - Fragments of samples containing 1-chalcopyrite, 2-pyrite, 3-magnetite (magnification x200)

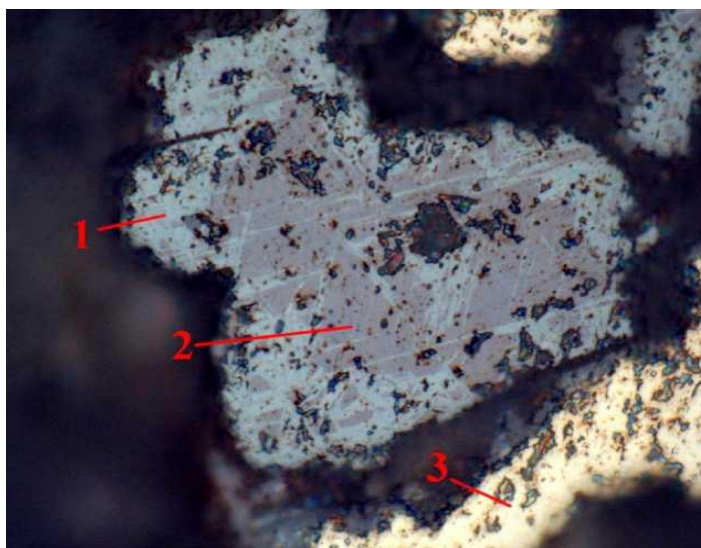


**Fig.4** - Fragments of samples containing 1-hematite, 2-magnetite, 3-chalcopyrite (magnification x100)

**Table 1** - Chemical composition of Almalyk MMC converter slags

No. slag	Content, wt. %								
	Cu	Zn	Pb	Fe	Fe <sub>3</sub> O <sub>4</sub>	SiO <sub>2</sub>	CaO	Al <sub>2</sub> O <sub>3</sub>	S
1	2.94	1.95	1.3	47.0	20.7	22.5	1.95	3.20	1.0
2	3.57	1.75	1.1	46.9	21.1	19.1	1.57	3.11	0.90

**Table 2** - Chemical composition of clinker from the zinc plant of Almalyk MMC

No. samples	Clinker content , wt. %								
	Cu	Pb	Zu	SiO <sub>2</sub>	S	C	Fe	Au	Ag
1	2.72	1.32	2.05	19.00	-	25.20	22.00	2.35 g/t	185 g/t

The process of recovering magnetite from converter slag composition: Cu-2.94; Zn-1.95; Pb-1.3; Fe-47.0; Fe<sub>3</sub>O<sub>4</sub>-20.7; SiO<sub>2</sub>-22.5; CaO-1.95; Al<sub>2</sub>O<sub>3</sub>-3.20; S-1.0 clinker occurs in solid and liquid phases, since the process takes place at a temperature of 1250 °C, and the melting point of iron is 1539 °C, carbon 3527 °C.

With such a content of magnetite in the converter slag, it becomes possible to mix it with concentrate and load it even into the Vanyukov autogenous furnace. In order to deplete converter slag as a recyclable product, tests were carried out on its preliminary recovery in the Vanyukov furnace. As a reducing agent for magnetite - ferric iron of the

iron silicate melt of copper production, clinker was used - a technogenic solid residue from the Waeltz process of zinc cakes from zinc production, containing more than 50% of reducing elements in the form of metallic iron and carbon.

### Discussion of the research results

It was settled (fig.5) that using clinker size + 5 - 10 mm when reducing converter slag in a converter from magnetite to wustite using technology (Fig. 6), more than 50.0% was restored in 10-15 minutes (the amount of magnetite decreased from 21.9% to 9.8%).

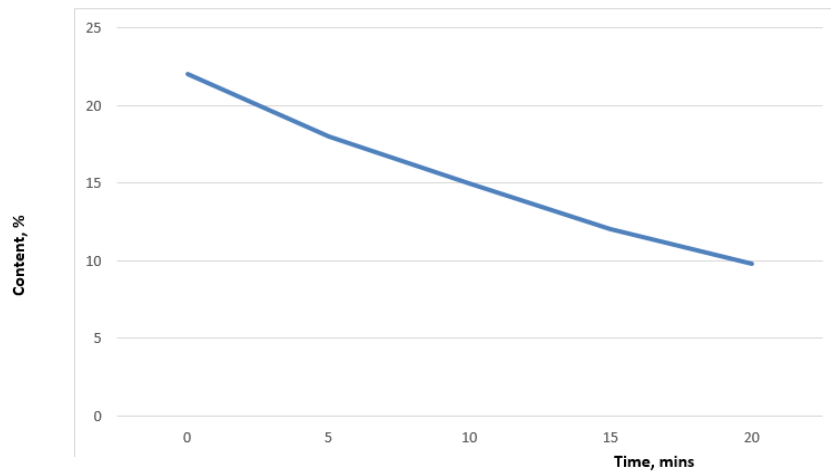


Fig. 5 - Dependence of magnetite reduction in the composition of converter slag from time to time.

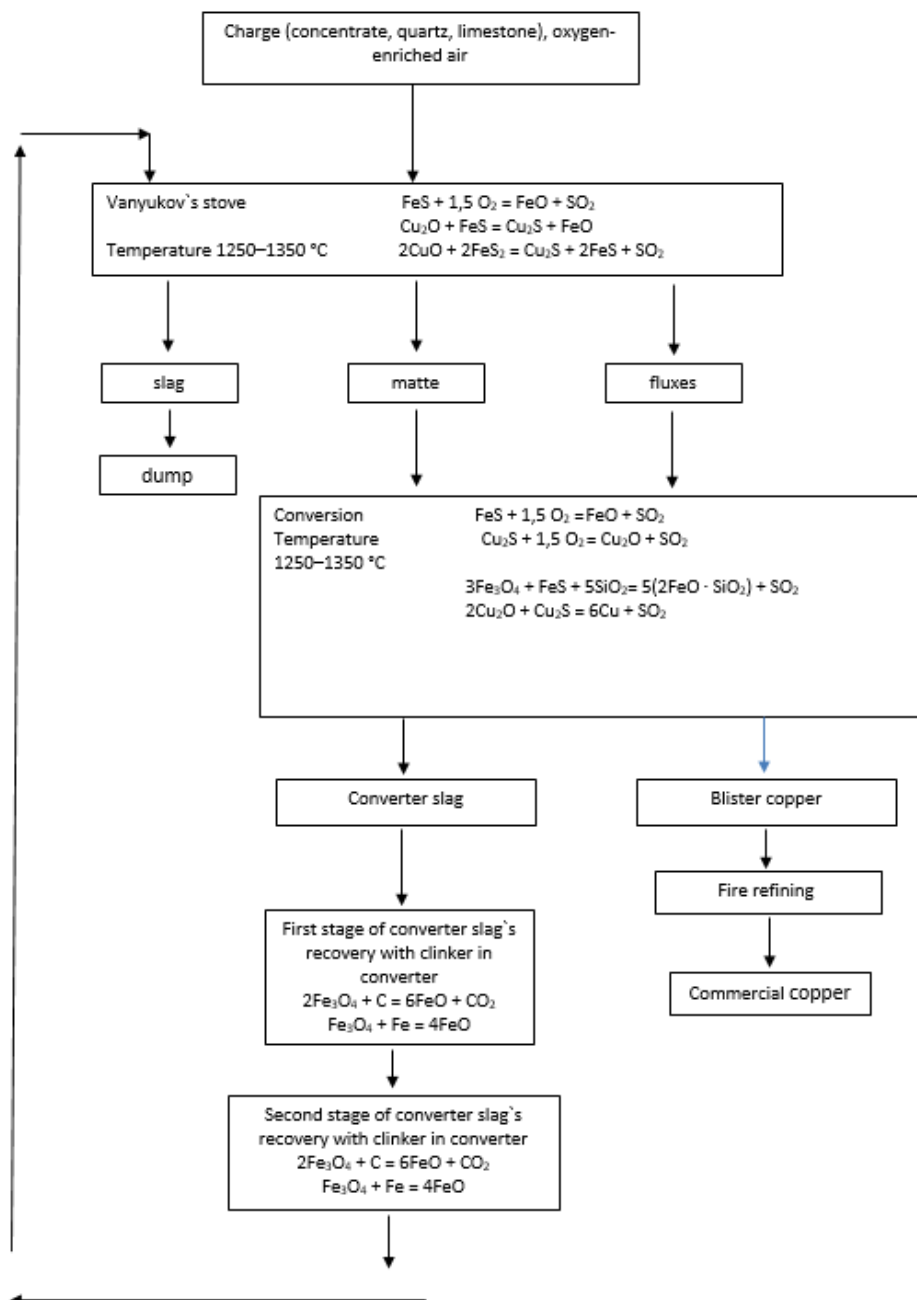


Fig.6 - Technology for processing recovered converter slag in the Vanyukov furnace

**Table 3** - Operation of the Vanyukov furnace in normal mode when smelting copper sulfide concentrate without the addition of converter slag concentrate as part of the charge.

Date Name of material slag hole.	Cu	SiO <sub>2</sub>	Fe	CaO
01.12.2022	0.64	28.84	50.11	2.80
02.12. 2022	0.73	26.40	49.27	2.63
03.12.2022	0.65	28.52	51.63	2.91
04.12.2022	0.54	29.92	51.08	2.80
05.12.2022	0.62	29.16	50.11	2.86
06.12.2022	0.56	32.52	46.64	2.57
07.12.2022	0.63	29.74	48.44	3.64
08.12.2022	0.60	28.86	52.60	2.46
09.12.2022	0.55	31.00	48.58	2.69

**Table 4** - Copper content in the dump slag of the PZHV, for 10 days from 10 – 19 December 2022 when processing recovered converter slag.

Date Name of material slag hole.	Cu	SiO <sub>2</sub>	Fe	CaO
12/10/2022	0.65	34.20	51.83	2.58
11.12. 2022	0.58	29.08	49.86	2.74
12/12/2022	0.59	27.56	50.27	2.35
12/13/2022	0.65	29.30	52.66	2.35
12/14/2022	0.69	30.24	52.35	2.69
12/15/2022	0.59	29.80	51.86	2.40
12/16/2022	0.61	29.40	50.58	2.24
12/17/2022	0.59	29.20	51.97	2.80
12/18/2022	0.68	29.12	52.05	2.40
12/19/2022	0.72	29.70	51.72	2.55

The amount of copper sulfide (semi-sulfide copper) has significantly decreased from its initial content from 3.6% to 1.96

In December 2022 The second stage of industrial testing of the processing of recovered converter slag from copper production in the liquid bath furnace (LBA) - the Vanyukov furnace - was continued in the conditions of Almayk MMC JSC. Table 3 shows the operation of the Vanyukov furnace in normal mode from 12/01/2022 to 12/09/2022, with copper content (standard for PV) in the matte: 45 - 50%.

Heat compensation from loading cold solid converter slags (metal oxides) from the dump occurs by loading clinker due to the exothermic reaction of oxidation of carbon and iron present in the clinker – a technogenic waste from the Almayk MMC JSC ACP plant.

In table 4 shows the copper content in the waste slag during the processing of recovered converter slag.

The data in Tables 4 show that the copper content in the dump slag when operating in the

PZhV mode for 10 days from 12/10/2022 to 12/19/2022 with the loading of recovered converter slag is 0.58% - 0.72%. They do not exceed the data on the copper content in the waste slag of the PZhV furnace (Vanyukov furnace) without loading converter slag.

### Conclusions

It was established and recommended that the use of clinker - technogenic waste from zinc production with a particle size of +5 - -10 mm when restoring converter slag in a converter from magnetite to wustite using the developed technology in 10-15 minutes decreased from 21.9% to 9.8%, with this contents can be loaded into the Vanyukov oven.

In the process of smelting sulfide copper concentrate and solid recovered converter slag from copper production in the Vanyukov furnace, no changes in technology indicators were observed.

The lack of heat during the smelting process in the Vanyukov furnace when loading reduced

converter slag in a cold state is compensated by additional clinker blending of technogenic waste raw materials from the zinc plant AGMK, which is a coolant (an exothermic oxidation reaction of metallic iron and clinker carbon), as well as additional raw materials of noble metals.

A two-stage technology for processing technogenic raw materials in the form of converter slag has been developed in copper production, in the first stage by restoring it in a converter, and in the second stage, after its recovery, it is mixed when melting sulfide copper concentrates in a single-zone Vanyukov furnace. Clinker-zinc production is used as a reducing agent; the iron and carbon contained in it reduce the excess part of magnetite, and 95% of noble metals are extracted from it. As a result, it was possible to deplete the converter slags of copper production in copper from 2.2-3.5% to a waste level of 0.58 - 0.72%, which is the goal of this technology.

**Conflict of interest.** On behalf of all authors, the correspondent author declares that there is no conflict of interest.

**Cite this article as:** Yakubov MM, Yoqubov MM, Kholikulov DB, Maksudhodjaeva MS. Depletion of converter slags to waste in the Vanyukov furnace during pyrometallurgical copper production at JSC Almalyk MMC. Kompleksnoe Ispolzovanie Mineralnogo Syra = Complex Use of Mineral Resources. 2024; 331(4):60-68. <https://doi.org/10.31643/2024/6445.39>

## «Алмалық ТМК» АҚ пирометаллургиялық мыс өндірісі кезінде Ванюков пешіндегі конверторлық шлактарды қалдықтарға шығару.

<sup>1</sup>Yakubov M.M., <sup>1</sup>Yoqubov M.M., <sup>2</sup>Kholikulov D.B., <sup>2</sup>Maksudhodjaeva M.S.

<sup>1</sup>«Алмалық қаласындағы MISIS Ұлттық зерттеу технологиялық университеті» Алмалық филиалы, Өзбекстан

<sup>2</sup>Ташкент мемлекеттік техникалық университетінің Алмалық филиалы, Өзбекстан

Мақала келді: 6 қараша 2023  
Сараптамадан өтті: 4 желтоқсан 2023  
Қабылданды: 4 қаңтар 2024

### ТҮЙІНДЕМЕ

Мақалада «Алмалық ТМК» АҚ-да техногендік түзілімдерді олардан түсті және асыл металдарды кешенді түрде алу мақсатында шлак және клинкер-мырыш түріндегі мыс пирометаллургиялық өндірісіне тарту мүмкіндігі көрсетілген. Мырыш өндірісінің техногендік қалдықтары болып табылатын клинкер құрамында металдық темір және көміртек түріндегі тотықсыздандырғыш элементтердің айтарлықтай мөлшері, сонымен қатар 2,3 г/т алтын және 250 г/т күміс бар. Ғылыми зерттеулерде клинкер конвертер қожында болатын магнетиттің жұтандауы кезінде және конвертер қожының жұтандауы (редукциясы) процесінде тотықсыздандырғыш ретінде жұмыс істейді, асыл металдар штейнге, содан кейін 95-98% дейін тазаланбаған мыс алынады. «Алмалық ТМК» АҚ мыс өндірісінің түрлендіргіш қождарында 2,0-3,5% мыс бар және олар айналым өнімі ретінде 75% мыс алынатын шағылыстырғыш пеште жұтандалады. Алайда, Ванюковтың автогендік пештерін енгізумен (оларда конвертер қождары өңделмейді) мыс өндіру үшін конвертер қождарының бір бөлігі, комбинаттың техногендік шикізатына айнала отырып, кен шикізатын байыту процесінде, конвертер қожынан тазаланбаған мысқа төмен өтпелі экстракциясы бар сульфидті мыс концентратын алу үшін байыту фабрикасына қайтарылады. Шағылыстырғыш және Ванюков пештеріндегі конверторлық шлактардан мыс шығымын арттыру үшін алдымен конвертер қожын тотықсыздандыру процестерінде жұтандатып, содан кейін өңдеуге беру керек.

**Түйін сөздер:** мыс, шлак, конвертерлік қож, жұтандату, магнетит, бөліп алу, клинкер, концентрат.



<b>Mahmud M. Yakubov</b>	<b>Авторлар туралы ақпарат:</b> Доктор, профессор, «Алмалық қаласындағы MISiS ұлттық зерттеу технологиялық университеті» Алмалық филиалы, Өзбекстан. E-mail: yakubovmahmud51@gmail.com
<b>Mahmud M. Yoqubov</b>	PhD, «Алмалық қаласындағы MISiS ұлттық зерттеу технологиялық университеті» Алмалық филиалы, Өзбекстан. E-mail: oybek.yoqubov6600@gmail.com
<b>Doniyor B. Kholikulov</b>	PhD, Ташкент мемлекеттік техникалық университетінің Алмалық филиалы, Өзбекстан. E-mail: doniyor_xb@mail.ru
<b>Mukhtabar S. Maksudhodjaeva</b>	PhD, Ташкент мемлекеттік техникалық университетінің Алмалық филиалы, Өзбекстан. E-mail: lawsecret@mail.ru

## Освобождение конвертерных шлаков в отходы в печи Ванюкова при пирометаллургическом производстве меди на АО «Алмалыкский ГМК»

<sup>1</sup>Yakubov M.M., <sup>1</sup>Yoqubov M.M., <sup>2</sup>Kholikulov D.B., <sup>2</sup>Maksudhodjaeva M.S.

<sup>1</sup>«Национальный исследовательский технологический университет МИСиС в Алмалыке» Алмалыкский филиал, Узбекистан

<sup>2</sup>Алмалыкский филиал Ташкентского государственного технического университета, Узбекистан

<p>Поступила: 6 ноября 2023 Рецензирование: 4 декабря 2023 Принята в печать: 4 января 2024</p>	<p><b>АННОТАЦИЯ</b></p> <p>В статье показана возможность вовлечения техногенных образований в пирометаллургическое производство меди в виде шлаков и клинкерно-цинкового производства с целью комплексного извлечения из них цветных и благородных металлов на АО «Алмалыкский ГМК». Клинкер – техногенный отход производства цинка – содержит значительное количество восстанавливающих элементов в виде металлического железа и углерода, а также золото в количестве 2,3 г/т и серебро 250 г/т. В исследованиях клинкер работает как восстановитель магнетита, содержащегося в конвертерном шлаке, при его обеднении и в процессе обеднения (восстановления) конвертерного шлака извлечение благородных металлов в штейн, а затем в черновую медь до 95-98 %. Конвертерные шлаки медного производства АО «Алмалыкский ГМК» содержат 2,0-3,5% меди и их, как оборотный продукт, обедняют в отражательной печи с извлечением меди 75%. Однако с внедрением автогенных печей Ванюкова (в них не перерабатываются конвертерные шлаки) для производства меди часть конвертерных шлаков, превращаясь в техногенное сырье комбината, возвращается на обогатительную фабрику в процессе обогащения рудного сырья, для получения сульфидного медного концентрата с низким сквозным извлечением из конвертерного шлака в черновую медь. Для увеличения выхода меди из конвертерного шлака в отражательных печах и печах Ванюкова необходимо сначала обеднить конвертерный шлак в восстановительных процессах, а затем передавать его на переработку.</p> <p><b>Ключевые слова:</b> медь, шлак, конвертерный шлак, обеднение, магнетит, извлечение, клинкер, концентрат.</p>
<b>Mahmud M. Yakubov</b>	<b>Информация об авторах:</b> Доктор, профессор, «Национальный исследовательский технологический университет МИСиС в Алмалыке» Алмалыкский филиал, Узбекистан. E-mail: yakubovmahmud51@gmail.com
<b>Mahmud M. Yoqubov</b>	PhD, «Национальный исследовательский технологический университет МИСиС в Алмалыке» Алмалыкский филиал, Узбекистан. E-mail: oybek.yoqubov6600@gmail.com
<b>Doniyor B. Kholikulov</b>	PhD, Алмалыкский филиал Ташкентского государственного технического университета, Узбекистан. E-mail: doniyor_xb@mail.ru
<b>Mukhtabar S. Maksudhodjaeva</b>	PhD, Алмалыкский филиал Ташкентского государственного технического университета, Узбекистан. E-mail: lawsecret@mail.ru

## References

- [1] Tsemekhman LSh, Paretsky V. M. Modern methods of processing sulfide copper-nickel concentrates. Non-ferrous metals. 2020; 1:24-31.
- [2] Marchuk RA, Krupnov LV, Morgoslep VI, Rummyantsev DV. Practice of operation of flash smelting furnaces in the Norilsk Nickel company in the conditions of processing finely dispersed raw materials with reduced energy potential. Non-ferrous metals. 2020; 6:47-54.
- [3] Bellemans I, De Wilde E, Moelans N, Verbeken K. Metal losses in pyrometallurgical operations. A review. Adv. Colloid Interface Sci. 2018; 255:47-63.
- [4] Tlotlo Solomon Gabasiane, Gwiranai Danha, Tirivaviri A Mamvura, Tebogo Mashifana, and Godfrey Dzinomwa. Environmental and Socioeconomic Impact of Copper Slag. A Review. Crystals. 2021; 11:1504. <https://doi.org/10.3390/cryst11121504>
- [5] Busolic D, Parada F, Parra R, Sanchez M, Palacios J, and Hino M. Recovery of Iron from Copper Flash Smelting Slags. Mineral Processing and Extractive Metallurgy. 2011; 120(1):32-6. <https://doi.org/10.1179/037195510X12772935654945>
- [6] Sanakulov KS, Kadyrov AA. Strategy for long-term innovative development of the Kyzylkum region. ISBN 978-3-943974-15-7. Publishing house Artem Cologne, Germany. 2021, 408.

- [7] Gabasiane TS, Danhaa G, Mamvuraa TA, Mashifanab T, Dzinomwac G. Characterization of copper slag for beneficiation of iron and copper. *Heliyon*. 2021; 7(4). <https://doi.org/10.1016/j.heliyon.2021.e06757>
- [8] Khursanov AKh. History and development prospects, problems of processing technogenic deposits of the Almalyk MMC. *Materials of the international research and development conference. Almalyk*. 2019, 3-15
- [9] Sanakulov KS. *Scientific and technical principles of processing waste from mining and metallurgical production*. Tashkent: Fan. 2009, 404.
- [10] Mirzanova ZA, Khasanov AU, Isroilov AT, Tashaliev FU, Rakhimjonov ZhB. Technology for processing technogenic waste containing non-ferrous metals. *Journal Coposition Materials*. 2021; 2:176-180.
- [11] Vanyukov AV. *Melting in a liquid bath*. Moscow. Ed. Metallry. 1988, 208.
- [12] Kupryakov YuP. *Copper smelting slags and their processing*. M.: Metallurgy. 1987, 201.
- [13] Dosmukhamedov NK, Fedorov AN. Distribution of Cu, Pb, Zn and As between the products of two-stage reductive depletion of high-copper slags. *Non-ferrous metals*. 2019; 7:30-35.
- [14] Vanyukov AV, Zaitsev VYa. *Theory of pyrometallurgical processes*. M.: Metallurgy. 1993, 384.
- [15] Yakubov MM, Abdukadyrov AA, Mukhametdzhanova ShA, Yokubov OM. Involvement in the production of man-made formations at the enterprise JSC Almalyk MMC. *Magazine Non-ferrous metals*. 2022; 5:36-41.
- [16] Yokubov OM, Khasanov AS, Yakubov MM, Mukhametdzhanova ShA. Improving the depletion of converter slags from copper production. *Uzbek Chemical Journal*. 2022; 1:30-34.
- [17] Kupryakov YuP. *Reflective smelting of copper concentrates*. M.: Metallurgy. 1976, 350.
- [18] Kenzhaliyev B, Kvyatkovskiy S, Dyussebekova M, Semenova A, Nurhadiyanto D. Analysis of Existing Technologies for Depletion of Dump Slags of Autogenous Melting. *Kompleksnoe Ispolzovanie Mineralnogo Syra = Complex Use of Mineral Resources*. 2022; 323(4): 23-29. <https://doi.org/10.31643/2022/6445.36>
- [19] Kezhou Song & Ari Jokilaakso. Transport Phenomena in Copper Bath Smelting and Converting Processes – A Review of Experimental and Modeling Studies, *Mineral Processing and Extractive Metallurgy Review*. 2022; 43(1):107-121. <https://doi.org/10.1080/08827508.2020.1806835>
- [20] Moskalyk RR, Alfantazi AM. Nickel sulphide smelting and electrorefining practice: A review. *Mineral Processing and Extractive Metallurgy Review*. 2002; 23(3-4):141-180. <https://doi.org/10.1080/08827500306893>



DOI: 10.31643/2024/6445.40

Earth sciences

## Prospects of oil and gas potential of the South Torgai sedimentary basin

\*Uakhiova A.A., Madisheva R.K., Askarova N.S., Adilkhanov R.K., Zheksenbaeva G.M.

NPJSC Abylkas Saginov Karaganda Technical University, Karagandy, Kazakhstan

\* Corresponding author email: ayauzhan.uakhiova@mail.ru

<p>Received: December 23, 2023 Peer-reviewed: January 3, 2024 Accepted: January 10, 2024</p>	<p><b>ABSTRACT</b></p> <p>One of the main directions for assessing the prospects of oil production is the study of oils. In this regard, modern geochemical studies are widely used in forecasting the oil and gas potential of the subsurface, occupying an important role in the question of the origin and source of hydrocarbons. The study is aimed at a comprehensive analysis of the geochemical characteristics of the South Torgai sedimentary basin in order to identify and assess the prospects for oil and gas potential. Comparing the composition of oils from different deposits makes it possible to determine the oil source strata, zones of oil formation and oil accumulation. The compounds in oils that are most or least susceptible to changes under the influence of factors such as water leaching, biodegradation and thermal transformation are subject to comparison. The relative content of individual classes of compounds in the oils of the Arysium trough, the geological characteristics of oil samples and the distribution of normal alkanes are presented. In this work, a comparative analysis of previously conducted geochemical studies was carried out to determine the composition and genesis of oils in the Arysium trough. Biomarkers in oils, which make it possible to restore the genetic properties of oils and determine the conditions of sedimentation of oil-generating organic substances, indicate the presence of suboxidation conditions, redox potential and predominantly oxidative environment in the process of sedimentation of organic substances. The results obtained are important for understanding the processes of oil formation and generation, as well as for further forecasting the oil content of the South Torgai sedimentary basin.</p>
	<p><b>Keywords:</b> oil and gas content, organic matter, oil, biomarker analysis, graben-syncline,orst-syncline.</p>
<p><b>Uakhiova Ayauzhan Aitpaevna</b></p>	<p><b>Information about authors:</b> Master student, The Department of «Geology and Exploration of Mineral Deposits», NPJSC Abylkas Saginov Karaganda Technical University, N. Nazarbayev Avenue 56, 100000, Karagandy, Kazakhstan. Email: ayauzhan.uakhiova@mail.ru</p>
<p><b>Madisheva Rima Kopbosynkyzy</b></p>	<p>Acting Associate Professor, PhD, The Department of «Geology and Exploration of Mineral Deposits», NPJSC Abylkas Saginov Karaganda Technical University, N. Nazarbayev Avenue 56, 100000, Karagandy, Kazakhstan. Email: rimma_kz@mail.ru</p>
<p><b>Askarova Nazym Srajadinkyzy</b></p>	<p>Doctor PhD, The Department of «Geology and Exploration of Mineral Deposits», NPJSC Abylkas Saginov Karaganda Technical University, N. Nazarbayev Avenue 56, 100000, Karagandy, Kazakhstan. Email: srajadin-nazym@mail.ru</p>
<p><b>Adilkhanov Ruslan Kayirgalievich</b></p>	<p>PhD student, The Department of «Geology and Exploration of Mineral Deposits», Abylkas Saginov Karaganda Technical University, N. Nazarbayev Avenue 56, 100000, Karagandy, Kazakhstan. Email: rkbnm82@mail.ru</p>
<p><b>Zheksenbaeva Gulmira Medinaevna</b></p>	<p>PhD student, The Department of «Geology and Exploration of Mineral Deposits», Abylkas Saginov Karaganda Technical University, N. Nazarbayev Avenue 56, 100000, Karagandy, Kazakhstan. Email: gulmira_zh91@mail.ru</p>

### Introduction

One of the main directions for assessing the prospects of oil production is the study of oils. Modern geochemical studies are widely used in predicting the oil and gas potential of the subsurface, occupying an important role in the question of the origin and source of hydrocarbons. Comparing the composition of oils from different

deposits makes it possible to determine the oil source strata, zones of oil formation and oil accumulation. The compounds in oils that are most or least susceptible to changes under the influence of factors such as water leaching, biodegradation and thermal transformation are subject to comparison.

Geochemical research methods, which are based on the analysis of the chemical composition

and properties of oil and gas, as well as related rocks, play an important role in the study of the origin of oil. It is important to note that the effectiveness of geochemical methods can be significantly increased with their combined use. This allows to get a more complete and accurate solution to the task.

The data on the composition of hydrocarbon biomarkers represented in oils by such compounds as alkanes (n-alkanes, isoprenoids), arenes (naphthalenes, phenanthrenes, etc.) and polycyclic naphthenes (heylantanes, steranes, gopanes) allow us to judge the source of oils, the conditions of accumulation and transformation of the initial organic matter [1]. These biomarkers can provide valuable information about the origin of oil, including the types of organisms that were present during its formation and environmental conditions. They may also indicate specific geological processes that led to the formation of oil. All these data are important for understanding the processes of oil formation and can help in identifying potential oil deposits.

Thus, Botwe Takyi and others in their work, referring to the studies of the authors Alberdi M. [2] and Avbovbo A. [3], subjected saturated substances to gas chromatographic mass spectrometric analysis (GC MS) for the presence of steranes, isoprenoids and n-alkanes, as well as chromatograms of the biomarkers triterpanes and gopanes. The composition of the biomarkers of the studied oils indicates low-oxygen and lowering environmental conditions for the studied samples, which corresponds to the marine delta deposition environment. The study [4] shows that oils are associated with a mixture of terrestrial and marine organic substances with a relatively high content of terrestrial and a lower content of seaweed [4]. In the work of Rabiati Abubakar et al. [5], gas chromatographic mass spectrometric (GC-MS) and gas chromatographic (GC) analyses were used to characterize biomarkers obtained from organic matter (oil and rock extracts) to determine the source of organic matter, deposition medium and maturity. 16 oil samples and 98 rock samples from 7 wells were examined. The study [5] showed that the distribution of these biomarkers suggests that the Cretaceous period oils were obtained from a mixed source of kerogen (marine and terrestrial) deposited in anoxic or suboxygenic conditions of

paleodeposition. The ratios of CPI, Ts/Tm and C29  $\beta\beta/(\beta\beta + \alpha\alpha)$  steranes, based on the ratios of C29 20S/(20S + 20R) steranes, indicate that the studied samples have a relatively low or medium maturity level [5]. In this regard, it is important to note the importance of a set of studies, which suggests that a more detailed understanding of the origin of oil can be obtained using the results of biomarker analysis of oil from all fields in combination with other methods such as carbon isotope analysis or oil fingerprinting.

### Experimental part

According to the «Map of prospects for oil and gas potential of Kazakhstan», the South Torgai sedimentary basin belongs to the Eastern oil and gas geological region (Figure 1) and is part of the Turan epigercine plate [6].

The basin is the youngest sedimentary basin in Kazakhstan, it consists of three blocks: the Zhilanshik, Aryskum troughs and the Mynbulak saddle between them (Figure 2). Sandy-argillaceous Mesozoic deposits are one of the main oil and gas bearing complexes in the section, within which the Lower Cretaceous (Aryskum horizon), middle-upper Jurassic and Lower Jurassic complexes are distinguished, in addition to of which the Upper Paleozoic promising oil and gas complex has also been identified [7].

The prospects of pre-Mesozoic formations are based on the presence of manifestations of hydrocarbons from weathered basement rocks up to industrial oil inflows (Kyzylkiya, Karavanchi, Kenlyk).

To date, 52 oil and gas fields and structures have been discovered in the South Torgai basin in total (Figure 2), the depletion of the initial recoverable reserves of some of them is quite high, for example, the depletion of the Kumkol field is 83% [8]. Due to the decrease in the residual recoverable oil reserves of almost all fields, the determination of the origin of oil and the forecast of the direction of hydrocarbon migration are an urgent topic for justifying deep drilling to the Paleozoic.

Despite the fact that significant studies have been conducted in the South Torgai basin using various methods and exploration work continues [[8], [9], [10], [11]], there is no single agreed opinion on the origin of oil.



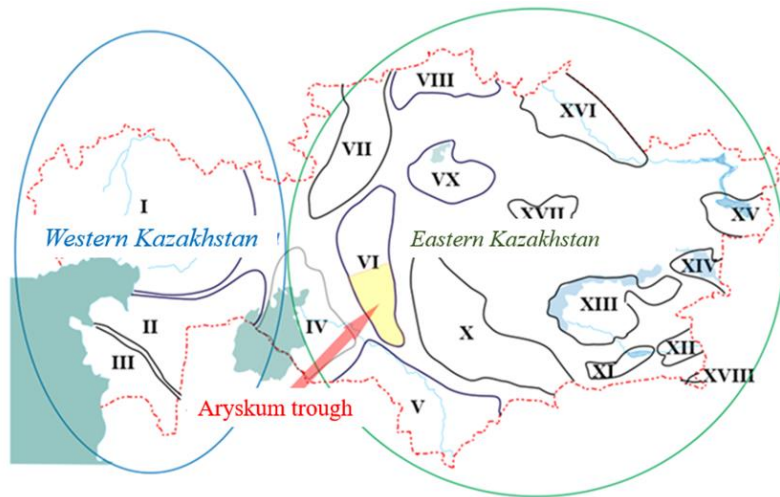


**Figure 1** - The scheme of the position of sedimentary basins of Kazakhstan [6]

I – Caspian; II – Ustyurt-Bozashy; III – Mangystau; IV – Aral; V – Syrdarya; VI – South Torgai; VII – North Torgai; VIII – North Kazakhstan; IX – Teniz; X – Shu-Sarysu; XI – West-Ili; XII – East-Ili; XIII – Balkhash; XIV – Alakol; XV – Zaysan; XVI – Irtysh; XVII – Karaganda; XVIII – Tekesko-Karkarinsky

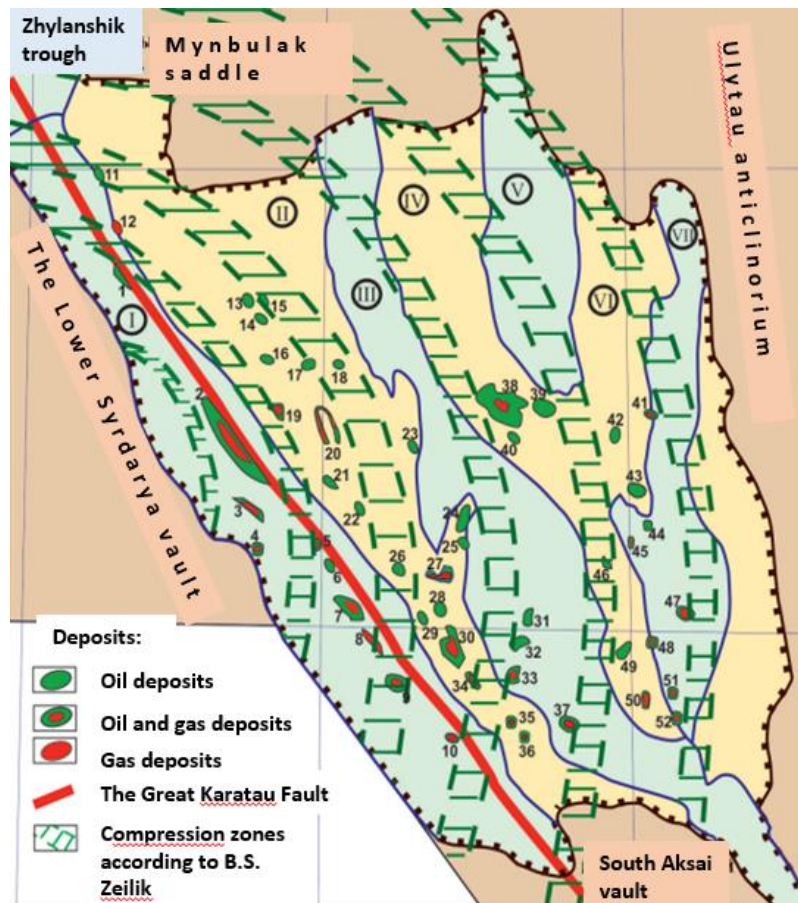


**Figure 2** - Placement of oil and gas fields in the South Torgai oil and gas region [9]

Graben-synclines: I – Aryskum, III – Akshabulak, V – Sarylan, VII – Bozingen. Gorst-anticlines: II – Aksai, IV – Aschisai, VI – Tabakbulak. Deposits: 1 – Maybulak, 2 – Aryskum, 3 – Doschan, 4 – South Doschan, 5 – Southeast Doschan, 6 – North Konys, 7 – Konys, 8 – South Konys, 9 – Bektas, 10 – North Ketekazgan, 11 – Zhylankyr, 12 – South Rovnoye, 13 – Bukharsai, 14 – South Karabulak, 15 – Karabulak, 16 – Eszhan, 17 – northwest Kyzylkiya, 18 – Kalzhan, 19 – Kenlyk, 20 – Kyzylkiya, 21 – Aktau, 22 – North Khairkeldy, 23 – Karavanshi, 24 – North Nuraly, 25 – Akshabulak North, 26 – Khairkeld, 27 – Nuraly, 28 – South Khairkeld, 29 – Taur, 30 – Aksai, 31 – East Akshabulak, 32 – Central Akshabulak, 33 – Akshabulak, 34 – South Aksai, 35 – West Tuzkol, 36 – Zhanbyrshy, 37 – Tuzkol, 38 – Kumkol, 39 – East Kumkol, 40 – South Kumkol, 41 – Karakol, 42 – Tabakbulak, 43 – Maikyzy, 44 – Sorkol, 45 – Kainar, 46 – Aschisai, 47 – Sarybulak, 48 – South Sarybulak, 49 – Blinovskoye, 50 – Arysskoye, 51 – North Priozernoye, 52 – South Arysskoye



The separation and identification of the alkane composition was carried out by gas-liquid chromatography on gas-liquid chromatographs «Chromatograph» (Model 3700) and Perkin-Elmer Sigma 2B using a flame ionization detector, helium was used as the carrier gas. In order to determine the genetic relationship between oils and the characteristics of their oil source rock, Seithaziev E. Sh. et al. [12] conducted a biomarker analysis on 39 oil samples on an Agilent 7890B chromatography-mass spectrometer in SIM mode.

The geochemical studies of oils carried out by different authors [[13], [14]] were carried out with an insufficient number of samples and less reliable methods. In this regard, it is important to combine and compare existing previously conducted studies and the results of their analyses. This will allow you to see the big picture, identify possible patterns and trends, and identify possible gaps in data or methodology. This approach can lead to a more accurate interpretation of the data, improved research methodology and, ultimately, a deeper understanding of the origin of oil.

## Results and Discussion

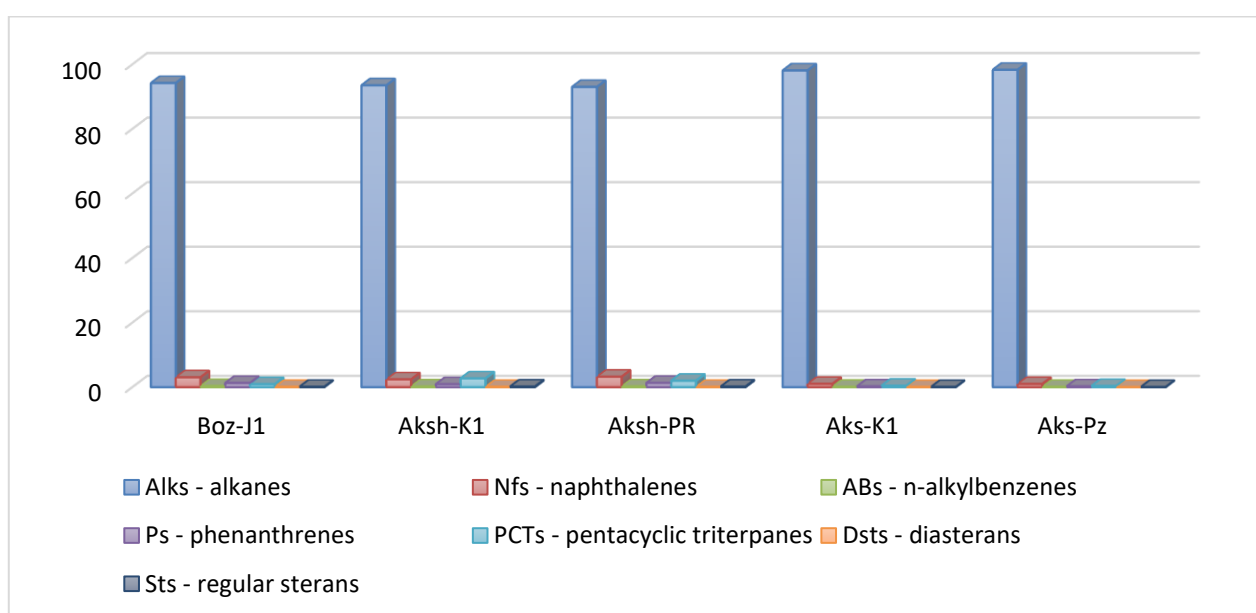
In general, the relative content of individual classes of compounds in the oils of the Arysium

trough is presented in Table 1. Thus, the studied oils are represented by such compounds as alkanes (n-alkanes, isoprenoids), polycyclic naphthenes (heylantanes, steranes, gopanes) and arenes (naphthalenes, phenanthrenes, etc.).

Normal alkanes, representing one of the main classes of hydrocarbons, are one of the most common classes of biogenic organic compounds in oil (Figure 3) [[16], [17]], the content of which among the identified compounds in the oils of the Bosingen and Akshabulak graben-syncline is 92-94% and will increase in the oils of the Aksai mountain anticline to 98% (Figure 4) [15].

Source hydrocarbon rocks are deposited in different conditions (marine, lacustrine, deltaic), in which certain microorganisms and biomass exist [13], the comparison of which makes it possible to decipher the genetic properties of oils. Biomarkers in oil retain information about these source organisms, and their analysis is used to determine the conditions of sedimentation of source rocks [18].

It is known that the ratio of pristane/phytane increases from oils formed by marine sapropel organic matter to oils generated by mixed and continental humus organic matter. But first of all, the ratio of pristane/phytane depends on the redox conditions in the sedimentation basin, given in Table 2 [15].

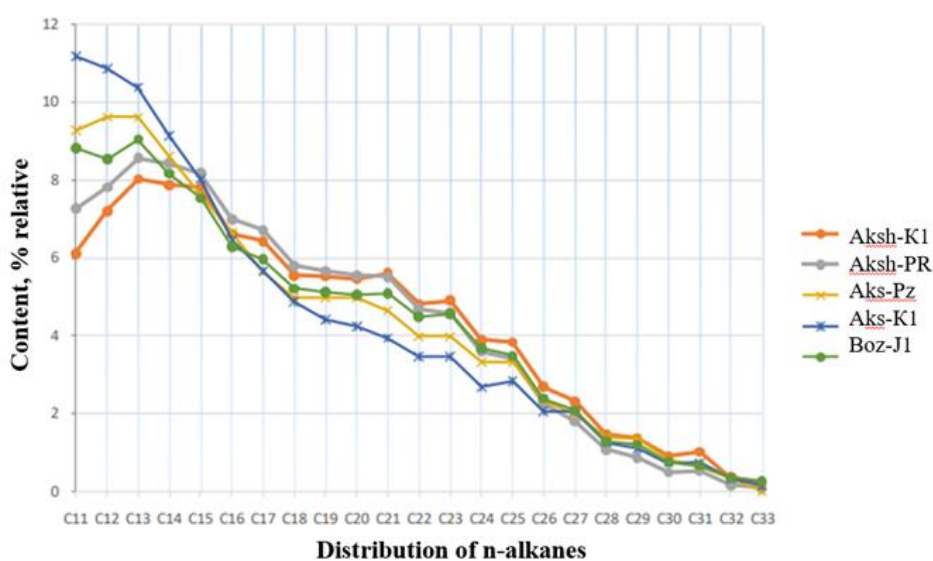


**Figure 3** – The relative content of certain classes of compounds in the oils of the Arysium trough

**Table 1** - The relative content of certain classes of compounds in the oils of the Aryskum trough [15]

Oil Index	Boz-J1	Aksh-K1	Aksh -PR	Aks-K1	Aks-Pz
<b>Group of compounds *</b>	<b>Content, % relative</b>				
Alks (m/z 57)	94.2	93.5	93.0	98.1	98.3
ABs (m/z 92)	0.35	0.22	0.24	0.11	0.09
Nfs (m/z 128 +142+156+170)	3.05	2.40	3.24	1.01	0.97
Ps (m/z 178 +192+206+220)	1.27	0.91	1.29	0.23	0.24
PCTs (m/z 191)	0.93	2.70	1.98	0.44	0.35
Dsts (m/z 217)	0.08	0.09	0.09	0.04	0.03
Sts (m/z 217)	0.09	0.18	0.17	0.04	0.03

\* Alks – alkanes, ABs – n-alkylbenzenes, Nfs – naphthalenes, Ps – phenanthrenes, PCTs – pentacyclic triterpanes, Dsts – diasterans, Sts – regular steranes.

**Figure 4** – Distribution of normal alkanes [13]**Table 2** - Dependence of the pristan /phytane ratio on redox conditions

The pristan /phytane ratio	Redox conditions
Pr/Ph <1.0	Sharply reducing sedimentation environment
Pr/Ph 1.0 – 1.5	Reducing environment
Pr/Ph 1.5 – 2.0	Weakly reducing environment or sub-oxidative sedimentation conditions
Pr/Ph >2.0	Oxidizing conditions

According to biomarker analysis [12], to determine the conditions of sedimentation of organic matter, a graph of the dependence of the ratio of pristan to phytane on the ratio of C29 sterane/ C30 gopan (Figure 5) and a trigonogram of terpane was used, according to the results of which

it was found that sedimentation of organic matter of the studied oils occurred in a predominantly oxidizing environment.

In the study [19], the same signals indicated in the previous work were used to diagnose saturated hydrocarbon fractions [12], and for aromatic fractions, the signals m/z 178, 184, 192 were selected to detect phenanthrenes, dibenzotifenes and methylphenanthrenes. This analysis was performed to characterize the oil source rocks of the studied oils: sedimentation conditions, lithology, thermal maturity and age of the oil source rocks.

According to the graph of the dependence of the ratio of pristan to phytane on the ratio of C29 sterane/ C30 gopan, which determines the conditions of sedimentation, the organic matter of the oils was formed in a lacustrine and oxidizing environment (Figure 6).

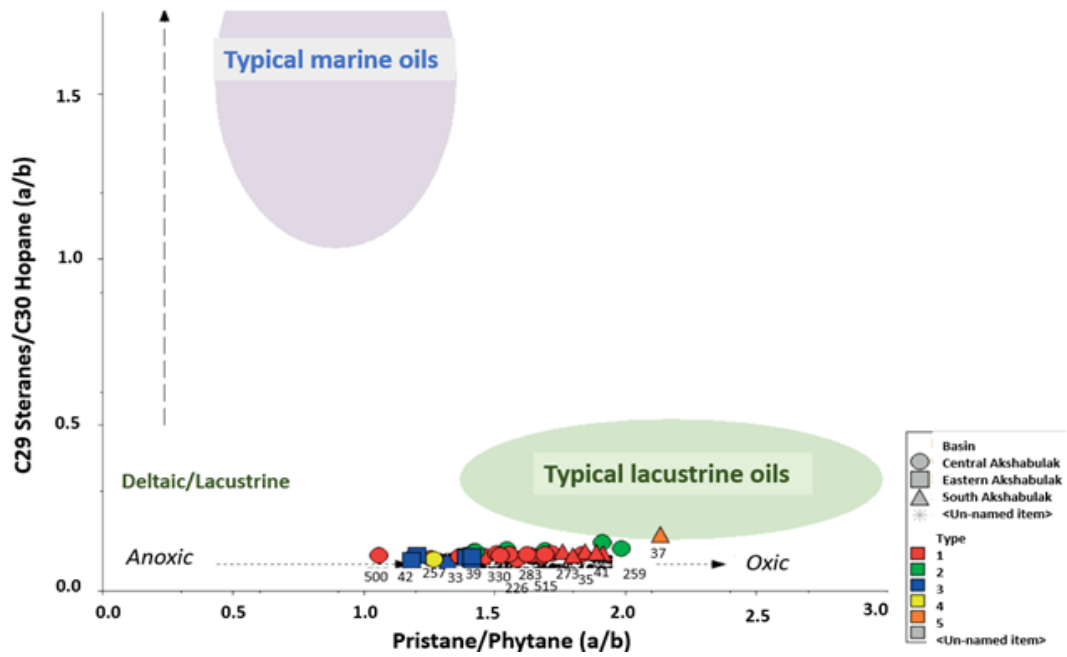


Figure 5 – Graph of the dependence of pristan/phytane (Pr/Ph) on sterane C29/ gopan C30 [12]

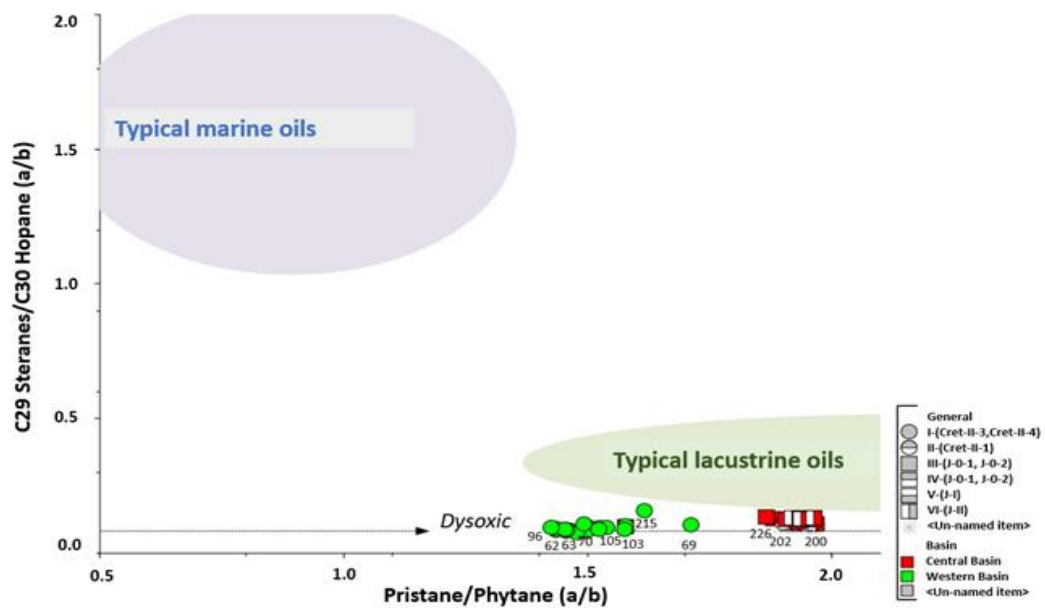


Figure 6 – Comparison of the ratio of pristan/phytane (Pr/Ph) with the ratio of C29 sterane / C30 gopan (according to Seithaziev E.Sh. et al.) [12]

Table 3 - Geological characteristics of oil samples

Oil Index	Boz-J1	Aksh-K1	Aksh -PR	Aks-K1	Aks-Pz
Structural element	Bosingen graben-syncline	Akshabulak graben-syncline		Aksai graben-syncline	
Age	J1-2 kr, J1-2ds	K1nc1ar	PR	K1nc1ar	Pz
Deposit	Sorkol	Akshabulak	Akshabulak	Kenlyk	Kenlyk
Pristane/phytane	3.1	1.6	1.8	2.6	2.7

According to the data in Table 3, it is known that in the oils of the Aryskum deflection, the value of the pristane /phytane ratio is higher than 1 and varies slightly within individual structures. In the Akshabulak graben-syncline, the values range from 1,6 to 1,8, while in the Aksai gorst-anticline from 2,7 to 2,6, which may indicate the formation of the initial organic matter that produced the oils of the Akshabulak oils under suboxidizing conditions, and the Aksai gorst-anticline under oxidizing conditions. The relatively increased value of pristan/phytane (3,1) in oil from the Lower Jurassic of the Bosingen graben-syncline indicates a higher redox potential [20].

Lithological studies of Jurassic sediments [11] indicate a lacustrine environment for the Aryskum graben-syncline. The lithology of source rocks also affects the composition of biomarkers in oil during its formation. No biomarker parameter is able to accurately identify the type of lithology of source rocks, however, it allows us to distinguish between clay or carbonate source rocks. Low C29/C30 gopan (29H/30H), low values of the homogopan index on the mass fragments of terpanes (m/z 191) of all studied oils [11] indicate the clay content of their source rocks [19].

## Conclusions

In this work, a comparative analysis of previously conducted geochemical studies was carried out to determine the composition and genesis of oils in the Aryskum trough. Studies have shown that the oils of this region are represented by the main classes of hydrocarbons, such as alkanes, polycyclic naphthenes and arenes. The content of normal alkanes in the studied oils ranged from 92% to 98%.

According to the analysis, it is known that biomarkers in oils, which allow to restore the genetic properties of oils and determine the conditions of sedimentation of oil-generating organic substances, indicate the presence of suboxidation conditions, redox potential and predominantly oxidative environment in the process of sedimentation of organic substances. The results obtained are important for understanding the processes of oil formation and generation, as well as for further forecasting the oil content of the South Torgai sedimentary basin.

**Conflicts of interest.** On behalf of all authors, the corresponding author states that there is no conflict of interest.

**Cite this article as:** Uakhiova AA, Madisheva RK, Askarova NS, Adilkhanov RK, Zheksenbaeva GM. Prospects of oil and gas potential of the South Torgai sedimentary basin. *Kompleksnoe Ispolzovanie Mineralnogo Syra = Complex Use of Mineral Resources*. 2024; 331(4):69-78. <https://doi.org/10.31643/2024/6445.40>

## Оңтүстік Торғай шөгінді алабының мұнайгаздылығының болашағы

Уахioва А.А., Мадисheва Р.К., Асқарова Н.С., Адилханов Р.К., Жексенбаева Г.М.

КЕАҚ Әбілқас Сағынов атындағы Қарағанды техникалық университеті, Қарағанды, Қазақстан

Мақала келді: 23 желтоқсан 2023  
Сараптамадан өтті: 3 қаңтар 2024  
Қабылданды: 10 қаңтар 2024

### ТҮЙІНДЕМЕ

Мұнайлылықты бағалаудың негізгі бағыттарының бірі мұнайды зерттеу болып табылады. Осыған байланысты қазіргі геохимиялық зерттеулер көмірсутектердің шығу тегі мен қайнар көзі туралы мәселеде маңызды рөл атқара отырып, жер қойнауының мұнайгаздылығын болжауда кеңінен қолданылады. Зерттеу мұнайгаздылықтың келешегін анықтау және бағалау мақсатында Оңтүстік Торғай шөгінді алабының геохимиялық сипаттамаларын кешенді талдауға бағытталған. Өртүрлі кен орындарының мұнайларының құрамын салыстыру мұнай көздерінің қабаттарын, мұнай түзілу аймақтарын және мұнайдың жинақталуын анықтауға мүмкіндік береді. Салыстыруға судың шайылуы, биодеградация және термиялық түрлендіру сияқты факторлардың әсерінен өзгерістерге ең көп немесе ең аз ұшырайтын мұнайдағы қосылыстар жатады. Бұл жұмыста Арысқұм иілісі мұнайындағы қосылыстардың жекелеген кластарының салыстырмалы құрамы, мұнай үлгілерінің геологиялық сипаттамасы және қалыпты алкандардың таралуы ұсынылған. Және Арысқұмдағы мұнайдың құрамы мен генезисін анықтау үшін бұрын жүргізілген геохимиялық зерттеулерге салыстырмалы талдау жүргізілді. Мұнайдың генетикалық сәйкестігін қалпына келтіруге және мұнай түзетін органикалық заттардың шөгу жағдайларын анықтауға мүмкіндік беретін майлардағы биомаркерлер органикалық заттардың тұндыру процесінде субтотықтырғыш жағдайлардың, тотығу-тотықсыздану потенциалының және басым тотықтырғыш ортаның болатынын көрсетеді. Алынған нәтижелер мұнайды қалыптастыру және өндіру процестерін түсіну үшін, сондай-ақ Оңтүстік Торғай шөгінді алабының мұнайлылығын одан әрі болжау үшін маңызды.

	<b>Түйін сөздер:</b> мұнайгаздылық, органикалық заттар, мұнай, биомаркерлік талдау, грабен-синклиналь, горст-синклиналь.
<b>Уахиова Аяужан Айтпаевна</b>	<b>Авторлар туралы ақпарат:</b> КЕАҚ Әбілқас Сағынов атындағы Қарағанды техникалық университетінің «Геология және пайдалы қазбалар кен орындарын барлау» кафедрасының магистранты, Н.Назарбаев даңғылы 56, 100000, Қарағанды, Қазақстан. Email: ayauzhan.uakhiova@mail.ru
<b>Мадишева Рима Копбосынқызы</b>	PhD докторы, КЕАҚ Әбілқас Сағынов атындағы Қарағанды техникалық университетінің «Геология және пайдалы қазбалар кен орындарын барлау» кафедрасының доцент м.а., Н.Назарбаев даңғылы 56, 100000, Қарағанды, Қазақстан. Email: rimta_kz@mail.ru
<b>Асқарова Назым Сражадинқызы</b>	PhD докторы, КЕАҚ Әбілқас Сағынов атындағы Қарағанды техникалық университетінің «Геология және пайдалы қазбалар кен орындарын барлау» кафедрасының оқытушысы, Н.Назарбаев даңғылы 56, 100000, Қарағанды, Қазақстан. Email: srajin-nazym@mail.ru
<b>Адилханов Руслан Кайырғалиевич</b>	КЕАҚ Әбілқас Сағынов атындағы Қарағанды техникалық университетінің «Геология және пайдалы қазбалар кен орындарын барлау» кафедрасының докторанты, Н.Назарбаев даңғылы 56, 100000, Қарағанды, Қазақстан. Email: rkbnt82@mail.ru
<b>Жексенбаева Гулмира Мединаевна</b>	КЕАҚ Әбілқас Сағынов атындағы Қарағанды техникалық университетінің «Геология және пайдалы қазбалар кен орындарын барлау» кафедрасының докторанты, Н.Назарбаев даңғылы 56, 100000, Қарағанды, Қазақстан. Email: gulmira_zh91@mail.ru

## Перспективы нефтегазоносности Южно-Торгайского осадочного бассейна

Уахиова А.А., Мадишева Р.К., Асқарова Н.С., Адилханов Р.К., Жексенбаева Г.М.

НАО Карагандинский технический университет имени Абылкаса Сагинова, Караганда, Казахстан

	<b>АННОТАЦИЯ</b> Одним из главных направлений оценки перспектив нефтеносности является изучение нефтей. В этой связи широкое практическое применение при прогнозировании нефтегазоносности недр находят современные геохимические исследования, занимая важную роль в вопросе о происхождении и об источнике углеводородов. Исследование направлено на комплексный анализ геохимических характеристик Южно-Торгайского осадочного бассейна с целью выявления и оценки перспектив нефтегазоносности. Сопоставление состава нефтей из различных залежей дает возможность определить нефтематеринские толщи, зоны нефтеобразования и нефтенакопления. Сравнению подлежат соединения в нефтях, которые наиболее или наименее подвержены изменениям под влиянием таких факторов, как вымывание водой, биодеградация и термическое преобразование. Представлено относительное содержание отдельных классов соединений в нефтях Арыскупского прогиба, геологическая характеристика образцов нефтей и распределение нормальных алканов. В данной работе был проведен сравнительный анализ ранее проведенных геохимических исследований для определения состава и генезиса нефтей в Арыскупском прогибе. Биомаркеры в нефтях, позволяющие восстановить генетические принадлежности нефтей и определить условия осадконакопления нефтегенерирующих органических веществ, свидетельствуют о наличии субокислительных условий, окислительно-восстановительном потенциале и преимущественно окислительной среде в процессе осадконакопления органических веществ. Полученные результаты имеют важное значение для понимания процессов формирования и генерации нефти, а также для дальнейшего прогнозирования нефтеносности Южно-Торгайского осадочного бассейна.
Поступила: 23 декабря 2023 Рецензирование: 3 января 2024 Принята в печать: 10 января 2024	<b>Ключевые слова:</b> нефтегазоносность, органическое вещество, нефть, биомаркерный анализ, грабен-синклиналь, горст-синклиналь.
<b>Уахиова Аяужан Айтпаевна</b>	<b>Информация об авторах:</b> Магистрант кафедры «Геология и разведка МПИ» НАО Карагандинского технического университета имени Абылкаса Сагинова, пр. Н.Назарбаева 56, 100000, Караганда, Казахстан. Email: ayauzhan.uakhiova@mail.ru
<b>Мадишева Рима Копбосынқызы</b>	Доктор PhD, и.о. доцента кафедры «Геология и разведка МПИ» НАО Карагандинского технического университета имени Абылкаса Сагинова, пр. Н.Назарбаева 56, 100000, Караганда, Казахстан. Email: rimta_kz@mail.ru
<b>Асқарова Назым Сражадинқызы</b>	Доктор PhD, преподаватель кафедры «Геология и разведка МПИ» НАО Карагандинского технического университета имени Абылкаса Сагинова, пр. Н.Назарбаева 56, 100000, Караганда, Казахстан. Email: srajin-nazym@mail.ru
<b>Адилханов Руслан Кайырғалиевич</b>	Докторант кафедры «Геология и разведка МПИ» НАО Карагандинского технического университета имени Абылкаса Сагинова, пр. Н.Назарбаева 56, 100000, Караганда, Казахстан. Email: rkbnt82@mail.ru
<b>Жексенбаева Гулмира Мединаевна</b>	Докторант кафедры «Геология и разведка МПИ» НАО Карагандинского технического университета имени Абылкаса Сагинова, пр. Н.Назарбаева 56, 100000, Караганда, Казахстан. Email: gulmira_zh91@mail.ru



## References

- [1] Peters KE, Walters CC, Moldowan JM. The biomarker guide I. Biomarkers and isotopes in the environment. 2nd ed. Cambridge: Cambridge University Press. 2005; 1:474.
- [2] Alberdi M, Lopez L. Biomarkers 18(H)-oleanane: A geochemical tool to assess Venezuelan petroleum systems. *Journal of South American Earth Sciences*. 2000; 13(8):751–759. [https://doi.org/10.1016/S0895-9811\(00\)00055-9](https://doi.org/10.1016/S0895-9811(00)00055-9)
- [3] Avbovbo AA. Tertiary Litho-stratigraphy of Niger Delta. *American Association of Petroleum Geologists Bulletin*. 1978; 62:295-300.
- [4] Botwe Takyi, Selegba Abrakassa, Udom GJ, Koffi Eugene Kouadio, Frederick k. Bempong & Eric Brantson Thompson. Source of organic matter and paleoenvironment of deposition of crude oils from the Niger Delta Basin. *Petroleum science and Technology*. 2022; 40(12):1479-1491. <https://doi.org/10.1080/10916466.2021.2024229>
- [5] Rabiatiu Abubakar, Kofi Adomako-Ansah, Solomon Adjei Marfo, Judith Ampomah Owusu & Clifford Fenyi. Origin and depositional environment of oils and sediments in the Cretaceous Deep-Water Tano Basin, Ghana: Constraints from biomarkers. *Petroleum science and Technology*. 2022. <https://doi.org/10.1080/10916466.2022.2143804>
- [6] Fishman IL. Geodinamicheskiye modeli Aralo-Kaspiyskogo regiona [Geodynamic models of the Aral-Caspian region]. *Almaty*. 2016, 156. (in Russ.).
- [7] Ozdoyev SM, Madisheva RK, Seylkanov TM, Portnov VS, Isayev I. O neftegazonosnosti kory vyvetrivaniya skladchatogo fundamenta Aryskumskogo progiba Yuzhno-Torgayskogo basseyna [On the oil and gas content of the weathering crust of the folded basement of the Aryskum trough of the South Torgai basin]. *Neft i gaz = Oil and gas*. 2020; 1(115):17-32. (in Russ.).
- [8] Aydarbekov KD. Istoriya otkrytiya i osvoyeniya mestorozhdeniya Kumkol [The history of the discovery and development of the Kumkol deposit]. *Neft i gaz = Oil and gas*. 2020; 3-4:(117-118, 180-186). (in Russ.).
- [9] Turkov OS. K voprosu o glubinnoy nefti Yuzhno-Torgayskogo basseyna [On the issue of deep oil in the South Torgai basin]. *Neft i gaz = Oil and gas*. 2020; 5(119):70-83. (in Russ.).
- [10] Zholtayev G, Zhylkaydarov SE. Otsenka prognoznnykh resursov uglevodorodnogo syria. Respubliki Kazakhstan v 3-kh knigakh. Kniga II. Tekst otcheta (neft, gaz, kondensat), otchet po Programme 46 [Assessment of the projected hydrocarbon resources of the Republic of Kazakhstan in 3 books. Book II. Text of the report (oil, gas, condensate), Program Report 46]. *Almaty*. 2003. (in Russ.).
- [11] Bolat E. Usloviya formirovaniya i zakonomernosti razmeshcheniya skopleniy nefi i gaza v Yuzhno-Turgayskom basseyne [Conditions of formation and patterns of placement of oil and gas accumulations in the South Turgai basin] *Dissertatsiya na soiskaniye uch. st. kand. geologo-mineral. nauk, Rossiyskiy Gosudarstvennyy geologorazvedochnyy universitet imeni Sergo Ordzhonikidze = Dissertation for the degree of Candidate of Geological and Mineral Sciences, Sergo Ordzhonikidze Russian State Geological Exploration University, Moskva*. 2020, 1-97. (in Russ.).
- [12] Seytkhaziyev Esh, Uteyev RN, Mustafayev MK, Lyu Sh, Sarsenbekov ND, Dosmukhambetov AK. Fingerprinting i biomarkernyy analiz nefi Akshabulakskoy gruppy dlya opredeleniya tipov neftey [Fingerprinting and biomarker analysis of oil of the Akshabulak group to determine the types of oils]. *Vestnik neftegazovoy otrasli Kazakhstana = Bulletin of the oil and gas industry of Kazakhstan*. 2021; 4(9):93-110. (in Russ.).
- [13] Madisheva RK. Issledovaniye geodinamicheskoy obstanovki osadkonakopleniya i formirovaniya neftegazonosnosti doyrskogo kompleksa Aryskumskogo progiba [Investigation of the geodynamic situation of sedimentation and formation of oil and gas potential of the pre-Jurassic complex of the Aryskum trough]. *Dissertatsiya na soiskaniye stepeni doktora filosofii, Karagandinskiy tekhnicheskii universitet = Dissertation for the degree of Doctor of Philosophy, Karaganda Technical University, Karaganda*. 2020, 1-68. (in Russ.).
- [14] Golyshev SI, Padalko NL, Madisheva RK, Ozdoyev SZh, Portnov VS, Isayev VI. Izotopnyy sostav neftey Aryskumskogo progiba (Yuzhnyy Kazakhstan) [The composition of biomarkers and the origin of oils of the Aryskum trough (South Kazakhstan)]. *Izvestiya Tomskogo politekhnicheskogo universiteta, Inzhiniring georesursov = Proceedings of Tomsk Polytechnic University, Georesource engineering*. 2020, 80-89. (in Russ.). <https://doi.org/10.18799/24131830/2020/3/2533>
- [15] Madisheva RK, Serebrennikova OV, Isayev VI, Portnov VS, Ozdoyev SM. Sostav biomarkerov i proiskhozhdeniye neftey Aryskumskogo progiba (Yuzhnyy Kazakhstan). [The composition of biomarkers and the origin of oils of the Aryskum trough (South Kazakhstan)]. *Izvestiya Tomskogo politekhnicheskogo universiteta, Inzhiniring georesursov = Proceedings of Tomsk Polytechnic University, Georesource engineering*, 2020; 331(7):116-130. (in Russ.). <https://doi.org/10.18799/24131830/2020/7/2724>
- [16] Tissot BP, Welte DH. Petroleum formation and occurrence. NewYork: Springer-Verlag. 1984, 699. <http://dx.doi.org/10.1007/978-3-642-87813-8>
- [17] Murillo WA, Horsfield B, Vieth-Hillebrand A. Unraveling petroleum mixtures from the South Viking Graben, North Sea: a study based on  $\delta^{13}C$  of individual hydrocarbons and molecular data. *Organic Geochemistry*. 2019; 137:103900. <https://doi.org/10.1016/j.orggeochem.2019.103900>
- [18] Seytkhaziyev Esh, Uteyev RN, Mustafayev MK, Lyu Sh, Sarsenbekov ND, Dosmukhambetov AK, Dzhumabayev TE. Primeneniye biomarkerov i fingerprintinga nefi dlya rasshifrovki geneticheskoy prinadlezhnosti nefi i prognozirovaniya puti migratsii nefi na mestorozhdenii Nuraly [The use of biomarkers and oil fingerprinting to decipher the genetic affiliation of oil and predict the

migration path of oil at the Nuraly field]. Vestnik neftegazovoy otrasli Kazakhstana = Bulletin of the oil and gas industry of Kazakhstan. 2021; 2(7):61-75. (in Russ.). <https://doi.org/10.54859/kjogi89490>

[19] Seytkhaziyev ESh, Dzhumabayev TE, Latipova AM, Dosmukhambetov AK. Otchet geokhimicheskoye issledovaniya prob nefti mestorozhdeniya Nuraly (v ramkakh proyekta «Pereschet zapasov nefti, gaza, kondensata i poputnykh komponentov mestorozhdeniya Nuraly) [Report on geochemical studies of oil samples from the Nuraly field (within the framework of the project "Recalculation of oil, gas, condensate, and associated components of the Nuraly field)]. Atyrauskiy filial TOO KMG Inzhiniring = Atyrau branch of KMG Engineering LLP. 2021, 1-88. (in Russ.).

[20] Madisheva RK, Portnov VS. O neftegazonosnosti Aryskumskogo progiba Yuzhno-Torgayskogo osadochnogo basseyna [On the oil and gas potential of the Aryskum trough of the South Torgai sedimentary basin]. Neft i gaz = Oil and gas. 2022; 5(131):65-76. (in Russ.). <https://doi.org/10.37878/2708-0080/2022-5.04>



DOI: 10.31643/2024/6445.41

Metallurgy



## Calculation of the thermoplastic beryllium oxide slurry molding with ultrasonic activation

<sup>1</sup> Zhabbasbayev U.K., <sup>1\*</sup> Ramazanova G.I., <sup>2</sup> Terekhov V.I., <sup>3</sup> Sattinova Z.K.

<sup>1</sup>Satbayev University, Almaty, Kazakhstan

<sup>2</sup>Kutateladze Institute of Thermophysics SB RAS, Novosibirsk, Russia

<sup>2</sup>L.N. Gumilev Eurasian National University, Astana, Kazakhstan

\*Corresponding author email: g.ramazanova@satbayev.university

<p>Received: October 5, 2023 Peer-reviewed: November 5, 2023 Accepted: January 11, 2024</p>	<p><b>ABSTRACT</b></p> <p>The article presents the results of assessing thermal shrinkage during the formation of beryllium oxide ceramics using the hot casting method. The thermoplastic slurry is a composite system with a dispersion medium (binder) that has a very low thermal conductivity compared to the dispersed phase (beryllium oxide). Ultrasonic treatment reduces the viscosity of the slurry and improves its casting properties. The formation of beryllium oxide slurry is carried out without disrupting the integrity of the system and depends on the casting speed and temperature factors. The combined influence of these factors determines the casting properties of the slurry. Cooling - solidification of the slurry in the casting mold occurs in stages in the liquid, amorphous states with a phase transition, and in the viscoplastic state of the casting. The cooling rate of the casting at all stages depends on the cavity design, the rheological properties of the slurry, and the casting process parameters. It is important to maintain the integrity of the casting due to temperature shrinkage.</p> <p><b>Keywords:</b> thermoplastic slurry, formation, shrinkage, casting properties, beryllium oxide, ultrasonic treatment.</p>
<p><b>Zhabbasbayev Uzak Kairbeekovic</b></p>	<p><b>Information about authors:</b> Doctor of Technical Sciences, Professor, Head of the Research and Production Laboratory "Modeling in Energy", Satbayev University, 22 Satpaev Street, 050013 Almaty, Kazakhstan. Email: uzak.zh@mail.ru</p>
<p><b>Ramazanova Gaukhar Izbasarovna</b></p>	<p>Candidate of physical and mathematical sciences, Leading Researcher. Research and Production Laboratory "Modeling in Energy", Satbayev University, 22 Satbayev str., 050013 Almaty, Kazakhstan. E-mail: g.ramazanova@satbayev.university</p>
<p><b>Terekhov Victor Ivanovich</b></p>	<p>Doctor of Technical Sciences, Professor, Chief Researcher of the Kutateladze Institute of Thermophysics, Siberian Branch of the Russian Academy of Sciences. 1 Academician Lavrentiev av., 630090 Novosibirsk, Russia. Email: terekhov@itp.nsc.ru</p>
<p><b>Sattinova Zamira Kanaevna</b></p>	<p>Candidate of physical and mathematical sciences, Associated Professor, L.N. Gumilev Eurasian National University, 2 Satpayev str., 010008 Astana, Kazakhstan. E-mail: sattinova.kz@gmail.com</p>

### Introduction

Currently, products made from beryllium oxide (BeO) ceramics, obtained through the slurry casting technology, are widely used in the following applications [[1], [2], [3], [4], [5], [6]]:

1) Refractory material for crucibles used in melting metallic beryllium, uranium, and precious metals.

2) Insulators and heat sinks, substrates for transistors, and microchips in the electronics, radio, and electrical industries.

3) Windows and insulators for microwave (MW) technology.

4) Dielectric discharge tubes, resonators, and hollow dielectric waveguides in gas lasers covering a wide spectral range.

5) Heat pipes in cryogenic engineering, where thermal conductivity at temperatures ranging from 45 to 50 K can reach tens of thousands of W/(m·K).

6) Material for the heat-generating matrix element in nuclear reactors.

7) Neutron reflectors as part of neutron filters, with additives (such as boron) for protection against neutrons of various energies.

Beryllium oxide ceramics possess high chemical, thermal, and radiation resistance [[1], [2], [6]]. Unlike other types of oxide ceramics, it can absorb and reflect neutrons of various energies [[1], [2], [6]]. It has exceptional thermal conductivity, up to 320 W/(m·K) [[1], [2], [3], [4], [5], [6]], and a sound velocity of over 12,000 m/s [2]. Without the addition of impurities, BeO ceramics exhibit high electrical

resistance and mechanical strength [[1], [2], [6]]. They are effective at transmitting various forms of electromagnetic radiation [[1], [2], [6]]. With the addition of TiO<sub>2</sub>, they can be used in powerful microwave energy absorbers [[2], [6]]. Beryllium oxide ceramics have a melting temperature of around 2843 K, while ceramics based on Al<sub>2</sub>O<sub>3</sub> melt at only 2323 K [[2], [6]]. When cooled to 50 K, the thermal conductivity of BeO monocrystals sharply increases to 13,500 W/(m·K), which is also characteristic of BeO ceramics [[2], [3]].

The process of forming ceramics through hot casting involves several stages [[2], [6], [7], [8], [9], [10], [11]]: movement and heat exchange in the liquid state; movement and heat exchange in the amorphous state; movement and heat exchange in the solid-plastic state.

The hydrodynamics of the slurry in the casting mold fall into the category of physical processes related to flow and deformation. The slurry retains its configuration after exiting the feeder. Experimental findings indicate that within the range of possible casting speeds, the slurry's movement in the casting mold is laminar [[6], [7], [8], [9]]. The slurry enters the casting mold at temperatures of 75-80°C and cools down to 35-40°C, allowing the casting to be removed from the mold without warping [[6], [7], [9]]. During the stage of filling the mold cavity, it is crucial to ensure maximum disruption of the structure to obtain a homogeneous suspension [[2], [6], [9]]. This is achieved through ultrasonic treatment [[6], [11], [12], [13]].

During the cooling - solidification process, there is a change in the volume of the slurry, which results in shrinkage occurring in three stages: in the liquid, amorphous, and solid-plastic states [[2], [6], [8]]. The main technological problem solved at this stage is to achieve compensation of internal shrinkage [[6], [8], [13]]. The importance of this operation lies in the fact that the absence or incomplete compensation of internal shrinkage can lead to internal defects (cracks, porosity) in castings and products [[6], [8], [13]]. During solidification, it is necessary to minimize friction against the mold walls and maximize plasticity without disrupting the newly forming structure of the casting [[6], [8], [13]].

In the previous works of the authors [[7], [9], [15]], the results of experiments and calculations of the motion and heat exchange of beryllium oxide

slurry with ultrasonic activation were presented. The experimental results established the process of forming a liquid slurry with a transition to a viscoplastic state. It was shown that the calculated and experimental data are in agreement and confirm the physical validity of the proposed mathematical model of the forming process [[7], [9], [15]].

This study presents calculations of the impact of casting speed and temperature factors on shrinkage during the formation of beryllium oxide slurry with ultrasonic activation.

## Forming Process

### Experimental Setup

The schematic of the ultrasonic casting setup is shown in Figure 1.

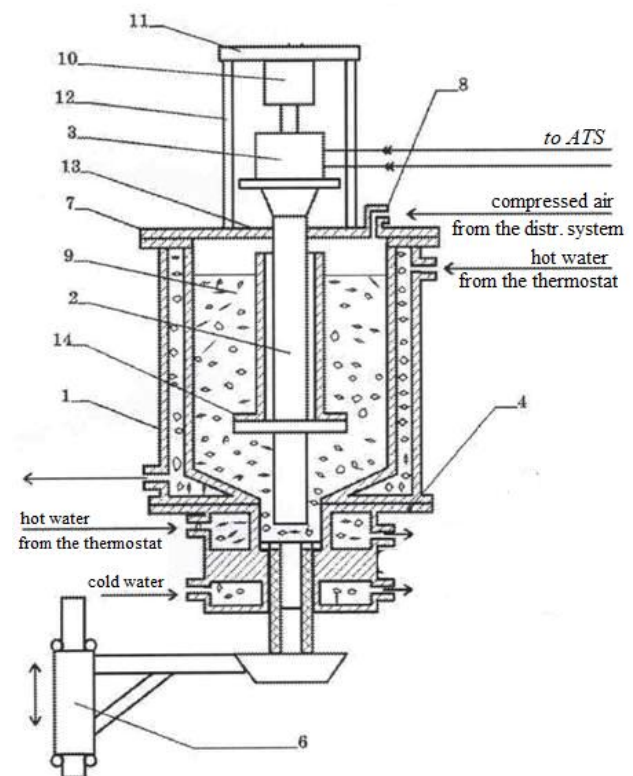


Figure 1 - Schematic of the experimental ultrasonic setup

The setup comprises a heated slurry tank 1 with an attached acoustic-technological system (ATS), consisting of a longitudinal waveguide 2 with a magnetostrictive transducer 3 of the PMS type, a three-loop filer 4, and a mechanism for controlling the movement of the billet 6.

The ultrasonic generator USG2-4 was used as the power source for the acoustic systems. The main parameters of the setup are provided in Table 1.

**Table 1** - Technical Characteristics of the Ultrasonic Casting Setup

Parameter Name	Value
General Information	
1. Power consumed by the equipment, kW	6.0
2. Operating voltage, V	220/380
3. Working tank volume, l	8
4. Casting speed (productivity), mm/min	10-120
Ultrasonic Equipment Data	
5. 5. Ultrasonic generator parameters: USG power, kW	4
6. Operating frequency, kHz	18±1.35
7. Operating voltage, V	220±44
8. Bias current, A	18±3
9. AFC accuracy, Hz	50
10. Radio interference level	According to GOST 23450-79
Utility product data	
11. Pressure, MPa	0.2
12. Water flow rate, m³/h	1.0
13. Water temperature, °C for the hot circuit of the die and slurry tank - for the warm circuit of the die - for the cold circuit of the die	80 56 40
14. Compressed gas pressure, MPa	Up to 1.0

*The die of the casting setup*

The formation of thermoplastic beryllium oxide slurry takes place within the die of the casting setup [[6], [8]]. The die has a round-shaped cavity (Fig. 2a) or a ring-shaped cavity (Fig. 2b) with a cooling circuit.

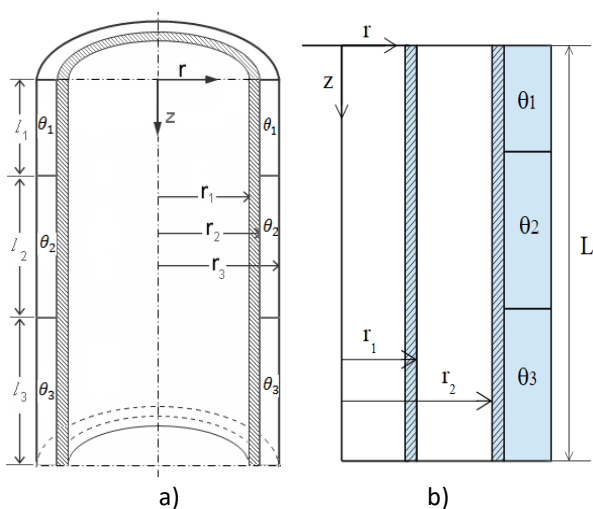


**Figure 2** - Schematic diagram of the die:

a) round-shaped cavity; b) ring-shaped cavity

In the calculations, the round cavity has a radius of  $r_1 = 0.006$  m and a length of  $L = 0.089$  m, while the ring-shaped cavity has radii of  $r_1 = 0.006$  m,  $r_2 = 0.00675$  m, and a length of  $L = 0.089$  m. Liquid slurry enters the die cavity with an initial temperature of  $t_0$ . As it progresses, the slurry mass cools down and solidifies. The slurry takes on a structural form, emerging from the round cavity as a rod (Fig. 2a) and as a tube from the ring-shaped cavity (Fig. 2b). The density of the slurry is variable and increases as it solidifies.

**Mass and Heat Transfer Model**

*Rheology of Thermoplastic Slurry*

In experiments [[6], [14]], BeO slurry exhibits the rheology of a non-Newtonian fluid with a yield stress and high viscosity. The effective (apparent) molecular viscosity of a viscoplastic fluid with a yield stress under shear can be expressed as [[15], [16], [17], [18]]:

$$\mu_{eff} = \begin{cases} \mu_p + \tau_0 |\dot{\gamma}|^{-1}, & \text{if } |\tau| > \tau_0 \\ \infty, & \text{if } |\tau| \leq \tau_0 \end{cases} \quad (1)$$

Here,  $\tau_0$  is the yield stress,  $|\tau| = \sqrt{\tau_{ij}\tau_{ij}}$  is the second invariant of the deviatoric stress tensor,  $\mu_p$  is the plastic viscosity,  $\dot{\gamma} = \sqrt{2S_{ij}S_{ij}} = S^2$  is the shear rate,  $S_{ij} = 0.5 \left( \frac{\partial U_i}{\partial x_j} + \frac{\partial U_j}{\partial x_i} \right)$  is the strain rate tensor.

The expression (1) corresponds to the Schwedoff-Bingham fluid model [18].

In regions where the shear stress is less than  $\tau \leq \tau_0$ , the effective viscosity exhibits singular behavior. The effective viscosity can be represented as a smooth function using the regularization approach [19]:

$$\mu_{eff} = \mu_p + \tau_0 \frac{[1 - \exp(-10^3 |S|)]}{|S|} \quad (2)$$

where  $m = 1000$  is a regularization parameter [19]. Expression (2) helps overcome the difficulties in the presence of the yield limit for the Schwedoff-Bingham fluids.

*Basic Equations*

The forming process occurs in a steady-state mode. The length of the cavities is greater than their



radial dimensions (Figure 1). Therefore, the motion equation can be written in the approximation of a narrow channel [7], taking into account the expression for effective viscosity (1):

$$\rho u \frac{\partial u}{\partial z} + \rho v \frac{\partial u}{\partial r} = -\frac{dp}{dz} + \frac{1}{r} \frac{\partial}{\partial r} \left( r \mu_{eff} \frac{\partial u}{\partial r} \right) + \rho g \quad (3)$$

$$\frac{\partial \rho u}{\partial z} + \frac{1}{r} \frac{\partial r \rho v}{\partial r} = 0 \quad (4)$$

Heat exchange occurs along the length and radius of the cavity due to the cooling of the slurry. As experiments show, the change in the slurry's phase state occurs within a temperature range from 59 to 54°C [7]. In this case, the heat of phase transition is taken into account using a model of apparent heat capacity [[20], [21], [22], [23], [24], [25]]. The heat transfer equation, with the adopted assumptions, can be written as [[7], [26]]:

$$\rho u c_p \frac{\partial t}{\partial z} + \rho v c_p \frac{\partial t}{\partial r} = \frac{\partial}{\partial z} \left( \lambda \frac{\partial t}{\partial z} \right) + \frac{1}{r} \frac{\partial}{\partial r} \left( r \lambda \frac{\partial t}{\partial r} \right) + \mu_p \left( \frac{\partial u}{\partial r} \right)^2 \quad (5)$$

Here,  $z$  and  $r$  are the axial and radial coordinates,  $u$  and  $v$  are velocity components,  $p$ ,  $\rho$ ,  $t$ ,  $c_p$ ,  $\mu_{eff}$ ,  $\mu_p$ ,  $\lambda$  are pressure, density, temperature, apparent heat capacity coefficient, effective and plastic viscosity, and thermal conductivity of the slurry, respectively.

The pressure gradient is determined from the conservation of mass flow rate [27]:

$$\int_S \rho u dS = \rho_o u_o S \quad (6)$$

where  $S$  is the cross-sectional area of the cavity.

The boundary conditions for this problem are standard: for the slurry velocity on the cavity walls in the liquid state, no-slip conditions are applied; in the transition and solidifying zones, slip conditions are used. For the slurry temperature, Dirichlet conditions are applied to the outer cavity wall, while Neumann conditions are applied to the axis or inner cavity wall.

The dependencies of density, physicochemical properties of the slurry on temperature with US activation, and the consideration of phase transition heat using the apparent heat capacity method are provided in [7]. The system of equations (1)-(6) is solved by a numerical method [27]. The pressure

gradient is determined by the method of splitting from the conservation of mass flow rate (6).

*Verification of Calculation Data*

Verification of the calculations was carried out using experimental data [[6], [15]] obtained for beryllium oxide slurry in a ring-shaped cavity. The calculations were performed under the same process parameters as in the experiments (Table 2). The cooling contour of the die is divided into three parts. In the first part, the cooling water temperature is  $\theta_1 = 80^\circ\text{C}$ , in the second part  $\theta_2 = 56^\circ\text{C}$ , and in the third part  $\theta_3 = 40^\circ\text{C}$ .

In the first cooling circuit, the wall temperature is  $\theta_1 = 80^\circ\text{C}$ . The temperature field shows a decrease in temperature from 80 to 78°C (Figure 3a), and the density field increases from 2260 to 2275 kg/m<sup>3</sup> (Figure 3b).

In the second cooling circuit, the wall temperature is  $\theta_2 = 56^\circ\text{C}$ . The dynamic viscosity  $\mu_p(t)$ , density  $\rho(t)$ , and yield shear stress  $\tau_0(t)$  increase as the temperature decreases. The slurry temperature decreases from 78°C to 54°C (Figure 3a), and the density increases from 2275 kg/m<sup>3</sup> to 2335 kg/m<sup>3</sup> (Figure 3b).

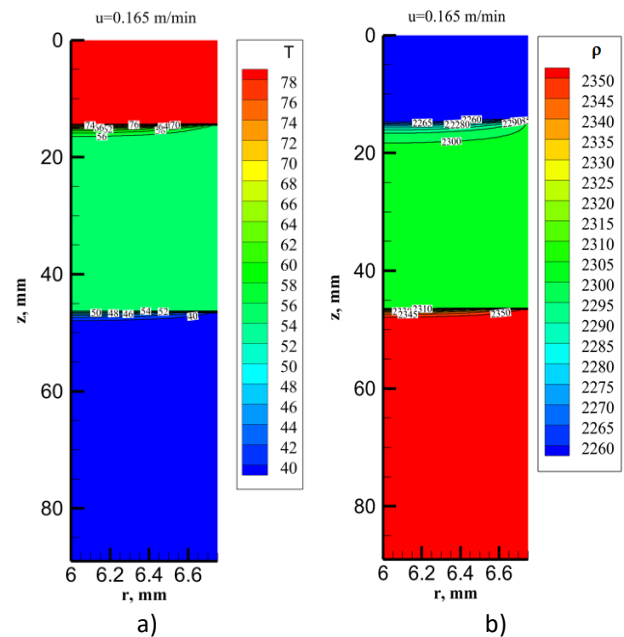


**Figure 3** – Calculated data for temperature and density at a binder mass fraction  $\omega = 0.117$

In the third cooling circuit, the wall temperature is  $\theta_3 = 40^\circ\text{C}$ . The slurry temperature decreases from 54°C to 40°C (Figure 3a), and the density increases from 2335 kg/m<sup>3</sup> to 2360 kg/m<sup>3</sup> (Figure 3b).

The isotherm at  $t=59^\circ\text{C}$  represents the upper limit of the transition zone, while the isotherm at  $t=54^\circ\text{C}$  represents the lower limit. Within this zone, the slurry is in an amorphous state.

**Table 2** - Slurry Parameters as a Function of Casting Speed in the Ring-Shaped Cavity [6]

Content of Binder in Slurry, Mass Fraction	Slurry Viscosity at $T_0 = 80^\circ\text{C}$ , Pa·s	Casting Ability of Slurry, mm	Casting Speed, mm/min	Mechanical Strength of Casting (Bending), MPa
0.117	2.80	89	165	8.17

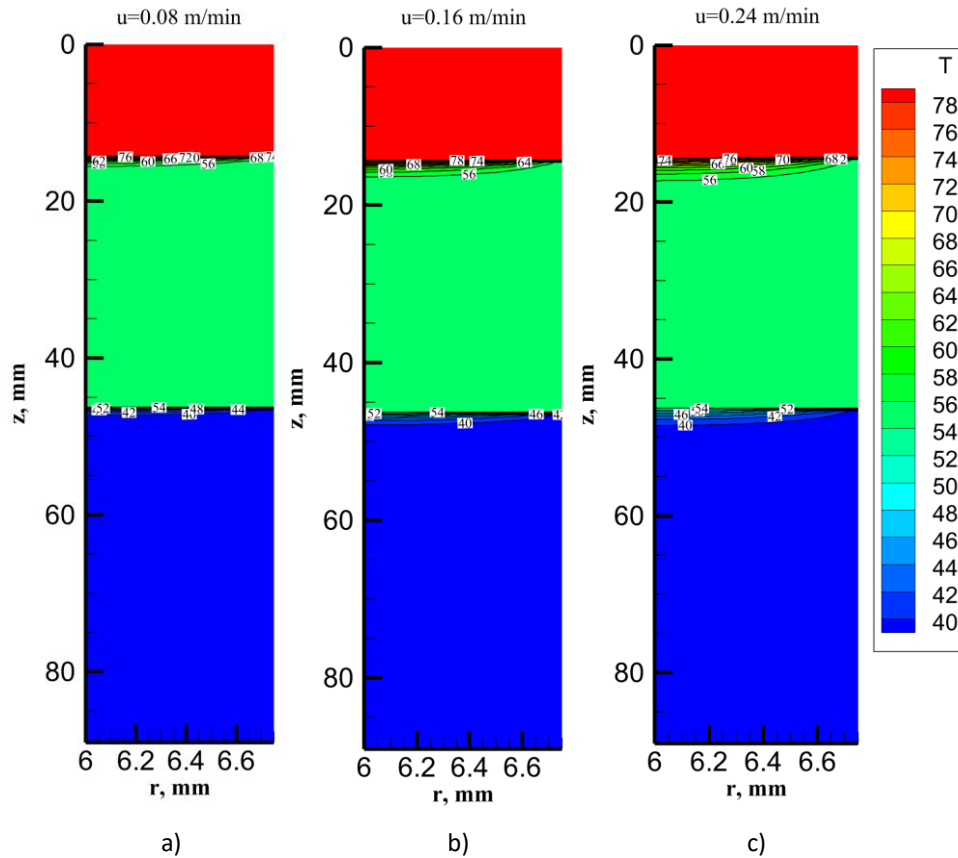


**Figure 4** – Temperature field of BeO slurry in the ring-shaped cavity at different casting speeds and a binder mass fraction of  $\omega = 0.117$

**The discussion of the calculation data**

Figure 4 illustrates the temperature distribution in the ring-shaped cavity for three cooling circuits of the die with a cavity thickness of  $r_2 - r_1 = 0.75$  mm and a length of  $L = 89$  mm. The casting speeds were  $u = 0.08$  m/min,  $0.16$  m/min, and  $0.24$  m/min. The water temperatures in the cooling circuits are  $\theta_1 = 80^\circ\text{C}$ ,  $\theta_2 = 56^\circ\text{C}$ , and  $\theta_3 = 40^\circ\text{C}$ .

The slurry temperature at the entrance to the ring-shaped cavity is constant across the section and equal to  $t_0 = 80^\circ\text{C}$ . In the first cooling circuit, the wall temperature is  $\theta_1 = 80^\circ\text{C}$ , and in this region, the slurry temperature decreases slightly from  $80^\circ\text{C}$  to  $78^\circ\text{C}$  (Figure 4).

It is known that heat is transferred due to thermal conductivity against the flow of the slurry [26]. This explains the temperature reduction in the first part of the cavity. The temperature field determines the rheological and thermophysical properties of the slurry mass in its liquid state.

In the second cooling circuit, the wall temperature is  $\theta_2 = 56^\circ\text{C}$ . The dynamic viscosity  $\mu_p(t)$ , density  $\rho(t)$ , and yield shear stress  $\tau_0(t)$  increase as the temperature decreases. The slurry slides along the cavity walls along the length of the second circuit. This causes the profile of the longitudinal velocity component downstream to become constant across the cavity cross-section

The increase in heat removal from the wall in the second cooling circuit results in a reduction in the

temperature field (Figure 4). At the beginning of the second circuit, there is a region where the temperature field is variable and indicates the transition of the slurry from a liquid to an amorphous state. In this region, the temperature decreases from 78 to 54°C, marking the onset of a change in the slurry's aggregate state [[6], [7], [8]].

In the third cooling circuit, where the wall temperature is  $\theta_3 = 40^\circ\text{C}$ , the temperature decreases from 54 to 40°C. In the third part of the cavity, the slurry transitions from an amorphous to a viscoplastic state. The slurry's sliding motion on the wall ensures the continuity of the slurry and the preservation of the structural form of the casting without warping.

The increase in casting speed leads to an expansion of the transition zone from liquid to amorphous state and from amorphous to viscoplastic state (see Figure 4).

The variation in density reflects the transition of the slurry within the cavity from one structural state to another. Figure 5 illustrates the density field in the ring-shaped cavity at casting speeds of  $u = 0.08$  m/min, 0.16 m/min, and 0.24 m/min. As shown in Figure 5, the slurry's density increases as the temperature decreases and the slurry cools along the length of the ring-shaped cavity.

In the first cooling circuit, there is a slight increase in slurry density, and the slurry remains in a liquid state. In the second cooling circuit, a significant increase in slurry density occurs, indicating the transition of the slurry from a liquid to an amorphous state. In this region, there is a change in the slurry's aggregate state with the crystallization of the binder material. Further increases in slurry density occur in the third circuit due to the solidification of the casting.

During the solidification stage, it is crucial to ensure compensation for the internal shrinkage of the casting. Without adequate compensation for internal shrinkage, internal defects such as shrinkage cavities and porosities can occur in castings and products.

In the ring-shaped cavity, the computational data consistently show a continuous change in density at all stages of forming, taking into account compensation for internal shrinkage through the supply of liquid slurry (Figure 5).

Therefore, the density field visually illustrates the entire forming stage with the shrinkage of beryllium oxide slurry.

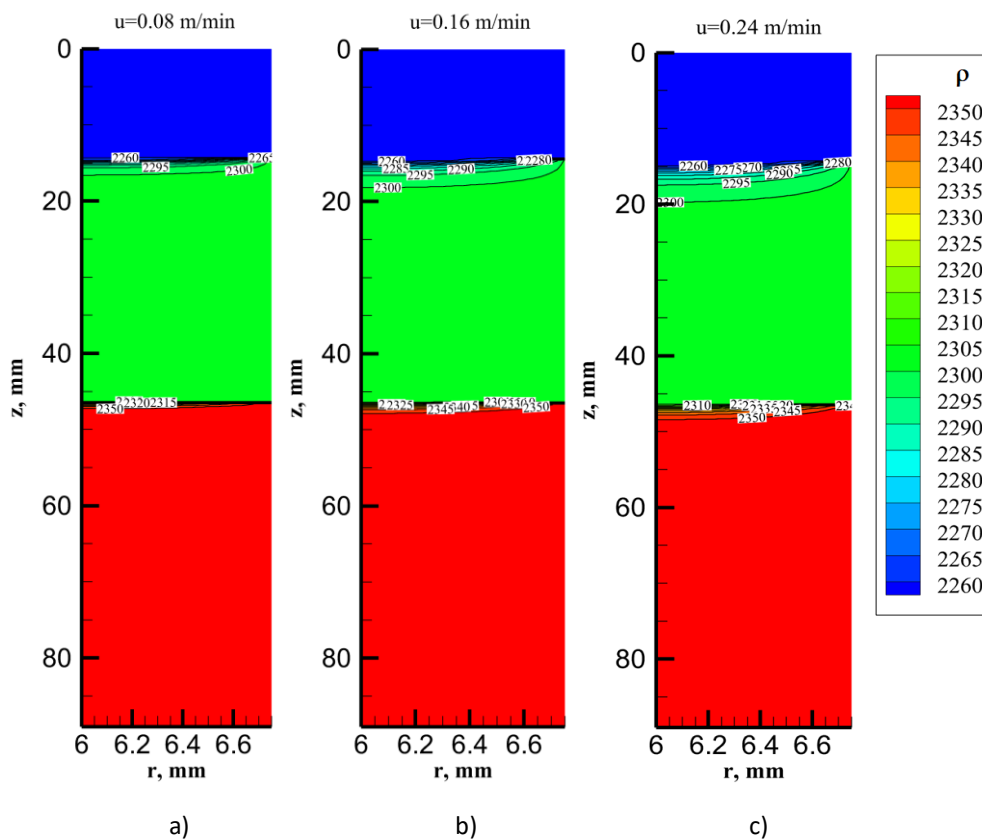


**Figure 5** – Beryllium oxide slurry density field in the ring-shaped cavity at different casting speeds and a binder mass fraction of  $\omega=0.117$

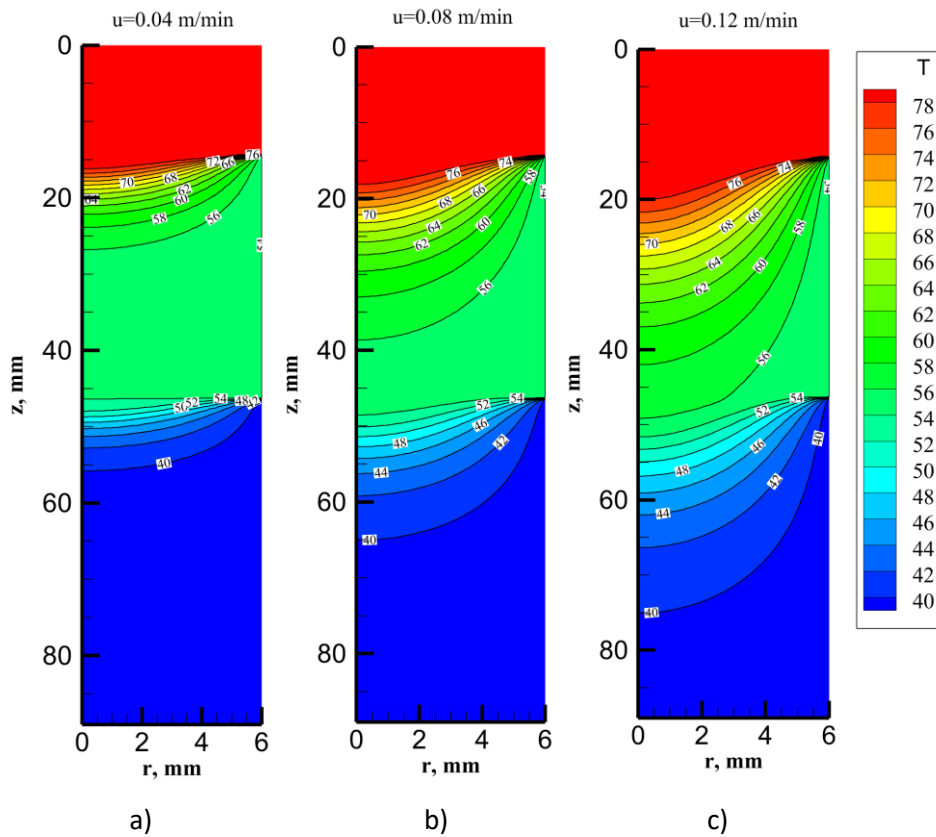


Figure 6 – Temperature field of BeO slurry in the round cavity at different casting speeds and a binder mass fraction of  $\omega=0.117$

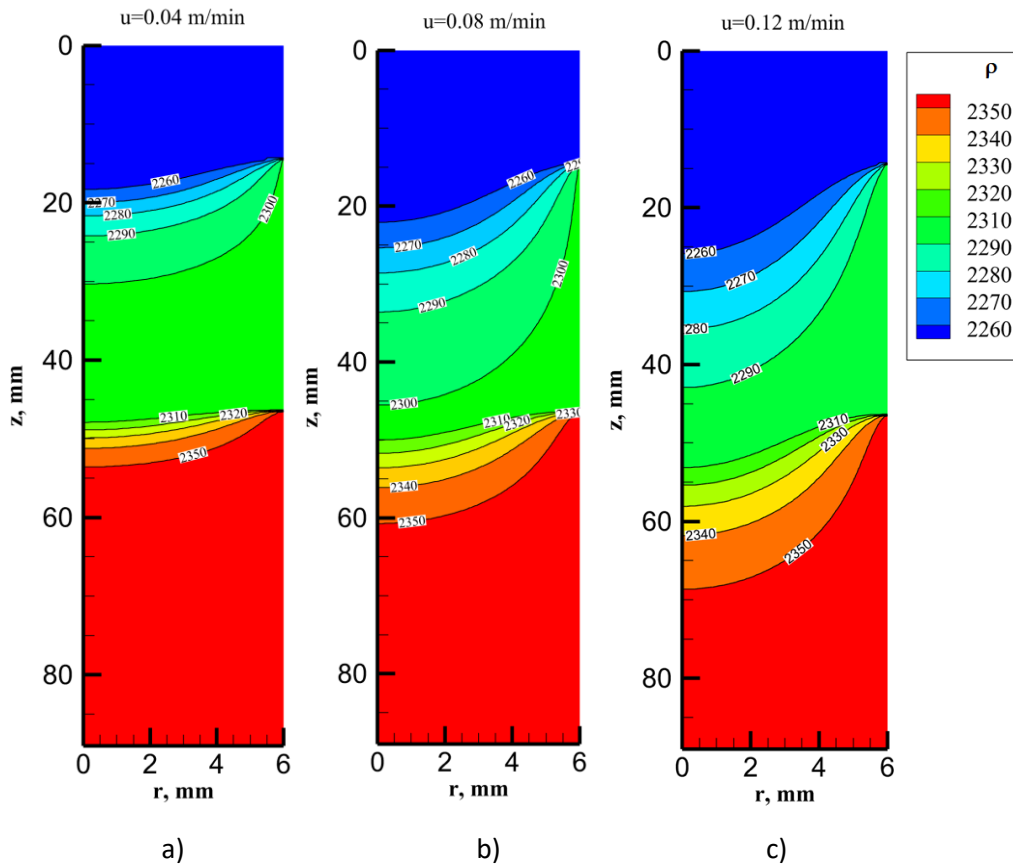


Figure 7 - Density field of BeO slurry in the round cavity at different casting speeds and a binder mass fraction of  $\omega=0.117$

The computed temperature data in the round cavity are shown in Figure 6 at casting speeds of  $u = 0.04$  m/min,  $0.08$  m/min, and  $0.12$  m/min. The radius of the cavity is  $0.006$  m, and the length is  $0.089$  m. The temperature of the slurry at the inlet of the round cavity is  $t_0=80^\circ\text{C}$ . In the cooling circuits, the water temperatures were as follows:  $\theta_1= 80^\circ\text{C}$ ;  $\theta_2= 56^\circ\text{C}$ ;  $\theta_3= 40^\circ\text{C}$ .

The casting speeds in the round cavity are lower than those in the ring-shaped cavity. In the ring-shaped cavity, a tube with a thin wall is formed, while in the round cavity, a rod is formed. The structural dimensions of the cavity determine the casting speed regimes for BeO ceramic products.

At a casting speed of  $u = 0.04$  m/min, the temperature distribution in the contact zones causes only minor thermal deformation of the casting (Figure 6).

However, temperature distributions in the contact zones at casting speeds of  $u = 0.08$  m/min and  $0.12$  m/min can result in significant thermal deformation of the casting (Figure 6).

The results of experimental studies [[6], [8], [13]] have shown that the increase in density (specific volume) during the cooling process in the liquid state amounts to 5-6%. However, during the cooling of slurry in amorphous and viscoplastic state there is a 70-80% of density (specific volume) increase due to temperature shrinkage [[6], [8], [13]].

From this, it can be inferred that the speed and temperature factors, along with the structural characteristics of the mold cavity, determine the changes in density (specific volume) in the amorphous and viscoplastic states of the slurry.

In the ring-shaped cavity, the increase in density represents only a small part of the amorphous and viscoplastic states of the slurry. Therefore, it can be considered that the flow rate of slurry with feeding provides compensation for thermal shrinkage.

In the round cavity, at a casting speed of  $u = 0.04$  m/min, the density increase occupies a small part of the amorphous and viscoplastic states of the slurry (see Figure 7). The slurry flow rate with feeding can provide compensation for thermal shrinkage.

At casting speeds of  $u = 0.08$  m/min and  $0.12$  m/min, density increases occupy a significant part of the amorphous and viscoplastic states of the slurry (see Figure 7). In these cases, it may be difficult to compensate for thermal shrinkage by supplying a slurry flow.

## Conclusion

The calculation results illustrate the entire process of forming beryllium oxide slurry, taking into account the changes in its aggregate state. Ultrasonic treatment improves the rheological properties and enhances the flowability of the slurry in the mold cavity.

The calculations demonstrate the influence of casting speed, temperature factors, and the structural parameters of the mold cavity on the cooling-solidification process of the casting. In the annular cavity, at casting speeds of  $u = 0.08$  m/min,  $0.16$  m/min, and  $0.24$  m/min, the increase in density occupies only a small part of the amorphous and solid-plastic state of the slurry. The flow of liquid slurry with feeding in the annular cavity compensates for the thermal shrinkage of the slurry.

In the round cavity, compensation for the thermal shrinkage of the slurry was achieved only at a casting speed of  $u = 0.04$  m/min. However, at casting speeds of  $u = 0.08$  m/min and  $0.12$  m/min, significant areas of density change due to thermal deformation exist. In these cases, it may be difficult to compensate for thermal shrinkage by supplying a slurry flow.

In the calculations, it is possible to determine the conditions for forming a slurry with solidification shrinkage using the hot casting method, which allows obtaining a cast product with a homogeneous structure of beryllium oxide.

**Conflict of interest.** On behalf of all the authors, the correspondent author declares that there is no conflict of interest.

**Acknowledgements.** This work is supported by the Science Committee of the Ministry of Science and Higher Education of the Republic of Kazakhstan (Grant number AP19680086 for 2023-2025).



## Ультрадыбыстық белсендіру арқылы бериллий оксидінің термопластикалық шликерін қалыптауды есептеу

<sup>1</sup> Жапбасбаев Ұ.Қ., <sup>1\*</sup> Рамазанова Г.І., <sup>2</sup> Терехов В.И., <sup>3</sup> Саттинова З.Қ.

<sup>1</sup>Сәтбаев университеті, Алматы, Қазақстан

<sup>2</sup>С.С. Кутателадзе атындағы Жылуфизика институты PFA СБ, Новосібір, Ресей

<sup>3</sup>Л.Н. Гумилев атындағы Еуразия ұлттық университеті, Астана, Қазақстан

<p>Мақала келді: 5 қазан 2023 Сараптамадан өтті: 5 қараша 2023 Қабылданды: 11 қаңтар 2024</p>	<p><b>ТҮЙІНДЕМЕ</b> Мақалада бериллий оксидінің керамикасын ыстық құю әдісімен қалыптау кезіндегі термиялық шөгуді бағалау нәтижелері берілген. Термопластикалық шликер – дисперсиялы ортамен (бериллий оксиді) салыстырғанда өте төмен жылу өткізгіш дисперсті фазасы (байланыстырушы) бар композициялық жүйе. Ультрадыбыстық өңдеу шликердің тұтқырлығын төмендетеді және оның құйылу қасиетін жақсартады. Бериллий оксидінің шликерін қалыптастыру жүйенің тұтастығын бұзбай жүзеге асырылады және құюдың жылдамдығы мен температуралық факторларына байланысты. Осы факторлардың бірлескен әсері шликердің құю қасиеттерін анықтайды. Құйма қалыптағы шликердің салқындау-қатуы фазалық ауысумен құйманың сұйық, аморфты және тұтқырлы пластикалық күйінде кезең-кезеңімен өтеді. Барлық кезеңдердегі құйманы салқындату жылдамдығы құюстың конструкциясына, шликердің реологиялық қасиеттеріне, сонымен қатар құйманың жұмыс параметрлеріне байланысты. Бұл жағдайда құйманың температуралық шөгуге байланысты оның тұтастығын сақтау маңызды.</p>
	<p><b>Түйін сөздер:</b> термопластикалық шликер, қалыптау, шөгу, құю қасиеті, бериллий оксиді, ультрадыбыстық өңдеу.</p>
<p><b>Жапбасбаев Ұзақ Қайырбекұлы</b></p>	<p><b>Авторлар туралы ақпарат:</b> Техника ғылымдарының докторы, профессор, "Энергетикадағы модельдеу" ғылыми-өндірістік зертханасының меңгерушісі, Сәтбаев университеті, Сәтбаев көшесі, 22 үй, 050013 Алматы, Қазақстан. Email: uzak.zh@mail.ru</p>
<p><b>Рамазанова Гаухар Ізбасарқызы</b></p>	<p>Физика-математика ғылымдарының кандидаты, жетекші ғылыми қызметкер, «Энергетикадағы модельдеу» ғылыми-өндірістік зертханасы, Сәтбаев университеті, Сәтбаев көшесі, 22 үй, 050013 Алматы, Қазақстан. Электрондық пошта: g.ramazanova@satbayev.university</p>
<p><b>Терехов Виктор Иванович</b></p>	<p>Техника ғылымдарының докторы, профессор, PFA Сібір бөлімі С.С. Кутателадзе атындағы Жылуфизика институтының бас ғылыми қызметкері. Ресей, 630090, Новосібір қ., Ак. Лаврентьев даңғылы, 1. Email: terekhov@itp.nsc.ru</p>
<p><b>Саттинова Замира Қанайқызы</b></p>	<p>Физика-математика ғылымдарының кандидаты, қауымдастырылған профессор, Л.Н. Гумилев атындағы Еуразия ұлттық университеті, Сәтбаев көшесі, 2 үй, 010008, Астана, Қазақстан. Email: sattinova.kz@gmail.com</p>

## Расчет формования термопластичного шликера оксида бериллия с ультразвуковой активацией

<sup>1</sup>Жапбасбаев У.К., <sup>1\*</sup>Рамазанова Г.И., <sup>2</sup>Терехов В.И., <sup>3</sup>Саттинова З.К.

<sup>1</sup>Satbayev University, Алматы, Казахстан

<sup>2</sup>Институт теплофизики им. С.С. Кутателадзе СО РАН, Новосибирск, Россия

<sup>3</sup>Евразийский национальный университет имени Л.Н. Гумилева, Астана, Казахстан

<p>Поступила: 5 октября 2023 Рецензирование: 5 ноября 2023 Принята в печать: 11 января 2024</p>	<p><b>АННОТАЦИЯ</b> В статье приводятся результаты оценки термической усадки при формовании керамики оксида бериллия способом горячего литья. Термопластичный шликер представляет собой композиционную систему с дисперсионной фазой (связующее вещество), имеющей очень низкую теплопроводность, по сравнению с дисперсной фазой (оксид бериллия). Ультразвуковая обработка снижает вязкость шликера и улучшает его литейное свойство. Формования шликера оксида бериллия проводится без нарушения сплошности системы и зависит от скоростных и температурных факторов литья. Совокупное влияние этих факторов определяет литейное свойство шликера. Охлаждение-отвердевание шликера в литейной форме происходит поэтапно в жидком, аморфном состояниях с фазовым переходом и вязкопластичном состоянии отливки. Темп охлаждения отливки на всех этапах зависит от конструкции полости, реологических свойств шликера, а также от режимных параметров литья. При этом важным является соблюдение сплошности отливки из-за температурной усадки.</p>
	<p><b>Ключевые слова:</b> термопластичный шликер, формование, усадка, литейное свойство, оксид бериллия, ультразвуковая обработка.</p>

<b>Жапбасбаев Узак Каирбекович</b>	<b>Информация об авторах:</b> Доктор технических наук, профессор, заведующий научно-производственной лабораторией "Моделирование в энергетике", Satbayev University, ул. Сатбаева 22, 050000, Алматы, Казахстан. Email: uzak.zh@mail.ru
<b>Рамазанова Гаухар Избасаровна</b>	Кандидат физико-математических наук, ведущий научный сотрудник. Научно-производственная лаборатория "Моделирование в энергетике", Satbayev University, ул. Сатбаева, 22, 050013 Алматы, Казахстан. E-mail: g.ramazanova@satbayev.university
<b>Терехов Виктор Иванович</b>	Доктор технических наук, профессор, главный научный сотрудник Института теплофизики им. С.С. Кутателадзе СО РАН. Россия, 630090, Новосибирск, пр. Ак. Лаврентьева, 1. Email: terekhov@itp.nsc.ru
<b>Саттинова Замира Канаевна</b>	Кандидат физ.-мат. наук, Ассоциированный профессор, Евразийский национальный университет имени Л.Н. Гумилева, Казахстан, 010008 Астана, ул. Сатбаева, 2. E-mail: sattinova.kz@gmail.com

## References

- [1] Akishin GP, Kiiko VS. Proizvodstvo VeO-keramiki v SSSR i yeye vozrozhdeniye v sovremennoy Rossii [Production of VeO-ceramics in the USSR and its revival in modern Russia]. New refractories [Novyye ognepury]. 2019; 5:127-132. (in Russ.).
- [2] Kiiko V, Makurin Yu, Ivanovsky A. Keramika iz oksida berilliya: proizvodstvo, fiziko-khimicheskiye svoystva, primeneniye [Beryllium Oxide Ceramics: production, physico-chemical properties, application]. Yekaterinburg: Ural'skoye otdeleniye RAN [Yekaterinburg: Ural Branch of the Russian Academy of Sciences. 2006. (in Russ.).
- [3] Kiiko VS, Vaispapor VY. Thermal conductivity and prospects for application of BeO ceramic in electronics. Glass Ceram. 2014; 71:387-391. <https://doi.org/10.1007/s10717-015-9694-6>
- [4] Akishin GP, Turnaev SK, Vaispapor VYa, Gorbunova MA, Makurin YN, Kiiko VS, Ivanovskii AL. Thermal conductivity of beryllium oxide ceramic. Refract. Ind. Ceram. 2009; 50:465-468. <https://doi.org/10.1007/s11148-010-9239-z>
- [5] Vajdi M, Shahedi Asl M, Nekahi S, Moghanlous FS, Jafargholinejad S, Mohammadi M. Numerical assessment of beryllium oxide as an alternative material for micro heat exchangers. Ceram. Int. 2020; 46:19248-19255. <https://doi.org/10.1016/j.ceramint.2020.04.263>
- [6] Shakhov SA, Bitsoev GD. Primeneniye ul'trazvuka v proizvodstve keramicheskikh izdeliy s vysokoy teploprovodnost'yu [Application of Ultrasound in the Manufacture of High Thermal Conductivity Ceramic Article]. Ust'-Kamenogorsk [Ust'-Kamenogorsk]. 1999. (in Russ.).
- [7] Zhabbasbayev U, Ramazanova G, Kenzhaliev B, Sattinova Z, Shakhov S. Experimental and calculated data of the beryllium oxide slurry solidification. Appl. Therm. Eng. 2016; 96:593-599. <https://doi.org/10.1016/j.applthermaleng.2015.11.114>
- [8] Akishin GP, Turnaev SK, Vaispapor VYa, Kiiko VS, Shein IR, Pletneva ED, Timofeeva MN, Iva AL. Composition of beryllium oxide ceramics. Refractories and Industrial Ceramics. 2011; 11:377-381.
- [9] Zhabbasbayev UK, Kaltayev A, Bitsoev GD, Turnayev SK. Hydrodynamics of moulding of ceramic articles for beryllia with ultrasonic activation. Proceedings ASME International Mechanical Engineering Congress and Exposition, Orlando. 2008, 1301-1307. <https://doi.org/10.1115/IMECE2005-79843>
- [10] Pivinskii YE, Grishpun EM, Gorokhovskii AM. Engineering, manufacturing, and servicing of shaped and unshaped refractories based on highly concentrated ceramic binding suspensions. Refract. Ind. Ceram. 2015; 56:243-253. <https://doi.org/10.1007/s11148-015-9823>
- [11] Shakhov S. Controlling the deformation behavior of thermoplastic slips with ultrasound. Glass and Ceramics. 2007; 64:354-356. <https://doi.org/10.1007/s10717-007-0088-2>
- [12] Shakhov SA. Use of ultrasound in order to intensify molding of high-temperature thermocouple sheaths, Refract. Ind. Ceram. 2008; 49:261-264. <https://doi.org/10.1007/s11148-008-9074-7>
- [13] Shakhov SA. Mechanism for compensating slip volume changes during hot casting of ceramic, Glass Ceram. 2007; 64:229-231. <https://doi.org/10.1007/s10717-007-0057-9>
- [14] Shakhov SA, Gagarin AE. Rheological characteristics of thermoplastic disperse systems treated with ultrasound. Glass Ceramics. 2008; 65:19-21.
- [15] Sattinova ZK, Bekenov TN, Assilbekov BK, Ramazanova GI, Zhabbasbayev UK, Nussupbek ZhT. Mathematical modeling of the rheological behavior of thermoplastic slurry in the molding process of beryllium ceramics. Ceram. Int. 2022; 48:31102-31111
- [16] Bingham EC. Fluidity and Plasticity. New York: McGraw-Hill. 1922.
- [17] Heever EVD, Sutherland A, Haldenwang R. Influence of the rheological model used in pipe-flow prediction techniques for homogeneous non-newtonian fluids. J. Hydraulic Eng. 2014; 140(12):04014059.
- [18] Singh J, Rudman M, Blackburn HM, Chryst A, Pullum L, Graham LJW. The importance of rheology characterization in predicting turbulent pipe flow of generalized Newtonian fluids. J. Non-Newtonian Fluid Mech. 2016; 232:11-21.
- [19] Papanastasiou TC. Flows of materials with yield. J. Rheology. 1987; 31:385-404.
- [20] Voller VR, Swaminathan CR, Thomas BG. Fixed grid techniques for phase change problems: a review. Int. J. Numerical Methods Eng. 1990; 30:875-898.

- [21] Jabbari M, Bulatova R, Tok AIY, Bahl CRH, Mitsoulis E, Hattel JH. Ceramic tape casting: a review of current methods and trends with emphasis on rheological behaviour and flow analysis, *Mater. Sci. Eng., B.* 2016; 212:39-61. <https://doi.org/10.1016/j.mseb.2016.07.011>
- [22] Moraga NO, Lemus-Mondaca RA. Numerical conjugate air mixed convection/non-Newtonian liquid solidification for various cavity configurations and rheological models. *Int. J. Heat Mass Tran.* 2011; 54:5116-5125. <https://doi.org/10.1016/j.ijheatmasstransfer.2011.07.032>
- [23] Yamamoto T, Komarov SV. Influence of ultrasound irradiation on transient solidification characteristics in DC casting process: numerical simulation and experimental verification. *J. Mater. Process. Technol.* 2021; 294:117116. <https://doi.org/10.1016/j.jmatprotec.2021.117116>
- [24] Carbona M, Cortes C. Numerical simulation of a secondary aluminum melting furnace heated by a plasma torch. *J. Mater. Process. Technol.* 2014; 214:334-346.
- [25] Bannach N. Phase Change: Cooling and Solidification of Metal. <https://www.comsol.com/blogs/phase-change-cooling-solidification-metal/2014>, accessed 12.08.14
- [26] Cebeci T, Bradshaw P. *Physical and Computational Aspects of Convective Heat Transfer. Physical and Computational Aspects of Convective Heat Transfer.* New York: Springer. 1988. <https://doi.org/10.1007/978-1-4612-3918-5>
- [27] Tannehill J, Pletcher R, Anderson D. *Vychislitel'naya mekhanika zhidkosti i teploperedacha [Computational Fluid Mechanics and Heat Transfer.* Moskva: Mir [Moscow: Mir]. 1990. (in Russ.).



DOI: 10.31643/2024/6445.42

Metallurgy



## Recycling of beryllium, manganese, and zirconium from secondary alloys by magnesium distillation in vacuum

Volodin V.N., Abdulvaliyev R.A., Trebukhov S.A., Nitsenko A.V., Linnik X.A.\*

\* Institute of Metallurgy and Ore Beneficiation, Satbayev University, Almaty, Kazakhstan

\*Corresponding author email: xenija\_linnik@mail.ru

<p>Received: November 28, 2023 Peer-reviewed: December 3, 2023 Accepted: January 12, 2024</p>	<p><b>ABSTRACT</b></p> <p>One of the methods for processing secondary magnesium raw materials containing rare refractory metals can be a distillation with the extraction of magnesium into condensate and the accumulation of rare metals in the distillation residue. The residue can be used as a master alloy for special alloys. To justify the possibility of this process, we calculated the boundaries of the vapor-liquid equilibrium fields for the regions of liquid solutions existence in the Mg – Be, Mg – Mn, and Mg – Zr systems at atmospheric pressure (101.33 kPa) and in vacuum (1.33 kPa). The value of the vacuum is due to the fact that a further increase in rarefaction will lead to the magnesium crystallization from the melt, and it will complicate the technology. We established that in the distillation process of magnesium removal from Mg – Be and Mg – Zr alloys, the vapor phase will be represented by more than 99.95% of magnesium. The presence of 0.45 mass.% Mn is possible in the Mg – Mn system at 1000 °C in the vapor phase – condensate. However, results of preliminary tests of the evaporation intensity established that the process conducted at 850-900 °C provides an acceptable evaporation rate of the volatile component (Mg) for technological conditions. Thus, we confirmed the possibility of the proposed method to process secondary light alloys containing beryllium, manganese, and zirconium, which can be involved in the main process intended to produce special alloys in the form of a master alloy with magnesium.</p> <p><b>Keywords:</b> magnesium, beryllium, manganese, zirconium, phase diagram, vapor-liquid equilibrium.</p>
<p><b>Volodin Valeriy Nikolaevich</b></p>	<p><b>Information about authors:</b> Doctor of Technical Sciences, Professor, Chief Researcher of the Vacuum Processes Laboratory of Institute of Metallurgy and Ore Beneficiation, Satbayev University, Shevchenko str., 29/133, 050010, Almaty, Kazakhstan. Email: volodinv_n@mail.ru</p>
<p><b>Abdulvaliyev Rinat Anvarbekovich</b></p>	<p>Candidate of Technical Sciences, Head of the Laboratory of Alumina and Aluminium of the Institute of Metallurgy and Ore Beneficiation, Satbayev University, Shevchenko str., 29/133, 050010, Almaty, Kazakhstan. Email: rin-abd@inbox.ru</p>
<p><b>Trebukhov Sergey Anatolyevich</b></p>	<p>Candidate of Technical Sciences, Professor, Leading Researcher of the Laboratory of Vacuum Processes Institute of Metallurgy and Ore Beneficiation, Satbayev University, Shevchenko str., 29/133, 050010, Almaty, Kazakhstan. Email: s.trebukhov@satbayev.university</p>
<p><b>Nitsenko Alina Vladimirovna</b></p>	<p>Candidate of Technical Sciences, Head of the Vacuum Processes Laboratory of Institute of Metallurgy and Ore Beneficiation, Satbayev University, Shevchenko str., 29/133, 050010, Almaty, Kazakhstan. Email: alina.nitsenko@gmail.com</p>
<p><b>Linnik Xeniya Alexandrovna</b></p>	<p>Master of Technical Sciences, Junior Researcher of the Vacuum Processes Laboratory of Institute of Metallurgy and Ore Beneficiation, Satbayev University, Shevchenko str., 29/133, 050010, Almaty, Kazakhstan. Email: xenija_linnik@mail.ru</p>

### Introduction

Magnesium alloys are used in a variety of industries due to their low specific gravity, high mechanical properties, high casting qualities, biological compatibility with the human body, and the possibility of recycling [[1], [2], and [3]]. A large number of new alloys are being developed now. New alloys have increased strength, ductility, heat resistance, corrosion resistance, variable crystal size in the matrix, and other properties. These

magnesium materials include additives of manganese [[4], [5], [6], [7], [8], and [9]], zirconium [[10], [11], [12], [13], [14], [15], [16], [17], and [18]] and beryllium [[19], [20], [21], [22], [23], [24], and [25]].

The expansion of the scope of magnesium and its alloy application entails an increase in the amount of returnable magnesium scrap represented by details exhausted their service life and by waste generated during the processing of products and semi-finished products.

Currently, secondary magnesium scrap corresponding to the magnesium alloy is melted in crucible furnaces and then cast into ingots. Most of the scrap containing non-ferrous, ferrous, and rare metals is melted in a salt furnace and then added to liquid raw magnesium to make standard alloys. Some magnesium-based scrap is used to remove sulfur from cast iron. The issue of selling these alloys resulted in the search for other processing methods.

An alternative method to recycling magnesium scrap containing rare refractory metals may be the distillation of volatile components, in particular magnesium, from secondary raw materials with a concentration of alloying rare metals in the residue. In this case, the residue can be used as a magnesium-based alloy during alloying of special alloys. The high magnesium vapor pressure relative to that of Zr, Mn, and Be at moderate temperatures (700 – 900 °C) allows to magnesium release into the vapor phase and then into the condensate. The judgment about the possibility of separating molten systems into components or the lack thereof follows from state diagrams that include the vapor-liquid equilibrium boundaries. The construction of such phase diagrams is possible based on the thermodynamic functions of the solutions' formation and evaporation, in particular the vapor pressure values of the components that make up the system.

In this article, we present the state magnesium diagrams with beryllium, manganese, and zirconium supplemented by vapor-liquid equilibrium fields. Since magnesium is the basis of the alloys, we calculated the boundaries of the vapor-liquid equilibrium fields in the concentration regions of the existence of liquid solutions based on experimental data on the values of the saturated vapor pressure of the components determined by us. The results of experiments and calculations are presented below.

### Experimental part

*Preparation of magnesium alloys with beryllium, manganese and zirconium.* In binary systems of magnesium with refractory metals - beryllium, manganese, and zirconium, the highest concentration field of liquid alloys existence is present in the system with beryllium. It is presumably up to 90 at. %Be. The existence of liquid solutions up to a concentration of 2-2.5 at. % was established in the magnesium-manganese

system, and up to 0.2 at. % Zr in the magnesium-zirconium system. Therefore, we prepared magnesium-beryllium alloys containing from 20.17 to 76.31 at. % Be (Table 1), magnesium-manganese alloys containing from 0.45 to 2.31 at. %Mn (Table 2), and magnesium-zirconium alloys with zirconium content from 0.051 to 0.180 at. % (Table 3) for research.

**Table 1** – Composition of magnesium – beryllium system alloys

Alloy No.	Wt. %		At. %	
	Mg	Be	Mg	Be
1	45.57	54.43	23.69	76.31
2	64.73	35.27	40.49	59.51
3	83.47	16.52	65.19	34.81
4	91.43	8.57	79.83	20.17

**Table 2** – Composition of the magnesium-manganese system alloys

Alloy No.	Wt. %		At. %	
	Mg	Mn	Mg	Mn
1	99.80	0.20	99.55	0.45
2	99.51	0.49	98.89	1.11
3	98.96	1.04	97.69	2.31

**Table 3** – Composition of the magnesium-zirconium system alloys

Alloy No.	Wt. %		At. %	
	Mg	Zr	Mg	Zr
1	99.986	0.014	99.949	0.051
2	99.971	0.029	99.880	0.110
3	99.952	0.048	99.820	0.180

To prepare the alloys, magnesium was used with a content of the main element of 99.99 wt. %, beryllium – 99.9%, manganese – 99.9%, zirconium – 99.6%. The alloys were synthesized using the ampoule method, which consists of the following. The initial components in the form of sawdust were loaded into quartz ampoules in quantities necessary for the alloy preparation of a given composition. The ampoules were washed several times with neutral gas (argon), evacuated, and sealed at a pressure of 1 Pa. The fusion of the components was carried out at a temperature of 800-850 °C for 12 hours, followed by quenching in water.

*Determination of the liquid-vapor phase transition boundaries.* The construction of the liquid-vapor phase transition boundaries of molten systems is complicated by the high boiling



temperatures of solutions, the difficulty in determining the concentration of components in the vapor phase that is in equilibrium with the alloy, and the problem of instrumentation design for ebulliometric measurements.

In this work, the boundaries of the melt and vapor coexistence fields were calculated based on the partial pressure of the saturated vapor of the alloy components. Due to the absence of the boiling process of liquid metal solutions because of the high density of the metals that form them, the boiling point was determined to be equal to the temperature at which the sum of the partial vapor pressures of the system's components under Dalton's law is equal to atmospheric (0.1 MPa) or other pressures corresponding to the conditions of vacuum technologies.

The composition of the vapor phase ( $y_1, y_2 = 1 - y_1$ ) above a solution of a certain composition ( $x_1, x_2 = 1 - x_1$ ) at the boiling point was determined based on the Clapeyron-Mendeleev equation:  $P_1V = n_1RT$ , from which:

$$y_1(y_2)[mole\ fraction] = \frac{n_1(n_2)}{n_1 + n_2} = \frac{p_1(p_2)}{p_1 + p_2},$$

where:  $x_1$  and  $x_2$  are the number of moles of the first and second metal in the alloy;  $n_1$  and  $n_2$  are number of moles of the first and second metal in the vapor phase;  $p_1$  and  $p_2$  are the partial pressures of saturated vapor of the first and second components.

Phase transformations of condensed phases at low pressures were not taken into account because the temperatures of phase transitions change by  $(5.0 - 5.6) \times 10^{-3}$  °C (calculated by us) during the move from atmospheric pressure to vacuum according to the authors [26].

*Determination of the saturated vapor pressure values of metals.* It should be noted during the assessment of magnesium, beryllium, manganese, and zirconium vapor pressure [27] that magnesium vapor pressure is incomparably higher concerning Be, Mn, and Zr. That is, the boiling point method should be considered the most acceptable way to determine the vapor pressure in binary systems of magnesium with the indicated metals. This method is based on a sharp increase in the evaporation rate of the volatile component near the equalization of the saturated vapor pressure of the metal and a given inert gas pressure. The boiling point method and the device for its implementation are described in detail in our work [28].

In this work, we present the method for determining the values of partial pressures of components over the studied magnesium alloys using the example of the Mg – Be system.

First, we determined the partial pressure values for saturated magnesium vapor ( $\bar{p}_{Mg}$ ). In this case, we assumed that the vapor above the melt is represented entirely by magnesium. Then, we found the activity coefficient under the definition of thermodynamic functions by equation:

$$\gamma_{Mg} = \frac{\bar{p}_{Mg}}{p_{Mg}^o \times x_{Mg}},$$

where:  $p_{Mg}^o$  is the vapor pressure over elemental magnesium;  $x_{Mg}$  is the atomic fraction of magnesium in the alloy.

The beryllium activity coefficient ( $\gamma_{Be}$ ) was calculated by numerical integration of the Gibbs-Duhem equation with the use of the auxiliary function proposed by Darken [29]. After transformation [30], this function relates  $\ln\gamma_{Mg}$  and  $\ln\gamma_{Be}$  in the form of an equation convenient for numerical integration:

$$\ln\gamma_{Be} = -\frac{\ln\gamma_{Mg} \times x_{Mg} \times x_{Be}}{x_{Be}} + \int_{x_{Mg}=0}^{x_{Mg}} \frac{\ln\gamma_{Mg}}{(1 - x_{Mg})^2} dx_{Mg},$$

where  $x_{Be}$  is the atomic fraction of magnesium in the alloy which is equal to  $x_{Be} = 1 - x_{Mg}$ .

As a result of this calculation, we can find the partial vapor pressure of beryllium ( $\bar{p}_{Be}$ ) as:  $\bar{p}_{Be} = p_{Be}^o \times \gamma_{Be} \times x_{Be}$  or  $\ln\bar{p}_{Be} = \ln p_{Be}^o + \ln\gamma_{Be} + \ln x_{Be}$ . Here  $p_{Be}^o$  is the vapor pressure above elemental beryllium.

## Results and Discussion

*Determination of the vapor pressure values over the Mg – Be, Mg – Mn and Mg – Zr melts.* The values of magnesium vapor pressure determined experimentally by the boiling point method ( $\bar{p}_{Mg}$ , experiment), as well as the vapor pressure values of magnesium ( $\bar{p}_{Mg}$ , calculation), beryllium ( $\bar{p}_{Be}$ ), manganese ( $\bar{p}_{Mn}$ ) and zirconium ( $\bar{p}_{Zr}$ ), calculated by approximating experimental data, are given in Tables 4-6.

**Table 4** – Partial vapor pressures of magnesium and beryllium over Mg – Be melts

Alloy composition, at. fraction		Temperature K/°C	$\bar{p}_{Mg}$ , experiment, kPa	$\bar{p}_{Mg}$ , calculated, kPa	$\bar{p}_{Be}$ , kPa	
Mg	Be					
0.2369	0.7631	1123 850	1.07	1.04	$2.61 \times 10^{-7}$	
			1.07			
			0.93			
		1223 950	3.60	3.62		$3.82 \times 10^{-6}$
			3.33			
			3.87			
0.4049	0.5951	1123 850	1.87	1.87	$1.98 \times 10^{-7}$	
			2.00			
			1.73			
		1223 950	6.93	6.93		$2.83 \times 10^{-6}$
			7.20			
			6.67			
0.6519	0.3481	1073 800	1.73	1.69	$2.08 \times 10^{-8}$	
			1.60			
			1.73			
		1173 900	6.93	6.85		$3.94 \times 10^{-7}$
			6.93			
			6.67			
0.7983	0.2017	1073 800	2.40	2.38	$8.18 \times 10^{-9}$	
			2.13			
			2.53			
		1173 900	9.33	9.15		$1.80 \times 10^{-7}$
			9.20			
			8.93			
1.0	–	1023 750	1.73	1.72	–	
			2.0			
			1.47			
		1273 1000	38.00	38.01		–
			37.20			
			38.80			

**Table 5** – Partial vapor pressures of magnesium and manganese over Mg – Mn melts

Alloy composition, at. fraction.		Temperature K/°C	$\bar{p}_{Mg}$ , experiment, kPa	$\bar{p}_{Mg}$ , calculated, kPa	$\bar{p}_{Mn}$ , kPa
Mg	Mn				
1.0	–	1023 750	1.73	1.72	–
			2.0		
			1.47		
		1273 1000	38.00	38.01	
			37.20		
			38.80		
0.9955	0.0045	1023 750	1.73	1.72	$1.66 \times 10^{-7}$
			1.70		
			1.76		
		1123 850	6.91	6.98	
			6.97		
			7.04		
0.9889	0.0111	1023 750	1.70	1.71	$3.08 \times 10^{-7}$
			1.75		
			1.71		
		1123 850	6.87	6.94	
			7.08		
			6.89		
0.9769	0.0231	1023 750	1.60	1.69	$5.09 \times 10^{-7}$
			1.69		
			1.79		
		1123 850	6.67	6.87	
			6.87		
			7.06		

**Table 6** – Partial vapor pressures of magnesium and zirconium over Mg – Zr melts

Alloy composition, at. fraction.		Temperature K/°C	$\bar{p}_{Mg}$ , experiment, kPa	$\bar{p}_{Mg}$ , calculated, kPa	$\bar{p}_{Zr}$ , kPa
Mg	Zr				
1.0	–	1023 750	1.73	1.72	–
			2.0		
			1.47		
		1273 1000	38.00	38.01	
			37.20		
			38.80		
0.9995	0.0005	1023 750	1.73	1.72	$1.63 \times 10^{-21}$
			1.76		
			1.71		
		1123 850	6.95	7.00	
			6.97		
			7.01		
0.9988	0.0012	1023 750	1.73	1.72	$3.15 \times 10^{-21}$
			1.75		
			1.71		
		1123 850	6.91	6.99	
			7.11		
			7.02		
0.9981	0.0018	1023 750	1.69	1.72	$4.27 \times 10^{-21}$
			1.71		
			1.71		
		1123 850	6.71	6.99	
			6.82		
			6.96		

After mathematical processing, we obtained the following temperature-concentration dependencies, expressing the partial pressure values of the component studied systems:

- for the Mg – Be system:

$$\ln \bar{p}_{Mg} [Pa] = (-14746x_{Mg}^3 + 35273x_{Mg}^2 - 23214x_{Mg} - 13395) \cdot T^{-1} + 12.452x_{Mg}^3 - 29.745x_{Mg}^2 + 20.106x_{Mg} + 20.367 + \ln x_{Mg}$$

$$\ln \bar{p}_{Be} [Pa] = (14746x_{Be}^3 - 31084x_{Be}^2 + 14836x_{Be} - 35780 + 3094 \ln x_{Be}) \cdot T^{-1} - 12.452x_{Be}^3 + 26.289x_{Be}^2 - 13.194x_{Be} + 24.574 - 1.028 \ln x_{Be}$$

- for the Mg – Mn system:

$$\ln \bar{p}_{Mg} [Pa] = (-301x_{Mg}^2 - 669x_{Mg} - 15153) \cdot T^{-1} + 0.254x_{Mg}^2 + 0.413x_{Mg} + 22.544 + \ln x_{Mg}$$

$$\ln \bar{p}_{Mn} [Pa] = (-301x_{Mn}^2 + 1873x_{Mn} - 31097 - 1271 \ln x_{Mn}) \cdot T^{-1} + 0.254x_{Mn}^2 - 1.429x_{Mn} + 25.363 + 1.921 \ln x_{Mn}$$

- for the Mg – Zr system:

$$\ln \bar{p}_{Mg} [Pa] = (-327x_{Mg}^2 - 973x_{Mg} - 14823) \cdot T^{-1} + 0.298x_{Mg}^2 + 0.745x_{Mg} + 22.168 + \ln x_{Mg}$$

$$\ln \bar{p}_{Zr} [Pa] = (-327x_{Zr}^2 + 2281x_{Zr} - 71967 - 1627 \ln x_{Zr}) \cdot T^{-1} + 0.298x_{Zr}^2 - 1.937x_{Zr} + 35.098 + 2.341 \ln x_{Zr}$$

*Construction and analysis of a phase diagram with a liquid-vapor phase transition.* The boundaries of the liquid and vapor coexistence fields at atmospheric pressure (L+V) and in vacuum (L+V 1.33 kPa, shaded) were calculated based on the partial pressure values of the vapor components in the region of existence of liquid solutions of the Mg – Be, Mg – Mn and Mg – Zr systems. The choice of the vacuum value (1.33 kPa) is because a decrease in pressure less than the specified value can lead to the crystallization of magnesium from the melt, this will complicate the distillation process.

We plotted the fields on existing state diagrams of condensed phases [[31], and [32]], shown in Fig. 1-3. From the analysis of the boundary location on phase diagrams, it is possible to conclude next.

The vapor phase for magnesium systems with beryllium and zirconium will be represented by elemental magnesium when the evaporation process is performed up to the boiling point of magnesium at atmospheric pressure (1107 °C). Distillation of magnesium at 1000 °C will be accompanied by the occurrence of 0.2 at. (0.45 mass) % Mn at vapor for liquid Mg – Mn alloys. However, preliminary tests of the evaporation process intensity have established that the process conducted at 850-900 °C provides an acceptable evaporation rate of the volatile component (Mg) for technological conditions.

The evaporation process for magnesium from its alloys with beryllium will be accompanied by the accumulation of the Be compound in the residue. Thus, when magnesium evaporates from its alloy with beryllium (10.0 mass. % Be) at 900 °C in a vacuum, the average evaporation rate was  $5,5 \times 10^{-3}$  kg/(m<sup>2</sup>×sec) with magnesium extraction into the condensate of 61.20% and accumulation of 22.26 mass. % Be. During the extraction of 96 % Mg into the vapor phase, the average evaporation rate amounted to  $2.61 \times 10^{-3}$  kg/(m<sup>2</sup>×sec) with the accumulation of 64.76 mass.% Be in the distillation residue.

When magnesium evaporated from an alloy with manganese (4.0 mass. % Mn) under similar conditions, the average evaporation rate was  $2.09 \times 10^{-3}$  kg/(m<sup>2</sup> × sec) with 94.12 % extracting into the condensate. 41.67 mass. % Mn being accumulated in the residue.

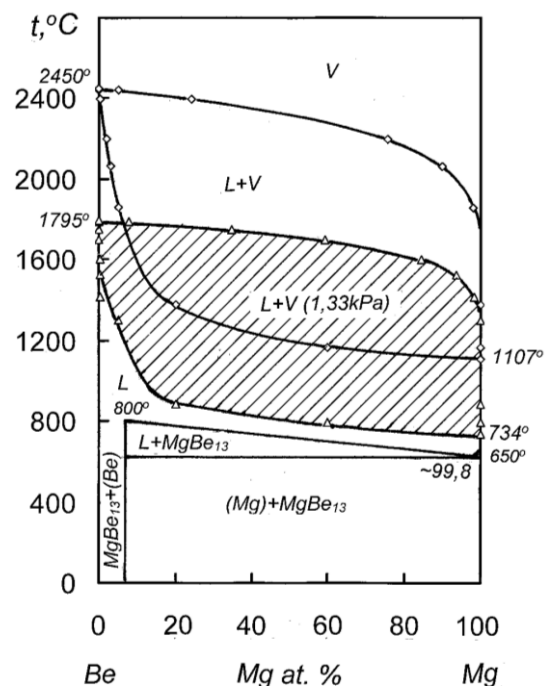


Figure 1– Mg–Be phase diagram



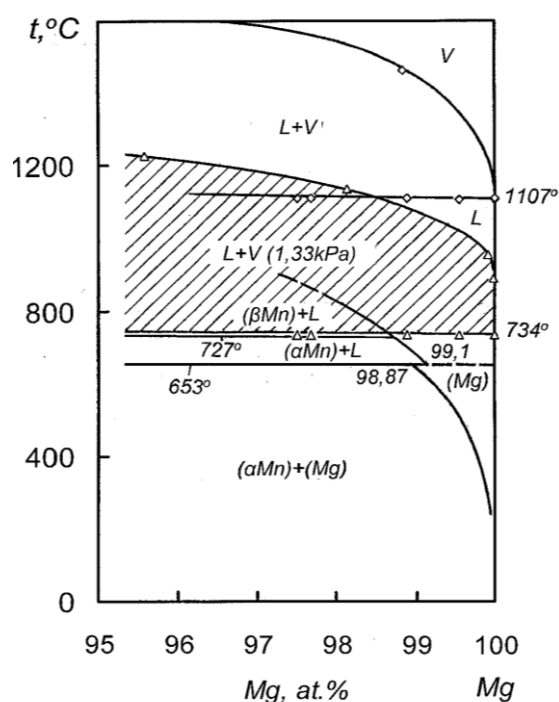


Figure 2 –Mg–Mn phase diagram

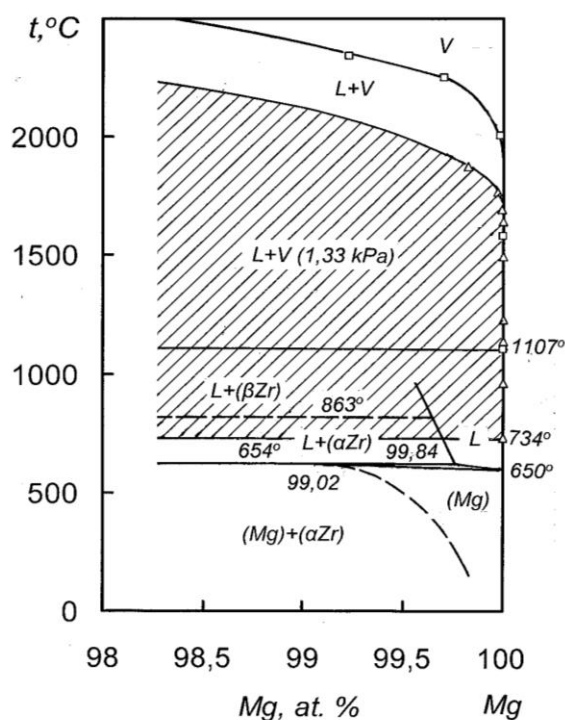


Figure 3 –Mg–Zr phase diagram

During the distillation of magnesium from its alloy with zirconium (1.85 mass. % Zr) within an hour at 900 °C, 92.56% Mg was extracted into the condensate with an accumulation of 20.11 wt. % Zr in the residue.

Thus, from secondary light alloys based on magnesium, the magnesium can be converted into condensate by distillation in a vacuum, which can be mixed with raw magnesium. The distillation residue with a significant content of beryllium, manganese and zirconium, with a combined or separate content of each, can be used as a master alloy in the production of special alloys. The latter ensures recycling – the return of rare refractory metals to the processes for manufacturing alloys with different physical properties.

## Conclusions

During the analysis of methods for processing secondary magnesium raw materials containing rare refractory metals, the use of the latter, including as a deoxidizer in ferrous metallurgy, was established. An alternative method intended to process secondary raw materials may be a distillation process with the extraction of magnesium into the condensate and the accumulation of rare metals in the distillation residue, followed by the use of the residue as a master alloy for special alloys.

Based on complete state diagrams of the Mg – Be, Mg – Mn, and Mg – Zr systems, including the liquid–vapor phase transition, the boundaries of which are calculated based on experimentally determined values of the components' saturated vapor pressure, the possibility of the proposed method to process secondary light alloys containing beryllium, manganese, and zirconium have been confirmed. The residues containing beryllium, manganese, and zirconium can be involved in the main process to produce special alloys in the form of a master alloy with magnesium.

Technological experiments have shown the possibility of technical implementation of the process with an intensity of magnesium evaporation acceptable for industrial production.

**Acknowledgement.** This study was funded by the Science Committee of the Ministry of Science and Higher Education of the Republic of Kazakhstan (Grant BR 18574018).

**Conflict of interest.** The corresponding author declares that there is no conflict of interest.

## Вакуумда магнийді айдау арқылы алынған қайталама қорытпалардан бериллий, марганец және цирконийді қайта өңдеу

Володин В.Н., Абдулвалиев Р.А., Требухов С.А., Ниценко А.В., Линник К.А.

Металлургия және кен байыту институты; Сәтбаев университеті, Алматы, Қазақстан

<p>Мақала келді: 28 қараша 2023 Сараптамадан өтті: 3 желтоқсан 2023 Қабылданды: 12 қаңтар 2024</p>	<p><b>ТҮЙІНДЕМЕ</b></p> <p>Құрамында сирек қиын балқитын металдар бар қайталама магний шикізатын өңдеу әдістерінің бірі магнийді конденсатқа бөліп алу және дистилляция қалдығында сирек металдарды жинақтау арқылы айдау процесі болуы мүмкін. Алынған қалдықтар арнайы қорытпалар үшін лигатура ретінде қолданылады. Магний қорытпаларын айдау арқылы өңдеу мүмкіндігін негіздеу үшін атмосфералық қысымда (101,33 кПа) және вакуумда (1,33 кПа) Mg – Be, Mg – Mn және Mg – Zr жүйелеріндегі сұйық ерітінділердің болу аймақтары үшін бу-сұйықтық тепе-теңдік өрістерінің шекаралары есептелді. Соңғысының шамасы қысым астында одан әрі жоғарылайды, нәтижесінде балқымадан Mg кристалданады, бұл технологияны қиындатады. Mg – Be және Mg – Zr қорытпаларынан магнийді кетіру процесінде бу фазасында магний 99,95-ден жоғары болатыны анықталды. Mg – Mn жүйесінде 1000 °C температурада бу фазасында (конденсат) 0,45 масс.% Mn болуы мүмкін. Дегенмен, булану процесінің қарқындылығын алдын ала сынаулар процесті 850-900 °C температурада жүргізу технологиялық жағдайлар үшін ұшпа компоненттің (Mg) булануының қолайлы жылдамдығын қамтамасыз ететінін анықтады. Осылайша, зерттеулер магниймен негізгі қорытпа түріндегі арнайы қорытпаларды алудың негізгі процесіне соңғыларын тарта отырып, құрамында бериллий, марганец және цирконий бар екінші реттік жеңіл қорытпаларды өңдеудің ұсынылған әдісінің мүмкіндігін растады.</p> <p><b>Түйін сөздер:</b> магний, бериллий, марганец, цирконий, қалыпты диаграмма, булы-сұйықтық тепе-теңдігі.</p>
<p><b>Володин Валерий Николаевич</b></p>	<p><b>Авторлар туралы ақпарат:</b> Техника ғылымдарының докторы, профессор, "Металлургия және кен байыту институты" АҚ Вакуумдық процестер зертханасының бас ғылыми қызметкері, Satbayev University, Шевченко көшесі 29/133, 0500100, Алматы, Қазақстан. Email: volodinv_n@mail.ru</p>
<p><b>Абдулвалиев Ринат Анварбекович</b></p>	<p>Техника ғылымдарының кандидаты, "Металлургия және кен байыту институты" АҚ глинозем және алюминий зертханасының меңгерушісі, Satbayev University, Шевченко көшесі 29/133, 0500100, Алматы, Қазақстан. Email: rin-abd@inbox.ru</p>
<p><b>Требухов Сергей Анатольевич</b></p>	<p>Техника ғылымдарының кандидаты, профессор, "Металлургия және кен байыту институты" АҚ Вакуумдық процестер зертханасының жетекші ғылыми қызметкері, Satbayev University, Шевченко көшесі 29/133, 0500100, Алматы, Қазақстан. Email: s.trebukhov@satbayev.university</p>
<p><b>Ниценко Алина Владимировна</b></p>	<p>Техника ғылымдарының кандидаты, "Металлургия және кен байыту институты" АҚ Вакуумдық процестер зертханасының меңгерушісі, Satbayev University, Шевченко көшесі 29/133, 0500100, Алматы, Қазақстан. Email: alina.nitsenko@gmail.com</p>
<p><b>Линник Ксения Александровна</b></p>	<p>Техника ғылымдарының магистрі, "Металлургия және кен байыту институты" АҚ Вакуумдық процестер зертханасының кіші ғылыми қызметкері, Satbayev University, Шевченко көшесі 29/133, 0500100, Алматы, Қазақстан. Email: xenija_linnik@mail.ru</p>

## Рециклинг бериллия, марганца и циркония дистилляцией магния в вакууме из вторичных магниевых сплавов

Володин В.Н., Абдулвалиев Р.А., Требухов С.А., Ниценко А.В., Линник К.А.

Институт металлургии и обогащения; Satbayev University, Алматы, Казахстан

<p>Поступила: 28 ноября 2023 Рецензирование: 3 декабря 2023 Принята в печать: 12 января 2024</p>	<p><b>АННОТАЦИЯ</b></p> <p>Одним из способов переработки вторичного магниевое сырьё, содержащего редкие тугоплавкие металлы, может быть дистилляционный передел с извлечением магния в конденсат и накоплением редких металлов в остатке от дистилляции. Полученный остаток возможно использовать в качестве лигатуры для специальных сплавов. Для обоснования возможности переработки магниевых сплавов дистилляцией рассчитаны границы полей парожидкостного равновесия для областей существования жидких растворов в системах Mg – Be, Mg – Mn и Mg – Zr при атмосферном давлении (101,33 кПа) и в вакууме (1,33 кПа). Величина последнего обусловлена тем, что дальнейшее увеличение разрежения приведет к кристаллизации Mg из расплава, что затруднит технологию. Было установлено, что в</p>
--	---

	дистилляционном процессе удаления магния из сплавов Mg – Be и Mg – Zr паровая фаза более, чем на 99,95 будет представлена магнием. В системе Mg – Mn при 1000 °С в паровой фазе (конденсате) возможно присутствие 0,45 mass.% Mn. Однако, предварительными испытаниями интенсивности процесса испарения было установлено, что ведение процесса при температурах 850-900 °С обеспечивает приемлемую для технологических условий скорость испарения летучего компонента (Mg). Таким образом, проведенными исследованиями подтверждена возможность предложенного способа переработки вторичных легких сплавов, содержащих бериллий, марганец и цирконий, с вовлечением последних в основной процесс получения специальных сплавов в виде лигатуры с магнием.
	<b>Ключевые слова:</b> магний, бериллий, марганец, цирконий, диаграмма состояния, парожидкостное равновесие.
<b>Володин Валерий Николаевич</b>	<b>Информация об авторах:</b> Доктор технических наук, профессор, главный научный сотрудник лаборатории вакуумных процессов АО «Институт металлургии и обогащения», Satbayev University, ул. Шевченко 29/133, 0500100, Алматы, Казахстан. Email: volodinv_n@mail.ru
<b>Абдувалиев Ринат Анварбекович</b>	Кандидат технических наук, заведующий лабораторией глинозема и алюминия АО «Институт металлургии и обогащения», Satbayev University, ул. Шевченко 29/133, 0500100, Алматы, Казахстан. Email: rin-abd@inbox.ru
<b>Требухов Сергей Анатольевич</b>	Кандидат технических наук, профессор, ведущий научный сотрудник лаборатории вакуумных процессов АО «Институт металлургии и обогащения», Satbayev University, ул. Шевченко 29/133, 0500100, Алматы, Казахстан. Email: s.trebukhov@satbayev.university
<b>Ниценко Алина Владимировна</b>	Кандидат технических наук, заведующий лабораторией вакуумных процессов АО «Институт металлургии и обогащения», Satbayev University, ул. Шевченко 29/133, 0500100, Алматы, Казахстан. Email: alina.nitsenko@gmail.com
<b>Линник Ксения Александровна</b>	Магистр технических наук, младший научный сотрудник лаборатории вакуумных процессов АО «Институт металлургии и обогащения», Satbayev University, ул. Шевченко 29/133, 0500100, Алматы, Казахстан. Email: xenija_linnik@mail.ru

## References

- [1] Rams J, Torres B, Pulido-González N, Garcia-Rodriguez S. Magnesium Alloys: Fundamentals and Recent Advances. Encyclopedia of Materials: Metals and Alloys. 2022; 1:2-10. <https://doi.org/10.1016/B978-0-12-819726-4.00082-X>
- [2] Satya Prasad SV, Prasad SB, Verma K, Kumar Mishra R, Kumar V, Singh S. The role and significance of Magnesium in modern day research-A review. Journal of Magnesium and Alloys. 2022; 1(10):1-61. <https://doi.org/10.1016/j.jma.2021.05.012>
- [3] Yang Y, Xiong X, Chen J, Peng X, Chen D, Pan F. Research advances of magnesium and magnesium alloys worldwide in 2022. Journal of Magnesium and Alloys. 2023; 8(11):2611-2654. <https://doi.org/10.1016/j.jma.2023.07.011>
- [4] She J, Zhou SB, Peng P, Tang AT, Wang Y, Pan HC., Yang CL, Pan FS. Improvement of strength-ductility balance by Mn addition in Mg – Ca extruded alloy. Materials Science and Engineering: A. 2020; 772:138796. <https://doi.org/10.1016/j.msea.2019.138796>
- [5] Li CC, Xia ZH, Qiao XG, Golovin IS, Zheng MY. Superior ductility Mg – Mn extrusion alloys at room temperature obtained by controlling Mn content. Materials Science and Engineering: A. 2023; 869:144508. <https://doi.org/10.1016/j.msea.2022.144508>
- [6] Wang T, Hua Z, Wang C, Zha M, Gao Y, Wang H. Realizing impressive superplasticity in a low-alloyed Mg – Zn – Ca – Al – Mn alloy: The roles of grain boundary segregation and dense  $\beta$ -Mn particles. Journal of Magnesium and Alloys. 2023; 31 July. <https://doi.org/10.1016/j.jma.2023.05.014>
- [7] Patel S, Rao V. Microstructure, mechanical properties and corrosion behavior of Mg – Cu and Mg – Cu – Mn alloys. Materialstoday: Proceedings. 2023; 7 July. <https://doi.org/10.1016/j.matpr.2023.06.284>
- [8] Somekawa H, Naito K. Grain boundary plasticity at intermediate temperatures in fine-grained Mg – Mn ternary alloys. Journal of Alloys and Compounds. 2023; 942:169012. <https://doi.org/10.1016/j.jallcom.2023.169012>
- [9] Dang C, Wang J, Wang J, Yu D, Zheng W, Xu C, Wang Z, Feng L, Chen X, Pan F. Simultaneous improvement of strength and damping of Mg – Mn alloy by tailoring bimodal grain structure. Vacuum. 2023; 215:112275. <https://doi.org/10.1016/j.vacuum.2023.112275>
- [10] Qian M, Stjohn DH, Frost MT. Characteristic zirconium-rich coring structures in Mg – Zr alloys. Scripta Materialia. 2002; 9(46):649-654. [https://doi.org/10.1016/S1359-6462\(02\)00046-5](https://doi.org/10.1016/S1359-6462(02)00046-5)
- [11] Qian M, Zheng L, Graham D, Frost MT, Stjohn DH. Settling of undissolved zirconium particles in pure magnesium melts. Journal of Light Metals. 2001; 3(1):157-165. [https://doi.org/10.1016/S1471-5317\(01\)000098](https://doi.org/10.1016/S1471-5317(01)000098)
- [12] Qian M, StJohn DH, Frost MT. Heterogeneous Nuclei size in magnesium – zirconium alloys. ScriptaMaterialia. 2004; 8(50) P:1115-1119. <https://doi.org/10.1016/j.scriptamat.2004.01.026>
- [13] Qian M, Das A. Grain refinement of magnesium alloys by zirconium: Formation of equiaxed grains. Scripta Materialia. 2006; 5(54):881-886. <https://doi.org/10.1016/j.scriptamat.2005.11.002>
- [14] Zhou H, Hou R, Yang J, Sheng Y, Li Z, Chen L, Li W, Wang X. Influence of Zirconium (Zr) on the microstructure, mechanical properties and corrosion behavior of biodegradable zinc – magnesium alloys. Journal Alloys and Compounds. 2020; 840:155792. <https://doi.org/10.1016/j.jallcom.2020.155792>
- [15] Chen Y, Ying T, Yang Y, Wang J, Zeng X. Regulating corrosion resistance of Mg alloys via promoting precipitation with trace Zr alloying. Corrosion Science. 2023; 216:111106. <https://doi.org/10.1016/j.corsci.2023.111106>

- [16] Zheng T, Hu Y, Jiang B, Fu L, Pan F, Nang A. A comparative study of deformation behaviors and ductility improvement in Mg – Gd – Zr and Mg – Zr cast alloys. *Journal of Materials Research and Technology*. 2023; 26:2082-2102. <https://doi.org/10.1016/j.jmrt.2023.08.052>
- [17] Zhong L, Wang L, Dou Y, Wang Y. Critical role dynamic precipitation on enhanced creep resistance in Mg – Zn alloy by Mn substitution for Zr. *Journal of Materials Research and Technology*. 2023; 24:9082-9095. <https://doi.org/10.1016/j.jmrt.2023.05.130>
- [18] Ablakatov IK, Ismailov MB, Mustafa LM, Sanin AF. Investigation of the Technology of Introducing Li, Mg and Zr Alloys into Aluminum Alloy. *Kompleksnoe Ispolzovanie Mineralnogo Syra = Complex Use of Mineral Resources*. 2023; 4(327):32-40. <https://doi.org/10.31643/2023/6445.37>
- [19] Zhabbasbayev UK, Ramazanova GI, Retnawati H, Sattinova ZK. Digitalization of the thermoplastic beryllium oxide slurryforming process using ultrasonic activation. *Kompleksnoe Ispolzovanie Mineralnogo Syra = Complex Use of Mineral Resources*. 2024; 3(330):5-12. <https://doi.org/10.31643/2024/6445.23>
- [20] Zeng XQ, Wang QD, Lü YZ, Ding WJ, Lu C, Zhu YP, Zhai CQ, Xu XP. Study on ignition proof magnesium alloy with beryllium and rare earth additions. *Scripta Materialia*. 2000; 5(43):403-409. [https://doi.org/10.1016/S1359-6462\(00\)00440-1](https://doi.org/10.1016/S1359-6462(00)00440-1)
- [21] Xiaogin Z, Qudong W, Yizhen L, Yanping Z, Wenjiang D, Yunhu Z. Influence of beryllium and rare earth additions on ignition-proof magnesium alloys. *Journal of materials Processing Technology*. 2001; 1(112):17-23. [https://doi.org/10.1016/S0924-0136\(00\)00854-2](https://doi.org/10.1016/S0924-0136(00)00854-2)
- [22] Cao P, Qian M, StJohn DH. Grain coarsening of magnesium alloys by beryllium. *Scripta Materialia*. 2004; 7(51):647-651. <https://doi.org/10.1016/j.scriptamat.2004.06.022>
- [23] Tan Q, Mo N, Jiang B, Pan F, Atrens A, Zhang M. Oxidation resistance of Mg – 9Al – 1Zn alloys micro-alloyed with Be. *Scripta Materialia*. 2016; 115:38-41. <https://doi.org/10.1016/j.scriptamat.2015.12.022>
- [24] Tan Q, Mo N, Jiang B, Pan F, Atrens A, Zhang M. Combined influence of Be and Ca on improving the high-temperature oxidation resistance of the magnesium alloy Mg – 9Al – 1Zn. *Corrosion Science*. 2017; 122:1-11. <https://doi.org/10.1016/j.corsci.2017.03.023>
- [25] Zhao Y, Xu Y, Chen P, Yuan Y, Qian Y, Li Q. Structural and electronic properties of medium-sized beryllium doped magnesium BeMg<sub>n</sub> clusters and their anions. *Results in Physics*. 2021; 26:104341. <https://doi.org/10.1016/j.rinp.2021.104341>
- [26] Clark JB, Richter PW. The determination of composition temperature-pressure phase diagrams of binary aloe systems. *Proceedings 7<sup>th</sup> International AIRAPT Conference “High Pressure Science and Technology”*; 1979 Le Creusot, Oxford. 1980. (V.1.) p.363-371.
- [27] Malyshev VP, Turdukozhayeva AM, Ospanov EA, Sarkenov B. Vaporizability and boiling of simple substances. Moscow: ScientificWorld. 2010, 304.
- [28] Nitsenko A, Volodin V, Linnik X, Burabaeva N, Trebukhov SA. Melt-Vapor Phase Transition in the Aluminum – Selenium System in Vacuum. *Metals*. 2023; 7(13):1297. <https://doi.org/10.3390/met13071297>
- [29] Darken LS, Gurry RW. *Physical chemistry of Metals*. New York, Toronto, London: McGraw-Hill Book Company. INC. 1953, 570.
- [30] Morachevsky AG. *Thermodynamics of molten metal and salt systems*. Moscow: Metallurgy. 1987, 240.
- [31] *State diagrams of double metallic systems: Reference book*. Ed. by Lyakishev N.P. M.: Engineering 1996, 992.
- [32] *State diagrams of double metallic systems: Reference book*. Ed. by Lyakishev N.P. M.: Engineering 2001, 872.



DOI: 10.31643/2024/6445.43

Metallurgy



## Research on the possibility of obtaining medium-carbon ferromanganese from the Djezdinskoe deposit

<sup>1</sup>Makhambetov Ye.N., <sup>1\*</sup>Abdirashit A.M., <sup>1</sup>Myngzhassar Ye.A.,  
<sup>1</sup>Burumbayev A.G., <sup>1</sup>Zhakan A.M., <sup>2</sup>Yucel Onuralp

<sup>1</sup>Zh.Abishev Chemical-Metallurgical Institute, Karaganda, Kazakhstan

<sup>2</sup>Istanbul Technical University, Istanbul, Turkey

\* Corresponding author email: a.abdirashit@ttu.edu.kz

<p>Received: December 10, 2023 Peer-reviewed: January 3, 2024 Accepted: January 12, 2024</p>	<p><b>ABSTRACT</b> In this article, the results of laboratory studies on the smelting of medium-carbon ferromanganese using Djezdinskoe ores are presented. Kazakhstan has significant reserves of manganese ores represented by iron-manganese and carbonate-oxide ores. The manganese ores of the Djezdinskoe deposit are characterized by a relatively high manganese content (48%) and low iron content (2-5%). Sieve analysis was used to study the particle size distribution of the ore. Based on the results of the sieve analysis of ore samples obtained after sieving, a high manganese content (53.54%), low iron content (0.47%), and silicon dioxide content (2.25%) were identified. Laboratory experiments were conducted on smelting medium-carbon ferromanganese in the high-temperature Tamman furnace. According to the results of the laboratory experiments, it is recommended to use the size classes of -5.0 + 0.0 mm to obtain high-quality low-phosphorus silicon-manganese alloy and the size class of +5.0 to produce medium-carbon ferromanganese. The average chemical composition of the metal and slag is as follows: % Mn – 86 – 88; Si – 0.04 – 0.35; Fe – 1.78 – 2.0; P – 0.06 – 0.09; C – 1.5 – 2.0; MnO – 19-20; SiO<sub>2</sub> – 13.94-14.5; CaO – 23.35 – 24.85; MgO – 13.25-14.0. Thus, an optimal technological scheme has been developed for the production of a wide range of manganese ferroalloys.</p>
	<p><b>Keywords:</b> Manganese ore, medium-carbon ferromanganese, low-phosphorus refined silicomanganese, differential thermal analysis, high-temperature furnace, ferroalloy.</p>
<p><b>Makhambetov Yerbolat Nysanaluly</b></p>	<p><b>Information about authors:</b> PhD, Head of the Laboratory of Ferroalloys and recovery processes, Zh.Abishev Chemical and Metallurgical Institute, Ermekova str., 63, 100009, Karaganda, Kazakhstan. Email: m.ye.n@mail.ru</p>
<p><b>Abdirashit Assylbek Miramkhanuly</b></p>	<p>Master of Technical Sciences, Junior Researcher of the Laboratory of Ferroalloys and recovery processes, Zh.Abishev Chemical and Metallurgical Institute, Ermekova str., 63, 100009, Karaganda, Kazakhstan. Email: a.abdirashit@ttu.edu.kz</p>
<p><b>Myngzhassar Yesmurat Amangalieovich</b></p>	<p>Master of Technical Sciences, Junior Researcher of the Laboratory of Pyrometallurgical Processes, Zh.Abishev Chemical and Metallurgical Institute, Ermekova str., 63, 100009, Karaganda, Kazakhstan. Email: ye.myngzhassar@gmail.com</p>
<p><b>Burumbayev Azamat Galymzhanovich</b></p>	<p>Master of Technical Sciences, Engineer of Ferroalloys and recovery processes, Zh.Abishev Chemical and Metallurgical Institute, Ermekova str., 63, 100009, Karaganda, Kazakhstan. Email: burumbayev.azamat@mail.ru</p>
<p><b>Zhakan Armat Medetuly</b></p>	<p>Engineer of Ferroalloys and recovery processes, Zh.Abishev Chemical and Metallurgical Institute, Ermekova str., 63, 100009, Karaganda, Kazakhstan. Email: armat.01.01@mail.ru</p>
<p><b>Yucel Onuralp</b></p>	<p>PhD, Professor of the Department of Metallurgy and Materials Science, Istanbul Technical University, Maslak 6449, Istanbul, Turkey. Email: yucel@itu.edu.tr</p>

### Introduction

Manganese is a crucial strategic metal with widespread industrial applications in various aspects of social economics. Approximately 90-95% of manganese is consumed in steel production, while the remaining portion is utilized in non-ferrous metallurgy, battery manufacturing, and food additives [1].

The applications of manganese stem from its physicochemical properties. It is well-known that adding manganese to steel enhances its mechanical properties such as wear resistance, ductility, and

strength [2]. Consequently, the primary consumer of manganese and its alloys is the metallurgical industry. Around 80% of extracted manganese ores are utilized in the production of manganese ferroalloys. This is because, from an economic perspective, the steelmaking industry generally prefers the use of manganese alloys with iron, such as ferromanganese.

In ferrous metallurgy, manganese alloys are essential for producing various types of steel, including carbon, low-alloy, tool, and corrosion-resistant steels, as well as for refined and cast iron. Manganese is also added to bronzes and brass.



Copper alloys with manganese are used for manufacturing turbine blades, while manganese bronzes are employed in producing propellers and other components requiring a blend of strength and corrosion resistance is required.

According to confirmed reserves of manganese ores, Kazakhstan ranks fourth in the world, and eighth in extraction, with a share of Kazakh ores in global reserves amounting to 8% [3]. The demand for manganese products continues to grow. Kazakhstan's reserves are found in oxide iron-manganese and carbonate-oxide manganese ores. The share of confirmed reserves of manganese ores by industrial categories is approximately 700 million tons, of which around 200 million tons are suitable for open-pit mining and 500 million tons for underground mining [4].

The average manganese content in Kazakhstan's ores is 19.4%, lower than in the ores of most countries worldwide (30–50%). The manganese ores of the Republic stand out for their low phosphorus and sulfur content, virtually lacking harmful impurities like arsenic and antimony, and featuring a significantly oxidized mineral composition. This characteristic advantageously distinguishes them from Ukrainian and Georgian ores. However, a drawback is the considerable iron content (ranging from 2 to 30%), and on certain sites, the presence of lead and zinc (up to 0.01-0.4%).

Out of 300 identified manganese deposits and occurrences, the State reserves balance accounts for 19 manganese deposits situated in Central Kazakhstan. In other regions, only isolated occurrences reach the size of small deposits. Many occurrences remain poorly studied, and the scale of manganese mineralization is limited by visual assessments. This limitation is primarily associated with the presence of rich ores at the Djezdinskoe deposit and the largest accumulations of manganese ores in the Atasu district. Consequently, the scope of work to study manganese mineralization in other regions of the Republic has been restricted [[5], [6], [7], [8], [9]]. Despite the impressive reserves of manganese ores in Kazakhstan, the production of medium-carbon ferromanganese has not been established.

The research was conducted to study the processes involved in smelting medium-carbon ferromanganese from manganese ore. The Djezdinskoe deposit was chosen as the subject of the study due to its status as one of the largest manganese ore deposits and its high industrial significance.

## Experimental part

The work was carried out at the Zh. Abishev Chemical-Metallurgical Institute. To conduct laboratory experiments, it was necessary to perform a particle size analysis. For determining the particle size distribution of the ore submitted for examination, a set of sieves according to GOST 9758-86 with the following opening sizes in mm was used: 40, 20, 10, 5, 2.5, 0.5, and 0.16 [[10], [11]]. A dry sieving analysis was conducted on the examined ore sample. Following the particle size analysis, thermal analysis of the ore was performed.

One of the widely adopted methods for studying calcination processes is thermal analysis [[12], [13], [14], [15]]. Therefore, this presented work includes calculations to determine the apparent activation energy using the non-isothermal kinetics method for phase transformations occurring in iron-manganese ores during heating. The possibility of determining the activation energy by three parallel paths using the heating curves of DTA (differential thermal analysis), DTG (differential thermogravimetric analysis), and TG (thermogravimetric analysis) derivatives was verified. Sequentially discussed are the physicochemical transformations occurring in iron-manganese ores in both oxidizing and reducing environments.

Differential thermal analysis was conducted in an oxidizing atmosphere of air and an inert argon atmosphere using a Paulik, Paulik, and Erdéy system derivatograph. This equipment allowed for the recording of changes in sample mass (TG), the rate of change of mass (DTG), and the temperature difference (DTA) between the sample and an inert reference during continuous heating at a specified rate. Derivatograms of manganese, iron-manganese, and iron ores (Table 1) revealed several endo- and exothermic effects associated with the dissociation and oxidation of manganese and iron-bearing minerals [[16], [17]]. These thermal effects and the related physicochemical transformations became the subject of investigation in this chapter. Temperature and differential curves were recorded using a platinum-platinum-rhodium thermocouple. The heating rate was set at 10 degrees per minute. The sensitivity of the DTA derivatograph was 1/10. Dissociation studies were conducted in an argon atmosphere. Samples, in powder form, were placed in a corundum crucible with a diameter of 10 mm and a height of 12 mm. The duration of the experiments was 100 minutes.

The interpretation of thermal effects was based on available literature data and the results of X-ray phase studies. In many cases, reference was made not only to individual publications on the thermoanalytical characteristics of minerals but also to summary tables that consolidate this data [[18], [19], [20]].

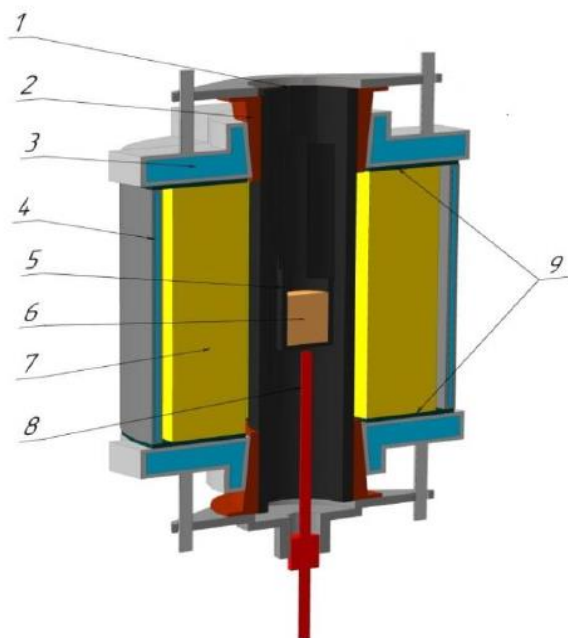


**Figure 1** - High-temperature Tamman furnace (in section) 1 - Carbon-graphite tube; 2 - Copper compression ring; 3 - Water-cooled cover; 4 - Water-cooled housing; 5 - Alumina crucible; 6 - Investigated charge; 7 - Protective lining; 8 - Thermocouple; 9 - Lower electrode.

Experimental studies on the smelting of medium-carbon ferromanganese were conducted in a high-temperature Tamman furnace, designed for modelling metallurgical processes (Figure 1). Its working zone is constructed with a graphite tube. Temperature regulation is achieved using a thyristor voltage regulator connected to the primary winding of the power transformer. This allows for obtaining a current of up to several thousand amperes on the output buses at voltages ranging from 0.5 to 15 volts. The furnace temperature was measured using a tungsten-rhenium thermocouple WR-5/20 in a corundum casing.

To conduct laboratory research on the process of smelting medium-carbon ferromanganese, we are evaluating the quality of the reducing properties of low-phosphorus refined silicomanganese, manganese ore from the Djezdinskoye deposit and lime.

## Results and Discussion

Initially, a dry sieving analysis was conducted on the material of the investigated sample with a size of  $-40.0 +0.0$  mm. The results of the analysis, showing the distribution by particle size classes and the content of manganese, iron, and silicon dioxide, are presented in Table 1. Based on the calculated granulometric composition of the ore obtained from dry sieving (Table 1), the weighted average content of manganese, iron, and silicon dioxide in the ore sample was determined to be 48.49%, 1.76%, and 5.59%, respectively. The particle size distribution curve corresponding to the dry sieving is depicted in Figure 2.

**Table 1** - Sieve analysis of the initial ore from the Djezdinskoe deposit.

№	Particle size class, mm	Output, %	The chemical composition, %			Extraction, %	
			Mn	Fe	SiO <sub>2</sub>	Mn	Fe
1	-40+20	26.36	53.54	0.47	2.25	29.11	7.02
2	-20+10	32.99	52.09	0.41	1.41	35.44	7.66
3	-10+5	26.88	49.19	2.06	4.64	27.27	31.36
4	-5+2.5	9.85	30.22	7.31	21.23	6.14	40.76
5	-2.5+1	3.74	25.67	5.84	30.65	1.98	12.36
6	-1+0.5	0.08	19.14	8.55	30.51	0.03	0.38
7	-0.5+0.16	0.02	21.53	7.55	25.17	0.01	0.09
8	-0.16+0	0.08	19.46	8.02	21.37	0.03	0.38
<b>Total (ore)</b>		<b>100</b>	<b>48.49</b>	<b>1.76</b>	<b>5.59</b>	<b>100</b>	<b>100</b>

The analysis of the results obtained from the dry sieving (Table 1) demonstrates relatively high outputs for particle size classes ranging from  $-40$  mm to  $+5.0$  mm. The highest output corresponds to the particle size class  $-20+10$  mm, accounting for 32.99%, gradually decreasing to 13.77% for the particle size class  $-5.0+0.0$  mm.

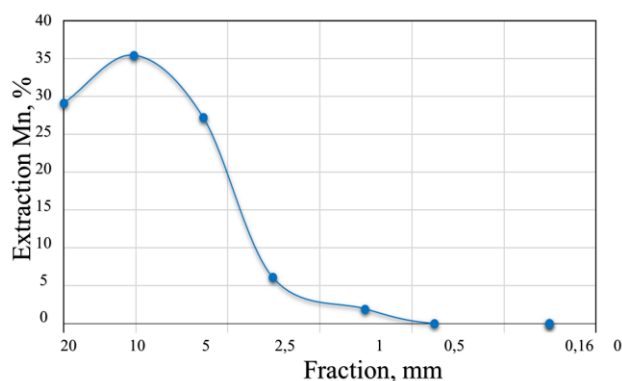


**Figure 2** - Sieve analysis of the initial ore (dry sieving)

The derivative thermograms of manganese ores from the Djezdinskoe deposit (Figures 3 and 4) are nearly identical. All derivative thermograms display two characteristic (similar) endothermic effects, differing only in their proportions. According to the derivative thermograms, the uniform removal of hygroscopic moisture smoothly progresses up to 250°C and abruptly transitions to the first endothermic effect within the temperature range of 285-400°C, corresponding to the loss of hydrated (structural) moisture associated with vernadite. At this temperature, presumably, the monohydrate dissociates, forming  $\alpha$ - $\beta$ -Mn<sub>2</sub>O<sub>3</sub>. The total moisture loss (hydrated and hygroscopic) amounts to 20 mg. The second endothermic effect at 500-570°C corresponds to the formation and decomposition of the  $\alpha$ -cryptomelane solid solution. At 660-675°C, there is an endothermic pyrolusite effect, indicating the formation of  $\beta$ -Mn<sub>2</sub>O<sub>3</sub> from  $\beta$ -pyrolusite ( $\beta$ -MnO<sub>2</sub>). At 810-825°C, a permanganate effect is observed (decomposition of psilomelane). Finally, at 970-980°C, a cryptomelane effect is identified, signifying the formation of  $\beta$ -hausmannite from  $\beta$ -Mn<sub>2</sub>O<sub>3</sub> ( $\beta$ -cryptomelane).

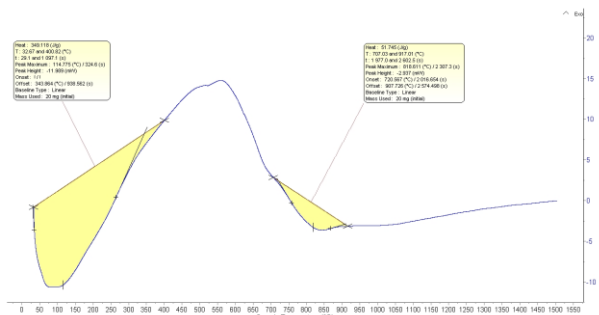


Figure 3 - Derivative thermogram of manganese ore (fraction +5 mm)

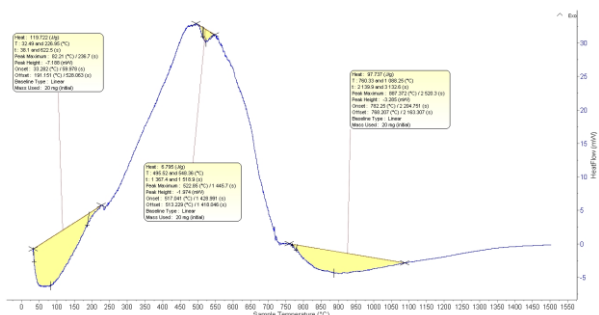


Figure 4 - Derivative thermogram of manganese ore (fraction -5 mm)

Phase composition of the primary manganese ore, as shown in Figure 5-9 for the fraction up to -40 mm, was determined using X-ray phase analysis. The results revealed that the main phases include pyrolusite (MnO<sub>2</sub>), hydrated manganese oxide

(MnO<sub>2</sub>(H<sub>2</sub>O)<sub>0.15</sub>), quartz (SiO<sub>2</sub>), magnesian calcite (Mg<sub>0.03</sub>Ca<sub>0.97</sub>)(CO<sub>3</sub>), lamontite (CaAl<sub>2</sub>Si<sub>4</sub>O<sub>12</sub>(H<sub>2</sub>O)<sub>2</sub>), gibbsite (Al(OH)<sub>3</sub>), potassium aluminium silicate (KAlSi<sub>3</sub>O<sub>8</sub>), calcium and manganese oxide (Ca<sub>2</sub>Mn<sub>8</sub>O<sub>16</sub>), iron oxide (Fe<sub>2</sub>O<sub>3</sub>), barium monoferrite (BaFe<sub>2</sub>O<sub>4</sub>), manganese-barium hollandite (BaMn<sub>8</sub>O<sub>16</sub>), and aluminium calcium (Al<sub>2</sub>Ca).

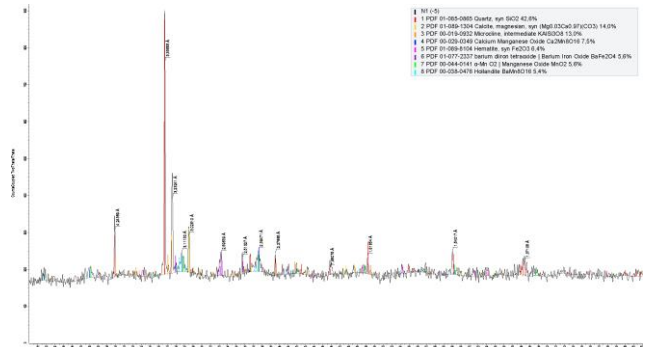


Figure 5 - X-ray diffraction pattern of manganese ores (fraction -5+2,5 mm)

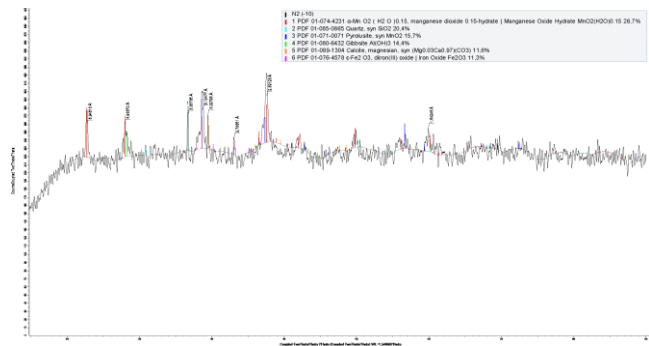


Figure 6 - X-ray diffraction pattern of manganese ores (fraction -10+5 mm)

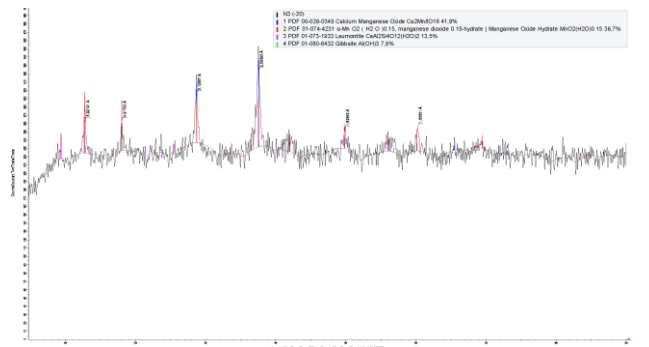


Figure 7 - X-ray diffraction pattern of manganese ores (fraction -20+10 mm)



Figure 8 - X-ray diffraction pattern of manganese ores (fraction -40+20 mm)

During the laboratory smelting process in the Tamman furnace, charge materials (ore, low-phosphorus silicomanganese, and limestone) were loaded into a corundum crucible. Upon reaching a temperature of 930°C, the gas release was observed in all experimental melts, characterized by a white deposit on the walls of the carbon tube lid. At 1330°C, the beginning of the charge melting was observed. Around 1450°C, a liquid melt appeared, indicated by the presence of an alloy adhered to the molybdenum wire. At a temperature of 1500°C, gases were formed and released in the crucible, resembling bubbles as if boiling water. At this temperature, the melt was maintained for 60 minutes and then allowed to cool in the furnace. As the temperature decreased to approximately ~200°C, the crucible was removed, and after cooling it to room temperature, the melt underwent sorting to separate the metal from the slag. Figure 9 shows a cross-section of a crucible (metal and slag).

The obtained alloy in terms of its chemical composition complied with the requirements of the GOST 4755-91 standard. The results of the smelting are presented in Table 2. As evident from the table, the compositions of the slags varied in terms of their basicity. The quantity of the reducing agent was adjusted to find the optimal value. During the laboratory experiments, it was noted that the reduction process in the crucible occurred very intensively, resulting in the complete melting of the entire charge and a clear separation between the metal and slag.

**Table 2** - Chemical composition of metal and slag, %

№	Metal, %				
	Mn	Fe	Si	C	P
1	86.38	10.30	0.21	2.0	0.06
2	86.45	10.25	0.35	2.0	0.07
3	86.51	10.18	0.34	2.0	0.08
4	88.14	9.97	0.03	1.5	0.07
5	88.44	10.00	0.04	1.88	0.08
6	88.35	9.98	0.04	1.78	0.09
№	Slag, %				
	MnO	SiO <sub>2</sub>	CaO	MgO	P
1	19.89	13.94	23.35	13.25	0.001
2	21.05	13.80	25.50	13.31	0.001
3	20.50	13.85	24.51	13.21	0.001
4	20.06	14.00	23.85	13.35	0.001
5	20.05	14.10	24.56	13.45	0.001
6	20.10	14.5	24.75	14.05	0.001

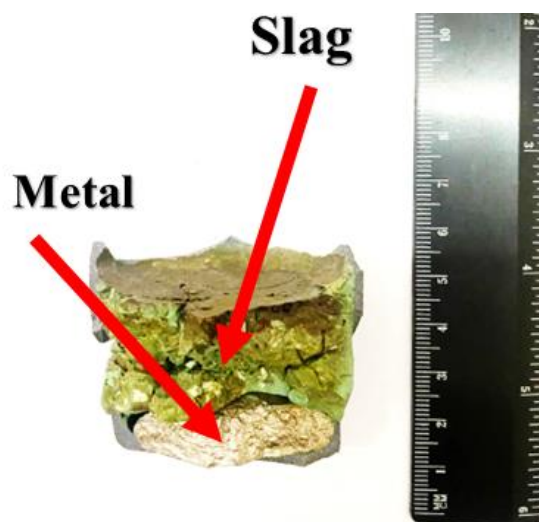


**Figure 9** - Cross section of a crucible (metal and slag)

As known, a range of technological indicators depends on the chemical composition of slag, especially its basicity (CaO/SiO<sub>2</sub>). As shown in Table 2, the basicity values range from 1.6 to 1.8. The choice of basicity largely determines the technological properties of the slag. In our case, the main goal was to improve the technical and economic indicators of the process, such as the degree of extraction of the leading element into the alloy, the technological efficiency, and the frequency of slag. The degree of manganese extraction from the ore into the alloy was ≥61%. Technological efficiency was characterized by fewer metal droplets entangled in the slag and clear separation of metal and slag when disassembling the solidified melt. A secondary task was to achieve slag stability at the given basicity. Slags from laboratory test melts were obtained in a stony state without signs of disintegration. The above information on optimal data corresponds to basicity values of 1.6-1.8. The recommended technological scheme for the metallurgical preparation of the Jezdinsky deposit is shown in Figure 10.

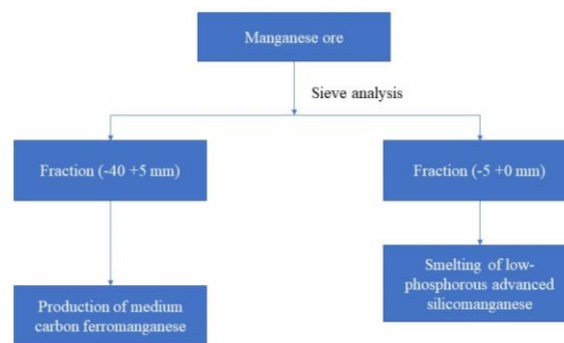


**Figure 10** - Recommended technological scheme for metallurgical preparation of the Dzhezdzinskaya deposit



## Conclusions

Based on the obtained research results, the following main conclusions can be drawn:

- It has been determined that in the dry sieving of crushed ore down to -80.0 mm, a significant amount of manganese is concentrated in the particle size class up to +5.0 mm, while the minimum amount of iron is concentrated in the particle size class down to -5.0 mm, suitable for low-phosphorus silicomanganese quality of charge materials.

- The phase transformations of charge materials in oxidizing and inert atmospheres were studied by differential thermal analysis (DTA). The experimental data obtained are consistent with the literature.

- The temperature range of the Tamman furnace operation is approximately from 1598 to 1698 K. The

entire smelting process was completed successfully, and the achieved temperature conditions at 1698 K allowed for the complete formation of metal and slag in the melting chamber.

This allows the establishment of optimal parameters for the technological mode to effectively smelt medium-carbon ferromanganese in the refined furnace. The obtained data from thermodynamic and laboratory studies provide a basis for conducting both laboratory and large-scale tests.

**Acknowledgements.** This work was carried out as part of a study funded by the Science Committee of the Ministry of Science and Higher Education of the Republic of Kazakhstan (grant no. AP14972750).

**Conflict of interest.** The corresponding author declares that there is no conflict of interest.

**Cite this article as:** Makhambetov YeN, Abdirashit AM, Myngzhassar YeA, Burumbayev AG, Zhakan AM, YucelO. Research on the possibility of obtaining medium-carbon ferromanganese from the Djezdinskoe deposit. *Kompleksnoe Ispolzovanie Mineralnogo Syra = Complex Use of Mineral Resources*. 2024; 331(4):101-108. <https://doi.org/10.31643/2024/6445.43>

## Жезді кен орнынан орташа көміртекті ферромарганец алу мүмкіндігін зерттеу

<sup>1</sup> Махамбетов Е.Н., <sup>1\*</sup> Әбдірашит А.М., <sup>1</sup>Мыңжасар Е.А.,  
<sup>2</sup>Бурумбаев А.Г., Жақан А.М., <sup>2</sup>Юсел Онуралп

<sup>1</sup> Ж.Әбішев атындағы Химия-металлургия институты, Қарағанда, Қазақстан

<sup>2</sup> Ыстамбұл техникалық университеті, Ыстамбұл, Түркия

<p>Мақала келді: 10 желтоқсан 2023 Сараптамадан өтті: 3 қаңтар 2024 Қабылданды: 12 қаңтар 2024</p>	<p><b>ТҮЙІНДЕМЕ</b> Бұл мақалада Жезді кендерін қолдана отырып, орташа көміртекті ферромарганецті балқыту бойынша зертханалық жұмыстардың нәтижелері келтірілген. Қазақстанда марганец кендерінің едәуір қоры бар, олар темір-марганец және карбонат-оксид кендері түрінде болады. Жезді кен орнының марганец кендерінде салыстырмалы түрде марганец жоғары мөлшерде (48 %) және темір аз мөлшерде (2-5%) болады. Кеннің гранулометриялық құрамын зерттеу үшін елек талдауы қолданылды. Електен бөлінгеннен кейін алынған кен үлгілерін гранулометриялық талдау нәтижелері бойынша марганецтің жоғары мөлшері (53,54 %), темірдің мөлшері (0,47 %) және кремний оксидінің аз мөлшері (2.25%) анықталды. Жоғары температуралы Тамман пешінде орта көміртекті ферромарганецті балқыту бойынша зертханалық жұмыстар жүргізілді. Зертханалық жұмыстардың нәтижелері бойынша жоғары сапалы төмен фосфорды өңдейтін силикомарганецті алу үшін -5+0,0 мм кластарды, орташа көміртекті ферромарганецті алу үшін өлшемі +5 класты қолдану ұсынылады. Металл мен қождың орташа өлшенген химиялық құрамы: %: Mn – 86 – 88; Si – 0,04 – 0,35; Fe – 1,78 – 2,0; R – 0,06 – 0,09; C – 1,5 – 2,0; MnO – 19-20; SiO2-13,94 – 14,5; CaO – 23,35 – 24,85; MgO-13,25-14.0. Осылайша, марганец ферроқорытпаларының кең спектрін өндірудің оңтайлы технологиялық схемасы жасалды.</p>
<p><b>Махамбетов Ерболат Нысаналыұлы</b></p>	<p><b>Түйін сөздер:</b> марганец кені, орташа көміртекті ферромарганец, төмен фосфорлы қайта өңделетін силикомарганец, дифференциалды термиялық талдау, жоғары температуралы пеш, ферроқорытпа.</p> <p><b>Авторлар туралы ақпарат:</b> PhD, ферроқорытпалар және тотықсыздандыру процестері зертханасының меңгерушісі, Ж.Әбішев атындағы химико-металлургиялық институт, Ермеков көшесі, 63, 100009, Қарағанды қ., Қазақстан. Email: m.ye.n@mail.ru</p>



<b>Әбдірашит Асылбек Мирамханұлы</b>	<i>Техника ғылымдарының магистрі, пирометаллургиялық процестер зертханасының кіші ғылыми қызметкері, Ж.Әбішев атындағы химико-металлургиялық институт, Еркемов көшесі, 63, 100009, Қарағанды қ., Қазақстан. Email: a.abdirashit@tttu.edu.kz</i>
<b>Мыңжасар Есмұрат Аманғалиұлы</b>	<i>Техника ғылымдарының магистрі, ферроқорытпалар және тотықсыздандыру процестері зертханасының кіші ғылыми қызметкері, Ж.Әбішев атындағы химико-металлургиялық институт, Еркемов көшесі, 63, 100009, Қарағанды қ., Қазақстан. Email: a.abdirashit@tttu.edu.kz</i>
<b>Бурумбаев Азамат Галымжанович</b>	<i>Техника ғылымдарының магистрі, ферроқорытпалар және тотықсыздандыру процестері зертханасының инженері, Ж.Әбішев атындағы химико-металлургиялық институт, Еркемов көшесі, 63, 100009, Қарағанды қ., Қазақстан. Email: burumbayev.azamat@mail.ru</i>
<b>Жақан Армат Медетулы</b>	<i>Ферроқорытпалар және тотықсыздандыру процестері зертханасының инженері, Ж.Әбішев атындағы химико-металлургиялық институт, Еркемов көшесі, 63, 100009, Қарағанды қ., Қазақстан. Email: armat.01.01@mail.ru</i>
<b>Юсел Онуэралп</b>	<i>PhD, Металлургия және материалтану кафедрасының профессоры, Ыстамбұл техникалық университеті, Маслак 6449, Ыстамбұл, Түркия. Email.ru: yucel@itu.edu.tr</i>

## Исследование возможности получение среднеуглеродистого ферромарганца из Джездинского месторождения

<sup>1</sup> Махамбетов Е.Н., <sup>1\*</sup> Абдирашит А.М., <sup>1</sup> Мынжасар Е.А.,  
<sup>1</sup> Бурумбаев А.Г., <sup>1</sup> Жакан А.М., <sup>2</sup> Юсел Онуэралп

<sup>1</sup> Химико-металлургический институт им.Ж.Абишева, Караганда, Казахстан

<sup>2</sup> Стамбульский технический университет, Стамбул, Турция

<p>Поступила: 10 декабря 2023 Рецензирование: 3 января 2024 Принята в печать: 12 января 2024</p>	<p><b>АННОТАЦИЯ</b></p> <p>В данной статье приведены результаты лабораторных работ по выплавке среднеуглеродистого ферромарганца с использованием Джездинских руд. В Казахстане имеются значительные запасы марганцевых руд, которые представлены железомарганцевыми и карбонатно-оксидными рудами. Марганцевые руды Джездинского месторождения характеризуются сравнительно высоким содержанием марганца (48 %) и низким содержанием железа (2-5 %). Для исследования гранулометрического состава руды был использован ситовый анализ. По результатам гранулометрического анализа образцов руды, полученных после ситового разделения, было выявлено высокое содержание марганца (53,54 %), низкое содержание железа (0,47 %) и кремнезема (2,25 %). Были проведены лабораторные работы по выплавке среднеуглеродистого ферромарганца в высокотемпературной печи Таммана. По результатам лабораторных работ рекомендуется использовать классы -5 + 0,0 мм для получения качественного низкофосфористого передельного силикомарганца, класс крупности +5 для получения среднеуглеродистого ферромарганца. Средневзвешенные химический состав металла и шлака: %: Mn – 86 – 88; Si – 0,04 – 0,35; Fe – 1,78 – 2,0; P – 0,06 – 0,09; C – 1,5 – 2,0; MnO – 19-20; SiO<sub>2</sub> – 13,94-14,5; CaO – 23,35 – 24,85; MgO – 13,25-14,0. Таким образом была разработана оптимальная технологическая схема для производства широкого спектра марганцевых ферросплавов.</p>
	<p><b>Ключевые слова:</b> марганцевая руда, среднеуглеродистый ферромарганец, низкофосфористый передельный силикомарганец, дифференциального термический анализ, высокотемпературная печь, ферросплав.</p>
	<p><b>Информация об авторах:</b> PhD, заведующий лабораторией ферросплавов и процессов восстановления, Химико-металлургический институт им. Ж.Абишева, ул. Еркемова, 63, 100009, г. Караганда, Казахстан. Email: m.ye.n@mail.ru</p>
	<p>Магистр технических наук, младший научный сотрудник лаборатории ферросплавов и процессов восстановления, Химико-металлургический институт им. Ж.Абишева, ул. Еркемова, 63, 100009, г. Караганда, Казахстан. Email: a.abdirashit@tttu.edu.kz</p>
	<p>Магистр технических наук, младший научный сотрудник лаборатории пирометаллургических процессов, Химико-металлургический институт им. Ж.Абишева, ул. Еркемова, 63, 100009, г. Караганда, Казахстан</p>
	<p>Магистр технических наук, инженер лаборатории ферросплавов и процессов восстановления, Химико-металлургический институт им. Ж.Абишева, ул. Еркемова, 63, 100009, г. Караганда, Казахстан. Email: burumbayev.azamat@mail.ru</p>
	<p>Инженер лаборатории ферросплавов и процессов восстановления, Химико-металлургический институт им. Ж.Абишева, ул. Еркемова, 63, 100009, г. Караганда, Казахстан. Email: armat.01.01@mail.ru</p>
	<p>PhD, профессор кафедры металлургии и материаловедение, Стамбульский технический университет, Маслак 6449, Стамбул, Турция. Email: yucel@itu.edu.tr</p>

## References

- [1] Gasik MI. Elektrometallurgiya margantsa [Elektrotermiya marganca]. Kiev, Tekhnika, 1979. (in Russ.).
- [2] Abdirashit A, Makhambetov Y, Yerzhanov A, Sarkulova Z, Aitkenov N, Aitbayev N. Large- scale laboratory tests for smelting medium-carbon ferromanganese using jezda manganese ore and simn17 silicomanganese fines. *Journal Metalurgija*. 2023; 62(1):139-141.
- [3] Akylbekov SA. Manganese of Kazakhstan. *Proceedings of the National Academy of Sciences of the Republic of Kazakhstan. Geological series*. 2006; 1:42-53.
- [4] Tastanova A, Kuldeev E, Temirova S, Abdykirova G, & Biryukova A. Processing of low-quality manganese-containing raw materials to obtain pellets for production ferromanganese alloys. *Review. Engineering Journal of Satbayev University*. 2023; 145(4):10-18. <https://doi.org/10.51301/ejsu.2023.i4.02>
- [5] Mukono T, Wallin M, Tangstad M. Phase Distribution During Slag Formation in Mn Ferroalloy Production. *Metallurgical and Materials Transactions B: Process Metallurgy and Materials Processing Science*. 2022; 53(2):1122-1135.
- [6] Mukono T, Wallin M, Tangstad M. Phase Distribution During Slag Formation in Mn Ferroalloy Production. *Metallurgical and Materials Transactions B: Process Metallurgy and Materials Processing Science*. 2022; 53(2):1122-1135.
- [7] Larssen TA, Tangstad M. Effect of Raw Materials on Temperature Development during Prereduction of Comilog and Nchwaning Manganese Ores. *Minerals*. 2023; 13(7):920. <https://doi.org/10.3390/min13070920>
- [8] Dyussenova SB, Lukhmenov AY, Imekeshova MA, Akimzhanov ZA. Investigation of the beneficiation of refractory ferromanganese ores "Zhomart" deposits. *Kompleksnoe Ispolzovanie Mineralnogo Syra= Complex Use of Mineral Resources*. 2024; 329(2):34-42. <https://doi.org/10.31643/2024/6445.14>
- [9] Tolyzbekov MZh. Margantsevorudnaya otrasl Kazakhstana [Manganese ore industry of Kazakhstan]. *Gornyy zhurnal Kazakhstana =Mining Magazine of Kazakhstan*. 2007; (2):2-5. (in Russ.).
- [10] Telkov ShA, Motovilov NI, Uysimbek A. Issledovaniye na obogatimost margantsevoy rudy rudoprovyavleniya kartobay [A study on the enrichment of manganese ore of the Kartabai ore occurrence]. *Gornyy zhurnal Kazakhstana =Mining Magazine of Kazakhstan*. 2021; 5:42-46. (in Russ.).
- [11] Nurumgaliev A, Makhambetov Y, Kuatbay Y, Yerekeyeva G, Abdirashit A, Mynzhassar Y. Study of softening temperatures of manganese ores in central Kazakhstan. *Journal Metalurgija*. 2023; 62(2):268-270.
- [12] Piloyan GO, Novikova OS. Termograficheskiy i termogravimetricheskiy metody opredeleniya energii aktivatsii protsessov dissotsiatsii [Thermographic and thermogravimetric methods for determining the activation energy of dissociation processes]. *Zhurnal neorganicheskoy khimii*. 1967; 12(3):602-604.
- [13] Djurdjevic MB. Application of thermal analysis in ferrous and nonferrous foundries. *Metallurgical and Materials Engineering*. 2021; 27(4):457-471.
- [14] Lascano D, Quiles-Carrillo L, Balart R, Boronat T, Montanes N. Kinetic analysis of the curing of a partially biobased epoxy resin using dynamic differential scanning calorimetry. *Polymers*. 2019; 11(3):391. <https://doi.org/10.3390/polym11030391>
- [15] Kelamanov B, Smailov S, Yerzhanov A, Adilhanov R, Kabykhanov S. The possibility of involvement in ferroalloy conversion of nickel ores of Kazakhstan. *Journal Metalurgija*. 2022; 61(3-4): 771-773.
- [16] Rong Y, Xu J. Forming Mechanism of Weld Cross Section and Validating Thermal Analysis Results Based on the Maximal Temperature Field for Laser Welding. *Metals*. 2022; 12(5):774.
- [17] Kelamanov B, Sariev O, Akuov A, Samuratov Y, Sultamuratova Z, Orynassar R. Study of nickel briquettes by thermographic method. *Journal Metalurgija*. 2022; 61(1):217-220.
- [18] Baisanov AS, Kairalapov ET, Sankai AN and others. Issledovaniye zheleznykh rud Lisakovskogo mestorozhdeniya metodom differentsialno-termicheskogo analiza [Investigation of iron ores of the Lisakovsky deposit by differential thermal analysis] *Materialy mezhdunar. nauchno-prakt. konf. «Zhidkost na granitse razdela faz – teoriya i praktika»*. posv. 70-letiyu Zh.N. Abisheva. [Materials of the international scientific and practical conference "Liquid at the interface of phases – theory and practice", dedicated to the 70th anniversary of J.N. Abishev] Karaganda, Kazakhstan. 2006, 685-689. (in Russ.).
- [19] Baisanov AS, Tolyzbekov AM, Takenov TD, Akulov AM, Almagambetov MS. Termodinamicheskiy analiz rastvorov so strukturoy shpineli v sisteme Mg-Fe-Sr-O [Thermodynamic analysis of solutions with spinel structure in the Mg-Fe-Cr-O system] *Respublikanskiy nauchnyy zhurnal Tekhnologiya proizvodstva metallov i vtorichnykh materialov=Republican scientific journal Technology of production of metals and secondary materials*. 2006; 10(2):8-13. (in Russ.).
- [20] Baisanov AS, Rustembekov KT, Nauryzbayeva VA, Samuratov EK. Issledovaniye protsessov vosstanovleniya zheleza i margantsa v zhelezo-margantsevykh rudakh metodom izotermicheskoy kinetiki [Study of the reduction processes of iron and manganese in iron-manganese ores by non-isothermal Kinetics] *Materialy mezhdunar. nauchno-prakt. konf. «Zhidkost na granitse razdela faz – teoriya i praktika»*. posv. 70-letiyu Zh.N. Abisheva [Materials of the international scientific and practical conference "Liquid at the interface of phases – theory and practice", dedicated to the 70th anniversary of J.N. Abishev] Karaganda, Kazakhstan. 2006, 690-693. (in Russ.).



## Overview of Technologies Used to Extract Scandium from Secondary Raw Materials

<sup>1</sup>Orynbayev B.M., <sup>1\*</sup>Baigenzhenov O.S., <sup>2</sup>Turan M.D.

<sup>1</sup>Satbayev University, Almaty, Kazakhstan

<sup>2</sup>Firat University, Elazig, Turkey

\*Corresponding author email: o.baigenzhenov@satbayev.university

<p>Received: December 10, 2023 Peer-reviewed: December 19, 2023 Accepted: January 17, 2024</p>	<p><b>ABSTRACT</b> The exceptional mechanical and chemical properties exhibited by scandium, characterized by its low density, high strength, and remarkable resistance to corrosion, have positioned it as a sought-after metal in diverse industrial applications. Consequently, a surge in market demand for scandium has been observed, highlighting its unique attributes compared to other metals. The Republic of Kazakhstan has identified potential sources of scandium in the waste generated by the titanium, uranium, and aluminum industries. By implementing efficient processing techniques for these production wastes, the country can effectively address the deficit of scandium while also mitigating man-made emissions, thus significantly improving the environmental landscape. This article aims to explore and evaluate contemporary methodologies that have been employed for the recovery of scandium from the aforementioned secondary sources. By examining and analyzing these techniques, we can gain insights into the most effective and sustainable approaches to harnessing scandium from waste materials in Kazakhstan. This research not only contributes to meeting market demands but also ensures the responsible utilization of scandium, benefiting not just the country's economy but also its environmental sustainability.</p>
	<p><b>Keywords:</b> titanium wastes, rare metals, scandium, rare earth elements, leaching, chlorination</p>
<p><b>Orynbayev Bauyrzhan Munarbaiuly</b></p>	<p><b>Information about authors:</b> PhD student, Non-commercial joint-stock company "Satbayev University", the department "Metallurgical processes, heat engineering and technology of special materials", st. Satpaeva 22, 050013, Almaty, Kazakhstan. E-mail: Bauyrzhan.Orynbayev@stud.satbayev.university</p>
<p><b>Baigenzhenov Omirserik Sabyrzhanovich</b></p>	<p>PhD, Professor, Non-commercial joint-stock company "Satbayev University", the department "Metallurgical processes, heat engineering and technology of special materials", st. Satpaeva 22, 050013, Almaty, Kazakhstan. E-mail: o.baigenzhenov@satbayev.university</p>
<p><b>Turan Mehmet Deniz</b></p>	<p>Professor, PhD, Firat University, Engineering Faculty, Metallurgical and Materials Engineering, Elazig, Turkey. E-mail: mdturan@firat.edu.tr</p>

### Introduction

The global market demand for rare and rare earth metals (REM) in the development and production of mineral resources is growing each year, driven by scientific and technological advancements [[1], [2], [3]]. Scandium, a rare and expensive metal, is primarily found dispersed in nature, although it also exists in its mineral called tortveitite. The extraction and purification of scandium involve multiple processes, which significantly contribute to its high price. In 2016, for example, scandium oxide cost reached \$4,200 per kilogram [[4], [5], [6]]. Scandium possesses unique properties such as low density, high strength, and excellent corrosion resistance, making it crucial for various industries including aviation, electronics, and energy. However, the natural sources of

scandium are limited, leading to increased research on its extraction [[7], [8]].

Although scandium is more prevalent in the Earth's crust compared to precious metals like gold and silver, it is a scattered element that does not form distinct deposits. Instead, scandium is widely distributed as a minor impurity in ores and minerals containing zircon, wolframite, beryl, cassiterite, uranium, and titanium [9]. Scandium is extracted from these ores as well as from waste generated during mineral production. In recycled mineral raw materials, scandium can constitute a fraction of around a dozen percent or more. Therefore, scandium concentrate is initially obtained from secondary raw materials, enabling the production of pure scandium through subsequent processing. Possible sources of secondary raw materials include slag, sludge, chlorine melts, and reverse solutions from underground leaching. The

processes for separating scandium from solutes are complex and may involve deposition, extraction, and ion exchange methods [[10], [11]].

The primary objective of this study is to provide an overview of industrial waste categories and the technological interventions employed in the extraction of scandium.

### Extraction from uranium raw materials

Scandium is primarily sourced from uranium ores, which typically contain concentrations of 0.001-0.0001% of this element. Higher concentrations of scandium can be found in specific minerals such as davidite (0.02%), xenotime (0.08-0.1%), and obrucheveite (0.08-0.2%) [12]. The annual production of scandium oxide ( $\text{Sc}_2\text{O}_3$ ) from uranium ores ranges from 50 to 500 tonnes, and the worldwide reserves of such ores are estimated to be around 600 million tonnes. When uranium ores are leached with sulphuric acid, scandium is transferred into the solution.

A technology scheme for the simultaneous extraction of scandium during the processing of uranium has been outlined in references [[12], [13]] (Figure 1). The process begins with leaching uranium ore using sulphuric acid, resulting in a solution containing up to 1 mg/l  $\text{Sc}_2\text{O}_3$ . Dodecylphosphoric acid (0.1 M) is used to fully extract uranium from this solution. Notably, scandium, thorium, and titanium are commonly co-extracted but remain in the organic phase after uranium re-extraction through a 10 M HCl solution.

Hydrofluoric acid treatment is employed to extract scandium and thorium from the organic solution. As a result, scandium and thorium form solid deposits (10%  $\text{Sc}_2\text{O}_3$  and 20%  $\text{ThO}_2$ ). The resulting precipitate is dissolved in a 15% sodium hydroxide solution at 75-90 °C for 4 hours, leading to the formation of scandium oxide. After filtration, the scandium hydroxide is dissolved in hydrochloric acid, and impurities such as titanium, zirconium, iron, and silicon are removed through hydrolysis. Subsequently, an oxalate purification method is applied.

Uranium is sorbed by anionites from these solutions while scandium remains in the solution. According to reference [14], the sorption of scandium can be achieved using ion exchange resins containing phosphorus, such as Lewatit TR 260. Laboratory experiments using authentic solutions have successfully achieved an overall dynamic capacity of scandium of 0.049 kg/m<sup>3</sup>. Desorption of scandium from a fully saturated sorbent, using eight specific volumes of  $\text{Na}_2\text{CO}_3$  solution (200 g/L), resulted in an 80% desorption efficiency. The desorbed substances were then subjected to the next stage of scandium absorption using the highly alkaline anion exchange resin Amberlite 920. From this resin, scandium is desorbed using a nitric acid solution containing ammonium nitrate. Additionally, an additional phase involves the precipitation of scandium oxalate from the desorbate of the second phase, followed by calcination to obtain  $\text{Sc}_2\text{O}_3$ .

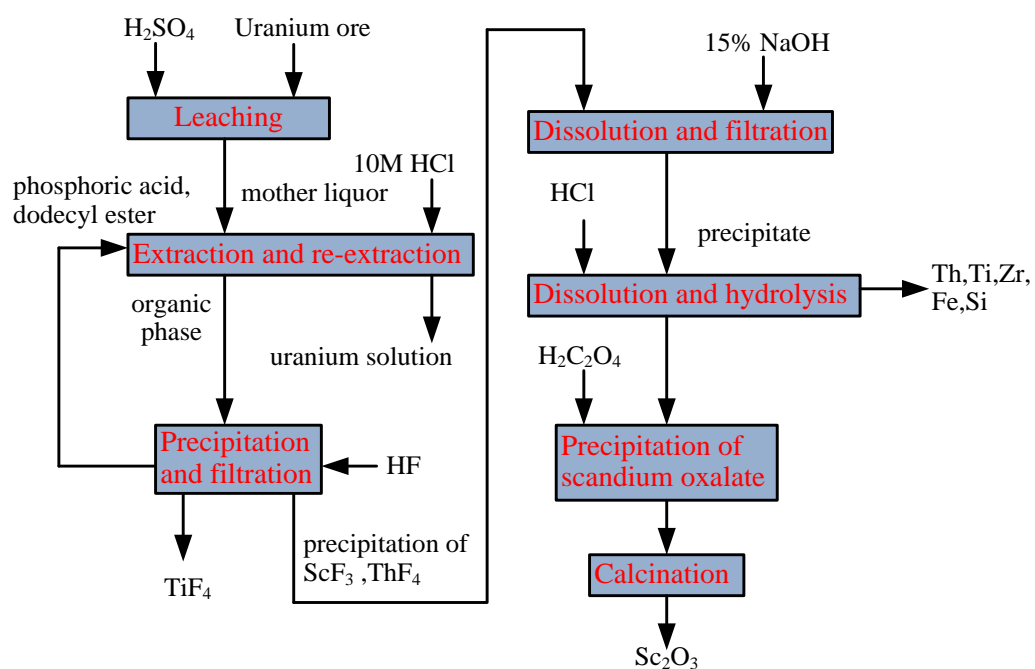


Figure 1 - Technological flow sheet of associated scandium extraction in uranium processing

In article [15], the authors examined the sorption capacities of Lewatit TP260 and Purolite MTS9580 sorbents. The results indicated that MTS9580 resin had an advantage over TP260, with an exchange capacity of 200 mg Sc/dm<sup>3</sup> compared to 59.7 mg Sc/dm<sup>3</sup> for TP260. It is important to note that Purolite MTS9580 has a significantly reduced dynamic exchange capacity for undesirable impurities such as Al, Fe, Ca, and others.

**Extraction of scandium from red mud.** A waste by-product of the Bayer bauxite treatment process presents a challenging technological task. Red mud production is significant, with approximately 1.1-1.2 tonnes generated for every tonne of bauxite alumina. Currently, red muds are typically deposited in designated lagoons due to limited disposal options. However, this practice poses environmental challenges and occupies large areas of land [[14], [15], [16]]. The global accumulation of red mud resulting from alumina production has reached around 1.5 billion tonnes, with this quantity increasing annually [[17], [18], [19]]. Despite current storage methods, environmental contamination from toxic substances contained in red mud remains a persistent issue. The extraction and recycling of metals from this waste can help mitigate these concerns.

Scandium, an essential component found in red mud, requires complex technological processes for retrieval. With the rapidly growing global consumption of scandium, there is a need to develop techniques to extract it in various chemical forms, such as oxide or fluoride.

A study conducted in [20] investigated the extraction of scandium from red mud obtained in Greece (see Figure 2). The red muds underwent sintering using sodium carbonates or sodium borates at 1100 °C for 20 minutes, followed by leaching with a 1.5 M HCl solution. The resulting solution was then subjected to ion exchange using Dowex 50W-X8 sulphocationite resin, enabling scandium and a significant portion of impurities to be extracted. The impurities were eluted with a 1.75 M HCl solution, and scandium was quantitatively desorbed using a 6 M HCl solution. The solution was subsequently neutralized with ammonia and passed through a liquid-liquid extraction step using a 0.05 M solution of D2EHPA in hexane. Scandium re-extraction was achieved using a 2 M NaOH solution. However, this recovery method is not cost-effective due to its lack of selectivity, requiring additional purification operations, and resulting in significant costs. To address this issue, the authors of [[21], [22]] have developed methods allowing for more selective leaching of scandium from red mud. The leaching of lanthanides, scandium, and yttrium from red mud was investigated using sulphuric, nitric, and hydrochloric acid solutions. Dilute HNO<sub>3</sub> (approximately 0.5 M) at room temperature provided the best results, with recoveries of 80% for scandium, 96% for yttrium, and 70% for ytterbium. Importantly, only 3% of iron was introduced into the solution.

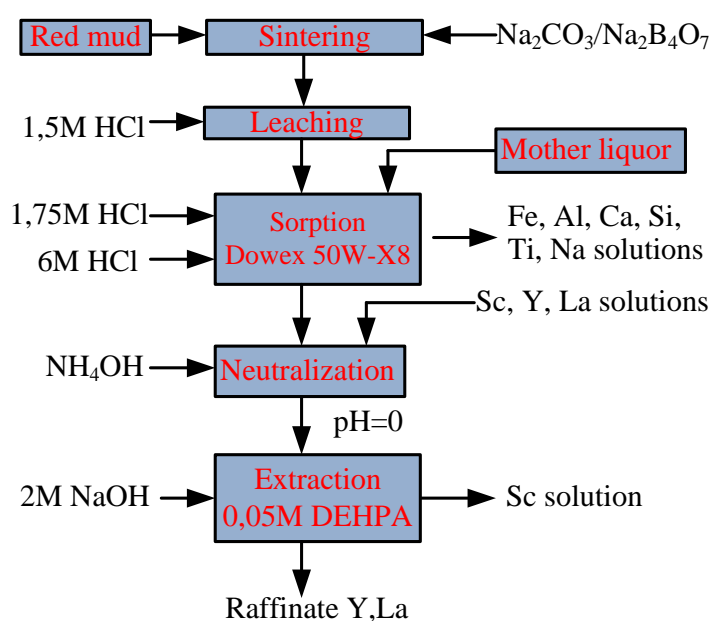


Figure 2 - Technological flow sheet of scandium extraction from red mud

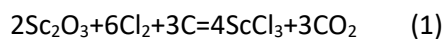


Furthermore, in [23], the alkaline method for scandium extraction from red sludge is described. The process involves treating red sludge with a  $\text{Na}_2\text{CO}_3$  solution, followed by hydrolytic precipitation of Sc(III) using a carrier (aluminium or zinc oxide solution in sodium hydroxide). The resulting precipitate is then treated with concentrated sodium hydroxide solution, transferred to the hydrochloric acid solution, and the filtrate is treated with an excess of stoichiometric proportions of ammonia or hydrofluoric acid solution. Experimental results indicate that this technique allows for the production of a scandium concentrate containing 10-30%  $\text{Sc}_2\text{O}_3$  in oxide form and 30-50%  $\text{ScF}_3$  in fluoride form.

When scandium is precipitated from an acidic solution using an ammonia solution, the recovery rate of scandium in the precipitate reaches 94-100%. Alternatively, when precipitation is done with hydrofluoric acid, the recovery rate ranges from 92-100%. However, it is important to acknowledge that this method involves multiple precipitation and filtration steps, which results in low productivity and complexity in terms of automation.

#### Extraction of Scandium from titanium production waste

Titanium concentrate is typically processed using two primary methods: sulfuric acid, which produces titanium oxide, and chlorination, which produces titanium tetrachloride. During the chlorination of titanium slag, a significant portion of scandium accumulates in the remaining melt of titanium chlorate. Scandium oxide undergoes chlorination through the reaction (1).



Scandium chloride is well soluble in water and hydrochloric acid solvents. Figure 3 shows the technology of the recovery of scandium. The bulk melt containing 0.01-0.03% scandium is alkalized in a weak solution of hydrochloric acid (20-40 g/l HCl). Scandium, located in the bulk melt in the form of chloride, is filtered and sent for extraction, adjusted for the content of ferric chloride. Scandium extraction is carried out with a 70% solution of tributyl phosphate in kerosene; the resulting scandium-enriched organic phase is washed from impurities with strong hydrochloric acid (220-240 g/l HCl); then the scandium extract is transferred to the aqueous phase (reextract) with a 7% hydrochloric acid solution. From the reextraction of oxalic acid, oxalates of scandium

and other metals are precipitated, the resulting pulp is filtered, a solid precipitate of oxalates is dried and heated at 700°C and a technical oxide containing 40-60%  $\text{Sc}_2\text{O}_3$  is obtained [[24], [25]].

The extraction of scandium from ilmenite slags obtained after smelting ilmenite concentrates is described in the referenced work (Figure 4). The proposed method involves grinding the slag and sintering it with  $\text{Na}_2\text{CO}_3$  at temperatures between 900-1000°C. The sintered material is then leached with a 30% HCl solution, maintaining a S:L ratio of 1:2 and a temperature of 80°C. Using an extraction solution of 30% D2EHPA in kerosene, 94% of scandium is extracted from the solution at a W:O ratio of 20:1. Iron is removed by washing the extracted solution with a 5M HCl solution, and scandium is further re-extracted with a 2M NaOH solution. The  $\text{Sc}(\text{OH})_3$  precipitate is dissolved in an HCl solution, and scandium oxalate is obtained through precipitation. The total recovery of scandium achieved is 90%.

Figure 4 provides an example of a process for obtaining scandium from the residual chlorination melt of titanium slag, as documented in previous research [20]. The process is based on the extraction of scandium as TBF from chloride solutions obtained through leaching with a 6M hydrochloric acid solution. The solution is then purified from radium by precipitating it together with newly formed barium sulfate. Scandium is subsequently extracted as a hydroxide by precipitating it with an  $\text{NH}_4\text{OH}$  solution after re-extraction with a 0.1M hydrochloric acid solution. Finally, the precipitate is heated to obtain  $\text{Sc}_2\text{O}_3$ .

The work [26] describes a method for processing a melt of titanium chlorators by obtaining  $\text{Sc}_2\text{O}_3$  and concentrating it in the aqueous phase of yttrium and manganese. The solution is based on the results of research on the extraction of Scandium, Yttrium, aluminum, iron(III), Titanium and manganese with a new nitrogen extractant N(2-hydroxy-5-nonylbenzyl)- $\beta$ ,  $\beta$ -dihydroxyethylamine (NBEA-1) in an organic thinner.

The method of separation of scandium and titanium is based on the use of an organic solution of NBEA for extraction [27]. For this process, a chloride solution containing titanium and scandium is used, to which hydrogen peroxide is added in a certain ratio with a titanium concentration from 0.8 to 10. Then the solution is neutralized, after which extraction is performed using a solution of NBEA in octanol with a concentration of 0.25 mol/l for 30 minutes at a pH of 2.25 to 3.45. This method allows to increase the metal separation coefficient from 450 to 26440.

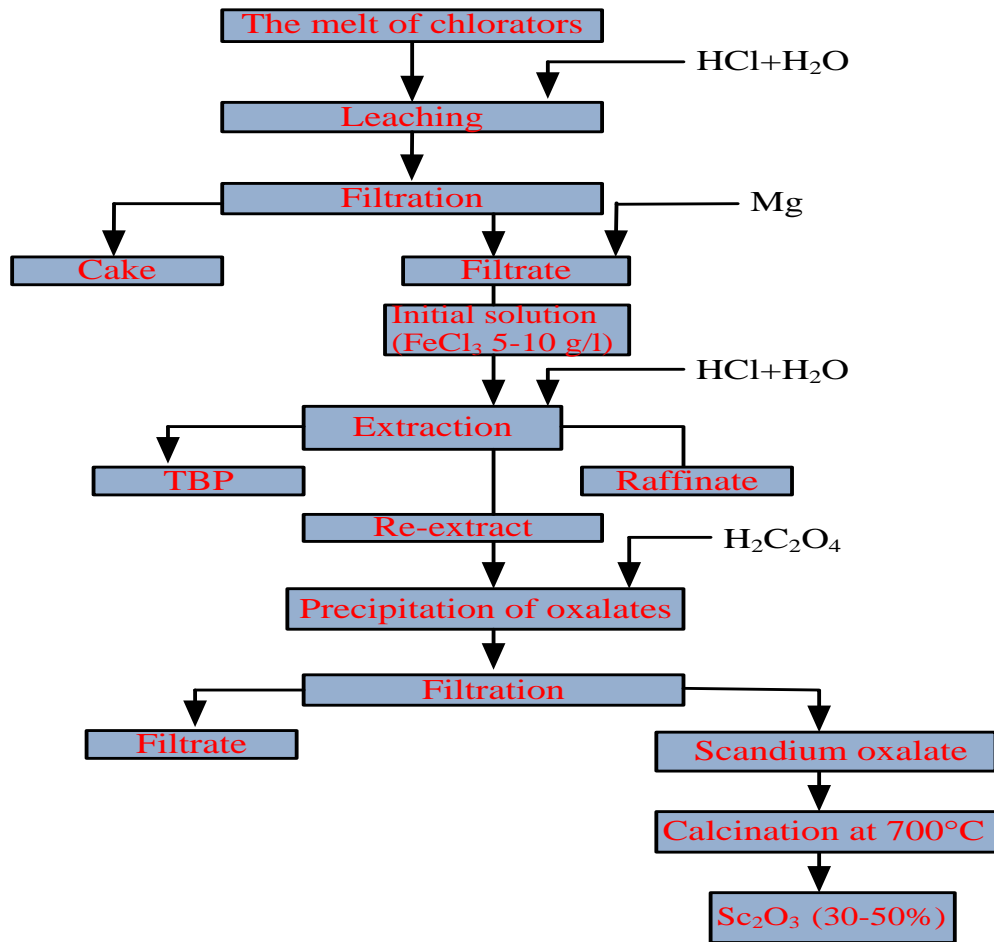


Figure 3 - Technological flow sheet for recovery scandium oxide from the spent melt of titanium chlorators

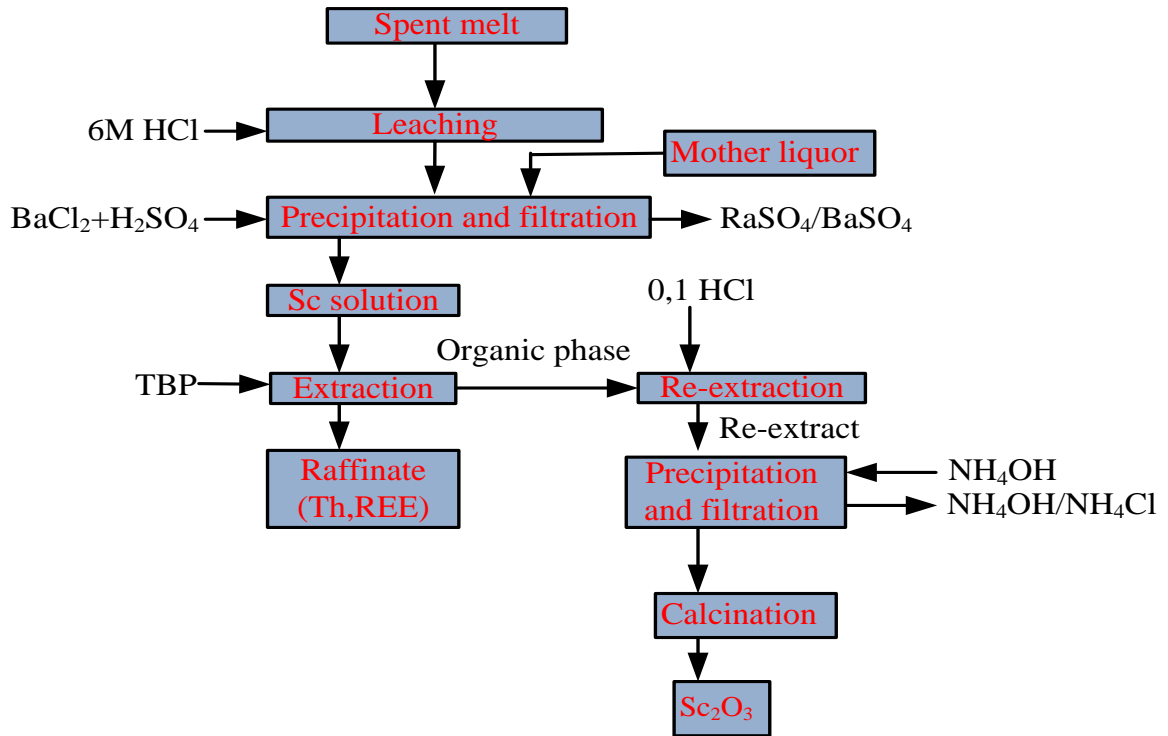


Figure 4 -Technological flow sheet for recovery scandium oxide from the spent melt of titanium chlorators

## Conclusion

In conclusion, the development of extraction technologies for scandium from secondary raw material sources is an important area of research, as it allows for improved resource efficiency and the recovery of valuable metals from waste materials. Effective methods for extracting scandium from feedstocks, with high recovery rates ranging from 85-90%, often involve sorption or extraction steps utilizing phosphorus-containing substances. These steps can be applied during the primary concentration of scandium as well as in subsequent

processing to remove unwanted impurities. Sorbents such as Lewatit TP260 and Purolite MTS9580 have shown promising selectivity towards scandium, and Dowex 50W-X8 has demonstrated high recovery not only of scandium but also other impurities. Further research will focus on the sorption capacities of Lewatit TP260 and Purolite MTS9580 in titanium waste solutions following aqueous leaching.

**Conflict of interest.** The corresponding author declares that there is no conflict of interest.

**Cite this article as:** Orynbayev BM, Baigenzhenov OS, Turan MD. Overview of Technologies Used to Extract Scandium from Secondary Raw Materials. *Kompleksnoe Ispolzovanie Mineralnogo Syra = Complex Use of Mineral Resources*. 2024; 331(4):109-116. <https://doi.org/10.31643/2024/6445.44>

## Скандийді қайталама шикізаттан алу үшін қолданылатын технологияларға шолу

<sup>1</sup>Орынбаев Б.М., <sup>1\*</sup>Байгенженов О.С., <sup>2</sup>Turan M.D.

<sup>1</sup>Сәтбаев университеті, Алматы, Қазақстан

<sup>2</sup>Фырат Университеті, Элязыг, Түркия

<p>Мақала келді: 10 желтоқсан 2023 Сараптамадан өтті: 19 желтоқсан 2023 Қабылданды: 17 қаңтар 2024</p>	<p><b>ТҮЙІНДЕМЕ</b></p> <p>Скандийдің тығыздығы төмен, беріктігі жоғары және коррозияға төзімділігімен ерекшеленетін ерекше механикалық және химиялық қасиеттері оны әртүрлі өнеркәсіптік салаларда сұранысқа ие металға айналдырды. Осыған байланысты скандийге нарықтық сұраныстың күрт өсуі байқалады, бұл оның басқа металдармен салыстырғанда қасиеттерінің ерекше екендігін көрсетеді. Қазақстан Республикасында титан, уран және алюминий өнеркәсібінің қалдықтарындағы скандийдің әлеуетті көздері анықталды. Осы өндіріс қалдықтарын өңдеудің тиімді технологияларын енгізу арқылы біздің ел скандий тапшылығы мәселесін тиімді шеше алады және сонымен бірге техногендік қалдықтарды азайтады, осылайша экологиялық жағдайды айтарлықтай жақсартады. Бұл мақаланың мақсаты – жоғарыда аталған қайталама шикізат көздерінен скандийді алу үшін қолданылатын заманауи әдістерді зерттеу және бағалау. Осы әдістерді зерделеп, талдай отырып, біз скандийді Қазақстандағы қалдықтардан алудың неғұрлым тиімді және орнықты тәсілдері туралы түсінік ала аламыз. Бұл зерттеу нарықтың қажеттіліктерін қанағаттандыруға ықпал етіп қана қоймайды, сонымен қатар скандийді жауапкершілікпен пайдалануды қамтамасыз етеді. Бұл елдің экономикасына ғана емес, оның экологиялық тұрақтылығына да пайда әкеледі.</p>
	<p><b>Түйін сөздер:</b> титан қалдықтары, сирек металдар, скандий, сирек жер элементтері, шаймалау, хлорлау</p>
<p><b>Орынбаев Бауыржан Мұнарбайұлы</b></p>	<p><b>Авторлар туралы ақпарат:</b> <i>Ph.D. докторант, «Сәтбаев университеті», «Металлургиялық процестер, жылу техникасы және арнайы материалдар технологиясы» кафедрасы, Алматы, Қазақстан. E-mail: B.Orynbayev@stud.satbayev.university</i></p>
<p><b>Байгенженов Омисерик Сабыржанович</b></p>	<p><i>Doctor Ph.D., профессор. «Сәтбаев университеті», «Металлургиялық процестер, жылу техникасы және арнайы материалдар технологиясы» кафедрасы, Алматы, Қазақстан. E-mail: o.baigenzhenov@satbayev.university</i></p>
<p><b>Turan Mehmet Deniz</b></p>	<p><i>Doctor Ph.D., проф., «Фырат университеті», «Металлургия және материалтану» кафедрасы, Элязыг, Түркия. E-mail: mdturan@firat.edu.tr</i></p>

## Обзор технологий, использовавшихся для извлечения скандия из вторичного сырья

<sup>1</sup>Орынбаев Б.М., <sup>1\*</sup>Байгенженов О.С., <sup>2</sup>Turan M.D.

<sup>1</sup>Satbayev University, Алматы, Казахстан

<sup>2</sup>Университет Фырат, Элязыг, Турция

<p>Поступила: 10 декабря 2023 Рецензирование: 19 декабря 2023 Принята в печать: 17 января 2024</p>	<p><b>АННОТАЦИЯ</b></p> <p>Исключительные механические и химические свойства скандия, характеризующиеся низкой плотностью, высокой прочностью и удивительной устойчивостью к коррозии, сделали его востребованным металлом в различных промышленных областях. В связи с этим наблюдается резкий рост рыночного спроса на скандий, что подчеркивает его уникальные свойства по сравнению с другими металлами. Республика Казахстан выявила потенциальные источники скандия в отходах титановой, урановой и алюминиевой промышленности. Внедрив эффективные технологии переработки этих отходов производства, страна сможет эффективно решить проблему дефицита скандия и одновременно снизить техногенные выбросы, тем самым значительно улучшив экологическую обстановку. Цель данной статьи - изучить и оценить современные методики, применяемые для извлечения скандия из вышеупомянутых вторичных источников. Изучив и проанализировав эти методы, мы сможем получить представление о наиболее эффективных и устойчивых подходах к извлечению скандия из отходов в Казахстане. Данное исследование не только способствует удовлетворению потребностей рынка, но и обеспечивает ответственное использование скандия, принося пользу не только экономике страны, но и ее экологической устойчивости.</p>
	<p><b>Ключевые слова:</b> титановые отходы, редкие металлы, скандий, редкоземельные элементы, выщелачивание, хлорирование</p>
<p><b>Орынбаев Бауыржан Мұнарбайұлы</b></p>	<p><b>Информация об авторах:</b> <i>Ph.D. докторант, Satbayev University, кафедра «Металлургические процессы, теплотехника и технология специальных материалов», Алматы, Казахстан. E-mail: B.Orynbayev@stud.satbayev.university</i></p>
<p><b>Байгенженов Омурсерик Сабыржанович</b></p>	<p><i>Доктор Ph.D., профессор, Satbayev University, кафедра «Металлургические процессы, теплотехника и технология специальных материалов», Алматы, Казахстан. E-mail: o.baigenzhenov@satbayev.university</i></p>
<p><b>Turan Mehmet Deniz</b></p>	<p><i>Доктор Ph.D., профессор, Firat University, факультет Инженерия, кафедра «Металлургия и материаловедение», Элязыг, Турция. E-mail: mduran@firat.edu.tr</i></p>

### References

- [1] Zhou J, Ning Sh, Meng J, Zhang Sh, Zhang W, Wang S, Chen Y, Wang X, Wei Y. Purification of scandium from concentrate generated from titanium pigments production waste. *Journal of Rare Earths*. 2021; 39(2): 194-200. <https://doi.org/10.1016/j.jre.2020.02.008>
- [2] Kenzhaliyev B, Surkova T, Azlan M, Yulusov S, Sukurov B, Yessimova D. Black shale ore of Big Karatau is a raw material source of rare and rare earth elements. *Hydrometallurgy*. 2021; 202:105733. <https://doi.org/10.1016/j.hydromet.2021.105733>
- [3] Baigenzhenov O, Yulusov S, Khabiyev A, Sydykanov M, Akbarov M. Investigation of the leaching process of rare-earth metals from the black shale ores of greater Karatau. *Complex Use of Mineral Resources*. 2019; 310(3):76-80. <https://doi.org/10.31643/2019/6445.31>
- [4] Ahmad Z. The Properties and Application of Scandium-Reinforced Aluminum. *JOM*. 2003; 55:35-39. <https://doi.org/10.1007/s11837-003-0224-6>
- [5] Reid S, Tam J, Yang M, Azimi G. Technospheric Mining of Rare Earth Elements from Bauxite Residue (Red Mud). *Process Optimization, Kinetic Investigation, and Microwave Pretreatment*. *Scientific Reports*. 2017; 7:1-9. <https://doi.org/10.1038/s41598-017-15457-8>
- [6] Zhang R, Khan S, Azimi G. Microstructured silicon substrates impregnated with bis (2,4,4-trimethylpentyl) phosphinic acid for selective scandium recovery. *Applied Surface Science*. 2023; 622:1-15. <https://doi.org/10.1016/j.apsusc.2023.156852>
- [7] Salman A, Juzsakova T, Mohsen S, Abdullah T, Le P-C, Sebestyen V, Sluser B, Cretescu I. Scandium Recovery Methods from Mining, Metallurgical Extractive Industries, and Industrial Wastes. *Materials*. 2022; 15(7):2376. <https://doi.org/10.3390/ma15072376>
- [8] Giret S, Hu Y, Masoumifard N, Boulanger J-F, Juère E, Kleitz F, Larivière D. Selective Separation and Pre-Concentration of Scandium with Mesoporous Silica, *ACS Applied Materials and Interfaces*. 2018; 10(1):448-457. <https://doi.org/10.1021/acsami.7b13336>
- [9] Vind J, Malfliet A, Bonomi C, Paiste P, Sajo J, Blanpain B, Tkaczyk A, Vassiliadou V, Panias D. Modes of occurrences of scandium in Greek bauxite and bauxite residue. *Minerals Engineering*. 2018; 123:35-48. <https://doi.org/10.1016/j.mineng.2018.04.025>

- [10] Wang W, Cheng CY. Separation and purification of scandium by solvent extraction and related technologies: a review. *Journal of Chemical Technology and Biotechnology*. 2011; 86:1237-1246. <https://doi.org/10.1002/jctb.2655>
- [11] Belosludtsev A, Yakimov Y, Mroczynski R, Stanionyte S, Skapas M, Buinovskis D, Kyžas N. Effect of Annealing on Optical, Mechanical, Electrical Properties and Structure of Scandium Oxide Films. *Physica Status Solidi*. 2019; 216(18):1900122. <https://doi.org/10.1002/pssa.201900122>
- [12] Xiao J, Peng Y, Ding W, Chen T, Zou K, Wang Z. Recovering Scandium from Scandium Rough Concentrate Using Roasting-Hydrolysis-Leaching Process. *Processes*. 2020; 8(3):365. <https://doi.org/10.3390/pr8030365>
- [13] Ghosh A, Dhiman S, Gupta A, Jain R. Process Evaluation of Scandium Production and Its Environmental Impact. *Environments*. 2023; 10(1):8-37. <https://doi.org/10.3390/environments10010008>
- [14] Yessimkanova U, Mataev M, Alekhina M, Kopbaeva M, Berezovskiy A, Dreisinger D. The study of the Kinetic Characteristics of Sorption of Scandium of Ion Exchanger Purolite MTS9580 from Return Circulating Solutions of Underground Leaching of Uranium Ores. *Eurasian Chemico-Technological Journal*. 2020; 22: 135-142.
- [15] Safulina A, Lizunov A, Semenov A, Baulin D, Baulin V, Tsvadze A, Aksenov S, Tananaev I. Recovery of Uranium, Thorium, and Other Rare Metals from Eudialyte Concentrate by a Binary Extractant Based on 1,5-bis[2-(hydroxyethoxyphosphoryl)-4-ethylphenoxy]-3-oxapentane and Methyl Trioctylammonium Nitrate. *Minerals*. 2022; 12(11):1469. <https://doi.org/10.3390/min12111469>
- [16] Toli A, Mikeli E, Marinos D, Balomenos E, Panias D. Assessing the Efficiency of Ion Exchange Resins for the Recovery of Scandium from Sulfuric Acid Leaching Solutions. *Separations*. 2023; 10(7):366. <https://doi.org/10.3390/separations10070366>
- [17] Abdulvaliev R, Akhmadieva N, Gladyshev C, Imangalieva L, Manapova A. The modified red mud reduction smelting. *Complex Use of Mineral Resources*. 2018; 306(3):15-20. <https://doi.org/10.31643/2018/6445.12>
- [18] Kenzhaliyev B, Surkova T, Yessimova D. Concentration of rare-earth elements by sorption from sulphate solutions. *Complex Use of Mineral Resources*. 2019; 310(3):5-9. <https://doi.org/10.31643/2019/6445.22>
- [19] Reddy PS, Reddy NG, Serjun V, et al. Properties and Assessment of Applications of Red Mud (Bauxite Residue): Current Status and Research Needs. *Waste and Biomass Valorization*. 2021; 12:1185-1217. <https://doi.org/10.1007/s12649-020-01089-z>
- [20] Mishra B, Gostu S. Materials sustainability for environment: Red-mud treatment. *Front. Chem. Sci. Eng.* 2017; 11:483-496. <https://doi.org/10.1007/s11705-017-1653-z>
- [21] Ochsenkuhn-Petropulu M, Lyberopulu Th, Ochsenkuhn KM, Parissakis G. Recovery of lanthanides and yttrium from red mud by selective leaching. *Anal. Chim. Acta*. 1996; 319:249-254.
- [22] Davris P, Balomenos E, Nazari G, Abrenica G, Patkar S, Xu W-Q, Karnachoritis Y. Viable Scandium Extraction from Bauxite Residue at Pilot Scale. *Mater. Proc.* 2021; 5:129-135. <https://doi.org/10.3390/materproc2021005129>
- [23] Shoppert A, Loginova I, Napol'skikh J, Kyrchikov A, Chaikin L, Rogozhnikov D, Valeev D. Selective Scandium (Sc) Extraction from Bauxite Residue (Red Mud) Obtained by Alkali Fusion-Leaching Method. *Materials*. 2022; 15(2):433. <https://doi.org/10.3390/ma15020433>
- [24] Toishybek A, Baigenzhenov O, Turan M, Kurbanova B, Merkitabeyev Y. A review of recovery technologies of rare and rare earth metals from wastes generated in titanium and magnesium production. *Complex Use of Mineral Resources*. 2023; 327(4):64-73. <https://doi.org/10.31643/2023/6445.41>
- [25] Karshyga Z, Ultarakova A, Lokhova N, Yessengaziyev A, Kassymzhanov K. Processing of Titanium-Magnesium Production Waste. *Journal of Ecological Engineering*. 2022; 23(7):215-225. <https://doi.org/10.12911/22998993/150004>
- [26] El Khalloufi M, Drevelle O, Soucy G. Titanium: An Overview of Resources and Production Methods. *Minerals*. 2021; 11(12):1425. <https://doi.org/10.3390/min11121425>
- [27] Kostikova GV, Mal'tseva IE, Krasnova OG, Sal'nikova EV, Zhilov VI. Use of Tetraoctyldiglycolamide for Concentration of Scandium by Extraction from Red-Mud Acid-Leaching Solutions. *Theoretical Foundations of Chemical Engineering*. 2022; 5: 900-907. <https://doi.org/10.1134/S0040579522050086>





DOI: 10.31643/2024/6445.45

Metallurgy



## Study of the leaching process for dust chamber sublimates followed by the extraction of niobium and zirconium into solution

\*Yessengaziyev A.M., Toishybek A.M., Mukangaliyeva A.O., Abdyldayev N.N., Yersaiynova A.A.

*Institute of Metallurgy and Ore Beneficiation, Satbayev University, Almaty, Kazakhstan*

*\*Corresponding author email: a.yessengaziyev@satbayev.university*

<p>Received: November 7, 2023 Peer-reviewed: January 4, 2024 Accepted: January 19, 2024</p>	<p><b>ABSTRACT</b></p> <p>The material composition of the sublimates from dust chambers in titanium chlorinators has been studied by chemical, X-ray and microprobe analysis methods. Studies of the phase composition of dust chamber sublimates have shown that the object consists of aqueous and anhydrous chloride phases to a greater extent. Two forms of niobium present, such as oxychloride and oxide niobium were found. The presence of zirconium in sublimates has a chloride and oxychloride nature. Experiments for the aqueous leaching of dust chamber sublimates were conducted to determine the optimal process conditions: S:L ratio = 1:8, leaching time = 1 hour, temperature = 25°C. Studies were conducted to choose an acidic reagent for cake leaching followed by the conversion of niobium and zirconium into a solution. A solution consisting of HF+H<sub>2</sub>SO<sub>4</sub> was selected as an acidic reagent for cake leaching. Optimal conditions for the extraction of niobium and zirconium into solution were established, such as 25% [18M HF] +75% [7M H<sub>2</sub>SO<sub>4</sub>], S:L ratio = 1:3, temperature = 90 °C, duration of the leaching process = 120 minutes. Under these leaching conditions, the extraction of niobium, zirconium, and titanium into solution was 94.06%, 84.95% and 32.35%, respectively. The elemental and phase composition of the residue from acid leaching of cake were determined.</p>
	<p><b>Keywords:</b> niobium, dust chamber sublimates, leaching, acid, solution.</p>
<p><b>Yessengaziyev Azamat Muratovich</b></p>	<p><b>Information about authors:</b> Ph.D., Researcher, Institute of Metallurgy and Ore Beneficiation, Satbayev University, Almaty, Kazakhstan. E-mail: a.yessengaziyev@satbayev.university</p>
<p><b>Toishybek Azamat Magaiyaully</b></p>	<p>Lead Engineer, Institute of Metallurgy and Ore Beneficiation, Satbayev University, Almaty, Kazakhstan. E-mail: a.toishybek@satbayev.university</p>
<p><b>Mukangaliyeva Arailym Omirzakkyzy</b></p>	<p>Lead Engineer, Institute of Metallurgy and Ore Beneficiation, Satbayev University, Almaty, Kazakhstan. E-mail: 000316650668-D@stud.satbayev.university</p>
<p><b>Abdyldayev Nurgaly Nurlanovich</b></p>	<p>Lead Engineer, Institute of Metallurgy and Ore Beneficiation, Satbayev University, Almaty, Kazakhstan. E-mail: n.abdyldayev@satbayev.university</p>
<p><b>Yersaiynova Albina Abatkyzy</b></p>	<p>Lead Engineer, Institute of Metallurgy and Ore Beneficiation, Satbayev University, Almaty, Kazakhstan. E-mail: a.yersaiynova@stud.satbayev.university</p>

### Introduction

In general, rare metals determine the development of such important fields as semiconductor electronics, nuclear power, aviation and rocket engineering, electro-vacuum technology, as well as the production of special steels and hard, heat-resistant and anticorrosive alloys. Rare refractory transition metals which form alloys of intermetallic compounds and solid solutions characterized by high intermolecular adhesion of atoms in crystals may be considered particularly in demand. The high rates of development of these technology branches determine the continuous increase in demand for rare metals which provides for further expansion of their production [[1], [2], [3]]. The use of titanium-magnesium production

waste abundant in rare metals can contribute to solving this problem [4]. Niobium and zirconium are a common satellite of titanium: therefore, they are found in titanium concentrates obtained from ores of ilmenite deposits. At Ust-Kamenogorsk Titanium and Magnesium Plant (UKTMP) JSC, during the processing of titanium-containing raw materials, the largest part of niobium and zirconium enters and concentrates in production waste.

When titanium tetrachloride is produced, a large amount of spent melt and pulps of chlorinators, sublimates and sludge of dust chambers is formed. An analysis of the distribution of niobium in solid waste from the chlorination process for titanium slags of the Ust-Kamenogorsk Titanium and Magnesium Plant shows that the highest content of niobium is found in dust chamber sublimates. Depending on the volume of titanium tetrachloride

production, up to 3.2 t/day of DC sublimates are formed and contain such valuable components as KCl, NaCl, FeCl<sub>2</sub>, FeCl<sub>3</sub>, MnCl<sub>2</sub>, CrCl<sub>3</sub>, TiCl<sub>4</sub>, NbCl<sub>5</sub>, ZrCl<sub>4</sub>, ThCl<sub>4</sub>, AlCl<sub>3</sub>, ScCl<sub>3</sub>, TaCl<sub>5</sub>. At the plant, DC distillates are washed with water, the resulting chloride pulp is discharged into an acidic sewer and then neutralized with lime milk. Here, all valuable components in the sublimates accumulate in sludge accumulators [[5], [6]].

Niobium is resistant to many acids and salt solutions. Orthophosphoric, diluted sulfuric and nitric acids have practically no effect on niobium. Only concentrated solutions of hydrochloric, sulfuric and hydrofluoric acid or their mixtures can be effectively used as reagents [[7], [8]].

There are well-known methods of hydrochloric acid opening for natural and secondary titanium, niobium and tantalum raw materials [[9], [10], [11]]. The work [12] studies the kinetics of niobium leaching with hydrochloric acid from titanium-magnesium production waste. The experiments determine the effect of the parameters of the leaching temperature (25-90 °C), HCl concentration (0.5 - 4 M), stirring rate (100-500 rpm) and the solid-liquid ratio. The maximum niobium extraction degree of more than 90% was achieved in 60 minutes by leaching residues in 4 M HCl at 70°C.

The work [13] studies the conditions for the niobium and tantalum leaching from the columbite concentrate of the Zashikhinskiy deposit with a solution of hydrofluoric and sulfuric acids. We can see that the concentration of acids and the temperature of the solution have a decisive effect on the extraction degree of both elements. In contrast, the dispersion of the concentrate and the duration of phase contact have a lesser effect. Under conditions ensuring the production of solutions with a total content of niobium and tantalum of at least 110-130 g/L. Large-scale laboratory tests of the process for the extraction of niobium 97.6% and tantalum 93.7% were performed. The separation of niobium and tantalum using 1-octanol as an extractant for the production of experimental samples of niobium oxide and tantalum oxide was studied under the conditions of a continuous extraction cascade.

Zirconium is also chemically resistant in many aggressive environments. Zirconium interacts with acids only when there are conditions for the oxidation of acids and the formation of anionic complexes. It reacts neither with hydrochloric and sulfuric acids (up to 50%) nor with alkali solutions. It interacts with nitric acid and Aqua regia at above 100

°C. It is soluble in hydrofluoric and hot concentrated (above 50%) sulfuric acids [14].

The work studies the effect of nitric, sulfuric and hydrochloric acids on the morphology, elemental composition, structural and chemical transformations of the mineral surface and the leaching efficiency of zirconium (eudialyte) concentrate with the use of a complex of modern analytical methods [15]. Specific features in the eudialyte destruction nature and the degree of the effect of various acids have been found.

The analysis of the scientific and technical literature shows that acidic methods of decomposition followed by selective extraction of the target components are used to a greater extent to open rare metal raw materials. Moreover, most studies in the literature are devoted to qualified sources of rare metal raw materials, and there are very few studies on the extraction of niobium and zirconium from titanium production waste. The main purpose of this research is to conduct experimental studies to leach dust chamber sublimates, followed by the extraction of niobium and zirconium into an acidic solution.

## Materials and methods

*Materials.* Mineral acids are high-purity hydrofluoric acid, chemically pure sulfuric acid, and chemically pure hydrochloric acid. A sample of the sublimates from dust chambers in titanium chlorinators was provided by UKTMP JSC. Content of the main components of dust chamber sublimates, wt. %: 7.44 Ti; 6.5 Fe; 5.025 K; 4.899 Al; 2.539 Zr; 1.105 Na; 0.797 Nb; 0.359 Si; 0.214 Mg; 44.35 Cl; 24.053 O.

*Equipment.* Shimadzu TW423L analytical balance (Japan); Velp Scientifica LS top-drive agitator (Italy); IV-6 vibration damper (Russia); LT-111a circulation thermostat (Russia); SNOL drying cabinet (Lithuania).

*Experiment method.* Agitation leaching of DC sublimates with water was performed with the use of a weight of 50 g, at different ratios of S:L, temperature, time and at a stirring rate of 300 rpm. After filtration, the resulting cakes were dried to a constant weight and tested. Subsequent acid leaching of the niobium-containing cake was performed similarly, using a wide range of process parameters. The liquid phase was filtered at the end of the process. The precipitate was washed with warm water to remove residual acid. The resulting solutions and cakes were analyzed for the content of niobium, zirconium, titanium, aluminum, and iron.

Analysis methods. X-ray phase analysis was performed with the BRUKER D8 ADVANCE device (Germany). X-ray fluorescence analysis was performed with Venus 200 PANalytical B.V. wave dispersion spectrometer (Holland). Chemical analysis of samples was performed with Optima 2000 DV, an optical emission spectrometer with inductively coupled plasma (United States). Electron probe analysis was performed with JEOL JXA 8230 microanalyzer (Japan).

## Results and discussion

**Physical and chemical study of dust chamber sublimates and their treatment with the removal of water-soluble components.** The results of the X-ray phase analysis are shown in Figure 1. For the most part, the object of study consists of aqueous and anhydrous chloride phases: Erythrosiderite  $K_2(FeCl_5(H_2O))$ , aqueous chloraluminite  $AlCl_3(H_2O)_6$ , rokühnite  $FeCl_2(H_2O)_2$ , sodium chloride  $NaCl$ , zirconium chloride  $ZrCl_2$ , niobium oxychloride  $NbOCl_3$ . The oxide components of the sublimate include the phases of rutile  $Ti_{0.924}O_2$ , titanium oxide  $Ti_6O_{11}$ , and niobium-aluminium-titanium oxide  $Ti_{0.8}Al_{0.1}Nb_{0.1}O_2$ .

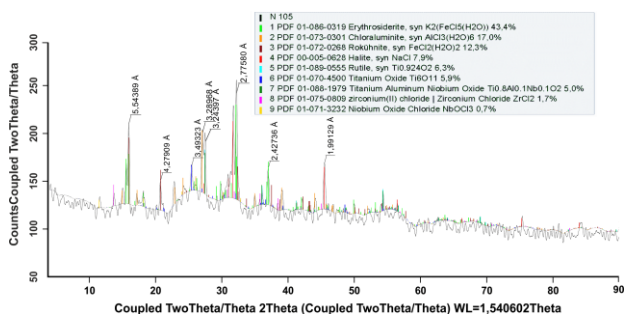


Figure 1 – Diffractogram of DC sublimates

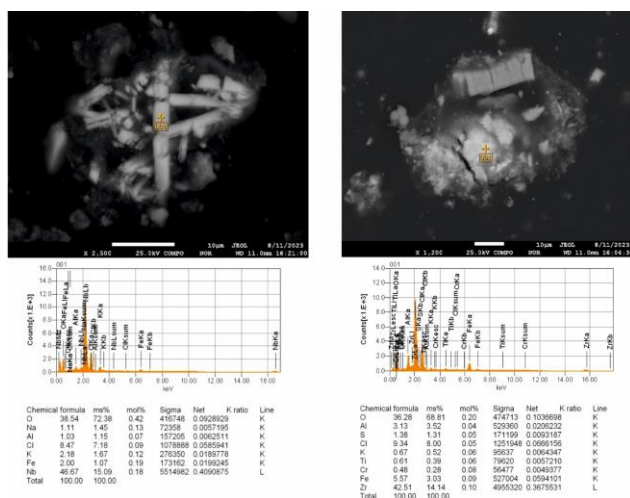


Figure 2 – COMPO image of DC sublimate. A particle of niobium and zirconium oxychlorides

A detailed study of the mineral structure of the DC sublimate sample was performed with the use of an electron probe microscope in the mode of backscattered electrons (COMPO). Several mineral points were analyzed using the electron probe microscope. Figure 2 shows particles of niobium ( $\times 2500$ ) and zirconium ( $\times 1200$ ) oxychlorides with a spectrum of various impurities.

Most hydrochloric acid salts are known to be freely soluble in water. Erythrosiderite contained in DC sublimates is a crystalhydrate of a complex salt of iron, potassium and hydrochloric acid  $FeCl_3 \cdot 2KCl \cdot H_2O$ . It is yellowish-red in color, hygroscopic, and soluble in water [16]. Hydrates of aluminum and iron chlorides are also hygroscopic crystalline substances that are easily soluble in water [[17], [18]]. Sodium chloride is the sodium salt of hydrochloric acid. It is moderately soluble in water and has a solubility that is slightly dependent on temperature. It is significantly reduced in the presence of chlorides of other metals. Pure sodium chloride is non-hygroscopic [19]. Zirconium oxide-dichloride has good solubility in cold water and is hydrolyzed in aqueous solution at above  $70^\circ C$  [20]. Niobium chloride and niobium oxychloride decompose with water, resulting in the formation of hydrated niobium pentoxide [21].

Experiments were conducted on its aqueous leaching taking into account the water-solubility of the chloride phases in DC sublimates. Table 1 shows the effect of the S:L ratio on the extraction degree of the main components of sublimating into the cake. Leaching experiments were performed at room temperature for 4 hours.

When the S:L ratio increases during the leaching of DC sublimates, a gradual decrease in cake yield is observed. The obtained pulps were filtered at a leisurely pace. At S: L = 1:10, the weight of the cake decreased 4 times while a slight decrease in the degree of niobium extraction into the cake was reported. When sublimates were leached at S: L= 1:8, the extraction of niobium into the cake was 83.85%. Ferric chloride showed high solubility in an aqueous medium and a relatively insignificant transition into cake. When the S:L ratio changes from 1:4 to 1:10, the extraction of aluminum and zirconium into the cake gradually decreases. At the same time, titanium showed low solubility and accumulation in the cake.

Table 2 shows the results of experiments on the effect of the leaching duration on the extraction degree of the main components of sublimating into the cake. The experiments were performed at process durations of 1,2,4,6 hours, temperature of  $25^\circ C$ , and S: L ratio of 1: 8.

**Table 1** – Effect of the S:L ratio on the extraction degree of the main components of sublimating into the cake

S:L ratio	Cake yield, %	Content in cake, %					Extraction into cake, %				
		Ti	Fe	Al	Zr	Nb	Ti	Fe	Al	Zr	Nb
1:4	28.00	24.23	7.45	19.67	4.14	2.25	91.19	32.08	62.72	45.63	79.15
1:6	27.60	24.34	5.45	16.71	4.13	2.29	90.31	23.13	52.51	44.87	79.41
1:8	27.00	25.74	3.59	13.42	3.93	2.48	93.42	14.92	41.26	41.76	83.85
1:10 AM	22.72	30.17	3.44	11.37	3.93	2.53	92.13	12.01	29.43	35.17	72.24

**Table 2** - Effect of leaching duration on the extraction degree of the main components of sublimate into the cake

Time, h	Cake yield, %	Content in cake, %					Extraction into cake, %				
		Ti	Fe	Al	Zr	Nb	Ti	Fe	Al	Zr	Nb
1	32.80	20.96	2.72	11.80	3.91	2.06	92.40	13.70	44.09	50.45	84.57
2	35.00	19.60	2.53	10.98	3.73	1.91	92.22	13.64	43.77	51.38	83.70
4	27.00	25.74	3.59	13.42	3.93	2.48	93.42	14.92	41.26	41.76	83.85
6	29.00	24.23	3.23	10.65	3.53	2.09	94.44	14.39	35.17	40.30	75.87

**Table 3** - Effect of temperature on the extraction degree of the main components of sublimate into the cake

T, °C	Cake yield, %	Content in cake, %					Extraction into cake, %				
		Ti	Fe	Al	Zr	Nb	Ti	Fe	Al	Zr	Nb
25	32.80	20.96	2.72	11.80	3.91	2.06	92.40	13.70	44.09	50.45	84.57
45	36.46	18.77	7.04	10.50	3.22	1.79	91.99	39.49	43.62	46.25	81.84
65	37.24	17.99	9.02	9.93	4.22	1.75	90.07	51.69	42.13	61.85	81.77
90	37.40	17.61	11.87	10.69	5.10	1.80	88.53	68.32	45.54	75.12	84.47

At a leaching duration of 1 hour, the extraction of niobium and zirconium into the cake was 84.57% and 50.45%, respectively. The table of the dependence of the extraction of sublimate components into cake on the duration of the experiment shows that when the duration increases, there is a decrease in the extraction of niobium and zirconium into cake, niobium and zirconium are leached into the solution. Therefore, the optimal leaching duration should be considered 1 hour for maximum extraction of the target components into the cake.

Table 3 shows the results of experiments on the effect of temperature on the extraction degree of the main components of sublimating into the cake. The study was performed at leaching temperatures of 25, 45, 65 and 90°C, and the following process parameters were kept constant: S: L ratio = 1: 8, duration = 4 hours, stirring rate = 300 rpm.

The results of the study presented in Table 3 show that increased leaching temperature leads to a slight increase in cake yield. At 90°C, the cake yield was 37.40%. There was a slight increase in the extraction of iron, aluminum, and zirconium into the cake, including chlorine cake, by 19.71%. It is worth

noting that an increase in temperature forms a gel-like, viscous pulp which is difficult to filter. It has been established that an increase in the temperature of the leaching process has a negative effect in terms of the conversion of chlorides into solution.

Therefore, the optimal conditions for the aqueous leaching of DC sublimate are S: L ratio = 1: 8, leaching time = 1 hour, and temperature = 25°C. At the same time, the extraction of niobium, titanium, aluminum, iron and zirconium into the cake was 84.57%, 92.40%, 44.09%, 13.70%, and 50.45%, respectively.

**Choice of an acidic reagent for the conversion of niobium and zirconium into solution.** The choice of solvents depends on many factors, including the corrosive effect on equipment, regenerability, and cost but not limited to the chemical and physical nature of the starting material. Besides, the state of rare refractory metals in acidic solutions is characterized by an extraordinary complexity and variety of forms. They can exist in the form of cationic and anionic mono- and polynuclear complex particles. Consequently, the subsequent extraction depends largely on the form of their existence in



**Table 4** – Content of Nb, Zr, Ti, Al, Fe in solution

Acidic reagent	Cake yield, %	Content in solution, g/L				
		Nb	Zr	Ti	Al	Fe
8M HCl	75.18	1.09	3.41	0.51	6.81	8.38
11M HCl	81.62	1.59	4.35	0.88	7.77	9.43
13M HF	55.60	6.75	9.47	22.37	20.47	16.38
18M HF	33.42	6.74	9.49	36.69	18.41	17.54
50%[13M HF]+50%[7M H <sub>2</sub> SO <sub>4</sub> ]	70.68	5.10	7.01	25.12	17.31	16.70
50%[18M HF]+50%[7M H <sub>2</sub> SO <sub>4</sub> ]	59.92	7.62	7.18	45.60	23.06	15.41

aqueous solutions which, in turn, are determined by their concentration of metal, and mineral acid, as well as the nature and concentration of other components.

To conduct experiments on acid leaching, 2 kg of cake was accumulated under the established optimal conditions of aqueous leaching of DC sublimates. Chemical composition of cake, wt.%: 28.33 Ti; 9.53 Al; 4.89 Zr; 3.66 Fe; 2.34 Nb; 1.5 Si; 33.28 O; 6.83 Cl; 0.46 Mn, etc. To compare the effectiveness of different acids concerning the conversion of the maximum amount of niobium and zirconium into filtrate, the niobium-containing cake was leached with solutions of HCl, HF and a mixture of acids with the composition of 50%HF+ 50%H<sub>2</sub>SO<sub>4</sub>. Considering that the completeness of the solubility of niobium and zirconium is achieved only in concentrated acids, agitation leaching of the cake was performed with the following solutions: 8M HCl, 11M HCl, 13M HF, 18M HF, 7M H<sub>2</sub>SO<sub>4</sub>. The cake suspension was processed for 2 hours at 25 °C and S:L ratio = 1:3. At the end of the process, the liquid phase was filtered. The precipitate was washed with warm water to remove residual acid. The resulting solutions were analyzed for the content of niobium, zirconium, titanium, aluminum, and iron. The results are shown in Table 4.

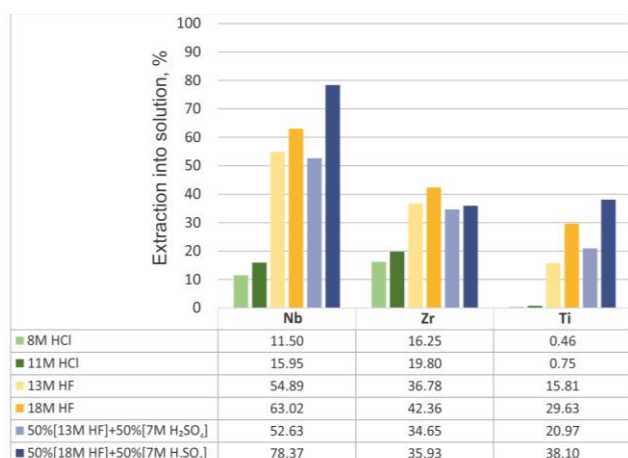


**Figure 3** – Dependence of the extraction degree of niobium, zirconium and titanium on the concentration and composition of the leaching solution

The graph of the dependence of the extraction degree of niobium, zirconium and titanium on the concentration and composition of the leaching solution was constructed. It is shown in Figure 3.

Studies on the identification of the effect of HCl, HF, HF+H<sub>2</sub>SO<sub>4</sub> on the degree of niobium extraction into the solution at a temperature of 25°C, the S:L ratio=1:3 and the agitation time of 2 hours showed the advantage of hydrofluoric acid and a HF+H<sub>2</sub>SO<sub>4</sub> mixture. When using hydrochloric acid under similar leaching conditions, the extraction of niobium and zirconium is 15.95% and 19.8%, respectively. Accordingly, about the conversion of niobium and zirconium into solution, concentrated hydrochloric acid turned out to be ineffective. The use of a mixture of hydrofluoric and sulfuric acids for cake leaching made it possible to achieve a relatively high extraction of the target components into the solution. The use of this mixture also helps to save on relatively expensive hydrofluoric acid. Therefore, a mixture of 50% [18M HF] + 50% [7M H<sub>2</sub>SO<sub>4</sub>] was chosen as the acidic reagent for cake leaching.

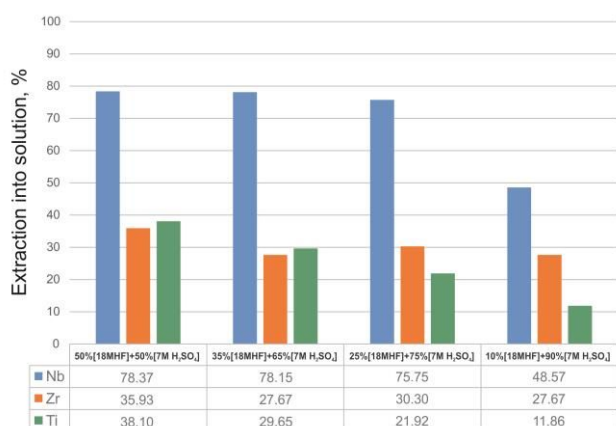
**Study of the effect of various parameters on acid leaching of cake.** Experiments on the effect of the ratio of a mixture of hydrofluoric and sulfuric acids were performed under the following conditions: S:L ratio=1:3, temperature = 25°C, duration = 240 minutes, stirring intensity = 300 rpm and acid ratios of 10% [18M HF] + 90% [5M H<sub>2</sub>SO<sub>4</sub>], 25% [18M HF] + 75% [5M H<sub>2</sub>SO<sub>4</sub>], 35% [18M HF] + 65% [7M H<sub>2</sub>SO<sub>4</sub>], 50% [18M HF] + 50% [7M H<sub>2</sub>SO<sub>4</sub>].

Figure 4 shows a histogram of the extraction of Nb, Zr, and Ti into solution at different ratios of hydrofluoric and sulfuric acids.

The figure shows that, in general, when the proportion of hydrofluoric acid in the mixture increases from 10% to 50%, the extraction of controlled elements into solution increases from 48.57 to 78.37% for niobium, from 27.67 to 35.93% for zirconium, and from 11.86 to 38.10% for titanium. The cake yield varies from 59.92% to



72.74%. At ratios of 35% [18M HF] +65% [7M H<sub>2</sub>SO<sub>4</sub>], 50% [18M HF] + 50% [7M H<sub>2</sub>SO<sub>4</sub>], the contamination of the solution with titanium and other impurities was higher; consequently, 25% [18M HF] +75% [7M H<sub>2</sub>SO<sub>4</sub>] was accepted as the optimal ratio of a mixture of hydrofluoric and sulfuric acids for the studied raw materials, at which the extraction of niobium and zirconium into solution is 75.75% and 30.3%, respectively. Further experiments on the effect of various parameters on the process of leaching niobium-containing cake were performed at the above ratio of hydrofluoric and sulfuric acids.



**Figure 4** – Histogram of the extraction of Nb, Zr, and Ti into solution at different ratios of hydrofluoric and sulfuric acids

Studies to leach niobium-containing cake at different ratios of solid and liquid phases were performed using solutions of a mixture of 25% [18M HF] +75% [7M H<sub>2</sub>SO<sub>4</sub>], temperature = 25°C, duration = 240 minutes, mixing intensity = 300 rpm. The results of the research are shown in Figure 5.

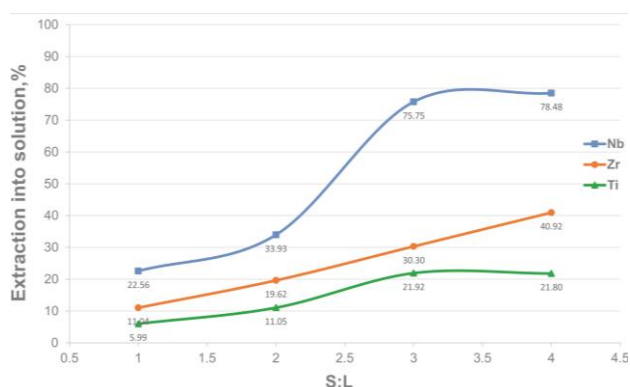


**Figure 5** – Dependence of the extraction of Nb, Zr, Ti into solution on the S:L ratio at 25%HF+75% H<sub>2</sub>SO<sub>4</sub>

The figure shows that the extraction of niobium into solution increases dynamically in the range of S:L ratios from 1:2 to 1:4. At the same time, the extraction of niobium into solution is comparatively lower at S:L ratios of 1:1 and 1:2. The extraction of zirconium and titanium into solution with a change in the S:L ratio increases in the range from ~ 11 to ~ 41% and from ~ 6 to ~ 22%, respectively. For that matter, these mineral forms of zirconium and titanium were moderately dissolved in solution under experimental conditions and remained mostly in the cake. Therefore, taking into account the consumption of the reagent during leaching, the S:L ratio = 1:3 can be considered the best option.

Further, the studies were performed at leaching temperatures of 25, 45, 65, 90°C and while maintaining constant the following process parameters: 25%HF + 75%H<sub>2</sub>SO<sub>4</sub>, S:L ratio =1:3, holding time = 240 minutes, and pulp stirring rate = 300 rpm. The results of the research are shown in Figure 6.

When the temperature of the leaching process increases, an increase in the extraction of Nb and Zr into the solution is reported. At the same time, there is a slight increase in the extraction of titanium into solution. In general, the increase in temperature had a positive effect on the intensification of the leaching process. At a leaching temperature of 90°C, the extraction into solution reached 94.73% for niobium, 33.67% for titanium, and 83.53% for zirconium. The cake yield varied between ~ 22 and 29%.

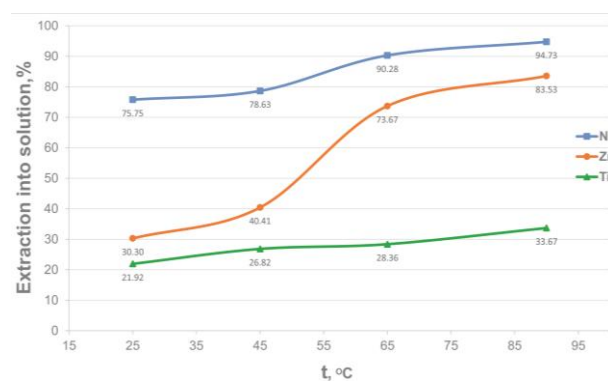


**Figure 6** – Dependence of the extraction of Nb, Zr, Ti into solution on the temperature at 25%HF+75% H<sub>2</sub>SO<sub>4</sub>

Experiments on the duration of leaching were performed while maintaining the duration of the process of 30, 60, 120 and 240 minutes, a temperature of 90°C, a ratio of S:L = 1:3 and a pulp stirring rate of 300 rpm. The experimental results are shown in Figure 7.

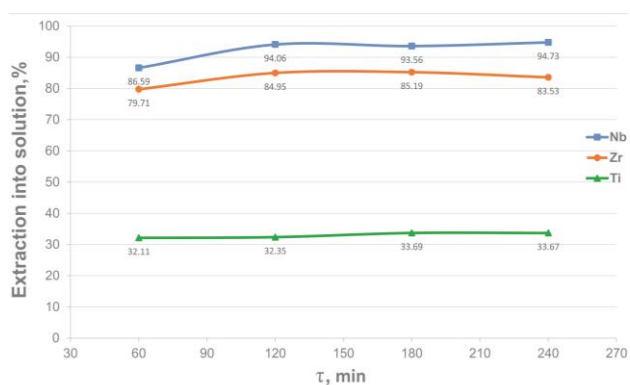


**Figure 7** – Dependence of the extraction of Nb, Zr, Ti into solution on duration at 25%HF+75% H<sub>2</sub>SO<sub>4</sub>

The extraction of niobium into the solution was 94.06% at a leaching duration of 120 minutes. Then, in the interval of the leaching duration of 120-240 minutes, it was kept at the level of ~ 93-95%. Over the entire period, the extraction of zirconium into solution was also consistently high, on average fluctuating in the range of ~80-85%. Titanium extraction is kept almost at the same level in the range of ~32-34%. The equilibrium in the system is established after 120 minutes of holding of pulp; therefore; there is no need to carry out the leaching process for more than 120 minutes. X-ray fluorescence analysis of the leaching residue was performed, wt. %: 55.22 Ti; 4.47 Fe; 1.04 Al; 0.75 Zr; 0.26 Nb; 0.21 Mg; 23.27 O; 7.5 Cl, etc.

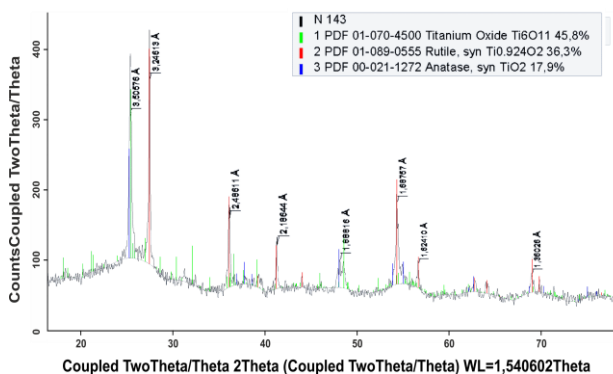


**Figure 8** – X-ray phase analysis of residual cake

According to the results of the XRF analysis (see Figure 8), the cake consists of titanium oxides of various natures, wt. %: 45,8 Ti<sub>6</sub>O<sub>11</sub>; 36,3 Ti<sub>0.924</sub>O<sub>2</sub>; 17,9 TiO<sub>2</sub>.

Thus, as a result of the experimental work on acid leaching of cake, the optimal conditions for the extraction of niobium and zirconium into solution were determined and are 25%HF +75%H<sub>2</sub>SO<sub>4</sub>, S:L ratio = 1:3, temperature = 90°C, duration of the leaching process = 120 minutes. At the same time,

the extraction of niobium into solution reached 94.06%, and the extraction of zirconium and titanium into solution amounted to 84.95% and 32.35%, respectively.

## Conclusions

We studied the material composition of the sublimates from dust chambers in titanium chlorinators. Chemical and X-ray fluorescence analyses determined the content of the main components, wt. %: 7.44 Ti; 6.5 Fe; 5.025 K; 4.899 Al; 2.539 Zr; 1.105 Na; 0.797 Nb; 0.359 Si; 0.214 Mg; 44.35 Cl; 24.053 O.

X-ray phase analysis found the presence of the following phases: erythrosiderite K<sub>2</sub> (FeCl<sub>5</sub>(H<sub>2</sub>O)), aqueous chloraluminite AlCl<sub>3</sub>(H<sub>2</sub>O)<sub>6</sub>, rokhnite FeCl<sub>2</sub>(H<sub>2</sub>O)<sub>2</sub>, sodium chloride NaCl, rutile Ti<sub>0.924</sub>O<sub>2</sub>, iron titanate Fe<sub>3</sub>Ti<sub>3</sub>O<sub>10</sub>, zirconium chloride ZrCl<sub>2</sub> and niobium oxychloride NbOCl<sub>3</sub>.

The study of the mineral structure of the DC sublimate sample using an electron probe microscope determined the presence of particles of niobium and zirconium oxychlorides.

Taking into account the water-solubility of the chloride phases in DC sublimates, experiments were conducted on its aqueous leaching at various parameters. The optimal conditions for aqueous leaching are S:L ratio = 1:8, leaching time = 1 hour, and temperature = 25°C. At the same time, the extraction of niobium, titanium, aluminum, iron and zirconium into the cake was 84.57%, 92.40%, 44.09 %, 13.70 %, and 50.45%, respectively.

We determined the quantitative elemental composition of a sample of niobium-containing cake obtained under optimal conditions of aqueous leaching, wt. %: 20.96 Ti; 11.8 Al; 3.91 Zr; 2.72 Fe; 2.06 Nb; 1.5 Si; 0.94 Na; 0.33 K; 0.15 Mg; 45.68 O; 6.8 Cl, etc.

Studies on the identification of the effect of HCl, HF, HF+H<sub>2</sub>SO<sub>4</sub> on the degree of niobium extraction into the solution at a temperature of 25°C, the S:L ratio=1:3 and the agitation time of 2 hours showed the advantage of hydrofluoric acid and a HF+H<sub>2</sub>SO<sub>4</sub> mixture. A mixture of 50% [18M HF] +50% [7M H<sub>2</sub>SO<sub>4</sub>] was chosen as the acidic reagent for cake leaching.

According to the results of the studies on the Study of the effect of various parameters on acid leaching of cake, optimal conditions for the extraction of niobium and zirconium into solution

were established: 25% [18M HF] +75% [7M H<sub>2</sub>SO<sub>4</sub>], S:L ratio = 1:3, temperature = 90 °C, duration of the leaching process = 120 minutes. Under these leaching conditions, the extraction of niobium, zirconium, and titanium into solution was 94.06%, 84.95% and 32.35%, respectively. X-ray fluorescence analysis of the residue, mass was performed, wt. %: 55.22 Ti; 4.47 Fe; 1.04 Al; 0.75 Zr; 0.26 Nb; 0.21 Mg; 23.27 O; 7.5 Cl, etc. Based on the results of the XRD

analysis, the phase composition of the residue, mass, was determined; wt. %: 45,8 Ti<sub>6</sub>O<sub>11</sub>; 36,3 Ti<sub>0.924</sub>O<sub>2</sub>; 17,9 TiO<sub>2</sub>.

**Acknowledgement.** This research was funded by the Science Committee of the Ministry of Science and High Education of the Republic of Kazakhstan, Grant Project No. AP19578854.

**Cite this article as:** Yessengaziyev AM, Toishybek AM, Mukangaliyeva AO, Abdyldayev NN, Yersaiynova AA. Study of the leaching process for dust chamber sublimates followed by the extraction of niobium and zirconium into solution. *Kompleksnoe Ispolzovanie Mineralnogo Syra = Complex Use of Mineral Resources.* 2024; 331(4):117-126. <https://doi.org/10.31643/2024/6445.45>

## Ниобий мен цирконий ерітіндіге шығарылатын шаң камераларының возгондарын шаймалау процесін зерттеу

\*Есенгазиев А. М., Тойшыбек А. М., Мұқанғалиева А.Ө., Абдылдаев Н.Н., Ерсайынова А.А.

*Металлургия және кен байыту институты, Сәтбаев Университеті, Алматы, Қазақстан*

<p>Мақала келді: 7 қараша 2023 Сараптамадан өтті: 4 қаңтар 2024 Қабылданды: 19 қаңтар 2023</p>	<p><b>ТҮЙІНДЕМЕ</b> Химиялық, рентгендік және микросондтық талдау әдістерімен титан хлораторларының шаң камераларының возгондарының заттық құрамы зерттелді. Шаң камераларының возгондарының фазалық құрамын зерттеу нәтижесінде олардың сулы және сусыз хлоридті фазалардан тұратыны анықталды. Возгондарда ниобий екі түрде - оксихлорид және оксид түрінде болады. Цирконий хлоридті және оксихлоридті сипатқа ие. Шаң камералары возгондарын сумен шаймалау бойынша тәжірибелер жүргізіліп, процестің оңтайлы жағдайлары анықталды: Қ:С=1:8, шаймалау уақыты 1 сағат, температура 25 °С. Ниобий мен цирконийді ерітіндіге айналдыра отырып, сүзіндіні шаймалау үшін реагентті таңдау бойынша зерттеулер жүргізілді. Реагент ретінде HF + H<sub>2</sub>SO<sub>4</sub> қышқылдарының қоспасынан тұратын ерітінді таңдалды. Ерітіндіге ниобий мен цирконийді алудың оңтайлы шарттары белгіленді: 25%[18m HF] +75%[7M H<sub>2</sub>SO<sub>4</sub>], Қ:С = 1: 3, температура 90 °C, шаймалау процесінің ұзақтығы 120 мин. Осы шаймалау жағдайында ниобийдің ерітіндіге өтуі 94,06%, цирконийдің 84,95%, титанның 32,35% болды. Сүзіндіні қышқылмен шаймалаудан қалған қалдықтың элементтік және фазалық құрамы анықталды.</p>
	<p><b>Түйін сөздер:</b> ниобий, шаң камераларының возгондары, шаймалау, қышқыл, ерітінді.</p>
<p><b>Есенгазиев Азамат Муратович</b></p>	<p><b>Авторлар туралы ақпарат:</b> PhD докторы, ғылыми қызметкер, <i>Металлургия және кен байыту институты, Сәтбаев Университеті, Алматы, Қазақстан.</i> E-mail: a.yessengaziyev@satbayev.university</p>
<p><b>Тойшыбек Азамат Мағауияұлы</b></p>	<p>Жетекші инженері, <i>Металлургия және кен байыту институты, Сәтбаев Университеті, Алматы, Қазақстан.</i> E-mail: a.toishybek@satbayev.university</p>
<p><b>Мұқанғалиева Арайлым Өмірзаққызы</b></p>	<p>Жетекші инженері, <i>Металлургия және кен байыту институты, Сәтбаев Университеті, Алматы, Қазақстан.</i> E-mail: 000316650668-D@stud.satbayev.university</p>
<p><b>Абдылдаев Нурғали Нурланович</b></p>	<p>Жетекші инженері, <i>Металлургия және кен байыту институты, Сәтбаев Университеті, Алматы, Қазақстан.</i> E-mail: n.abdyldaev@satbayev.university</p>
<p><b>Ерсайынова Альбина Абатқызы</b></p>	<p>Жетекші инженері, <i>Металлургия және кен байыту институты, Сәтбаев Университеті, Алматы, Қазақстан.</i> E-mail: a.yersaiynova@stud.satbayev.university</p>

## Исследование процесса выщелачивания возгонов пылевых камер с извлечением ниобия и циркония в раствор

\*Есенгазиев А. М., Тойшыбек А. М., Мұқанғалиева А.Ө., Абдылдаев Н.Н., Ерсайынова А.А.

*Институт металлургии и обогащения, Сәтбаев Университет, Алматы, Казахстан*

<p>Поступила: 7 ноября 2023 Рецензирование: 4 января 2024 Принята в печать: 19 января 2024</p>	<p><b>АННОТАЦИЯ</b></p> <p>Изучен вещественный состав возгонов пылевых камер титановых хлораторов методами химического, рентгеновского и микронзондового анализа. Исследования фазового состава возгонов пылевых камер показало, что объект в большей степени состоит из водных и безводных хлоридных фаз. Выявлены две формы присутствия ниобия - оксихлоридной и оксидной. Нахождения циркония в возгонах имеет хлоридную и оксихлоридную природу. Проведены опыты по водному выщелачиванию возгонов пылевых камер с определением оптимальных условий процесса: Т:Ж=1:8, время выщелачивания 1 часа, температура 25 °С. Проведены исследования по выбору кислотного реагента для выщелачивания кека с переводом ниобия и циркония в раствор. В качестве кислотного реагента для выщелачивания кека выбран раствор, состоящий из смеси HF+H<sub>2</sub>SO<sub>4</sub>. Установлены оптимальные условия извлечения ниобия и циркония в раствор: 25%[18M HF] +75%[7M H<sub>2</sub>SO<sub>4</sub>], Т:Ж = 1:3, температура 90 °С, продолжительность процесса выщелачивания 120 мин. При данных условиях выщелачивания, извлечение в раствор ниобия 94,06%, циркония 84,95%, титана 32,35%. Определен элементный и фазовый состав остатка от кислотного выщелачивания кека.</p> <p><b>Ключевые слова:</b> ниобий, возгоны пылевых камер, выщелачивание, кислота, раствор.</p>
<p><b>Есенгазиев Азамат Муратович</b></p>	<p><b>Информация об авторах:</b> Доктор PhD, научный сотрудник, Институт металлургии и обогащения, Сампаев Университет, Алматы, Казахстан. E-mail: a.yessengaziyev@satbayev.university</p>
<p><b>Тойшыбек Азамат Мағауияұлы</b></p>	<p>Ведущий инженер, Институт металлургии и обогащения, Сампаев Университет, Алматы, Казахстан. E-mail: a.toishybek@satbayev.university</p>
<p><b>Мұқанғалиева Арайлым Өмірзаққызы</b></p>	<p>Ведущий инженер, Институт металлургии и обогащения, Сампаев Университет, Алматы, Казахстан. E-mail: 000316650668-D@stud.satbayev.university</p>
<p><b>Абдылдаев Нурғали Нурланович</b></p>	<p>Ведущий инженер, Институт металлургии и обогащения, Сампаев Университет, Алматы, Казахстан. E-mail: n.abdyldaev@satbayev.university</p>
<p><b>Ерсайынова Альбина Абатқызы</b></p>	<p>Ведущий инженер, Институт металлургии и обогащения, Сампаев Университет, Алматы, Казахстан. E-mail: a.yersayynova@stud.satbayev.university</p>

## References

- [1] Zhilina YeM, Krasikov SA, Agafonov SN, Zhidovinova SV, Russkikh AS, Osinkina TV. Vydeleniye tugoplavkikh redkikh metallov iz otkhodov zharoprochnykh nikelvykh splavov [Isolation of refractory rare metals from waste heat-resistant nickel alloys]. Trudy Kol'skogo nauchnogo tsentra RAN [Proceedings of the Kola Scientific Center of the Russian Academy of Sciences]. 2018; 269-271, (in Russ.). <https://doi.org/10.25702/KSC.2307-5252.2018.9.1.269-271>
- [2] Bakhytuly N, Kenzhegulov A, Nurtanto M, Aliev A, & Kuldeev E. Microstructure and tribological study of TiAlCN and TiTaCN coatings. Kompleksnoe Ispolzovanie Mineralnogo Syra= Complex use of mineral resources. 2023; 327(4):99-110.
- [3] Alipovna MA, Karaulovich KA, Vladimirovich PA, Zhanuzakovich AZ, Bolatovna KB, Wieleba W, Bakhytuly N. The study of the tribological properties under high contact pressure conditions of TiN, TiC and TiCN coatings deposited by the magnetron sputtering method on the AISI 304 stainless steel substrate. Materials Science-Poland. 2023; 41(1):1-14.
- [4] Ultarakova AA, Yessengaziyev AM, Kuldeyev EI, Kassymzhanov KK, Uldakhanov Okh. Processing of titanium production sludge with the extraction of titanium dioxide. Metallurgija. 2021; 60(3-4):411-414.
- [5] Kudryavsky YuP, Kudryavskiy YUP. Kompleksnaya pererabotka vozgonov titanovykh khloratorov [Complex processing of titanium chlorinator sublimates]. Tsvetnyye metally [Non-ferrous metals]. 1998; 7:56-58. (in Russ.).
- [6] Kolobov GA, Pecheritsa KA, Prokhorov SV. Osnovnyye tendentsii sovershenstvovaniya magniyetermicheskogo sposoba proizvodstva titana gubchatogo [Main trends in improving the magnesium-thermal method for the production of titanium sponge]. Teoriya i praktika metallurgii [Theory and practice of metallurgy]. 2010; 5(6):43-45. (in Russ.).
- [7] Kalinnikov VT, Nikolaev AI, Zakharov VI. Gidrometallurgicheskaya kompleksnaya pererabotka netraditsionnogo titano-redkometall'nogo i alyumosilikatnogo syr'ya [Hydrometallurgical complex processing of non-traditional titanium-rare metal and aluminosilicate raw materials]. Apatity: Izd. KNTS RAN [Apatity: Publishing house. KSC RAS]. 1999, 225. (in Russ.).
- [8] Kalinnikov VT, Zots NV, Nikolaev AI. and others. Gidrometallurgicheskiye tekhnologii netraditsionnogo titano-redkometall'nogo syr'ya [Hydrometallurgical technologies of non-traditional titanium-rare metal raw materials]. Metallurgiya tsvetnykh i redkikh metallov: sb. st. Rossiysko-indiyskogo simpoz [Metallurgy of non-ferrous and rare metals: collection. Art. Russian-Indian symposium], M. 2002; 199-203. (in Russ.).
- [9] Korovin SS, Drobot DV, Fedorov PI. Redkiye i rasseyannyye elementy: Khimiya i tekhnologiya [Rare and trace elements: Chemistry and technology]. kn. 2. M.: MISIS [book 2. M.: MISIS]. 1999, 464. (in Russ.).
- [10] Patent RF №2201987. Sposob vskrytiya loparitovogo kontsentrata [Method for opening loparite concentrate]. Zots NV, Petrov VB, Kasikov AG. Publ. 10.04.03, Byul. № 10. (in Russ.).
- [11] Patent RF 2149908. Sposob razlozheniya mineral'nogo i tekhnogen'nogo syr'ya [Method of decomposition of mineral and technogenic raw materials]. Skiba GS, Korovin VN, Voskoboynikov NB, I dr. Publ. 27.05.00, byul. № 15. (in Russ.).
- [12] Terence M, Animesh J, Stephen S. Kinetics of hydrochloric acid leaching of niobium from TiO<sub>2</sub> residues. International Journal of Mineral Processing. 2016; 157:1-6. <https://doi.org/10.1016/j.minpro.2016.09.001>

- [13] Smirnov AV, Sibilev AS, Nechayev AV, Spynu AYU. Gidrometallurgicheskaya pererabotka kolumbitovogo konsentrata zashikhinskogo mestorozhdeniya [Hydrometallurgical processing of columbite concentrate from the Zashikha deposit]. Trudy KNTS (Khimiya i materialovedeniye) [Proceedings of KSC (Chemistry and Materials Science)]. 2015; 5:94-97. (in Russ.).
- [14] Zelikman AN, Meerson GA. Metallurgiya redkikh metallov [Metallurgy of rare metals], M. 1973; 608. (in Russ.).
- [15] Chanturia VA, Minenko VG, Koporulina EV, Ryazantseva MV, Samusev AL. Vliyaniye razlichnykh kislot na effektivnost' izvlecheniya tsirkoniya i redkozemel'nykh metallov pri vyshchelachivaniy evdialitovogo konsentrata [The effect of various acids on the efficiency of extraction of zirconium and rare earth metals during leaching of eudialyte concentrate]. Zhurnal «Fiziko-tehnicheskiye problemy razrabotki poleznykh iskopayemykh» [Journal "Physical and technical problems of mineral development"]. 2019; 6:140-151. (in Russ.).
- [16] Khimicheskaya entsiklopediya [Chemical Encyclopedia]. Redkol.: Knunyants I.L. i dr. M.: Sovetskaya entsiklopediya [Editorial Board: Knunyants I.L. and others. M.: Soviet Encyclopedia]. 1990; 2:671. (in Russ.).
- [17] Alyuminiy khloristyy 6-vodnyy [Aluminum chloride 6-water]. [Electronic resource]. <https://reaktivtorg.ru/alyuminiy-khloristyy-6-vodnyy>, (Access date: 6.07.2023). (in Russ.).
- [18] Ramazanova, J.M., and M.G. Zamalitdinova. 2019. Physical and Mechanical Properties Investigation of Oxide Coatings on Titanium. Kompleksnoe Ispolzovanie Mineralnogo Syra = Complex Use of Mineral Resources 309 (2):34-41. <https://doi.org/10.31643/2019/6445.14>.
- [19] Lidin RA, Molochko VA, Andreyeva LL. Khimicheskiye svoystva neorganicheskikh veshchestv: Ucheb. posobiye dlya vuzov [Chemical properties of inorganic substances: Textbook. manual for universities]. M.: Khimiya [M.: Chemistry]. 1996. (in Russ.).
- [20] Khimicheskaya entsiklopediya [Chemical Encyclopedia]. Redkol.: Zefirov NS, i dr. M.: Bol'shaya Rossiyskaya entsiklopediya [Editorial Board: Zefirov N.S. and others. M.: Great Russian Encyclopedia]. 1998; 5:783. (in Russ.).
- [21] Pererabotka titano-niobiyevotantalovogo syr'ya po sposobu khlorirovaniya [Processing of titanium-niobium-tantalum raw materials using the chlorination method]. [Electronic resource]. URL: <https://metal-archive.ru/redkie-metally/4267-pererabotka-titano-niobievo-tantalovogo-syr'ya-po-sposobu-hlorirovaniya.html> (Access date: 7.07.2023). (in Russ.).



**МАЗМУНЫ  
СОДЕРЖАНИЕ  
CONTENTS**

**ENGINEERING AND TECHNOLOGY**

*Barmenshinova M.B., Motovilov I.Y., Telkov Sh.A., Omar R.S.*  
STUDY OF THE MATERIAL COMPOSITION OF REFRACTORY GOLD-BEARING ORE FROM THE AKTOBE DEPOSIT ..... 5

*Sabergaliyev M.M., Yeligbayeva G.Z, Khassanov D.A., Muradova S.R., Orazalin Z.K., Ainakulova D.T., Sharipov R.Kh., Negim El-Sayed*  
MODIFIED BITUMEN-POLYMER MASTIC TO PROTECT METAL COATINGS FROM CORROSION..... 12

*Yeligbayeva G., Khaldun M. A., Abdassalam A. Alfergani, Tleugaliyeva Zh., Karabayeva A., Bekbayeva L., Zhetpisbay D.S., Shadin N.A., Atabekova Z.*  
POLYURETHANE AS A VERSATILE POLYMER FOR COATING AND ANTI-CORROSION APPLICATIONS: A REVIEW ..... 21

*Chang S.C., Yusoff A.H., Mohamed C.A.R., Liu S.F., Shoparwe N.F., Husain N.A, Azlan M.N.*  
GEOCHEMISTRY OF RARE EARTH ELEMENTS IN PAHANG RIVER SEDIMENT, MALAYSIA..... 42

**EARTH SCIENCES**

*Zhunussova G.E., Igenderlina M.B., Abekov U.E.*  
ANALYZING GEODETIC LEVELING AND SUBSIDENCE OF BENCHMARKS: DATA AND CONCLUSIONS FOR ZHEZKAZGAN AND GEV-LERMONTOVO VILLAGES ..... 51

*Yakubov M.M., Yoqubov M.M., Kholikulov D.B., Maksudhodjaeva M.S.*  
DEPLETION OF CONVERTER SLAGS TO WASTE IN THE VANYUKOV FURNACE DURING PYROMETALLURGICAL COPPER PRODUCTION AT JSC ALMALYK MMC..... 60

*Uakhiova A.A., Madisheva R.K., Askarova N.S., Adilkhanov R.K., Zheksenbaeva G.M.*  
PROSPECTS OF OIL AND GAS POTENTIAL OF THE SOUTH TORGAI SEDIMENTARY BASIN..... 69

**METALLURGY**

*Zhapbasbayev U.K., Ramazanova G.I., Terekhov V.I., Sattinova Z.K.*  
CALCULATION OF THE THERMOPLASTIC BERYLLIUM OXIDE SLURRY MOLDING WITH ULTRASONIC ACTIVATION ..... 79

*Volodin V.N., Abdulvaliyev R.A., Trebukhov S.A., Nitsenko A.V., Linnik X.A.*  
RECYCLING OF BERYLLIUM, MANGANESE, AND ZIRCONIUM FROM SECONDARY ALLOYS BY MAGNESIUM DISTILLATION IN VACUUM..... 90

*Makhambetov Ye.N., Abdirashit A.M., Myngzhassar Ye.A., Burumbayev A.G., Zhakan A.M., Yucel Onuralp*  
RESEARCH ON THE POSSIBILITY OF OBTAINING MEDIUM-CARBON FERROMANGANESE FROM THE DJEZDINSKOE DEPOSIT..... 101

*Orynbayev B.M., Baigenzhenov O.S., Turan M.D.*  
OVERVIEW OF TECHNOLOGIES USED TO EXTRACT SCANDIUM FROM SECONDARY RAW MATERIALS..... 109

*Yessengaziyev A.M., Toishybek A.M., Mukangaliyeva A.O., Abdyldayev N.N., Yersaiynova A. A.*  
STUDY OF THE LEACHING PROCESS FOR DUST CHAMBER SUBLIMATES FOLLOWED BY THE EXTRACTION OF NIOBIUM AND ZIRCONIUM INTO SOLUTION ..... 117

Техникалық редакторлар:  
*Г.К. Қасымова, Н.М.Айтжанова, Т.И. Қожахметов*

Компьютердегі макет:  
*Г.К. Қасымова*

Дизайнер:  
*Г.К. Қасымова, Н.М.Айтжанова*

Металлургия және кен байыту институты; Сәтбаев Университеті  
050010, Қазақстан Республикасы, Алматы қаласы, Шевченко к-сі, 29/133

Жариялауға 19.01.2024 жылы қол қойылды

Технические редакторы:  
*Г.К. Касымова, Н.М. Айтжанова, Т.И. Кожахметов*

Верстка на компьютере:  
*Г.К. Касымова*

Дизайнер:  
*Г.К. Касымова, Н.М.Айтжанова*

Институт металлургии и обогащения; Сатпаев Университет  
050010, г. Алматы, Республика Казахстан. ул. Шевченко, 29/133

Подписано в печать 19.01.2024г.

Technical editors:  
*G.K. Kassymova, N.M. Aitzhanova, T.I. Kozhakhmetov*

The layout on a computer:  
*G.K. Kassymova*

Designer:  
*G.K. Kassymova, N.M. Aitzhanova*

Institute of Metallurgy and Ore Beneficiation; Satbayev University,  
050010, Almaty city, the Republic of Kazakhstan. Shevchenko str., 29/133

Signed for publication on 19.01.2024